ANALYSIS OF CARBON AND ENERGY FLUXES DURING NITROGEN DEPRIVATION IN CHLAMYDOMONAS

By

Matthew Thomas Juergens

A DISSERTATION

Submitted to
Michigan State University
in partial fulfillment of the requirements
for the degree of

Plant Biology—Doctor of Philosophy

2016

ABSTRACT

ANALYSIS OF CARBON AND ENERGY FLUXES DURING NITROGEN DEPRIVATION IN CHLAMYDOMONAS

By

Matthew Thomas Juergens

Algae have been considered as sources for renewable bioenergy due their ability to accumulate high cellular percentages of biomass as energy dense molecules, namely starch and triacylglycerols. The accumulation of these compounds is most readily induced through exposing cells to nutrient deprivation, especially from the macronutrient nitrogen. Multiple large scale studies have been carried out to study the metabolism behind starch and oil accumulation in an effort to increase production; however, no sufficient strategy for over accumulation has been determined. Additionally, little is known about the actual motivations for algae to accumulate these compounds in the first place. Current hypothesized roles for these molecules range from aiding recovery from nutrient deprivation to providing sinks for overflowing photosynthetic energy as metabolism slows. The exact relationship between carbon accumulation and photosynthesis remains unresolved.

To study the interaction between photosynthesis (energy and carbon input) and carbon accumulation (stored carbon and energy), *Chlamydomonas reinhardtii* was chosen as a model. Chlamydomonas is the premier algal model system and can accumulate significant amounts of starch and TAG. Second, it can grow auto-, mixo-, and heterotrophically enabling experimentation under a range of light and media conditions. Further, extensive information available on the genome, transcriptome, proteome, and metabolic environment of Chlamydomonas allow for deeper interpretation of systems biology approaches.

In this dissertation I explore the relationship between photosynthesis and carbon accumulation during nitrogen deprivation from the perspective of carbon and energy fluxes. Through systems biology methods, physiological measurements, and biomass analysis across multiple stages of nutrient deprivation I show that carbon accumulation is not dependent upon photosynthesis under mixotrophic conditions, pointing to a storage role for starch and TAG, most likely to aid nutrient recovery. Further, through flux modeling efforts using measured constraints, I report on the complexity of starch and TAG accumulations and how they change over the course of nutrient deprivation. This work suggests deeper regulatory interactions between starch and TAG accumulation based upon cellular programming and not simply energy overflows. It is my sincere hope that this work will help guide future engineering efforts concerning biofuel production in algae.

TABLE OF CONTENTS

LIST OF TABLES

LIST OF FIGURES

KEY TO ABBREVIATIONS

(CCM) Carbon Concentrating Mechanism

(CDW) Cell Dry Weight

(Chl) Chlorophyll

(CEF) Cyclic electron flow

(DIRK) Dark Interval Relaxation Kinetics

(DGDG) Digalactosyldiacylglycerol

(ECS) Electrochromic Shift

(G.E.O) Gross Evolved Oxygen rates

(LED) Light Emitting Diodes

(LHC) Light Harvesting Centers

(LEF) Linear electron flow

(MGDG) Monogalactosyldiacylglycerol

(N) Nitrogen

(OH) Overflow Hypothesis

($P700^{+}$) Oxidized primary donor of photosystem I

(PG) Phosphatidylglycerol

(PS) Photosystem

(PMF) Proton motive force

(P700) PSI Primary Electron Donor

(Q_A) PSII Primary Quinone A

(qL) Percent of open Q_A based upon the lake model

(qP) Percent of open Q_A based upon the puddle model

(Φ_{II}) Quantum Efficiency of PS II photochemistry in the light

(ROS) Reactive Oxygen Species

(SQGD) Sulfoquinovosyldiacylglycerol

(SCX) Strong Cation Exchange

($\boldsymbol{\nu}_{\mathbf{H}}^{+}$) Total Proton Efflux

(TAG) Triacyl glycerol

(TAP) Tris-Acetate-Phosphate

CHAPTER- 1

Algae and Their Use in Biofuel Production: A Literature Review

Foreword

Algae are a diverse group of photosynthetic eukaryotes that play deeply important roles in the natural world. Ranging in size from microscopic single cells to multicellular bodies over 50m in length, these primarily aquatic organisms provide one of the largest primary food sources for the planet. In addition, through their photosynthetic activities (accounting for 25% of global CO_2 fixation (Jardillier *et al.* 2010)), these organisms have affected the global carbon balances, oxygen levels, and global ecosystems. During the last two hundred years, algae have also been employed in research on cell physiology, photosynthesis, and biofuel production (Beijerinck 1904, Ehrenberg 1838, Merrill 1916, Van Iterson *et al.* 1921, Williams 2012).

The work described in this thesis concerns the flows of carbon and energy in the model alga *Chlamydomonas reinhardtii* during nitrogen deprivation. Studies focusing on photosynthetic structure and function, storage compound accumulation and system wide metabolic fluxes are described in chapters 2-4 in the form of publication manuscripts. An analysis of photosynthesis, biomass, and storage compound utilization during nitrogen recovery is described in chapter 5. Conclusions and synthesis are presented in the final chapter. While each chapter introduces the specific literature and methods used, this introduction chapter aims to provide a broader context. First, there is a brief discussion of algal evolution and its relation to both higher plants and cyanobacteria. Next there is a discussion of algal culturing for industrial purposes as well as products and services that are derived from them. Following, there is an introduction to nutrient deprivation responses in algae, carbon compounds accumulated (starch and triacylglycerols) and the metabolism that supports those accumulations. The final section reviews what is known about algae during nutrient recovery and the roles that accumulated carbon compounds may play in the process.

Evolution and phylogeny of Algae and their relationship to Higher Plants and Cyanobacteria

Algae are a diverse group of eukaryotic organisms originating from one or more endosymbiotic events between heterotrophic eukaryotic cells and photosynthetic cyanobacteria (Bhattacharya *et al.* 1998, Bjorkman *et al.* 1987). Algae arising from initial (primary) endosymbiotic events include the green algae (Chlorophyta) which are thought to have given rise to higher plants (Leliaert *et al.* 2012), red algae (Rhodophyta), and the less studied Glaucophyta (Figure 1.1). Secondary endosymbiotic events with heterotrophic eukaryotes engulfing and forming an endosymbiosis with green algae gave rise to Euglenoids and Chlorarachniophytes (Keeling 2010). Similarly, endosymbiotic events with red algae serving as the endosymbiont gave rise to other important algal phyla including the Heterokonts (golden algae, diatoms, and brown algae), Haptophyta (coccolithophores), Cryptomonads, and the Dinoflagellates (Keeling 2009). Algae from single endosymbiotic events have two membranes around their chloroplast (inner and outer membranes) while algae arising from further endosymbiosis will have 3 or 4 (peri- and epi-plastidic membranes) depending on the number of events and how the event occurred or if one of the membranes was subsequently lost (Keeling 2009).

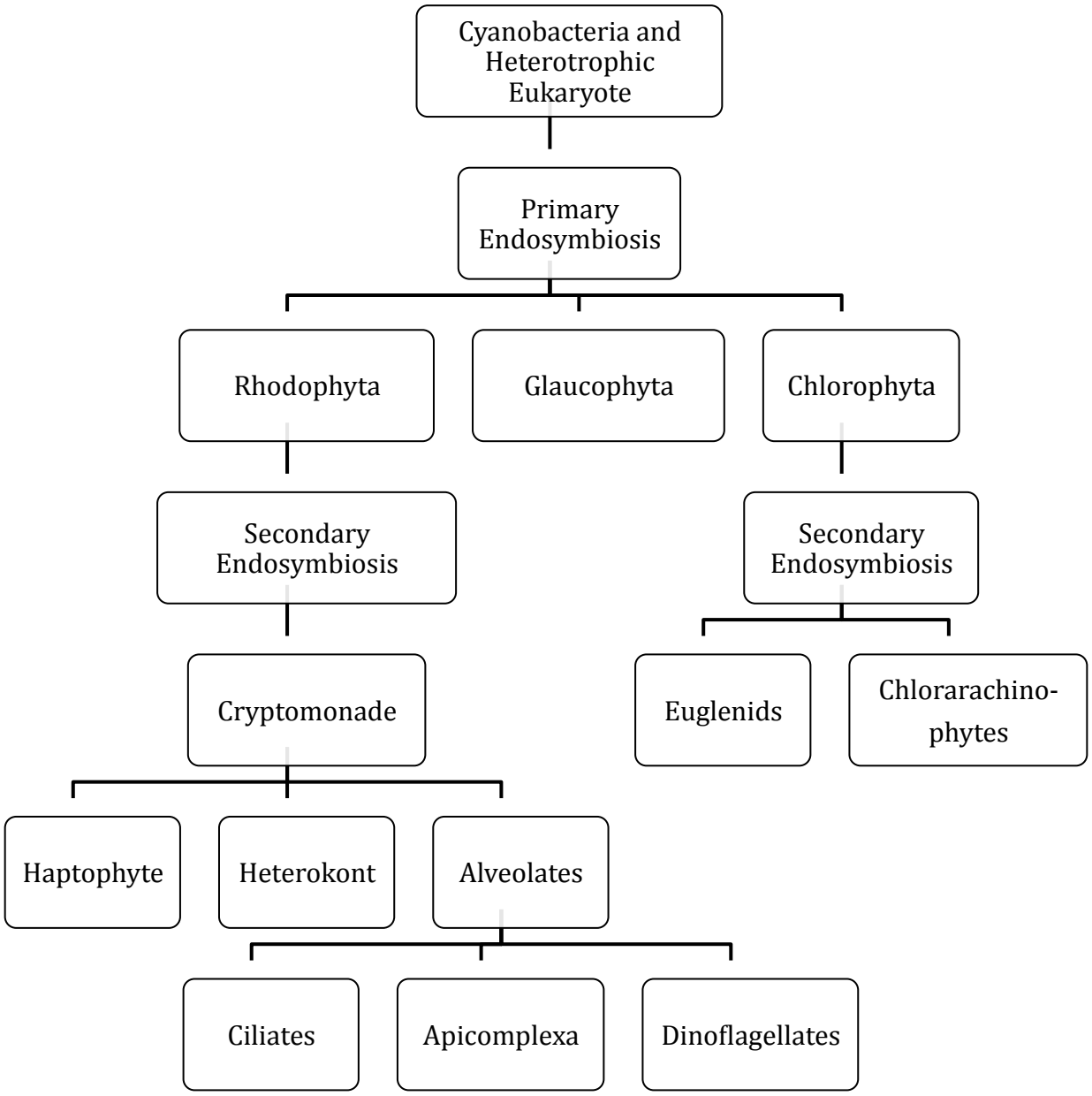

Figure 1.1. Algal Phylogeny. All algae are derived from the endosymbiosis of a cyanobacteria and a heterotrophic eukaryote. Primary endosymbiosis gave rise to the Glaucophytes, the Chlorophytes (Green algae), and Rhodophytes (Red algae). The green algae underwent secondary endosymbiosis giving rise to the Euglinids and the Chlorarachinophytes. Red algae also underwent secondary endosymbiosis, generating the Cryptomonades, Haptophytes, Heterokonts, and the Alveolates which comprises the ciliates, Apicomplexa and the Dinoflagellates. The figure was adapted from Archibald and Keeling, 2002, Trends in Genetics.

Algal lineages are characterized by different carbon storage and photosynthetic strategies. First, while most algae store their carbon as starch, the location differs, with Chlorophyte lineages storing it in the chloroplast while Rhodophyte and Glaucophyte lineages store it in the cytosol (Ball *et al.* 2011, Plancke *et al.* 2008). Starch is replaced as a major storage compound by triacylglycerol (TAG) lipid and chrysolaminaran (polysaccharide similar to starch except with β(1:3) and β(1:6) glycosidic bonds) in algae such as the diatoms (i.e. *Phaeodactylum triconum* (Kroth *et al.* 2008)) and other members of the heterokonts including Nannochloropsis species (Radakovits *et al.* 2012). In comparing the photosynthetic light harvesting apparatus of algae, the Rhodophyte and Glaucophyte lineages contain chlorophyll *a* and use the phycobilisome with phycobilin pigments phycocyanin and phycoerythrin as accessory light pigments for light capture (Larkum 2003, Larkum *et al.* 2007). Chlorophytes on the other hand have lost their cyanobacteria-derived phycobilisome structures and use chlorophyll *a* and *b* incorporated into light harvesting complexes, similar to the arrangement in higher plants (Larkum 2003). Chlorophyte lineages also have stacked thylakoid structures while Rhodophyte and Glaucophyte lineages do not (Douglas 1998). Glaucophyta are thought to be the oldest algal lineage and distinguish themselves from both Rhodophyta and Chlorophyta by having chloroplasts that maintain the endosymbiont's peptidoglycan wall (Douglas 1998, Jackson *et al.* 2015).

Algae have many structural and biochemical differences from cyanobacteria, especially in relation to photosynthesis. First, cyanobacteria contain no traditional organelles and one genome while algae contain several organelles and three genomes, one each in the chloroplast, mitochondria, and nucleus. This makes the genetic modification of cyanobacteria easier than algae. Next, cyanobacteria primarily store carbon as glycogen while algae store carbon as starch and/or triacylglycerols (Ball, et al. 2011). Cyanobacteria and some algae possess carbon-

concentrating systems; however, these differ in structure in the two groups. Cyanobacteria contain a specialized protein encapsulated bacterial microcompartment, the carboxysome, which houses the CO_2/bicarbonate interconverting carbonic anhydrase enzyme and the carbon fixing enzyme RuBisCO in a crystalline matrix (Cameron *et al.* 2013, Rae *et al.* 2013). Many algae on the other hand contain the pyrenoid, a starch encapsulated (Ramazanov *et al.* 1994) compartment containing several carbonic anhydrases and close interaction with the thylakoid membrane to increase CO_2 concentrations around RuBisCO (Morita *et al.* 1997). Further distinguishing the physiology of algae and cyanobacteria, some cyanobacteria can fix atmospheric nitrogen in special heterocyst cells (*Anabaena*) or in the dark (*Trichodesmium*) while algae cannot (Stal 2001, Wolk 1996). Finally, although both cyanobacteria and algae can be motile, they use different methods. Cyanobacteria depend upon a poorly understood gliding method for motility dependent upon manipulation of their cell surface while algae predominantly use flagellae, a feature that is believed to have been inherited from the symbiotic, eukaryotic heterotroph (Hoiczyk 2000).

Although a common ancestor is shared with higher land plants (including bryophytes, mosses, and hornworts and above), members of the algal lineage are distinguished by a number of important differences (Bhattacharya, et al. 1998, Leliaert, et al. 2012). First, even though some algae such as seaweeds are multicellular, they do not form a vascular system, leaf structure or a true root structure found in higher plants. In addition, higher plants rely on stomata for gas exchange while algal cells are directly exposed to the environmental gases (usually dissolved) (Farquhar *et al.* 1982, Spalding 2009). Next, while algae have pyrenoid CO_2 concentrating structures, most higher plants do not (the exception being the nonvascular hornworts (Villarreal *et al.* 2012)). Some plants however have evolved C4 and CAM photosynthetic mechanisms that

concentrate CO_2 at RuBisCO and which require specialized metabolic and anatomical developments (Ramazanov, et al. 1994, Sage *et al.* 2012). Many algae contain the betaine membrane lipid diacylglyceryl-*O*-4′-(*N,N,N,*-trimethyl) homoserine (DGTS) while higher land plants are generally devoid of it (Klug *et al.* 2001). Transient (day/night cycle) and long term (nutrient deprivation, hibernation) carbon storage compounds such as starch and TAG are handled differently in algae and higher land plants. Algae store both transient and long term carbon molecules in individual cells while higher land plants store transient carbon as starch in the leaves and long term storage carbon in specialized cell types in their stems, roots and tubers. Finally, the vast majority of higher plants are true autotrophs (with the exception of a small number of parasitic and insectivorous species or those like orchids that are heterotrophic at the earliest developmental stages) while many algae may be capable of mixotrophic or heterotrophic growth.

Chlamydomonas reinhardtii

Several algal species have served as important research tools in the investigation of photosynthetic organisms, none more prominently than the green alga *Chlamydomonas reinhardtii* (Goodenough 2015, Harris 2001, Merchant *et al.* 2012b). This organism is a haploid unicellular flagellate, has a rapid doubling time (<10hrs), can grow on reduced carbon substrates such as acetate, and can reproduce both sexually and asexually (Harris 2009a, Levine *et al.* 1960). The Chlamydomonas genus was originally described in the 1830s by G.C. Ehrenberg (Ehrenberg 1838) and it took another 50 years before *Chlamydomonas reinhardtii* was described (Proschold *et al.* 2001). Work by early geneticists and physiologists used *Chlamydomonas* to gain valuable insight into cell reproduction, growth, light responses, motility, and photosynthesis

(Desroche 1912, Levine 1960, Pasher 1918). Foundational research on the cell cycle, genetic recombination, and gene transfer were done with Chlamydomonas (Ebersold 1967, Ebersold *et al.* 1959, Ebersold *et al.* 1962, Levine *et al.* 1958a, Levine *et al.* 1958b, Levine, et al. 1960, Rosen *et al.* 1972, Smyth *et al.* 1975). Chlamydomonas has also provided in depth information about sexual reproduction and mating types through early work on nutrient deprivation (Armbrust *et al.* 1995, Martin *et al.* 1975a). Researchers also found this organism valuable in elucidating the components, structures, and formations of flagella (Harris *et al.* 2009, Lewin 1953, Silflow *et al.* 2001, Witman *et al.* 1972). Further, this organism has contributed to our understanding of day night cycles, lipid metabolism, and the mechanisms behind carbon concentrating mechanisms (Cross *et al.* 2015, Giroud *et al.* 1988, Liu *et al.* 2013, Mittag *et al.* 2003, Moroney *et al.* 1987). Finally, as it is able to grow heterotrophically on acetate, photosynthetic mutations that would have otherwise prevented the growth of autotrophs can be cultured and studied, which has provided a wealth of insights into the components and mechanisms of photosynthesis (Dent *et al.* 2001, Rochaix 2002, Spreitzer *et al.* 1981).

In recent years, a wealth of information has been assembled on this Chlamydomonas species including an annotated 121 megabase genome (Blaby *et al.* 2014, Grossman *et al.* 2003, Merchant *et al.* 2007), several proteomic and metabolomic libraries (Lee do *et al.* 2008, May *et al.* 2008, Wang *et al.* 2014), in addition to multiple large scale omic studies of this organism's response to different environmental stresses (Blaby *et al.* 2013, Bolling *et al.* 2005, Jamers *et al.* 2009, Juergens *et al.* 2015, Lee do, et al. 2008, Miller *et al.* 2010, Park *et al.* 2014, Schmollinger *et al.* 2014). Building on these large systems level data sets, system-wide metabolic modeling studies using metabolic flux analysis (MFA) and flux balance analysis (FBA) have been used to computationally study Chlamydomonas's metabolic networks (Boyle *et al.* 2009, Chang *et al.*

2011a, Chapman *et al.* 2015, Dal'Molin *et al.* 2011, Imam *et al.* 2015, Kliphuis *et al.* 2012, Lopez Garcia de Lomana *et al.* 2015, Wienkoop *et al.* 2010). Here physiological and systems data provide constraints on the possible solution space of Chlamydomonas metabolism, allowing metabolism to be predicted and studied via computational perturbation (Chapman, et al. 2015). Further expanding the use of Chlamydomonas as a model organism, extensive mutant libraries exist for Chlamydomonas, which increases the ease with which gene-phenotype relationships can be studied. One such library has 1935 mapped mutants with ~75% confidence and has helped identify genes related to TAG production (Li *et al.* 2016).

Algal aquaculture, biofuels and high value products

Humans have been culturing algae since ancient times as they provide many valuable products and functions (Buchholz *et al.* 2012). Civilizations with the longest known history of algal utilization include those from Asia (Japan) (Tamura 1966) and South America (Chile) (Dillehay *et al.* 2008). The oldest method of algal cultivation is open water algal farms in coastal areas where macroalgae are attached to a scaffold such as a rope and grown in shallow waters. Scientists in the 1800s attempted to culture microalgae but Beijerinck was the first to obtain true axenic cultures (Beijerinck 1904). Both macroalgae (seaweeds) and microalgae are cultivated for food products, fuel sources, high value specialty chemicals, and for purposes such as feed for aquatic animal farming and wastewater remediation (Mathiesen 2012, Muller-Feuga 2000, Schmidt *et al.* 2003, Selvaratnam *et al.* 2014).

These diverse organisms play a great role in the natural world. It is estimated that marine algae contribute 44% of oceanic CO_2 fixation (Jardillier, et al. 2010). Algae also play central roles in global aquatic nutrient cycles including those of nitrogen and phosphate which are

frequently limiting in environments such as the ocean. In aquatic environments of high nitrogen and phosphate concentrations, such as where fertilizer and sewage runoff have collected, algae can bloom causing eutrophication of the local environment along with hypoxia and/or toxin secretion (Anderson *et al.* 2008, Le *et al.* 2010). As such, algae are important primary producers and members of nutrient cycles in food webs and environments.

Algae produce a range of valuable products and services spanning from food products, to fuels. Macroalgae have traditionally been cultivated for use in foods, one of which we commonly see as nori (the wrapping on sushi (Garcia-Jimenez *et al.* 2015)). Algae are additionally cultivated for producing bioactive carotenoids (astaxanthin), and antioxidants, as well as proteins and biomass for animal feeds (Gimpel *et al.* 2015, Lemoine *et al.* 2010). Additionally, important long chain polyunsaturated fatty acids (PUFAS) necessary for many higher life forms including eicosapentanoic acid (EPA 20:5n-3) and docosahexanoic acid (DHA, 22:6n-3) are produced in large quantities by algae (Abedi *et al.* 2014, Gladyshev *et al.* 2013). Humans have limited capacity to produce these compounds and diets supplemented with DHA and EPA have been shown to benefit brain development in children (Innis 2007). Markets are rapidly growing for algal products such as raw biomass food supplements worth $80 million annually, PUFAS worth $300 million annually (Enxing *et al.* 2014), and the carotenoid market worth up to $1.2 billion (Sun *et al.* 2014). Researchers are also developing algae for the biomanufacturing of bioactive metabolites and proteins that are hard to produce in other systems (Borowitzka 2013, Mayfield *et al.* 2007, Rasala *et al.* 2015). Algae provide a system for proper post translational modification of various proteins with uses ranging from food additives to anticancer agents (Rasala, et al. 2015). Other heavily used algal products include the silica shell of diatoms which are harvested and used as fine polish in toothpaste and agarose gelatin which is used in the biotech industry

(Lebeau *et al.* 2003, Renn 1984). As an example of the scale and value of algal products, more than 10,000 tons of agar are produced globally each year from cultivation of red algae from the genera Gracilaria and Gelidium (most prominantly *Gelidium amansii*) with a market value of over $175 million (Bixler *et al.* 2011). Algae are also cultivated as a nutrient source for the fish, shrimp, and mollusk farming industries (valued at $106 billion globally), enabling animal feed to be grown onsite (Mathiesen 2012, Muller-Feuga 2000). Algae are also being assessed for their ability to recover nutrients and provide treatment services in waste water treatment plants (Schmidt, et al. 2003).

In addition to food and bioactive compounds, considerable research has been undertaken to make algae a competitive renewable energy resource (Durrett *et al.* 2008, Hu *et al.* 2008). Early researchers pioneered these efforts through the analysis of methane production from anaerobic digestion of the algal carbohydrate fraction (Meier 1955, Oswald *et al.* 1960). This work was revived during the energy crisis of the1970s and included research on hydrogen production (Benemann *et al.* 1977, Miyamoto *et al.* 1979, Uziel *et al.* 1975, Weissman *et al.* 1977). Further responding to the energy crisis, then US President Carter launched the Solar Energy Research Institute (SERI) in 1978 as part of the Department of Energy (DOE), currently known as the National Renewable Energy Laboratory (NREL). Within SERI, the Aquatic Species Program (ASP), whose work is summarized in a final report (Sheehan *et al.* 1998) was founded to research renewable energy from aquatic plants. Over two decades this program discovered over 3000 strains of algae, isolated and characterized the first plant-related acetyl-CoA carboxylase enzyme, which initiates fatty acid synthesis, developed protocols for pond system culturing of algae, and performed cost and resource analyses for cultivation. However, after much progress and effort, no clear method or organism was determined as an economically

competitive source. This along with decreased oil costs in the late 1980's and early nineties led to the termination of that program. As oil prices rose, concern about rising atmospheric CO_2 levels increased, and the future of energy security became subjects of public policy planning, intensive efforts to study algae as a renewable energy source were renewed (Pienkos *et al.* 2009).

To further develop algal bioenergy, several multifaceted programs were funded. One of the most recent was the National Alliance for Advanced Biofuels and Bioproducts (NAABB), funded by the DOE from 2010 to 2013. Research in NAABB was focused on 7 areas: Algal Biology, Cultivation, Harvesting Processes, Extraction Processes, Direct Conversion processes, Lipid Conversion Processes, and lipid extracted algae conversion and application (Olivares 2013). Major breakthrough came from the development of new algal strains, improved algal cultivation with the ARID pond system, decreases in harvesting cost through electrocoagulation and most importantly, improvements to hydrothermal liquefaction processing of biomass (see below). This expansive effort helped bring the price of algae biocrude from $240/gal to $7.50/ gal (Olivares 2013). Other National and Institutional programs, including both the Navy and Department of Defense, have contributed to research aimed at developing algal bioenergy applications. Several of these have involved researchers at Michigan State University, including, the DOE funded Plant Research Laboratory, the Center for Advanced Biofuels systems (CABS), the California Center for Algae Biotechnology (Cal-CAB), The Algal Biotechnology Consortium (ABC)(Cambridge), the International Center for Advanced Renewable Energy and Sustainability (I-CARES) and the Arizona Center for Algae Technology and Innovation (AzCATI). A large focus of many of these programs in on the advancement of algal culturing and growth regimes.

Algae are cultivated today in a variety of ways (Brennan *et al.* 2010, Chen *et al.* 2011a, Chisti 2007, Costa *et al.* 2014, Jones *et al.* 2012). Recent developments have led to algae being grown in large ponds or under artificial, controlled environment bioreactors (Chaumont , Grima *et al.* 1999, Pulz 2001). In the pond method, algae are typically grown in circular ponds or elongated raceways with pumps, stirrers, or large paddles being used to keep them suspended and mixed, with or without aeration. Cultures in these open-air ponds rely on sunlight for photosynthesis, which are kept shallow to prevent excessive shading. Additional challenges with ponds include exposure to contaminants including dust, competing natural algae, algal predators such as rotifers, and viruses that can devastate cultures (Carney *et al.* 2014). Finally, as ponds are exposed to the environments, they can only be productively utilized at those times and places when temperature and light intensity are compatible with moderate-to-high algal growth rates. To address these challenges, some algae being considered or used for open air ponds are extremophiles, being able to grow in saline water, high or low pHs, variable temperatures, or being able to produce allopathic toxins (Barnard *et al.* 2010). Examples of these include *Sulphuraria galdieria*, *Nannochloropsis* species, and *Cyanidium caldarium* (Luca *et al.* 1981, Schmidt *et al.* 2005, Sukenik *et al.* 2009).

Photobioreactors on the other hand are closed system growth chambers that use natural or artificial light and environmental control to allow for continuous regulated growth of algae (Brennan, et al. 2010, Chaumont , Chen, et al. 2011a, Grima, et al. 1999, Pulz 2001, Yen *et al.* 2014). Here, contamination is minimized and growth conditions can be optimized and tailored to an organism's needs or to the synthesis of desired products. These reactors however require many times more energy than ponds to operate. In general, low cost commodity products from algae such as fuels or total biomass are produced via raceway ponds while high value products

such as target pharmaceuticals and other health products with high standards are best suited to controlled bioreactors.

In culturing algae for bioenergy purposes, they are grown under either optimal or stressed conditions (Chisti 2007). Under optimal conditions, algae undergo rapid growth and biomass accumulation. While it is advantageous to have high lipid accumulations, frequently no major biomass component (protein, lipid, carbohydrate, etc.) is selected for during optimal growth as each contributes to biocrude formation using hydrothermal liquefaction (HTL, see below). Alternatively, growers may induce stress on the organism through nutrient deprivation (nitrogen deprivation is the most prominent, see below) to increase energy-enriched carbohydrate (starch) and/or triacylglycerol (TAG) contents. Through strain selection or transgenic manipulation, TAG compositions can be tailored to specific needs and be directly converted to biodiesel while the remaining biomass and carbohydrates can be used for anaerobic digestion (hydrogen and methane production), HTL or animal feed. Nutrient stress (particularly sulphur deprivation) can be used to produce hydrogen gas from green algae under anaerobic, illuminated conditions (Melis *et al.* 2000). Here, PSII and catabolic processes provide electrons for ferredoxin production of hydrogen (Antal *et al.* 2003, Posewitz *et al.* 2004, Tsygankov *et al.* 2006).

In addition to considering the energy yields of the biomass component during culturing, energy expenditures in downstream harvesting and processing need to be considered. One of the largest challenges associated with this is the separation of algae from culture media which is energy intensive. Residual water can reduce the downstream quality of generated products. During logarithmic growth, Wet Algal biomass is over 99% water by weight and needs to be "dewatered" to 50% water or better depending on the intended use of the biomass. Current dewatering strategies include concentrating cells through flocculation with different pH or

chemical shocks and then further concentration through centrifugation and filtration (Danquah *et al.* 2009, Uduman *et al.* 2010). The dewatering process is one of the most costly aspects of algal cultivation. After collection, biomass can be treated in a number of ways. If TAG accumulation was the focus of the culturing method, biodiesel can be generated through chemical extraction of TAGs and transmethylation after extensive dewatering (Meher *et al.* 2006). With the biomass/ growth strategy, cells are processed by hydrothermal liquefaction (HTL) (Barreiro *et al.* 2013, Biller *et al.* 2011, Sudasinghe *et al.* 2014), to generate biocrude. HTL generates biocrude fuel through the controlled medium temperature/ high pressure depolymerization of still-wet biomass. Different temperature/ pressure schemes can generate different pyrolysis component/ qualities depending on the downstream usage of the product (Elliott *et al.* 2015, Sudasinghe, et al. 2014). While HTL has the advantage of require less dewatering, it does require special equipment and careful monitoring (Li *et al.* 2014). Nutrient deprivation strategies increase both the energy density of individual cells as well as reduce processing energy costs by having a near drop in fuel product.

Nutrient stress and the induction of storage metabolism in algae

Like other organisms, algae require mineral micro- and macronutrients such as nitrogen, phosphate, sulfur, and iron, for growth and reproduction. In almost all natural environments the levels of one or more of these nutrients limit growth at different times. Algae have evolved sophisticated mechanisms to survive nutrient deprivation and to respond quickly once a resource becomes available. Many algae reside in aquatic environments such as the open ocean where mineral nutrients are usually limiting, with some ecosystems relying on coastal runoff or periodic upwelling from lower waters. In response to nutrient limitation algae accumulate carbon stores

and upregulate nutrient fixation pathways to facilitate uptake and incorporation of different forms of the limited resource (Miller, et al. 2010, Msanne *et al.* 2012, Park, et al. 2014). Intense competition for resources puts selective pressure favoring organisms that can respond rapidly. As algae are poised to uptake nutrients rapidly, giant algal blooms can occur when pollutants such as fertilizers, sewage, or other waste accumulate in water sources (Anderson *et al.* 2002, Heisler *et al.* 2008). These blooms can deprive local environments of oxygen (eutrophication) and in some cases secrete toxins that are harmful to other life forms such as fish and invertebrates(Anderson, et al. 2002).

The study of the relation between algae and their nutrient environment began in the mid to late 1880s when scientists began to culture them from pond and river sources (Beijerinck 1904, Van Iterson, et al. 1921). Martinus Beijerinck was a notable pioneer in algal and cyanobacterial isolation and physiology who conducted experiments on both nutrient excess and deprivation. He seems to have been the first to describe carbon accumulations during nitrogen deprivation as well as nitrogen fixation in cyanobacteria (Beijerinck 1904, Van Iterson, et al. 1921). Further work sought to understand how the nutrient environment affect the composition of biocomponents (protein, carbohydrate, lipid) (Spoehr *et al.* 1949).

Algal TAG accumulation has been studied during deprivation or limitation of several nutrients including iron, sulfur, and phosphate with the most frequently investigated being nitrogen (Blaby, et al. 2013, Bolling, et al. 2005, Cakmak *et al.* 2012, Grossman 2000, Grossman *et al.* 2010a, Hsieh *et al.* 2013, Moseley *et al.* 2002, Urzica *et al.* 2013, Wykoff *et al.* 1998). Nutrient deprivation induces a complex array of changes in algae at multiple regulatory and physiological levels. The most rapid system-wide changes occur early during the first 48hrs of nutrient deprivation with a secession of cell growth, increases in cell size and mass, and

falling chlorophyll levels. Functional measures of photosynthesis and respiration have been found to progressively decrease during the first days of nutrient deprivation suggesting a slowing of metabolism (Berges *et al.* 1996, Juergens, et al. 2015, Plumley *et al.* 1989b, Schmollinger, et al. 2014, Simionato *et al.* 2013, Young *et al.* 2003). To aid in the long term survival of nutrient deprivation some algae such as Chlamydomonas undergo gametogenesis, where cells produce vegetative zygotes better able to handle dormancy (Martin *et al.* 1975b, Sager *et al.* 1954). Under various nutrient deprivation stresses, cells have also been shown to decrease the expression of genes related growth, photosynthesis and respiration metabolism as well as upregulating genes responsible for nutrient assimilation as well as starch and fatty acid metabolism at both transcript and protein levels (Blaby, et al. 2013, Collier *et al.* 1992, Dong *et al.* 2013, Juergens, et al. 2015, Miller, et al. 2010, Msanne, et al. 2012, Nguyen *et al.* 2011, Park, et al. 2014, Tsai *et al.* 2014, Yang *et al.* 2013a). Expression of nutrient uptake transporters and associated proteins poises cells to rapidly uptake and utilize a nutrient once it returns. Several studies have reported increases in carotenoid concentrations as well (Simionato, et al. 2013, Solovchenko *et al.* 2014).

In the case of nitrogen deprivation, nitrogen is scavenged from any non-essential protein, free amino acids, and other nitrogen containing compounds to support stress response protein production. Carbon to nitrogen ratios increase as carbon accumulates and nitrogen levels per cell stay the same (Schmollinger, et al. 2014). Nutrient deprivation time courses in *Chlamydomonas reinhardtii* and *Scenedesmus obliquus* show that carbon accumulation is sequential with starch accumulating first and then TAG (Breuer *et al.* 2014, Fan *et al.* 2012, Siaut *et al.* 2011). TEM images show multiple large starch and lipid droplets after several days of nitrogen deprivation (Goodenough *et al.* 2014, Juergens, et al. 2015, Moellering *et al.* 2010, Siaut, et al. 2011,

Warakanont *et al.* 2015) with membrane lipid levels falling as TAG levels rise. Starch and lipid metabolism, especially in response to nitrogen deprivation are reviewed in the following sections of this chapter, as they are at the heart of carbon fluxes related to energy handling in both natural and cultivation systems.

Starch biosynthesis in Chlamydomonas and how it changes during N deprivation

In Chlamydomonas, starch synthesis is upregulated rapidly after the onset of nutrient deprivation resulting in large early increases in starch accumulation. Electron microscopy images show multiple large starch granules appear in the chloroplast of Chlamydomonas within the first 6 hrs of N deprivation (Fan, et al. 2012, Juergens, et al. 2015, Siaut, et al. 2011). During nutrient replete growth starch levels rise and fall during day/night cycles, however these levels dramatically increase upon nutrient deprivation (Ball *et al.* 1990, Hicks *et al.* 2001).

Starch is a semi-crystalline polymer of glucose held together by α(1-4) and α(1-6) glucosidic linkages. The α(1-4) linkages produce long glucose chains which are branched at α(1-6) linkages. Unbranched chains of glucose of at least 1000 glucose residues are referred to as amylose while large chains with branches are referred to as amylopectin (Ball *et al.* 2009) To make these starch structures, glucose is first phosphorylated by ADP-Glucose Phosphorylase. The ADP-glucose that is formed is then bound to a glycan chain by starch synthase using the α(1-4) bond. Branching enzymes are used to make α(1-6) glucosidic linkages to form amylopectin (Figure 1. 2**)**. Starch accumulation precedes TAG biosynthesis in Chlamydomonas and accumulates to a greater extent. In other algal types such as the diatoms and brown algae, starch plays a much less important role in both diurnal carbon storage and in response to stress.

These organisms accumulate chrysolaminarin and TAG predominantly (Beattie *et al.* 1961, Percival *et al.* 1951).

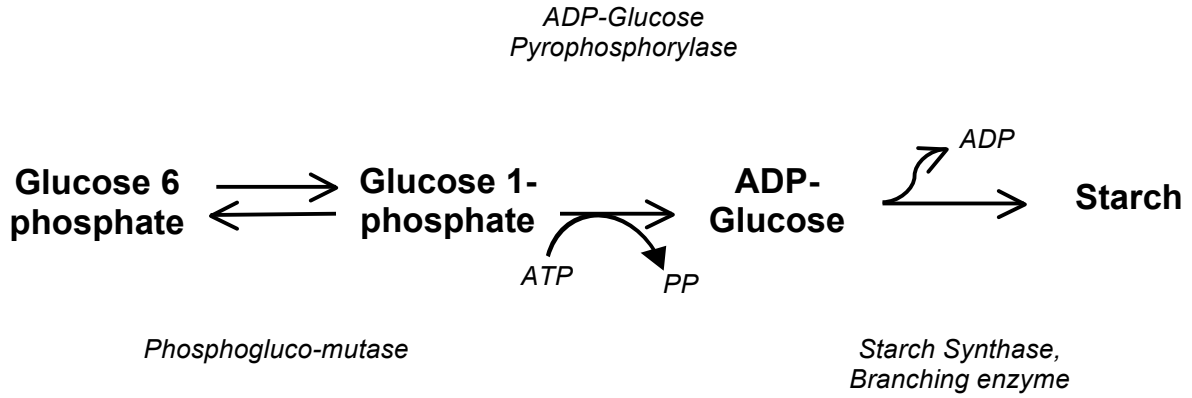

Figure 1.2. **Starch Synthesis in Chlamydomonas**. Starch Is synthesized in the plastid starting Glucose-6-phosphate being converted to Glucose-1-phosphate(G-1-P) via Phosphoglucomutase. Next, ADP-Glucose Pyrophosphorylase converts G-1-P into Adenosine diphosphate(ADP) Glucose via reaction with an Adenosine triphosphate. Starch Synthase then forms a α-1,4- glycosidic bond between the activated ADP-Glucose and a glucan chain. The branching enzyme will also add glucose monomers to glycan chains via α-1,6- glycosidic bonds.

During nitrogen deprivation, our work in Chapter 2 found an increase in expression of starch synthesis genes such as starch synthase I and branching enzyme within four hrs. Additionally, we have found starch degradation enzymes upregulated which we interpret as enzymes accumulating poised to degrade starch when Nitrogen returns. We additionally found starch to accumulate linearly immediately after the onset of N stress. These levels appeared to top off after 72hrs of stress under multiple light conditions and are presented in Chapter 3. This information demonstrates an immediate importance of starch metabolism in nutrient deprivation in Chlamydomonas as well as regulation of starch metabolism after several days of nutrient stress that is not currently understood.

Triacylglycerol metabolism during nutrient deprivation

Our current understanding of lipid metabolism in Chlamydomonas and literature on which it is based has been described in recent reviews by the labs of Benning (Liu, et al. 2013), Merchant (Merchant, et al. 2012b), and Fan (Fan *et al.* 2011). Because of its relevance to the work of this thesis, it is summarized here (Figure 1.3). During nutrient deprivation genes related to fatty acid biosynthesis, lipid remodeling, and TAG synthesis are upregulated, changes that are associated with large accumulations of TAG. TAGs consist of a glycerol backbone with three fatty acid chains attached by ester bonds. Fatty acids are produced in the chloroplast from 2 carbon acetyl-CoA precursors. Initially an acetyl CoA is carboxylated to produce malonyl CoA by the Acetyl-CoA Carboxylase enzyme. Another acetyl-CoA is condensed with malonyl CoA by β-Ketoacyl-ACP Synthase III, producing β-Ketoacyl-Acyl Carrier Protein (ACP) and releasing carbon dioxide. Ketoacyl-ACP is then reduced using NAPH –by Ketoacyl-ACP Reductase. The β-Hydroxyacyl-ACP product is then dehydrated with β-Hydroxyacyl-ACP

dehydratase to form trans-Δ2-enoyl-ACP. This product is further reduced with NADPH in the Enoyl-ACP reductase-catalyzed reaction to form a 4 carbon Acyl-ACP. This Acyl-ACP will then be further extended, starting with β-Ketoacyl-ACP Synthase III and another AcetylCoA. This cycle is terminated when the chain lengths are typically either 16 or 18 carbons in length. At this point fatty acids can be used for lipid synthesis or further modified by desaturation enzymes which introduce double bonds at specific carbon:carbon bond positions (Ratledge 2004, Ratledge *et al.* 2002). Animals and fungi have the fatty acid synthesis enzymes joined in one multi-functional polypeptide operating in the cytosol (eukaryotic pathway) while chloroplasts and bacteria have separate enzymes for different reactions (prokaryotic fatty acid synthase complex (Wakil 1989)). Generated fatty acids are used for the synthesis of membrane lipids, di- and triacylglycerols, for the acylation of proteins and other biomolecules, and in some tissues for the production of the hydrocarbon components of waxes and other surface lipids.

To make membrane glycerolipids and triacylglycerols, fatty acids must be first attached to a glycerol backbone. In the Kennedy pathway, Acyl-ACP-glycerol 3-phosphate acyl-transferase carries out the first transfer of a fatty acid to glycerol 3-phosphate forming lysophosphatidic acid. A second fatty acid is added to form phosphatidic acid. The phosphate is then removed via a phosphatase reaction to form diacylglycerol (DAG). DAGs can be further processed to form the glycolipids monogalactosyldiacylglycerol (MGDG) and digalactosyldiacylglycerol (DGDG), the phospholipids phosphatidylenthanolamine (PtdEtn), phosphatidylglycerol (PtdGro), phosphatidylinositol (PtdIns), the sulpholipids such as sulfoquinovosyldiacylglycerol (SQDG), the betain lipid diacylglyceryl-N,N,N-trimethylhomoserine (DGTS) or can be directly acylated to produce TAG. In TAG synthesis

fatty acids can also be transferred via various membrane lipid pools, with different desaturation and/or elongation modifications of fatty acids being catalyzed while attached to different glycerophospholipid moieties. While TAG biosynthesis was thought to be produced in the endoplasmic reticulum, recent studies have provided evidence that Chlamydomonas produces TAG also at the chloroplast (Fan, et al. 2011). In most eukaryotes, one of the most important membrane lipids for fatty acids trafficking and modification is phosphatidylcholine (Kennedy 1956, Kennedy *et al.* 1956, Li *et al.* 2013). This membrane lipid is absent from the model alga *Chlamydomonas reinhardtii* (Giroud, et al. 1988) and thought to be functionally replaced by the betaine lipid DGTS (Liu, et al. 2013, Moore *et al.* 2001, Sato *et al.* 1991, Schlapfer *et al.* 1983). Several genes related to fatty acid trafficking and oil filling have been implicated or experimentally verified (Boyle *et al.* 2012, Deng *et al.* 2012, La Russa *et al.* 2012, Li *et al.* 2012a, Li *et al.* 2012b).

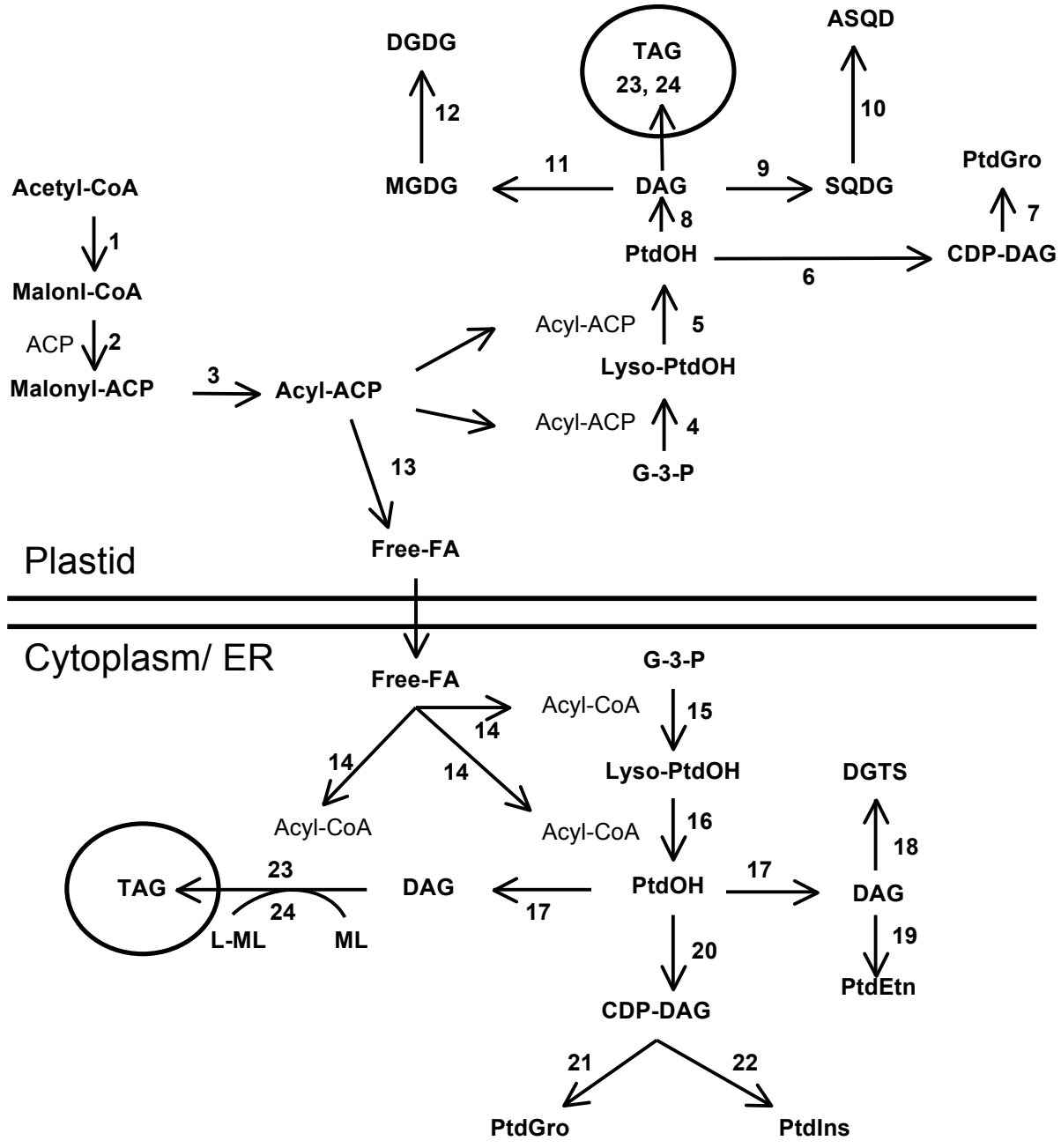

Figure 1.3. Glycerolipid biosynthesis in Chlamydomonas.

Figure 1. 3. (cont'd). This figure shows the metabolic pathways and distribution of the major glycerolipids in the plastid and cytoplasm/endoplasmic reticulum(ER) in Chlamydomonas. Numbers indicate enzyme reactions listed below, Bold indicates base molecules that are added to or modified. Enzymes. 1, Acetyl-CoA carboxylase; 2, Malonyl-CoA: ACP transacylase; 3, Fatty acid synthase complex; 4, Glycerol-3-P: Acyl-ACP acyltransferase; 5, Lyso-phosphatidate: Acyl-ACP acyltransferase; 6, CDP-diacylglycerol synthetase; 7, Phosphatidylglycerolphosphate synthase, Phosphatidylglycerolphosphate phosphatase; 8, Phosphatidate phosphatase; 9, Sulfolipid synthase; 10, Sulfolipid 2 - O-acyltransferase; 11, Monogalactosyldiacylglycerol synthase; 12, Digalactosyldiacylglycerol synthase; 13, Acyl-ACP thioesterase,; 14, Long-chain acyl-CoA synthetase; 15, Glycerol-3-P: Acyl-CoA acyltransferase; 16, Lyso-phosphatidate: Acyl-CoA acyltransferase; 17, Phosphatidate phosphatase; 18, Betaine lipid synthase; 19, CDP-ethanolamine: diacylglycerol ethanolamine phosphotransferase; 20, CDP-diacylglycerol synthetase; 21, Phosphatidylglycerolphosphate synthase,Phosphatidylglycerolphosphate phosphatase; 22, CDP-DAG: Inositol phosphotransferase; 23, and acyl-CoA: diacylglycerol acyltransferase; 24, phospholipid: diacylglycerol acyltransferase . Abbreviations: ACP, acyl carrier protein; ASQD, 2 - O-acyl-sulfoquinovosyldiacylglycerol; CDP, cytidine-5 -diphosphate; CoA, coenzyme A; DAG, diacylglycerol; DGDG, digalactosyldiacylglycerol; DGTS, diacylglyceryl-N,N,N-trimethylhomoserine; FA, fatty acid; G-3-P, glycerol-3-phosphate; MGDG, monogalactosyldiacylglycerol; ML, Membrane glycerolipidl;, Lyso-membrane glycerolipid; PtdEtn, phosphatidylethanolamine; PtdGro, phosphatidylglycerol; PtdGroP, phosphatidylglycerolphosphate; PtdIns, phosphatidylinositol; PtdOH, phosphatidic acid; SQ, sulfoquinovose; SQDG, sulfoquinovosyldiacylglycerol.; TAG, Triacylglycerol Figure modified from Riekof and Benning, 2009, and from Liu and Benning, 2013.

Several mutant algal lines defective in either starch or TAG accumulation have been studied in relation to their effect on total biofuel production. Starch accumulation was prevented in the starch synthase mutant Sta6 (BAFJ5) and found to induce higher accumulations of TAG during nutrient deprivation (Blaby, et al. 2013, Goodenough, et al. 2014, Li *et al.* 2010, Work *et al.* 2010). It was postulated that energy that would have gone into starch was redirected into FA metabolism, resulting in higher TAG accumulations. Surprisingly, the Sta6 mutant was also found to contain plastidic TAG bodies, a feature not seen in other algae (Goodson *et al.* 2011). Work from Siaut et al. provides data contradicting the idea of TAG accumulating the carbon not

put into starch in starchless mutants. They find no noticeable increases in TAG during N deprivation and attribute other labs increased TAG claims to the comparison of different cell lines as opposed to mutants and their complementation lines(Siaut, et al. 2011). Mutant screens for Chlamydomonas deficient in TAG production led to the discovery of an MGDG lipase mutant (PGD1) implicated in the trafficking of de novo FA into TAG during nutrient deprivation. This mutant showed phenotypes of increased rates of chlorosis and photosynthetic degradation and decreases in cell survival and Total FA accumulation (Li, et al. 2012b).

Why do algae make TAG under N limitation?

Several explanations have been proposed for the induction of TAG accumulation in algae under stress, ranging from storing reduced carbon as an energy source for survival and/or future recovery, to lipid reorganization during photosynthetic down-regulation and/or subsequent up-regulation, to photo-protection (Akita *et al.* 2015, Grossman, et al. 2010a, Khozin-Goldberg *et al.* 2005, Klok *et al.* 2014, Kohlwein 2010, Murphy 2001). Roessler (Roessler 1990) appears to have been the first to postulate that algae accumulate TAG as a sink for excess photosynthetic energy and reductant to prevent photochemical damage. In this explanation, photosynthetic carbon and energy assimilation that can no longer be directed to growth when population increase is inhibited by nutrient deficiency or other stresses results in overflow products, particularly TAG. The concept of overflow metabolism has traditionally been associated with the export of metabolites by heterotrophic microbes (Neijssel *et al.* 1975) and has more recently also been applied to photosynthetic metabolism in cyanobacteria (Courchesne *et al.* 2009, Grundel *et al.* 2012, Hays *et al.* 2015) and higher plants (Weise *et al.* 2011). In microalgal work, the idea of photosynthetic overflow (excess photosynthetic energy and carbon) as the driver of oil

accumulation has become a widely accepted explanation (see for example (Hu, et al. 2008, Klok, et al. 2014, Li, et al. 2012b, Li, et al. 2013, Solovchenko 2012). This Overflow Hypothesis strongly influences research efforts and the interpretation of results in biological and engineering studies of microalgal metabolism and TAG accumulation and also has important implications for the ecophysiology of photosynthetic microbes. While frequently invoked in interpreting the results of nutrient deprivation studies, the Overflow Hypothesis protective role vs. storage role question has not been systematically assessed.

Others have suggested a storage role for TAG accumulation. This idea posits that starch and TAG accumulate as storage compounds to be used for nutrient recovery, providing either energy for biosynthesis or carbon for a backbone for nitrogen reuptake and amino acid synthesis. Fan et al. has demonstrated a link between total carbon availability and TAG accumulation, an idea that supports a storage role vs. a protective role (Fan, et al. 2012). Once a nutrient returns, being able to quickly recover normal activities would give an algal an advantage over local competitors. Having evolved over millions of years to survive the common situation of nutrient deprivation this should come as no surprise.

Recovery from nutrient deprivation

The roles of starch and TAG in the nutrient stress condition can be further explored during recovery after the return of nutrient supply. Despite much effort to study carbon accumulation during nutrient deprivation, very little has been spent on the fates of starch and TAG once nitrogen returns. In *Chlamydomonas reinhardtii* basic analysis of starch and TAG levels after nitrogen is returned has shown starch and TAG levels decrease, starting with starch and then TAG a few hrs later (Siaut, et al. 2011, Tsai, et al. 2014). During this initial degradation

cells appear to recover themselves with minimal increases in cell number and then divide after roughly 24 hrs (Plumley, et al. 1989b). The transcriptome, proteome, and metabolome of nitrogen deprived and recovered cells shows cells rapidly responding to nitrogen return with upregulation of starch and TAG degradatory metabolism along with that of protein and nucleic acid synthesis (Plumley, et al. 1989b, Tsai, et al. 2014, Valledor *et al.* 2014).

Although this work demonstrates starch and TAG are rapidly degraded after N recovery it fails to show actual roles for these compounds. The Chlamydomonas CHT7 mutant, which is unable to recover from the nitrogen deprived "quiescent" state stops accumulating TAG but remains chlorotic and degrades TAG much more slowly than the wild-type (WT) (Tsai, et al. 2014). Further, a mating regulatory mutant (mat3) with decreased cell size was found to have a lag time before recovery(Armbrust, et al. 1995). Although unmeasured, it is imaginable that decreased starch and TAG accumulations in the smaller cells may partly cause the delay in recovery.

Outside of Chlamydomonas there have been a number of studies analyzing cells during nutrient recovery. While these studies are dominated by the study of nitrogen metabolism (Syrett *et al.* 1988) or cell physiology (Brussaard *et al.* 1998, Cagnon *et al.* 2013, Zhao *et al.* 2015), some give insight into the carbon metabolism. C^{14} radiolabeling studies in *Parietochloris incisa* has demonstrated that the fatty acid arachidonic acid accumulated in TAG is partially reutilized to form chloroplastic membrane lipids, demonstrating a carbon storage role for TAG (Khozin-Goldberg, et al. 2005). The focus of this study was on only one fatty acid and it is possible that not all fatty acids are treated in the same way during nutrient recovery. This group has additionally shown that the algae recover their nitrogen replete pigment characteristics rapidly after N repletion (Merzlyak *et al.* 2007). Work in *Dunaleilla Tertiolecta* further demonstrated a

rapid return of photosynthetic function after nitrogen deprivation and re-supply (Young, et al. 2003). Even after long periods of nitrogen deprivation (1 month), *Nannochloropsis oceanica* has been demonstrated to recover full photosynthetic efficiency after 3 just days (Dong, et al. 2013). Finally, a study in the carotenogenic alga *Chromochloris zofingiensis* presented detailed timecourses of starch, TAG, and carotenoid degradation during nitrogen recovery (Mulders *et al.* 2015). While they do not follow the carbon stores in the organism they do suggest cells could be recovered in the dark and feed of the TAG and starch.

REFERENCES

REFERENCES

Abedi, E. and Sahari, M.A. (2014) Long-chain polyunsaturated fatty acid sources and evaluation of their nutritional and functional properties. *Food Science & Nutrition*, **2**, 443-463.

Akita, T. and Kamo, M. (2015) Theoretical lessons for increasing algal biofuel: Evolution of oil accumulation to avert carbon starvation in microalgae. *Journal of theoretical biology*, **380**, 183-191.

Anderson, D.M., Burkholder, J.M., Cochlan, W.P., Glibert, P.M., Gobler, C.J., Heil, C.A., Kudela, R.M., Parsons, M.L., Rensel, J.E.J., Townsend, D.W., Trainer, V.L. and Vargo, G.A. (2008) Harmful algal blooms and eutrophication: Examining linkages from selected coastal regions of the United States. *Harmful Algae*, **8**, 39-53.

Anderson, D.M., Glibert, P.M. and Burkholder, J.M. (2002) Harmful algal blooms and eutrophication: Nutrient sources, composition, and consequences. *Estuaries*, **25**, 704-726.

Antal, T.K., Krendeleva, T.E., Laurinavichene, T.V., Makarova, V.V., Ghirardi, M.L., Rubin, A.B., Tsygankov, A.A. and Seibert, M. (2003) The dependence of algal H2 production on Photosystem II and O2 consumption activities in sulfur-deprived Chlamydomonas reinhardtii cells. *Biochimica et biophysica acta*, **1607**, 153-160.

Armbrust, E.V., Ibrahim, A. and Goodenough, U.W. (1995) A Mating Type-Linked Mutation That Disrupts the Uniparental Inheritance of Chloroplast DNA Also Disrupts Cell-Size Control in Chlamydomonas. *Mol Biol Cell*, **6**, 1807-1818.

Ball, S., Colleoni, C., Cenci, U., Raj, J.N. and Tirtiaux, C. (2011) The evolution of glycogen and starch metabolism in eukaryotes gives molecular clues to understand the establishment of plastid endosymbiosis. *J Exp Bot*, **62**, 1775-1801.

Ball, S.G. and Deschamps, P. (2009) Chapter 1 - Starch Metabolism In *The Chlamydomonas Sourcebook (Second Edition)*. London: Academic Press, pp. 1-40.

Ball, S.G., Dirick, L., Decq, A., Martiat, J.C. and Matagne, R.F. (1990) Physiology of Starch Storage in the Monocellular Alga Chlamydomonas-Reinhardtii. *Plant Sci*, **66**, 1-9.

Barnard, D., Casanueva, A., Tuffin, M. and Cowan, D. (2010) Extremophiles in biofuel synthesis. *Environ Technol*, **31**, 871-888.

Barreiro, D.L., Prins, W., Ronsse, F. and Brilman, W. (2013) Hydrothermal liquefaction (HTL) of microalgae for biofuel production: State of the art review and future prospects. *Biomass Bioenerg*, **53**, 113-127.

Beattie, A., Hirst, E.L. and Percival, E. (1961) Studies on the metabolism of the Chrysophyceae. Comparative structural investigations on leucosin (chrysolaminarin) separated from diatoms and laminarin from the brown algae. *Biochem J*, **79**, 531-537.

Beijerinck, M. (1904) Das Assimilationsprodukt der Kohlensäure in den Chromatophoren der Diatomeen. *Recueil Travaux Botaniques Néerlandais*, **1**, 28-32.

Benemann, J.R., Weissman, J.C., Koopman, B.L. and Oswald, W.J. (1977) Energy production by microbial photosynthesis. *Nature*, **268**, 19-23.

Berges, J.A., Charlebois, D.O., Mauzerall, D.C. and Falkowski, P.G. (1996) Differential effects of nitrogen limitation on photosynthetic efficiency of photosystems I and II in microalgae. *Plant Physiol*, **110**, 689-696.

Bhattacharya, D. and Medlin, L. (1998) Algal phylogeny and the origin of land plants. *Plant Physiol*, **116**, 9-15.

Biller, P. and Ross, A.B. (2011) Potential yields and properties of oil from the hydrothermal liquefaction of microalgae with different biochemical content. *Bioresource Technology*, **102**, 215-225.

Bixler, H.J. and Porse, H. (2011) A decade of change in the seaweed hydrocolloids industry. *J. Appl. Phycol.*, **23**, 321-335.

Bjorkman, O. and Demmig, B. (1987) Photon yield of O2 evolution and chlorophyll fluorescence characteristics at 77 K among vascular plants of diverse origins. *Planta*, **170**, 489-504.

Blaby, I.K., Blaby-Haas, C.E., Tourasse, N., Hom, E.F., Lopez, D., Aksoy, M., Grossman, A., Umen, J., Dutcher, S., Porter, M., King, S., Witman, G.B., Stanke, M., Harris, E.H., Goodstein, D., Grimwood, J., Schmutz, J., Vallon, O., Merchant, S.S. and Prochnik, S. (2014) The Chlamydomonas genome project: a decade on. *Trends in plant science*, **19**, 672-680.

Blaby, I.K., Glaesener, A.G., Mettler, T., Fitz-Gibbon, S.T., Gallaher, S.D., Liu, B.S., Boyle, N.R., Kropat, J., Stitt, M., Johnson, S., Benning, C., Pellegrini, M., Casero, D. and Merchant, S.S. (2013) Systems-Level Analysis of Nitrogen Starvation-Induced Modifications of Carbon Metabolism in a Chlamydomonas reinhardtii Starchless Mutant. *The Plant cell*, **25**, 4305-4323.

Bolling, C. and Fiehn, O. (2005) Metabolite profiling of *Chlamydomonas reinhardtii* under nutrient deprivation. *Plant Physiol*, **139**, 1995-2005.

Borowitzka, M.A. (2013) High-value products from microalgae-their development and commercialisation. *J. Appl. Phycol.*, **25**, 743-756.

Boyle, N.R. and Morgan, J.A. (2009) Flux balance analysis of primary metabolism in *Chlamydomonas reinhardtii*. *BMC systems biology*, **3**, 4.

Boyle, N.R., Page, M.D., Liu, B.S., Blaby, I.K., Casero, D., Kropat, J., Cokus, S.J., Hong-Hermesdorf, A., Shaw, J., Karpowicz, S.J., Gallaher, S.D., Johnson, S., Benning, C., Pellegrini, M., Grossman, A. and Merchant, S.S. (2012) Three Acyltransferases and Nitrogen-responsive Regulator Are Implicated in Nitrogen Starvation-induced Triacylglycerol Accumulation in *Chlamydomonas*. *J Biol Chem*, **287**, 15811-15825.

Brennan, L. and Owende, P. (2010) Biofuels from microalgae—A review of technologies for production, processing, and extractions of biofuels and co-products. *Renewable and Sustainable Energy Reviews*, **14**, 557-577.

Breuer, G., de Jaeger, L., Artus, V.P.G., Martens, D.E., Springer, J., Draaisma, R.B., Eggink, G., Wijffels, R.H. and Lamers, P.P. (2014) Superior triacylglycerol (TAG) accumulation in starchless mutants of Scenedesmus obliquus: (II) evaluation of TAG yield and productivity in controlled photobioreactors. *Biotechnology for biofuels*, **7**.

Brussaard, C.P.D., Brookes, R., Noordeloos, A.A.M. and Riegman, R. (1998) Recovery of nitrogen-starved cultures of the diatom Ditylum brightwellii (Bacillariophyceae) upon nitrogen resupply. *J Exp Mar Biol Ecol*, **227**, 237-250.

Buchholz, C.M., Krause, G.H. and Buck, B.H. (2012) Seaweed and Man. In *Seaweed Biology, Ecological studies* (Wiencke, C. and Bischof, K. eds). Berlin Heidelberg: Spring-Verlag, pp. 471-493.

Cagnon, C., Mirabella, B., Nguyen, H.M., Beyly-Adriano, A., Bouvet, S., Cuine, S., Beisson, F., Peltier, G. and Li-Beisson, Y. (2013) Development of a forward genetic screen to isolate oil mutants in the green microalga Chlamydomonas reinhardtii. *Biotechnology for biofuels*, **6**.

Cakmak, T., Angun, P., Demiray, Y.E., Ozkan, A.D., Elibol, Z. and Tekinay, T. (2012) Differential effects of nitrogen and sulfur deprivation on growth and biodiesel feedstock production of *Chlamydomonas reinhardtii*. *Biotechnology and bioengineering*, **109**, 1947-1957.

Cameron, J.C., Wilson, S.C., Bernstein, S.L. and Kerfeld, C.A. (2013) Biogenesis of a bacterial organelle: the carboxysome assembly pathway. *Cell*, **155**, 1131-1140.

Carney, L.T. and Lane, T.W. (2014) Parasites in algae mass culture. *Front Microbiol*, **5**, 278.

Chang, R.L., Ghamsari, L., Manichaikul, A., Hom, E.F., Balaji, S., Fu, W., Shen, Y., Hao, T., Palsson, B.O., Salehi-Ashtiani, K. and Papin, J.A. (2011) Metabolic network reconstruction of *Chlamydomonas* offers insight into light-driven algal metabolism. *Molecular systems biology*, **7**, 518.

Chapman, S.P., Paget, C.M., Johnson, G.N. and Schwartz, J.M. (2015) Flux balance analysis reveals acetate metabolism modulates cyclic electron flow and alternative glycolytic pathways in Chlamydomonas reinhardtii. *Frontiers in plant science*, **6**, 474.

Chaumont, D. Biotechnology of algal biomass production: a review of systems for outdoor mass culture. *J. Appl. Phycol.*, **5**, 593-604.

Chen, C.Y., Yeh, K.L., Aisyah, R., Lee, D.J. and Chang, J.S. (2011) Cultivation, photobioreactor design and harvesting of microalgae for biodiesel production: a critical review. *Bioresour Technol*, **102**, 71-81.

Chisti, Y. (2007) Biodiesel from microalgae. *Biotechnology Advances*, **25**, 294-306.

Collier, J.L. and Grossman, A.R. (1992) Chlorosis induced by nutrient deprivation in Synechococcus sp. strain PCC 7942: not all bleaching is the same. *Journal of bacteriology*, **174**, 4718-4726.

Costa, J.A.V. and de Morais, M.G. (2014) Chapter 1 - An Open Pond System for Microalgal Cultivation. In *Biofuels from Algae* (Soccol, A.P.-J.L.C.R. ed. Amsterdam: Elsevier, pp. 1-22.

Courchesne, N.M., Parisien, A., Wang, B. and Lan, C.Q. (2009) Enhancement of lipid production using biochemical, genetic and transcription factor engineering approaches. *Journal of biotechnology*, **141**, 31-41.

Cross, F.R. and Umen, J.G. (2015) The Chlamydomonas cell cycle. *Plant J*, **82**, 370-392.

Dal'Molin, C.G., Quek, L.E., Palfreyman, R.W. and Nielsen, L.K. (2011) AlgaGEM--a genome-scale metabolic reconstruction of algae based on the *Chlamydomonas reinhardtii* genome. *Bmc Genomics*, **12 Suppl 4**, S5.

Danquah, M.K., Ang, L., Uduman, N., Moheimani, N. and Fordea, G.M. (2009) Dewatering of microalgal culture for biodiesel production: exploring polymer flocculation and tangential flow filtration. *J Chem Technol Biot*, **84**, 1078-1083.

Deng, X.D., Gu, B., Li, Y.J., Hu, X.W., Guo, J.C. and Fei, X.W. (2012) The roles of acyl-CoA: diacylglycerol acyltransferase 2 genes in the biosynthesis of triacylglycerols by the green algae Chlamydomonas reinhardtii. *Mol Plant*, **5**, 945-947.

Dent, R.M., Han, M. and Niyogi, K.K. (2001) Functional genomics of plant photosynthesis in the fast lane using *Chlamydomonas reinhardtii*. *Trends in plant science*, **6**, 364-371.

Desroche, P. (1912) *Reactions des Chlamydomonas aux Agents Physiques* Schulz, Paris.

Dillehay, T.D., Ramirez, C., Pino, M., Collins, M.B., Rossen, J. and Pino-Navarro, J.D. (2008) Monte Verde: seaweed, food, medicine, and the peopling of South America. *Science*, **320**, 784-786.

Dong, H.P., Williams, E., Wang, D.Z., Xie, Z.X., Hsia, R.C., Jenck, A., Halden, R., Li, J., Chen, F. and Place, A.R. (2013) Responses of *Nannochloropsis oceanica* IMET1 to Long-Term Nitrogen Starvation and Recovery. *Plant Physiol*, **162**, 1110-1126.

Douglas, S.E. (1998) Plastid evolution: origins, diversity, trends. *Curr Opin Genet Dev*, **8**, 655-661.

Durrett, T.P., Benning, C. and Ohlrogge, J. (2008) Plant triacylglycerols as feedstocks for the production of biofuels. *Plant J*, **54**, 593-607.

Ebersold, W.T. (1967) Chlamydomonas reinhardi: heterozygous diploid strains. *Science*, **157**, 447-449.

Ebersold, W.T. and Levine, R.P. (1959) A genetic analysis of linkage group I of Chlamydomonas reinhardi. *Z Vererbungsl*, **90**, 74-82.

Ebersold, W.T., Levine, R.P., Levine, E.E. and Olmsted, M.A. (1962) Linkage maps in Chlamydomonas reinhardi. *Genetics*, **47**, 531-543.

Ehrenberg, C.G. (1838) *Die Infusionsthierchen als vollkommene Organismen.* Leipzig, Germany.

Elliott, D.C., Biller, P., Ross, A.B., Schmidt, A.J. and Jones, S.B. (2015) Hydrothermal liquefaction of biomass: developments from batch to continuous process. *Bioresour Technol*, **178**, 147-156.

Enxing, C., Ploeg, M., Barbosa, M., Sijtsma, L., Vigani, M., Parisi, C. and Rodriguez Cerezo, E. (2014) Microalgae-base products for the foos and feed sector: an outlook for Europe. In *Institute for Porspective Technological Studies*: IPTS.

Fan, J., Andre, C. and Xu, C. (2011) A chloroplast pathway for the de novo biosynthesis of triacylglycerol in *Chlamydomonas reinhardtii*. *Febs Letters*, **585**, 1985-1991.

Fan, J., Yan, C., Andre, C., Shanklin, J., Schwender, J. and Xu, C. (2012) Oil accumulation is controlled by carbon precursor supply for fatty acid synthesis in *Chlamydomonas reinhardtii*. *Plant & cell physiology*, **53**, 1380-1390.

Farquhar, G.D. and Sharkey, T.D. (1982) Stomatal Conductance and Photosynthesis. *Annu Rev Plant Phys*, **33**, 317-345.

Garcia-Jimenez, P. and Robaina, R.R. (2015) On reproduction in red algae: further research needed at the molecular level. *Frontiers in plant science*, **6**.

Gimpel, J.A., Henriquez, V. and Mayfield, S.P. (2015) In Metabolic Engineering of Eukaryotic Microalgae: Potential and Challenges Come with Great Diversity. *Front Microbiol*, **6**, 1376.

Giroud, C., Gerber, A. and Eichenberger, W. (1988) Lipids of Chlamydomonas reinhardtii. Analysis of Molecular Species and Intracellular Site(s) of Biosynthesis. *Plant and Cell Physiology*, **29**, 587-595.

Gladyshev, M.I., Sushchik, N.N. and Makhutova, O.N. (2013) Production of EPA and DHA in aquatic ecosystems and their transfer to the land. *Prostag Oth Lipid M*, **107**, 117-126.

Goodenough, U. (2015) Historical perspective on Chlamydomonas as a model for basic research: 1950–1970. *The Plant Journal*, **82**, 365-369.

Goodenough, U., Blaby, I., Casero, D., Gallaher, S.D., Goodson, C., Johnson, S., Lee, J.H., Merchant, S.S., Pellegrini, M., Roth, R., Rusch, J., Singh, M., Umen, J.G., Weiss, T.L. and Wulan, T. (2014) The path to triacylglyceride obesity in the sta6 strain of Chlamydomonas reinhardtii. *Eukaryot Cell*, **13**, 591-613.

Goodson, C., Roth, R., Wang, Z.T. and Goodenough, U. (2011) Structural Correlates of Cytoplasmic and Chloroplast Lipid Body Synthesis in Chlamydomonas reinhardtii and Stimulation of Lipid Body Production with Acetate Boost. *Eukaryotic Cell*, **10**, 1592-1606.

Grima, E.M., Fernandez, F.G.A., Camacho, F.G. and Chisti, Y. (1999) Photobioreactors: light regime, mass transfer, and scaleup. *Journal of biotechnology*, **70**, 231-247.

Grossman, A. (2000) Acclimation of *Chlamydomonas reinhardtii* to its nutrient environment. *Protist*, **151**, 201-224.

Grossman, A.R., Gonzalez-Ballester, D., Shibagaki, N., Pootakham, W., Moseley, J. and Pootakham, W. (2010) *Responses to Macronutrient Deprivation*.

Grossman, A.R., Harris, E.E., Hauser, C., Lefebvre, P.A., Martinez, D., Rokhsar, D., Shrager, J., Silflow, C.D., Stern, D., Vallon, O. and Zhang, Z. (2003) Chlamydomonas reinhardtii at the Crossroads of Genomics. *Eukaryotic Cell*, **2**, 1137-1150.

Grundel, M., Scheunemann, R., Lockau, W. and Zilliges, Y. (2012) Impaired glycogen synthesis causes metabolic overflow reactions and affects stress responses in the cyanobacterium Synechocystis sp. PCC 6803. *Microbiology*, **158**, 3032-3043.

Harris, E.H. (2001) Chlamydomonas as a Model Organism. *Annu Rev Plant Physiol Plant Mol Biol*, **52**, 363-406.

Harris, E.H. (2009) The life of an acetate flagellate. In *The Chlamydomonas Sourcebook: Introduction to Chlamydomonas and Its Laboratory Use* (Harris, E.H. ed. Oxford, UK: Elsevier, pp. 159-210.

Harris, E.H., D., S. and Witman, G.B. (2009) Preface to Volume 3. In *The Chlamydomonas Sourcebook (Second Edition)*. London: Academic Press, pp. xi-xii.

Hays, S.G. and Ducat, D.C. (2015) Engineering cyanobacteria as photosynthetic feedstock factories. *Photosynth. Res.*, **123**, 285-295.

Heisler, J., Glibert, P.M., Burkholder, J.M., Anderson, D.M., Cochlan, W., Dennison, W.C., Dortch, Q., Gobler, C.J., Heil, C.A., Humphries, E., Lewitus, A., Magnien, R., Marshall, H.G., Sellner, K., Stockwell, D.A., Stoecker, D.K. and Suddleson, M. (2008) Eutrophication and harmful algal blooms: A scientific consensus. *Harmful Algae*, **8**, 3-13.

Hicks, G.R., Hironaka, C.M., Dauvillee, D., Funke, R.P., D'Hulst, C., Waffenschmidt, S. and Ball, S.G. (2001) When simpler is better. Unicellular green algae for discovering new genes and functions in carbohydrate metabolism. *Plant Physiol*, **127**, 1334-1338.

Hoiczyk, E. (2000) Gliding motility in cyanobacteria: observations and possible explanations. *Archives of microbiology*, **174**, 11-17.

Hsieh, S.I., Castruita, M., Malasarn, D., Urzica, E., Erde, J., Page, M.D., Yamasaki, H., Casero, D., Pellegrini, M., Merchant, S.S. and Loo, J.A. (2013) The Proteome of Copper, Iron, Zinc, and Manganese Micronutrient Deficiency in Chlamydomonas reinhardtii. *Molecular & Cellular Proteomics*, **12**, 65-86.

Hu, Q., Sommerfeld, M., Jarvis, E., Ghirardi, M., Posewitz, M., Seibert, M. and Darzins, A. (2008) Microalgal triacylglycerols as feedstocks for biofuel production: perspectives and advances. *Plant J*, **54**, 621-639.

Imam, S., Schauble, S., Valenzuela, J., Lopez Garcia de Lomana, A., Carter, W., Price, N.D. and Baliga, N.S. (2015) A refined genome-scale reconstruction of Chlamydomonas metabolism provides a platform for systems-level analyses. *Plant J*, **84**, 1239-1256.

Innis, S.M. (2007) Dietary (n-3) fatty acids and brain development. *J Nutr*, **137**, 855-859.

Jackson, C., Clayden, S. and Reyes-Prieto, A. (2015) The Glaucophyta: the blue-green plants in a nutshell. *Acta Soc Bot Pol*, **84**, 149-165.

Jamers, A., Blust, R. and De Coen, W. (2009) Omics in algae: paving the way for a systems biological understanding of algal stress phenomena? *Aquat Toxicol*, **92**, 114-121.

Jardillier, L., Zubkov, M.V., Pearman, J. and Scanlan, D.J. (2010) Significant CO2 fixation by small prymnesiophytes in the subtropical and tropical northeast Atlantic Ocean. *ISME J*, **4**, 1180-1192.

Jones, C.S. and Mayfield, S.P. (2012) Algae biofuels: versatility for the future of bioenergy. *Curr Opin Biotechnol*, **23**, 346-351.

Juergens, M.T., Deshpande, R.R., Lucker, B.F., Park, J.J., Wang, H., Gargouri, M., Holguin, F.O., Disbrow, B., Schaub, T., Skepper, J.N., Kramer, D.M., Gang, D.R., Hicks, L.M. and Shachar-Hill, Y. (2015) The Regulation of Photosynthetic Structure and Function during Nitrogen Deprivation in Chlamydomonas reinhardtii. *Plant Physiol*, **167**, 558-573.

Keeling, P.J. (2009) Chromalveolates and the Evolution of Plastids by Secondary Endosymbiosis. *J Eukaryot Microbiol*, **56**, 1-8.

Keeling, P.J. (2010) The endosymbiotic origin, diversification and fate of plastids. *Philos Trans R Soc Lond B Biol Sci*, **365**, 729-748.

Kennedy, E.P. (1956) The biological synthesis of phospholipids. *Can J Biochem Physiol*, **34**, 334-348.

Kennedy, E.P. and Weiss, S.B. (1956) The function of cytidine coenzymes in the biosynthesis of phospholipides. *J Biol Chem*, **222**, 193-214.

Khozin-Goldberg, I., Shrestha, P. and Cohen, Z. (2005) Mobilization of arachidonyl moieties from triacylglycerols into chloroplastic lipids following recovery from nitrogen starvation of the microalga Parietochloris incisa. *Bba-Mol Cell Biol L*, **1738**, 63-71.

Kliphuis, A.M.J., Klok, A.J., Martens, D.E., Lamers, P.P., Janssen, M. and Wijffels, R.H. (2012) Metabolic modeling of *Chlamydomonas reinhardtii:* energy requirements for photoautotrophic growth and maintenance. *J. Appl. Phycol.*, **24**, 253-266.

Klok, A.J., Lamers, P.P., Martens, D.E., Draaisma, R.B. and Wijffels, R.H. (2014) Edible oils from microalgae: insights in TAG accumulation. *Trends in biotechnology*, **32**, 521-528.

Klug, R.M. and Benning, C. (2001) Two enzymes of diacylglyceryl-O-4'-(N,N,N,-trimethyl)homoserine biosynthesis are encoded by btaA and btaB in the purple bacterium Rhodobacter sphaeroides. *Proc Natl Acad Sci U S A*, **98**, 5910-5915.

Kohlwein, S.D. (2010) Triacylglycerol homeostasis: insights from yeast. *J Biol Chem*, **285**, 15663-15667.

Kroth, P.G., Chiovitti, A., Gruber, A., Martin-Jezequel, V., Mock, T., Parker, M.S., Stanley, M.S., Kaplan, A., Caron, L., Weber, T., Maheswari, U., Armbrust, E.V. and Bowler, C. (2008) A model for carbohydrate metabolism in the diatom Phaeodactylum tricornutum deduced from comparative whole genome analysis. *PloS one*, **3**, e1426.

La Russa, M., Bogen, C., Uhmeyer, A., Doebbe, A., Filippone, E., Kruse, O. and Mussgnug, J.H. (2012) Functional analysis of three type-2 DGAT homologue genes for triacylglycerol production in the green microalga *Chlamydomonas reinhardtii*. *Journal of biotechnology*, **162**, 13-20.

Larkum, A.D. (2003) Light-Harvesting Systems in Algae. In *Photosynthesis in Algae* (Larkum, A.D., Douglas, S. and Raven, J. eds): Springer Netherlands, pp. 277-304.

Larkum, A.W., Lockhart, P.J. and Howe, C.J. (2007) Shopping for plastids. *Trends in plant science*, **12**, 189-195.

Le, C., Zha, Y., Li, Y., Sun, D., Lu, H. and Yin, B. (2010) Eutrophication of Lake Waters in China: Cost, Causes, and Control. *Environ Manage*, **45**, 662-668.

Lebeau, T. and Robert, J.M. (2003) Diatom cultivation and biotechnologically relevant products. Part II: Current and putative products. *Appl. Microbiol. Biotechnol.*, **60**, 624-632.

Lee do, Y. and Fiehn, O. (2008) High quality metabolomic data for *Chlamydomonas reinhardtii*. *Plant methods*, **4**, 7.

Leliaert, F., Smith, D.R., Moreau, H., Herron, M.D., Verbruggen, H., Delwiche, C.F. and De Clerck, O. (2012) Phylogeny and Molecular Evolution of the Green Algae. *Crit Rev Plant Sci*, **31**, 1-46.

Lemoine, Y. and Schoefs, B. (2010) Secondary ketocarotenoid astaxanthin biosynthesis in algae: a multifunctional response to stress. *Photosynth Res*, **106**, 155-177.

Levine, R.P. (1960) Genetic Control of Photosynthesis in Chlamydomonas Reinhardi. *Proc Natl Acad Sci U S A*, **46**, 972-978.

Levine, R.P. and Ebersold, W.T. (1958a) Gene recombination in Chlamydomonas reinhardi. *Cold Spring Harb Symp Quant Biol*, **23**, 101-109.

Levine, R.P. and Ebersold, W.T. (1958b) The relation of calcium and magnesium to crossing over in Chlamydomonas reinhardtii. *Z Vererbungsl*, **89**, 631-635.

Levine, R.P. and Ebersold, W.T. (1960) The genetics and cytology of Chlamydomonas. *Annu Rev Microbiol*, **14**, 197-216.

Lewin, R.A. (1953) Studies on the flagella of algae. Il. Formation of flagella by Chlamydomonas in light and darkness. *Annals of the New York Academy of Sciences*, **56**, 1091-1093.

Li, H., Liu, Z., Zhang, Y., Li, B., Lu, H., Duan, N., Liu, M., Zhu, Z. and Si, B. (2014) Conversion efficiency and oil quality of low-lipid high-protein and high-lipid low-protein microalgae via hydrothermal liquefaction. *Bioresour Technol*, **154**, 322-329.

Li, X., Benning, C. and Kuo, M.-H. (2012a) Rapid Triacylglycerol Turnover in *Chlamydomonas reinhardtii* Requires a Lipase with Broad Substrate Specificity. *Eukaryotic Cell*, **11**, 1451-1462.

Li, X., Moellering, E.R., Liu, B., Johnny, C., Fedewa, M., Sears, B.B., Kuo, M.H. and Benning, C. (2012b) A galactoglycerolipid lipase is required for triacylglycerol accumulation and survival following nitrogen deprivation in Chlamydomonas reinhardtii. *The Plant cell*, **24**, 4670-4686.

Li, X., Zhang, R., Patena, W., Gang, S.S., Blum, S.R., Ivanova, N., Yue, R., Robertson, J.M., Lefebvre, P., Fitz-Gibbon, S.T., Grossman, A.R. and Jonikas, M.C. (2016) An

indexed, mapped mutant library enables reverse genetics studies of biological processes in Chlamydomonas reinhardtii. *The Plant cell*.

Li, Y., Han, D., Hu, G., Sommerfeld, M. and Hu, Q. (2010) Inhibition of starch synthesis results in overproduction of lipids in Chlamydomonas reinhardtii. *Biotechnology and bioengineering*, **107**, 258-268.

Li, Y., Han, D., Yoon, K., Zhu, S., Sommerfeld, M. and Hu, Q. (2013) Molecular and Cellular Mechanisms for Lipid Synthesis and Accumulation in Microalgae: Biotechnological Implications. In *Handbook of Microalgal Culture*.

Liu, B.S. and Benning, C. (2013) Lipid metabolism in microalgae distinguishes itself. *Current Opinion in Biotechnology*, **24**, 300-309.

Lopez Garcia de Lomana, A., Schauble, S., Valenzuela, J., Imam, S., Carter, W., Bilgin, D.D., Yohn, C.B., Turkarslan, S., Reiss, D.J., Orellana, M.V., Price, N.D. and Baliga, N.S. (2015) Transcriptional program for nitrogen starvation-induced lipid accumulation in Chlamydomonas reinhardtii. *Biotechnology for biofuels*, **8**, 207.

Luca, P.D., Musacchio, A. and Taddei, R. (1981) Acidophilic algae from the fumaroles of Mount Lawu (Java, locus classicus of Cyanidium caldarium Geitler. *Giornale botanico italiano*, **115**, 1-9.

Martin, N.C. and Goodenough, U.W. (1975a) Gametic differentiation in Chlamydomonas reinhardtii. I. Production of gametes and their fine structure. *The Journal of cell biology*, **67**, 587-605.

Martin, N.C. and Goodenough, U.W. (1975b) Gametic Differentiation in Chlamydomonas-Reinhardtii .1. Production of Gametes and Their Fine-Structure. *Journal of Cell Biology*, **67**, 587-605.

Mathiesen, A.M. (2012) The Sate of World Fisheries and Aquaculture. Rome: FAO Fisheries and Aquaculture Department: Food and Agriculture Organization of the united Nations.

May, P., Wienkoop, S., Kempa, S., Usadel, B., Christian, N., Rupprecht, J., Weiss, J., Recuenco-Munoz, L., Ebenhoh, O., Weckwerth, W. and Walther, D. (2008) Metabolomics- and proteomics-assisted genome annotation and analysis of the draft metabolic network of Chlamydomonas reinhardtii. *Genetics*, **179**, 157-166.

Mayfield, S.P., Manuell, A.L., Chen, S., Wu, J., Tran, M., Siefker, D., Muto, M. and Marin-Navarro, J. (2007) Chlamydomonas reinhardtii chloroplasts as protein factories. *Current Opinion in Biotechnology*, **18**, 126-133.

Meher, L.C., Sagar, D.V. and Naik, S.N. (2006) Technical aspects of biodiesel production by transesterification - a review. *Renew. Sust. Energ. Rev.*, **10**, 248-268.

Meier, R.L. (1955) Biological cycles in the transformation of solar energy into useful fuels. In *Solar Energy Research* (Daniels, F. and Duffie, J.A. eds). Madison, WI: University of Wisconsin Press, pp. 179-183.

Melis, A., Zhang, L., Forestier, M., Ghirardi, M.L. and Seibert, M. (2000) Sustained photobiological hydrogen gas production upon reversible inactivation of oxygen evolution in the green alga Chlamydomonas reinhardtii. *Plant Physiol*, **122**, 127-136.

Merchant, S.S., Kropat, J., Liu, B., Shaw, J. and Warakanont, J. (2012) TAG, You're it! *Chlamydomonas* as a reference organism for understanding algal triacylglycerol accumulation. *Current Opinion in Biotechnology*, **23**, 352-363.

Merchant, S.S., Prochnik, S.E., Vallon, O., Harris, E.H., Karpowicz, S.J., Witman, G.B., Terry, A., Salamov, A., Fritz-Laylin, L.K., Marechal-Drouard, L., Marshall, W.F., Qu, L.H., Nelson, D.R., Sanderfoot, A.A., Spalding, M.H., Kapitonov, V.V., Ren, Q., Ferris, P., Lindquist, E., Shapiro, H., Lucas, S.M., Grimwood, J., Schmutz, J., Cardol, P., Cerutti, H., Chanfreau, G., Chen, C.L., Cognat, V., Croft, M.T., Dent, R., Dutcher, S., Fernandez, E., Fukuzawa, H., Gonzalez-Ballester, D., Gonzalez-Halphen, D., Hallmann, A., Hanikenne, M., Hippler, M., Inwood, W., Jabbari, K., Kalanon, M., Kuras, R., Lefebvre, P.A., Lemaire, S.D., Lobanov, A.V., Lohr, M., Manuell, A., Meier, I., Mets, L., Mittag, M., Mittelmeier, T., Moroney, J.V., Moseley, J., Napoli, C., Nedelcu, A.M., Niyogi, K., Novoselov, S.V., Paulsen, I.T., Pazour, G., Purton, S., Ral, J.P., Riano-Pachon, D.M., Riekhof, W., Rymarquis, L., Schroda, M., Stern, D., Umen, J., Willows, R., Wilson, N., Zimmer, S.L., Allmer, J., Balk, J., Bisova, K., Chen, C.J., Elias, M., Gendler, K., Hauser, C., Lamb, M.R., Ledford, H., Long, J.C., Minagawa, J., Page, M.D., Pan, J., Pootakham, W., Roje, S., Rose, A., Stahlberg, E., Terauchi, A.M., Yang, P., Ball, S., Bowler, C., Dieckmann, C.L., Gladyshev, V.N., Green, P., Jorgensen, R., Mayfield, S., Mueller-Roeber, B., Rajamani, S., Sayre, R.T., Brokstein, P., Dubchak, I., Goodstein, D., Hornick, L., Huang, Y.W., Jhaveri, J., Luo, Y., Martinez, D., Ngau, W.C., Otillar, B., Poliakov, A., Porter, A., Szajkowski, L., Werner, G., Zhou, K., Grigoriev, I.V., Rokhsar, D.S. and Grossman, A.R. (2007) The *Chlamydomonas* genome reveals the evolution of key animal and plant functions. *Science*, **318**, 245-250.

Merrill, E.D. (1916) Osbeck's Dagbok Ofwer en Ostindsk Resa. *Am J Bot*, **3**, 571-588.

Merzlyak, M.N., Chivkunova, O.B., Gorelova, O.A., Reshetnikova, I.V., Solovchenko, A.E., Khozin-Goldberg, I. and Cohen, Z. (2007) Effect of nitrogen starvation on optical properties, pigments, and arachidonic acid content of the unicellular green alga Parietochloris incisa (Trebouxiophyceae, Chlorophyta). *Journal of Phycology*, **43**, 833-843.

Miller, R., Wu, G., Deshpande, R.R., Vieler, A., Gartner, K., Li, X., Moellering, E.R., Zauner, S., Cornish, A.J., Liu, B., Bullard, B., Sears, B.B., Kuo, M.H., Hegg, E.L., Shachar-Hill, Y., Shiu, S.H. and Benning, C. (2010) Changes in transcript abundance in *Chlamydomonas reinhardtii* following nitrogen deprivation predict diversion of metabolism. *Plant Physiol*, **154**, 1737-1752.

Mittag, M. and Wagner, V. (2003) The circadian clock of the unicellular eukaryotic model organism Chlamydomonas reinhardtii. *Biol Chem*, **384**, 689-695.

Miyamoto, K., Hallenbeck, P.C. and Benemann, J.R. (1979) Nitrogen fixation by thermophilic blue-green algae (cyanobacteria): temperature characteristics and potential use in biophotolysis. *Applied and environmental microbiology*, **37**, 454-458.

Moellering, E.R. and Benning, C. (2010) RNA interference silencing of a major lipid droplet protein affects lipid droplet size in Chlamydomonas reinhardtii. *Eukaryot Cell*, **9**, 97-106.

Moore, T.S., Du, Z. and Chen, Z. (2001) Membrane lipid biosynthesis in Chlamydomonas reinhardtii. In vitro biosynthesis of diacylglyceryltrimethylhomoserine. *Plant Physiol*, **125**, 423-429.

Morita, E., Kuroiwa, H., Kuroiwa, T. and Nozaki, H. (1997) High localization of ribulose-1,5-bisphosphate carboxylase/oxygenase in the pyrenoids of Chlamydomonas reinhardtii (Chlorophyta), as revealed by cryofixation and immunogold electron microscopy. *Journal of Phycology*, **33**, 68-72.

Moroney, J.V., Kitayama, M., Togasaki, R.K. and Tolbert, N.E. (1987) Evidence for Inorganic Carbon Transport by Intact Chloroplasts of Chlamydomonas reinhardtii. *Plant Physiol*, **83**, 460-463.

Moseley, J.L., Allinger, T., Herzog, S., Hoerth, P., Wehinger, E., Merchant, S. and Hippler, M. (2002) Adaptation to Fe-deficiency requires remodeling of the photosynthetic apparatus. *Embo J*, **21**, 6709-6720.

Msanne, J., Xu, D., Konda, A.R., Casas-Mollano, J.A., Awada, T., Cahoon, E.B. and Cerutti, H. (2012) Metabolic and gene expression changes triggered by nitrogen deprivation in the photoautotrophically grown microalgae Chlamydornonas reinhardtii and Coccomyxa sp C-169. *Phytochemistry*, **75**, 50-59.

Mulders, K.J.M., Lamers, P.P., Wijffels, R.H. and Martens, D.E. (2015) Dynamics of biomass composition and growth during recovery of nitrogen-starved Chromochloris zofingiensis. *Appl. Microbiol. Biotechnol.*, **99**, 1873-1884.

Muller-Feuga, A. (2000) The role of microalgae in aquaculture: situation and trends. *J. Appl. Phycol.*, **12**, 527-534.

Murphy, D.J. (2001) The biogenesis and functions of lipid bodies in animals, plants and microorganisms. *Prog Lipid Res*, **40**, 325-438.

Neijssel, O.M. and Tempest, D.W. (1975) The regulation of carbohydrate metabolism in Klebsiella aerogenes NCTC 418 organisms, growing in chemostat culture. *Archives of microbiology*, **106**, 251-258.

Nguyen, H.M., Baudet, M., Cuine, S., Adriano, J.M., Barthe, D., Billon, E., Bruley, C., Beisson, F., Peltier, G., Ferro, M. and Li-Beisson, Y. (2011) Proteomic profiling of oil

bodies isolated from the unicellular green microalga *Chlamydomonas reinhardtii*: With focus on proteins involved in lipid metabolism. *Proteomics*, **11**, 4266-4273.

Olivares, J.A. (2013) National Alliance for Advanced Biofuels and Bioproducts(NAABB): Synopsis: U.S. Department of Energy: Office of Energy Efficiency and Renewable Energy.

Oswald, W.J. and Golueke, C.G. (1960) Biological transformation of solar energy. *Adv Appl Microbiol*, **2**, 223-262.

Park, J., Wang, H., Gargouri, M., Deshpande, R., Skepper, J., Holguin, F.O., Juergens, M., Shachar-Hill, Y., Hicks, L. and Gang, D.R. (2014) The response of Chlamydomonas reinhardtii to nitrogen deprivation: A systems biology analysis. *Submitted*.

Pasher, A. (1918) Über die Beziehung der Reduktionsteilung zur Mendelschen Spaltung. *Ber. Deutsch. Bot. Ges.*, **36**, 163-168.

Percival, E.G.V. and Ross, A.G. (1951) 156. The constitution of laminarin. Part II. The soluble laminarin of Laminaria digitata. *Journal of the Chemical Society (Resumed)*, 720-726.

Pienkos, P.T. and Darzins, A. (2009) The promise and challenges of microalgal-derived biofuels. *Biofuels, Bioproducts and Biorefining*, **3**, 431-440.

Plancke, C., Colleoni, C., Deschamps, P., Dauvillee, D., Nakamura, Y., Haebel, S., Ritte, G., Steup, M., Buleon, A., Putaux, J.L., Dupeyre, D., d'Hulst, C., Ral, J.P., Loffelhardt, W. and Ball, S.G. (2008) Pathway of cytosolic starch synthesis in the model glaucophyte Cyanophora paradoxa. *Eukaryotic Cell*, **7**, 247-257.

Plumley, F.G. and Schmidt, G.W. (1989) NITROGEN-DEPENDENT REGULATION OF PHOTOSYNTHETIC GENE-EXPRESSION. *P Natl Acad Sci USA*, **86**, 2678-2682.

Posewitz, M.C., Smolinski, S.L., Kanakagiri, S., Melis, A., Seibert, M. and Ghirardi, M.L. (2004) Hydrogen photoproduction is attenuated by disruption of an isoamylase gene in Chlamydomonas reinhardtii. *The Plant cell*, **16**, 2151-2163.

Proschold, T., Marin, B., Schlosser, U.G. and Melkonian, M. (2001) Molecular phylogeny and taxonomic revision of Chlamydomonas (Chlorophyta). I. Emendation of Chlamydomonas Ehrenberg and Chloromonas Gobi, and description of Oogamochlamys gen. nov. and Lobochlamys gen. nov. *Protist*, **152**, 265-300.

Pulz, O. (2001) Photobioreactors: production systems for phototrophic microorganisms. *Appl. Microbiol. Biotechnol.*, **57**, 287-293.

Radakovits, R., Jinkerson, R.E., Fuerstenberg, S.I., Tae, H., Settlage, R.E., Boore, J.L. and Posewitz, M.C. (2012) Draft genome sequence and genetic transformation of the oleaginous alga *Nannochloropsis gaditana*. *Nature Communications*, **3**.

Rae, B.D., Long, B.M., Whitehead, L.F., Forster, B., Badger, M.R. and Price, G.D. (2013) Cyanobacterial Carboxysomes: Microcompartments that Facilitate CO2 Fixation. *J Mol Microb Biotech*, **23**, 300-307.

Ramazanov, Z., Rawat, M., Henk, M.C., Mason, C.B., Matthews, S.W. and Moroney, J.V. (1994) The Induction of the Co2-Concentrating Mechanism Is Correlated with the Formation of the Starch Sheath around the Pyrenoid of Chlamydomonas-Reinhardtii. *Planta*, **195**, 210-216.

Rasala, B.A. and Mayfield, S.P. (2015) Photosynthetic biomanufacturing in green algae; production of recombinant proteins for industrial, nutritional, and medical uses. *Photosynth. Res.*, **123**, 227-239.

Ratledge, C. (2004) Fatty acid biosynthesis in microorganisms being used for Single Cell Oil production. *Biochimie*, **86**, 807-815.

Ratledge, C. and Wynn, J.P. (2002) The biochemistry and molecular biology of lipid accumulation in oleaginous microorganisms. *Adv Appl Microbiol*, **51**, 1-51.

Renn, D.W. (1984) Agar and Agarose - Indispensable Partners in Biotechnology. *Ind Eng Chem Prod Rd*, **23**, 17-21.

Rochaix, J.D. (2002) Chlamydomonas, a model system for studying the assembly and dynamics of photosynthetic complexes. *FEBS Lett*, **529**, 34-38.

Roessler, P.G. (1990) Environmental-Control of Glycerolipid Metabolism in Microalgae - Commercial Implications and Future-Research Directions. *Journal of Phycology*, **26**, 393-399.

Rosen, H. and Ebersold, W.T. (1972) Recombination in relation to ultraviolet sensitivity in Chlamydomonas reinhardi. *Genetics*, **71**, 247-253.

Sage, R.F., Sage, T.L. and Kocacinar, F. (2012) Photorespiration and the evolution of C4 photosynthesis. *Annu Rev Plant Biol*, **63**, 19-47.

Sager, R. and Granick, S. (1954) Nutritional Control of Sexuality in Chlamydomonas Reinhardi. *J Gen Physiol*, **37**, 729-742.

Sato, N. and Murata, N. (1991) Transition of Lipid Phase in Aqueous Dispersions of Diacylglyceryltrimethylhomoserine. *Biochimica et biophysica acta*, **1082**, 108-111.

Schlapfer, P. and Eichenberger, W. (1983) Evidence for the Involvement of Diacylglyceryl (N,N,N-Trimethyl) Homoserine in the Desaturation of Oleic and Linoleic Acids in Chlamydomonas-Reinhardi (Chlorophyceae). *Plant Sci Lett*, **32**, 243-252.

Schmidt, I., Sliekers, O., Schmid, M., Bock, E., Fuerst, J., Kuenen, J.G., Jetten, M.S.M. and Strous, M. (2003) New concepts of microbial treatment processes for the nitrogen removal in wastewater. *FEMS microbiology reviews*, **27**, 481-492.

Schmidt, R.A., Wiebe, M.G. and Eriksen, N.T. (2005) Heterotrophic high cell-density fed-batch cultures of the phycocyanin-producing red alga Galdieria sulphuraria. *Biotechnology and bioengineering*, **90**, 77-84.

Schmollinger, S., Muhlhaus, T., Boyle, N.R., Blaby, I.K., Casero, D., Mettler, T., Moseley, J.L., Kropat, J., Sommer, F., Strenkert, D., Hemme, D., Pellegrini, M., Grossman, A.R., Stitt, M., Schroda, M. and Merchant, S.S. (2014) Nitrogen-Sparing Mechanisms in Chlamydomonas Affect the Transcriptome, the Proteome, and Photosynthetic Metabolism. *The Plant cell*.

Selvaratnam, T., Pegallapati, A.K., Montelya, F., Rodriguez, G., Nirmalakhandan, N., Van Voorhies, W. and Lammers, P.J. (2014) Evaluation of a thermo-tolerant acidophilic alga, Galdieria sulphuraria, for nutrient removal from urban wastewaters. *Bioresour Technol*, **156**, 395-399.

Sheehan, J., Dunahay, T., Benemann, J. and Roessler, P.G. (1998) A Look Back at the U.S. Department of Energy's Aquatic Species Program: Biodiesel from Algae. *National Renewable Energy Laboratory*.

Siaut, M., Cuine, S., Cagnon, C., Fessler, B., Nguyen, M., Carrier, P., Beyly, A., Beisson, F., Triantaphylides, C., Li-Beisson, Y.H. and Peltier, G. (2011) Oil accumulation in the model green alga *Chlamydomonas reinhardtii*: characterization, variability between common laboratory strains and relationship with starch reserves. *Bmc Biotechnol*, **11**.

Silflow, C.D. and Lefebvre, P.A. (2001) Assembly and motility of eukaryotic cilia and flagella. Lessons from Chlamydomonas reinhardtii. *Plant Physiol*, **127**, 1500-1507.

Simionato, D., Block, M.A., La Rocca, N., Jouhet, J., Marechal, E., Finazzi, G. and Morosinotto, T. (2013) Response of *Nannochloropsis Gaditana* to Nitrogen Starvation Includes a De Novo Biosynthesis of Triacylglycerols, a Decrease of Chloroplast Galactolipids and a Reorganization of the Photosynthetic Apparatus. *Eukaryot Cell*.

Smyth, R.D., Martinek, G.W. and Ebersold, W.T. (1975) Linkage of six genes in Chlamydomonas reinhardtii and the construction of linkage test strains. *Journal of bacteriology*, **124**, 1615-1617.

Solovchenko, A., Lukyanov, A., Solovchenko, O., Didi-Cohen, S., Boussiba, S. and Khozin-Goldberg, I. (2014) Interactive effects of salinity, high light, and nitrogen starvation on fatty acid and carotenoid profiles in Nannochloropsis oceanica CCALA 804. *European Journal of Lipid Science and Technology*, **116**, 635-644.

Solovchenko, A.E. (2012) Physiological Role of Neutral Lipid Accumulation in Eukaryotic Microalgae under Stresses. *Russ. J. Plant Physiol.*, **59**, 167-176.

Spalding, M.H. (2009) Chapter 8 - The CO2-Concentrating Mechanism and Carbon Assimilation. In *The Chlamydomonas Sourcebook (Second Edition)* (Witman, E.H.H.B.S.B. ed. London: Academic Press, pp. 257-301.

Spoehr, H.A. and Milner, H.W. (1949) The Chemical Composition of Chlorella - Effect of Environmental Conditions. *Plant Physiol*, **24**, 120-149.

Spreitzer, R.J. and Mets, L. (1981) Photosynthesis-Deficient Mutants of *Chlamydomonas-Reinhardii* with Associated Light-Sensitive Phenotypes. *Plant Physiol*, **67**, 565-569.

Stal, L.J. (2001) Nitrogen Fixation in Cyanobacteria. In *eLS*: John Wiley & Sons, Ltd.

Sudasinghe, N., Dungan, B., Lammers, P., Albrecht, K., Elliott, D., Hallen, R. and Schaub, T. (2014) High resolution FT-ICR mass spectral analysis of bio-oil and residual water soluble organics produced by hydrothermal liquefaction of the marine microalga Nannochloropsis salina. *Fuel*, **119**, 47-56.

Sukenik, A., Beardall, J., Kromkamp, J.C., Kopecky, J., Masojidek, J., van Bergeijk, S., Gabai, S., Shaham, E. and Yamshon, A. (2009) Photosynthetic performance of outdoor *Nannochloropsis* mass cultures under a wide range of environmental conditions. *Aquatic Microbial Ecology*, **56**, 297-308.

Sun, Z., Liu, J., Bi, Y. and Zhou, Z. (2014) Microalgae as the production platform for Carotenoids. In *Recent Advances in Microalgal Biotechnology* (Liu, J., Sun, Z. and Gerken, H. eds). Foster City, CA, USA: OMICS Group ebooks.

Syrett, P.J. and Peplinska, A.M. (1988) Effects of Nitrogen-Deprivation, and Recovery from It, on the Metabolism of Microalgae. *New Phytol*, **109**, 289-296.

Tamura, T. (1966) *Marine aquaculture. 2nd Edition (Translated from Japanese)* Springfield, VA, USA.

Tsai, C.H., Warakanont, J., Takeuchi, T., Sears, B.B., Moellering, E.R. and Benning, C. (2014) The protein Compromised Hydrolysis of Triacylglycerols 7 (CHT7) acts as a repressor of cellular quiescence in Chlamydomonas. *Proc Natl Acad Sci U S A*, **111**, 15833-15838.

Tsygankov, A.A., Kosourov, S.N., Tolstygina, I.V., Ghirardi, M.L. and Seibert, M. (2006) Hydrogen production by sulfur-deprived Chlamydomonas reinhardtii under photoautotrophic conditions. *Int J Hydrogen Energ*, **31**, 1574-1584.

Uduman, N., Qi, Y., Danquah, M.K., Forde, G.M. and Hoadley, A. (2010) Dewatering of microalgal cultures: A major bottleneck to algae-based fuels. *J Renew Sustain Ener*, **2**.

Urzica, E.I., Vieler, A., Hong-Hermesdorf, A., Page, M.D., Casero, D., Gallaher, S.D., Kropat, J., Pellegrini, M., Benning, C. and Merchant, S.S. (2013) Remodeling of Membrane Lipids in Iron Starved Chlamydomonas. *J Biol Chem*.

Uziel, M., Oswald, W.J. and Golueke, C.G. (1975) Solar Energy Fixation and conversion with Algal Bacterial Systems. SERL, University of California, Berleley.

Valledor, L., Furuhashi, T., Recuenco-Munoz, L., Wienkoop, S. and Weckwerth, W. (2014) System-level network analysis of nitrogen starvation and recovery in Chlamydomonas reinhardtii reveals potential new targets for increased lipid accumulation. *Biotechnology for biofuels*, **7**, 171.

Van Iterson, G., Jong, L.E.d.d.D.d. and Kluyver, A.j. (1921) *Martinus Willem Beijerinck: His Life and his Work* The Hague: Martinus Nijhoff.

Villarreal, J.C. and Renner, S.S. (2012) Hornwort pyrenoids, carbon-concentrating structures, evolved and were lost at least five times during the last 100 million years. *P Natl Acad Sci USA*, **109**, 18873-18878.

Wakil, S.J. (1989) Fatty acid synthase, a proficient multifunctional enzyme. *Biochemistry-Us*, **28**, 4523-4530.

Wang, H., Gau, B., Slade, W.O., Juergens, M., Li, P. and Hicks, L.M. (2014) The global phosphoproteome of Chlamydomonas reinhardtii reveals complex organellar phosphorylation in the flagella and thylakoid membrane. *Molecular & cellular proteomics : MCP*, **13**, 2337-2353.

Warakanont, J., Tsai, C.H., Michel, E.J., Murphy, G.R., 3rd, Hsueh, P.Y., Roston, R.L., Sears, B.B. and Benning, C. (2015) Chloroplast lipid transfer processes in Chlamydomonas reinhardtii involving a TRIGALACTOSYLDIACYLGLYCEROL 2 (TGD2) orthologue. *Plant J*.

Weise, S.E., van Wijk, K.J. and Sharkey, T.D. (2011) The role of transitory starch in C(3), CAM, and C(4) metabolism and opportunities for engineering leaf starch accumulation. *J Exp Bot*, **62**, 3109-3118.

Weissman, J.C. and Benemann, J.R. (1977) Hydrogen production by nitrogen-starved cultures of Anabaena cylindrica. *Applied and environmental microbiology*, **33**, 123-131.

Wienkoop, S., Weiss, J., May, P., Kempa, S., Irgang, S., Recuenco-Munoz, L., Pietzke, M., Schwemmer, T., Rupprecht, J., Egelhofer, V. and Weckwerth, W. (2010) Targeted proteomics for Chlamydomonas reinhardtii combined with rapid subcellular protein fractionation, metabolomics and metabolic flux analyses. *Mol Biosyst*, **6**, 1018-1031.

Williams, R.B. (2012) The editions, issues, states and dates of William Henry Harvey's A manual of the British algae. *Archives of Natural History*, **39**, 312-320.

Witman, G.B., Carlson, K., Berliner, J. and Rosenbaum, J.L. (1972) Chlamydomonas flagella. I. Isolation and electrophoretic analysis of microtubules, matrix, membranes, and mastigonemes. *The Journal of cell biology*, **54**, 507-539.

Wolk, C.P. (1996) Heterocyst formation. *Annu Rev Genet*, **30**, 59-78.

Work, V.H., Radakovits, R., Jinkerson, R.E., Meuser, J.E., Elliott, L.G., Vinyard, D.J., Laurens, L.M., Dismukes, G.C. and Posewitz, M.C. (2010) Increased lipid

accumulation in the Chlamydomonas reinhardtii sta7-10 starchless isoamylase mutant and increased carbohydrate synthesis in complemented strains. *Eukaryot Cell*, **9**, 1251-1261.

Wykoff, D.D., Davies, J.P., Melis, A. and Grossman, A.R. (1998) The regulation of photosynthetic electron transport during nutrient deprivation in Chlamydomonas reinhardtii. *Plant Physiol*, **117**, 129-139.

Yang, Z.-K., Ma, Y.-H., Zheng, J.-W., Yang, W.-D., Liu, J.-S. and Li, H.-Y. (2013) Proteomics to reveal metabolic network shifts towards lipid accumulation following nitrogen deprivation in the diatom *Phaeodactylum tricornutum*. *J. Appl. Phycol.*

Yen, H.-W., Hu, I.C., Chen, C.-Y. and Chang, J.-S. (2014) Chapter 2 - Design of Photobioreactors for Algal Cultivation. In *Biofuels from Algae* (Soccol, A.P.-J.L.C.R. ed. Amsterdam: Elsevier, pp. 23-45.

Young, E.B. and Beardall, J. (2003) PHOTOSYNTHETIC FUNCTION IN DUNALIELLA TERTIOLECTA (CHLOROPHYTA) DURING A NITROGEN STARVATION AND RECOVERY CYCLE. *Journal of Phycology*, **39**, 897-905.

Zhao, Y., Wang, Y. and Quigg, A. (2015) The 24 hour recovery kinetics from n starvation in Phaeodactylum tricornutum and Emiliania huxleyi. *Journal of Phycology*, **51**, 726-738.

Chapter-2

The Regulation of Photosynthetic Structure and Function During Nitrogen Deprivation in *Chlamydomonas reinhardtii*

This research was published in:
Matthew T. Juergens, Rahul R. Deshpande, Ben F. Lucker, Jeong-Jin Park, Hongxia Wang, Mahmoud Gargouri, F. Omar Holguin, Bradley Disbrow, Tanner Schaub, Jeremy N. Skepper, David M. Kramer, David R. Gang, Leslie M. Hicks, and Yair Shachar-Hill(2015)The Regulation of Photosynthetic Structure and Function During Nitrogen Deprivation in *Chlamydomonas reinhardtii. Plant Physiology*
In this work, Lesli Hicks, JJ Park, Hongxia Wang, Mahmoud Gargouri and David Gang generated proteomic and transcript data. I assisted in the annotation of the transcripts and proteins and generated the heat maps based upon that data. I also generated the hierarchical clustering and k means clustering analysis with the assistance of Omar Holguin. Further, I carried out all of the physiological photosynthetic measurements and figures generated in the work. Additionally, I generated cell samples for Jeremy Skepper to analyze via electron microscopy. Bradley Disbrow assisted me in the starch quantification and gene annotation and analysis. The manuscript was drafted by myself with the assistance of Yair Shachar-hill and Bradley Disbrow. Ben Lucker and David Kramer provided training and assistance in the interpretation of photosynthetic experiments.

ABSTRACT

The accumulation of carbon storage compounds by many unicellular algae after nutrient deprivation occurs despite declines in their photosynthetic apparatus. To aid in understanding the regulation and roles of photosynthesis during this potentially bioenergetically valuable process, we analyzed photosynthetic structure and function after nitrogen deprivation in the model alga *Chlamydomonas reinhardtii*. Transcriptomic, proteomic, metabolite and lipid profiling, and microscopic time course data were combined with multiple measures of photosynthetic function. Levels of transcripts and proteins of photosystem I and II and most antenna genes fell with differing trajectories; thylakoid membrane lipid levels decreased while their proportions remained similar and thylakoid membrane organization appeared to be preserved. Cellular chlorophyll content decreased more than two-fold within 24 hrs and we conclude from transcript, protein, and ^{13}C labelling rates that chlorophyll synthesis was down regulated both pre- and post-translationally and that chlorophyll levels fall because of a rapid cessation in synthesis and dilution by cellular growth rather than because of degradation. Photosynthetically driven oxygen production and the efficiency of photosystem II as well as $P700^{+}$ reduction and electrochromic shift kinetics all decreased over the time course without evidence of substantial energy overflow. The results also indicate that linear electron flow fell ~15% more than cyclic flow over the first 24 hrs. Comparing Calvin-Benson cycle transcript and enzyme levels with changes in photosynthetic $^{13}CO_2$ incorporation rates also point to a coordinated multi-level down regulation of photosynthetic fluxes during starch synthesis before the induction of high triacylglycerol accumulation rates.

INTRODUCTION

Our current dependence on fossil fuels is unsustainable, motivating the development of bioenergy resources. Among these, microalgal oil and biomass production has shown promise (Atabani *et al.* 2012, Chisti 2007, Ohlrogge *et al.* 2009, Williams *et al.* 2010) because of the photoautotrophic growth of algae and their ability to reach high cell densities, accumulate high dry weight percentages of triacylglycerol (TAG), and their potential for much higher productivity per hectare than terrestrial biofuel crops (Hu, et al. 2008, Wijffels *et al.* 2010). The unicellular green alga *Chlamydomonas reinhardtii* is among the most widely studied models of photosynthesis (Rochaix 2002) and other cellular processes including lipid accumulation by algae under stress (Merchant, et al. 2012b). Its advantages for studying photosynthetic mechanisms and regulation include the ability to grow both photo- and heterotrophically so that photosynthetic down regulation and photosynthetically impaired mutants can be isolated (Dent, et al. 2001), a fully sequenced genome, collections of mutants, and the ease with which its growth, physiology, and photosynthetic rates can be measured.

In a range of microalgae, nitrogen (N) deprivation induces high accumulation of starch and TAG (Granum *et al.* 2002, Hu, et al. 2008, Liu, et al. 2013, Martin, et al. 1975a, Shifrin *et al.* 1981). In an effort to understand algal TAG production during N deprivation and to guide engineering of higher oil yields, omics-based approaches have been employed (Jamers, et al. 2009). Using the annotated *Chlamydomonas* genome (Merchant, et al. 2007), the *Chlamydomonas* transcriptome was analyzed before and after N deprivation, which revealed multiple changes in gene expression that affect diverse parts of metabolism (Blaby, et al. 2013, Goodenough, et al. 2014, Miller, et al. 2010, Schmollinger, et al. 2014). In addition, proteomics have been used to profile the changes in protein expression during N deprivation in

Phaeodactylum tricornutum (Yang, et al. 2013a), *Chlamydomonas reinhardtii* (Longworth *et al.* 2012, Nguyen, et al. 2011, Schmollinger, et al. 2014), and *Nannochloropsis oceanica* (Dong, et al. 2013) and metabolomics have been used to assess changes in metabolite pools sizes (Bölling *et al.* 2005, Lee *et al.* 2012). These and other studies point to wide ranging changes in the structure and operation of the metabolic and other cellular networks. Several studies have considered the relationships among metabolic processes including how carbon and energy fixation by photosynthesis affects oil accumulation during N deprivation (Johnson *et al.* 2013, Miller, et al. 2010, Msanne, et al. 2012). However an integrated systems analysis of both the machinery and the physiological functioning of the photosynthetic apparatus during nutrient deprivation is still lacking, and this limits our understanding of the multilevel regulation of energy and carbon fluxes.

During N deprivation in algae, energy and carbon for de novo synthesis of TAG can come directly from photosynthesis (Msanne, et al. 2012) or from external carbon substrates (Johnson, et al. 2013, Wang *et al.* 2009). Photosynthetic yields decrease during N deprivation, even under phototrophic conditions where cells are entirely dependent upon photosynthesis (Philipps *et al.* 2012, Simionato, et al. 2013). Chlorophyll (Chl) fluorescence, which is sensitive to environmental changes and stress conditions that induce alterations in photosynthetic components (Iwai *et al.* 2008), can monitor the efficiency of linear electron flow (Baker *et al.* 2007) and has indicated that in Nannochloropsis (Simionato *et al*. 2013) and other algae, including Chlamydomonas, *(Berges, et al. 1996, Blaby, et al. 2013, Li, et al. 2010)* photosynthetic efficiency falls after N deprivation. Photosynthetically driven metabolic fluxes can also be probed by supplying ^{13}C labeled bicarbonate/CO_2 and quantifying ^{13}C incorporation into metabolite pools (Feng *et al.* 2010, Shastri *et al.* 2007, Young *et al.* 2011).

Thylakoid membrane lipids are central to photosynthetic function, including the stabilization of photosynthetic complexes and oxygen evolution (Boudière *et al.* 2013, Jarvis *et al.* 2000, Jones 2007, Leng *et al.* 2008, Mizusawa *et al.* 2012) . The most abundant classes are the neutral lipids monogalactosyldiacylglycerol (MGDG), digalactosyldiacylglycerol (DGDG), and the anionic lipids sulfoquinovosyldiacylglycerol (SQGD) and phosphatidylglycerol (PG) (Frentzen 2004, Mizusawa, et al. 2012, Shimojima *et al.* 2010). Stress, nutrient deprivation, or changing environmental conditions cause changes in lipid composition, leading to effects on photosynthetic yield and efficiency (Li, et al. 2012b, Philipps, et al. 2012). Cellular Chl and carotenoid concentrations provide additional measures of photosynthetic potential. Carotenoids play a role in protecting cells from excess energy harvesting and act as structural components in the photocenters (Takaichi 2011). In *Chlamydomonas*, decreasing Chl content is associated with down regulation of synthesis genes and potentially also degradation and follows a decrease in photosynthetic yield during N deprivation (Li, et al. 2010, Philipps, et al. 2012).

This paper examines photosynthetic changes at the level of transcript, protein, lipid, and functional fluxes during the first 48 hrs after N deprivation. Until recently studies of nutrient limitation in microalgae have focused on the effects seen one to several days after deprivation (Moseley, et al. 2002, Urzica, et al. 2013, Wykoff, et al. 1998) when oil accumulation rates are high (Li, et al. 2010, Miller, et al. 2010, Philipps, et al. 2012, Plumley, et al. 1989b, Simionato, et al. 2013, Yang *et al.* 2013b) and photosynthetic functions are already substantially diminished. Here we focus on the induction phase to investigate the transition into a nutrient deprived, oil accumulating state and the regulation of photosynthesis during that transition. The results demonstrate coordinated changes in photosynthetic gene expression as well as the levels of the photosynthetic machinery and their activities. Photosynthetic transcripts and to a lesser extent

protein levels for different parts of the photosynthetic infrastructure were down-regulated as were the levels of thylakoid lipids and Chl. Photosynthetic function as measured by dynamic optical parameters indicated modest decreases in the efficiency of light utilization during the first 24 hrs and a relative decrease in linear compared to cyclic electron flow. Calvin cycle protein and transcript levels decreased modestly after 6 hrs though ^{13}C labeling incorporation from CO_2 was significantly reduced by that time. The results provide a multilevel description of the controlled down-regulation of photosynthetic components and photosynthetic fluxes, highlight the value of combined multiomic and functional measurements, and have significant implications for current hypotheses about the relationship between photosynthesis and TAG accumulation in algae.

RESULTS

Changes in the levels of transcripts and proteins of photosynthesis

C. reinhardtii samples were harvested at 0, 0.5, 1, 2, 4, 6, 12, and 24 hrs after N deprivation and transcripts were analyzed by high throughput sequencing as described in Park et al. (Park, et al. 2014). Nitrogen replete cells (time 0) were used as the reference for all subsequent time points. Quantitative proteomic analysis was performed using iTRAQ labeling combined with strong cation exchange (SCX) fractionation and nanoLC-ESI-MS/MS at all the time points except for 0.5 hrs. 192 photosynthetically related genes with putative or confirmed annotations were collected using genomic annotation, the literature and additional databases (see Methods). Genes were classed as belonging to the following functional groups: photosynthetic reaction center complexes, light harvesting complexes, electron transport, photosynthetic antennae, carbon concentrating mechanisms, the Calvin-Benson cycle, oxidative stress responses, and pigment production and degradation. The transcript and protein level changes for these are presented in Figures 2.1 and 2.2. As previously reported, (Merchant, et al. 2007, Schmollinger, et al. 2014), expression of most photosynthetic genes is down regulated during N deprivation with a wide range of trajectories.

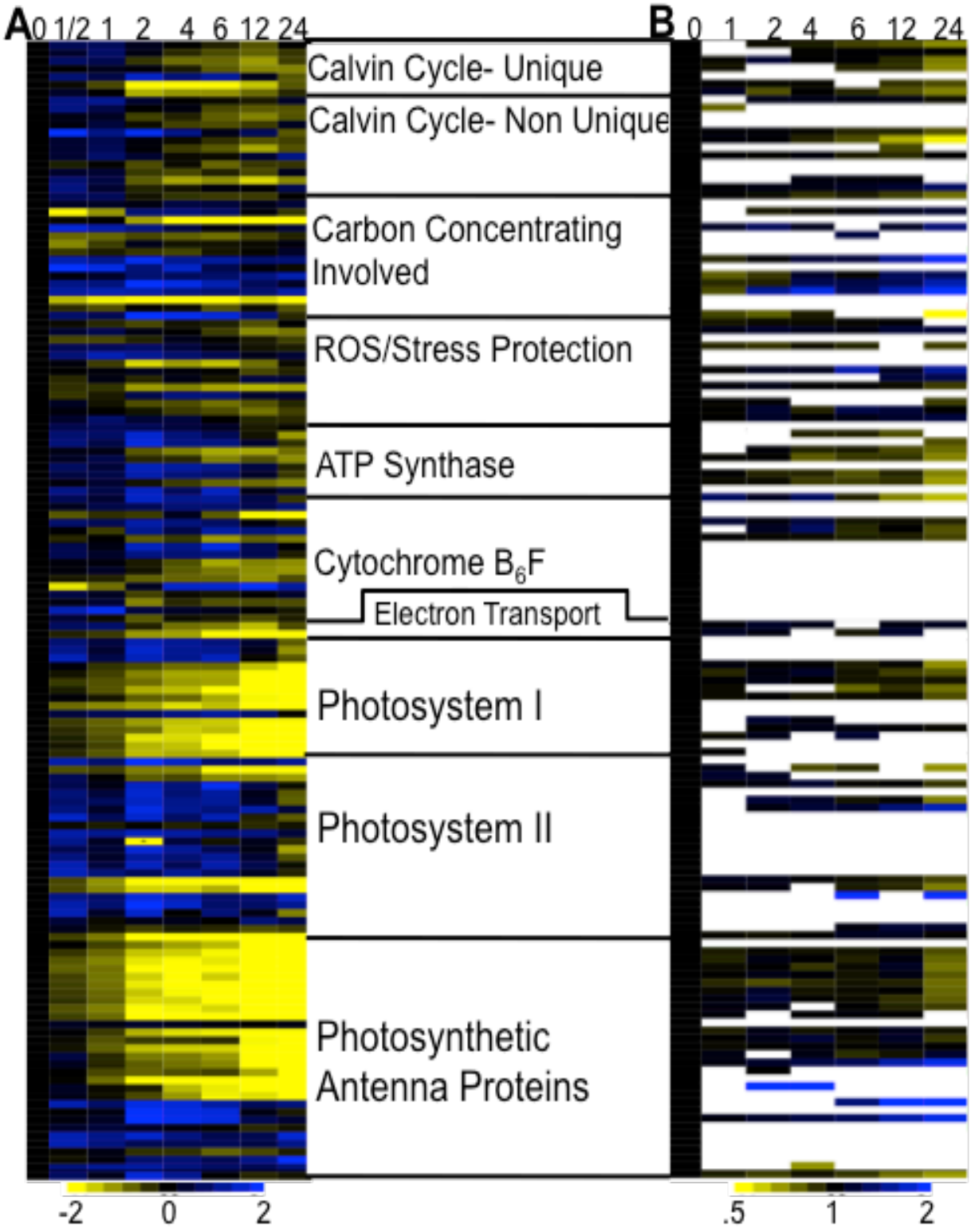

Figure 2.1. Photosynthetic transcripts and protein expression

Figure 2.1. (cont'd). Expression levels represented for the first 24 hrs of N deprivation for transcripts (left hand panel) and the corresponding proteins (right hand panel). Details of quantification and validation of transcript and proteomic levels are presented in (Park et al 2014). Expression values are normalized to N replete expression levels with yellow indicating down-regulation and blue indicating up-regulation; the range shown for transcripts is +/- $\log_2$ and for proteins is two-fold up or down. Some expression levels are outside this range and are shown as saturated. Spaces left blank indicate that transcript/ protein detection did not meet the quality criteria for inclusion.

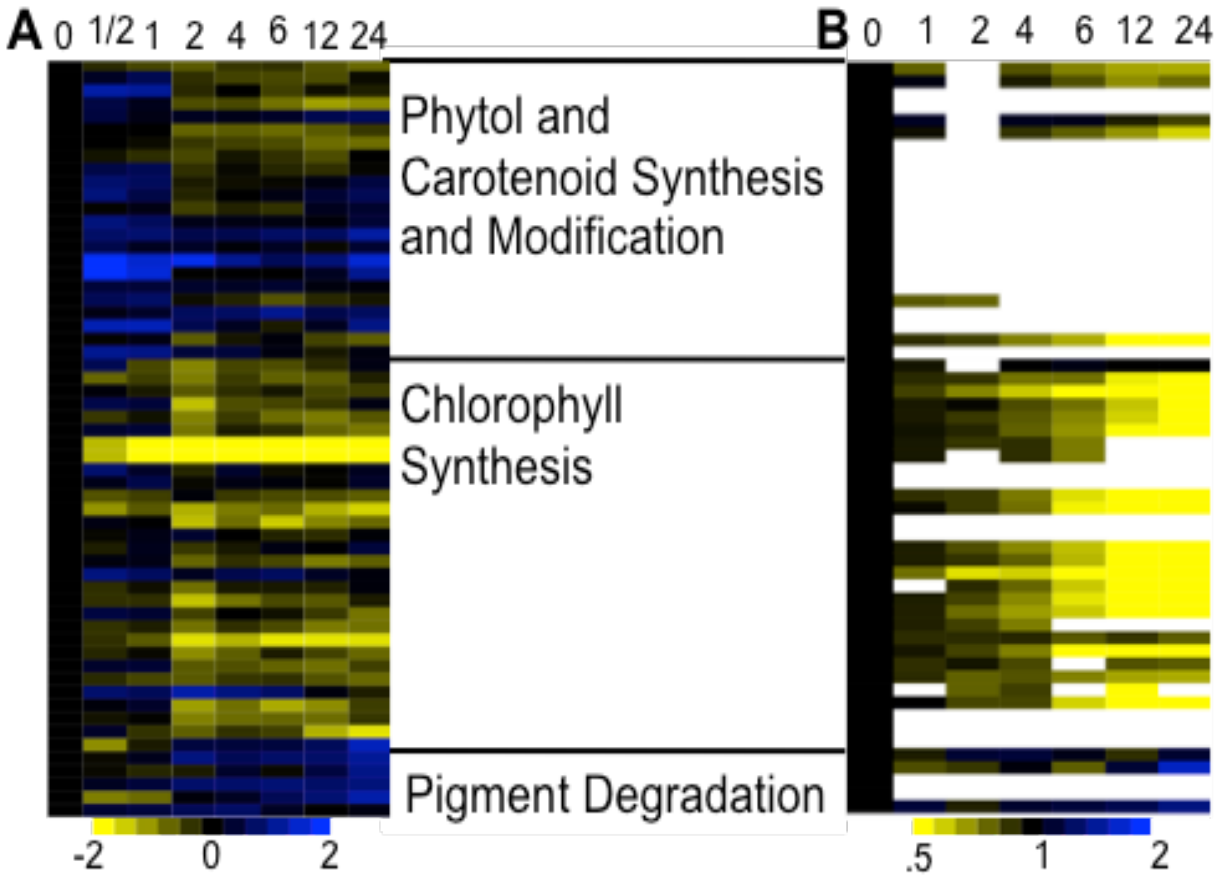

Figure 2.2. The levels of transcripts (A) and proteins (B) of photosynthetic pigment metabolism and starch metabolism. Details of quantification and validation of transcript and proteomic levels are presented in **(Park, et al. 2014).** Expression values are normalized to N replete expression levels. The range shown for transcripts is +/- $\log_2$ and for proteins is two-fold up or down. Spaces left blank indicate that transcript/ protein detection did not meet the quality criteria for inclusion.

In order to analyze gene expression for different functional groups within photosynthesis in a statistically objective manner, Kmeans clustering was performed, which divided the transcripts into 7 different expression patterns or classes (average 2.1 within class variance over 50 iterations) (Fig 2.3A). Agglomerative hierarchical clustering of the expression classes demonstrated 4 overarching expression trends with Classes 5, 3, 2, and 7, clustering together and class 6; class 1; class 4 by themselves. The distribution of the genes for each functional group across the expression pattern classes (K-means classes) are shown in Fig2.3B and the

contribution of genes from each functional group to the different K-means classes is shown in Fig 2.3C.

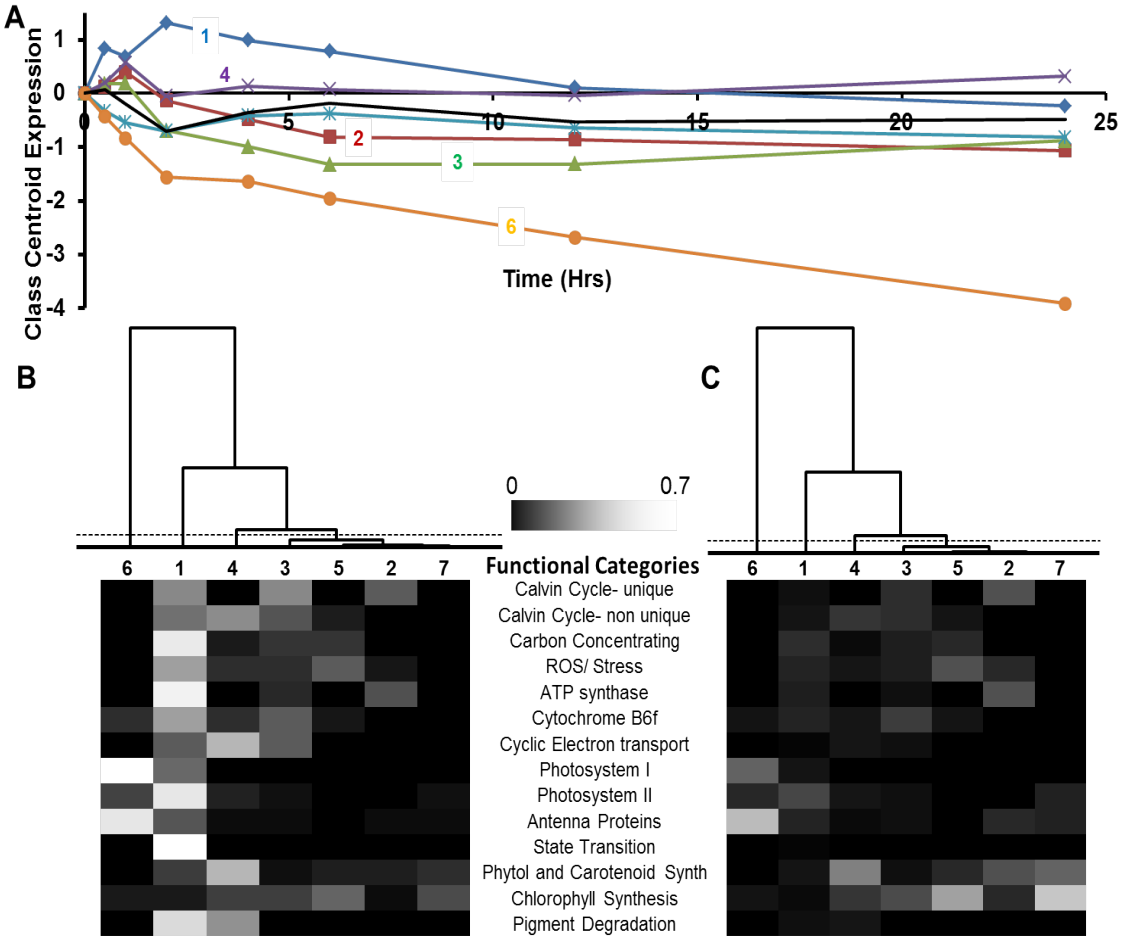

Figure 2.3. Statistical analysis of photosynthetic transcripts. A) K means clustering class centroid expression (log fold change (+/- $\log_2$)) of classes derived from statistical analysis. Class1:blue diamond, 2: red square, 3: green triangle, 4: purple X, 5: teal star, 6: orange circle, 7: black cross. Panels B) and C) present heatmaps of class fractional enrichment by functional group member totals (Rows total normalized to add to 1) and class member totals (Columns total normalized to equal 1). 0 member enrichment is indicated by black while enrichment of 0.7 or more is indicated by white. Gene functional categories are listed between panels B and C. Dendograms above B and C heatmaps represent statistical difference between each expression class in Panel A while numbers indicate class number being presented.

The transcript levels for many genes involved in the photosynthetic light reactions decreased within 30 min after N deprivation and continuing to 24 hrs. There are several notable exceptions, especially those found in expression class 1, including genes encoding the Photosystem (PS) II 22kDa protein and cytochrome c6, whose transcripts increased in abundance. Additionally, PSII and PSI genes in general appear in two different expression classes with PSII dominantly in expression class 1 while PSI appears in expression class 6; this difference in photosystem regulation has been found in other organisms (Berges, et al. 1996). The decrease in transcript abundance was greatest for three genes corresponding to oxygen evolution enhancers 1-3 in PSII and for most genes in PSI, with decreases of the order of 10 to 100 fold. Photosynthetic antenna proteins showed 10 to 20 fold decreases in transcript abundance for both light harvesting centers 1 (LHC1) and 2 during the first 24 hrs of N deprivation. LHC stress related proteins LHCSR1, LHCSR2, LHCSR3 (Class1), also involved in non-photochemical quenching (Maruyama *et al.* 2014, Peers *et al.* 2009, Tokutsu *et al.* 2013), increased in protein abundance by 2.5 fold. Transcript abundance for most genes of the Calvin-Benson cycle are found in expression class 1, increasing in the first four h and then dropping to the original values or lower by 24 hrs. Calvin-Benson cycle protein abundances are maintained through 12 hrs and then decrease slightly by 24 hrs.

While PSI and PSII genes were down regulated, genes implicated in both cyclic electron flow (CEF) pathways were upregulated. In the PGR5 mediated pathway, Proton Gradient Regulation 5 (PGR5) and PGR-Like-1B (PGRL-1B), both found in green algae and higher plants, aid transfer of electrons from reduced ferredoxin to plastoquinol (Hertle *et al.* 2013, Johnson *et al.* 2014, Munekage *et al.* 2002, Petroutsos *et al.* 2009). These genes both doubled in

transcript abundance within 1 hr with levels falling to N replete levels by 24 hrs, similar to values reported in (Schmollinger, et al. 2014); protein levels were not reliably quantified. PGRL1 was also found to respond to iron deficiency (Petroutsos, et al. 2009). A type 2 NADPH Dehydrogenase, NDA2, is thought to be responsible for the second CEF pathway in Chlamydomonas (Jans *et al.* 2008, Johnson, et al. 2014). NDA2 Transcript abundances increased slightly by 24 hrs while protein level increased 1.5 fold by 24 hrs suggesting that CEF through this route may increase during N deprivation.

Carbon concentrating mechanism (CCM) related genes (reviewed in Wang *et al.* (2011)) such as the carbonic anhydrases CAH1 (Van *et al.* 1999) and CAH3 and carbon limiting associated genes Carbon Concentrating protein 1(CCP1), CCP2, Low Carbon Induced E(LCIE), and LCI9 showed increased transcript abundance in the first 4 hrs which then decreased, represented by expression Class 1 while protein abundance increased by 24 hrs. This was likewise found in the marine alga *Dunaliella tertiolecta* Butcher (Young *et al.* 2005) and Chlorella (Beardall *et al.* 1982, Beardall *et al.* 1991), where both Fe and N limitation led to an increased affinity for inorganic carbon. Others such as CAH2 showed a decrease in transcript expression over time (Class 7). CAH1 and similar proteins have been found in the periplasm and growth media under ambient air CO_2 concentrations (Coleman *et al.* 1984).

Genes involved with removing radical oxygen species such as Iron superoxide dismutase 1 (FSD1) (Myouga *et al.* 2008) and Catalase 1 (CAT1) (Yoshida *et al.* 2003) showed declines in transcript and protein levels. An exception is GPX5 (a glutathione peroxidase), whose transcript levels increased by ~30% by 24 hrs of deprivation and whose protein abundance increased ~20%. GPX5 is known to metabolize peroxide, and like other oxidative stress response genes is

known to be up regulated under photosynthetic stress conditions like high light (Fischer *et al.* 2009). Protein levels followed transcript changes 6 to 12 hrs after N deprivation.

Questions have been raised about the importance and mechanisms of alternative electron acceptor pathways, such as chlororespiration, in regulating photosynthetic energy fluxes during N deprivation (Peltier *et al.* 1991). The alternative oxidases, plastid plastoquinol terminal oxidases 1 and 2 (PTOX1, PTOX2), are thought to be involved in the chlororespiration in Chlamydomonas (Bailleul *et al.* 2010, Houille-Vernes *et al.* 2011, Rumeau *et al.* 2007) and changes in protein and transcript abundance have been found to be associated with nutrient deprivation in algae, particularly iron deprivation (Cardol *et al.* 2008) as well as light stress (Houille-Vernes, et al. 2011). PTOX1&2 transcripts decreased in abundance 1.5 fold within the first half hour but then increased through 24 hrs to slightly less or greater than N replete conditions. PTOX2 protein values increased 2.4 fold by 24 hrs suggesting that during N deprivation, in addition to linear and cyclic electron transport being down regulated, additional electrons are returned to oxygen, which may help to regulate the ATP/NADPH ratio and photosynthetic output (Peltier, et al. 1991). This may help explain why we observed only minor decreases in the oxidation level of PSII primary quinone A (Q_A) (Figure 2.8D, below).

Pigment levels and their regulation

Chlorophyll content decreased during N deprivation with levels dropping from ~33 $\mu g \cdot mg^{-1}$ cell dry weight (CDW) to less than 10 $\mu g \cdot mg^{-1}$ CDW after 24 hrs of N deprivation (Fig.2.4A), with decreases being most rapid soon after deprivation. Chl content per million cells (Fig 2.4B) fell from 0.9 to 0.63 μg Chl/million cells within the first 12 hrs and then declined more slowly to 0.43 μg Chl/million cells by 48hrs. The ratio of Chl *a* to Chl *b* was not

significantly altered. However Figure 2.4 B shows that Chl levels per culture volume were initially unchanged after N deprivation, and decreased rather slowly after 6 hrs.

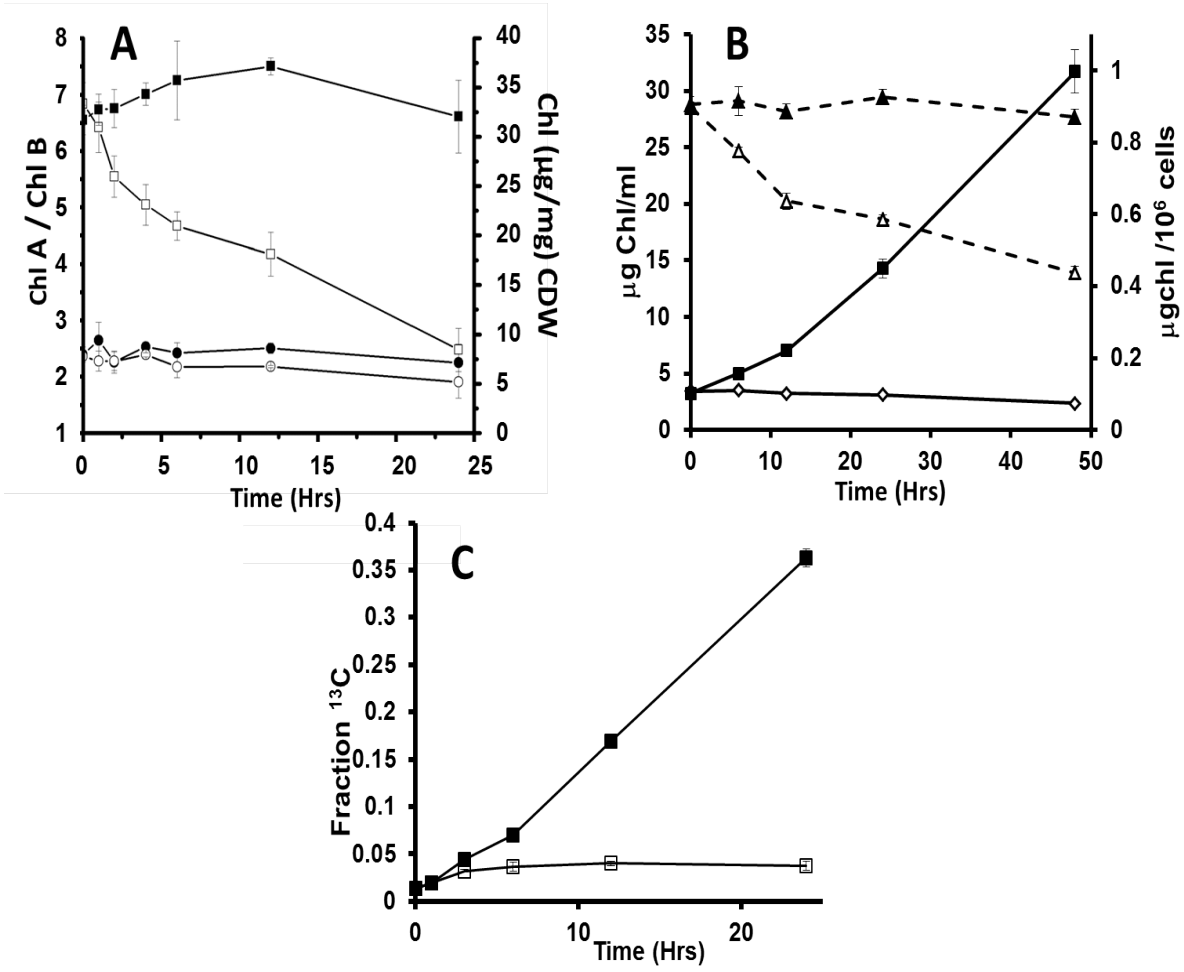

Figure 2.4. Chlorophyll concentrations and synthesis. (A) Chl concentration per cell dry weight (CDW) in N replete and N depleted cultures (solid and open rectangles respectively). The ratio of Chl *a* to Chl *b* for N replete and N depleted (solid and open circles respectively). (B) µgChl per culture volume of N replete (solid square) and N deplete (hollow square). (C) ^{13}C incorporation into phytol chains (as percent of molecules containing ^{13}C label) in N replete and N depleted cultures (solid and open rectangles respectively). Error bars indicate standard deviation, N=3

Chl synthesis genes for both the porphyrin ring and phytol chain were rapidly down-regulated at both the transcript and protein levels with transcripts falling by one half and proteins by ~30% of initial values by 2 hrs, while transcript abundances for Chl catabolic genes, such as chlorophyllase, were significantly elevated after 1hrs. ^{13}C labeling and analysis of phytol ^{13}C contents was therefore used to follow Chl synthesis rates during N deprivation (Fig. 2.4C). N depleted cells supplied with ^{13}C acetate incorporated ^{13}C into Chl or phytol only within the first 3 hrs, indicating that *de novo* Chl synthesis ceases soon after N deprivation. This, together with the continued growth (cell division continued for 12 hrs after N deprivation substantial rates of biomass increase continued beyond that), is sufficient to account for the large decreases in Chl content over the first 24 hrs without significant Chl degradation. It has been suggested that Chl decreases following N deprivation in cyanobacteria are due to dilution from cell growth (Collier, et al. 1992) which we demonstrate here with ^{13}C labeling. Chl degradation has been previously inferred to occur both to remobilize nitrogen (from both Chl and associated proteins) and to reduce light stress (Allen *et al.* 1969, Geider *et al.* 1998).

Carotenoids are involved with light absorption and energy dissipation, reducing radical oxygen species production (Lohr 2009). Within the first 4 hrs of N deprivation, the expression of some carotenoid synthesis and modification genes were strongly upregulated while most stayed at the same level or decreased. After 4 hrs, most of the related transcript abundances decreased, although they were still elevated compared with N replete conditions. Transcript levels of the degradation enzymes carotenoid cleavage dioxygenases 1 and 2 were elevated during N deprivation. Carotenoid levels, determined by HPLC at 450nm (Figure 2.5 A-F) showed that levels of the xanthophyll cycle carotenoid violaxanthin (Jahns *et al.* 2012) decreased continuously, being undetectable by 48 hrs, while zeaxanthin levels doubled by 24 hrs relative to

time 0 hrs levels then returned to initial levels at 48 hrs after N deprivation. Levels of other xanthin carotenoids, neoxanthin and loraxanthin, and lutein also decreased after N deprivation with neoxanthin falling to undetectable levels after 48 hrs of deprivation. β-carotene levels showed a trend similar to free zeaxanthin with an increase to 24 hrs then a decrease back to initial values at 48 hrs.

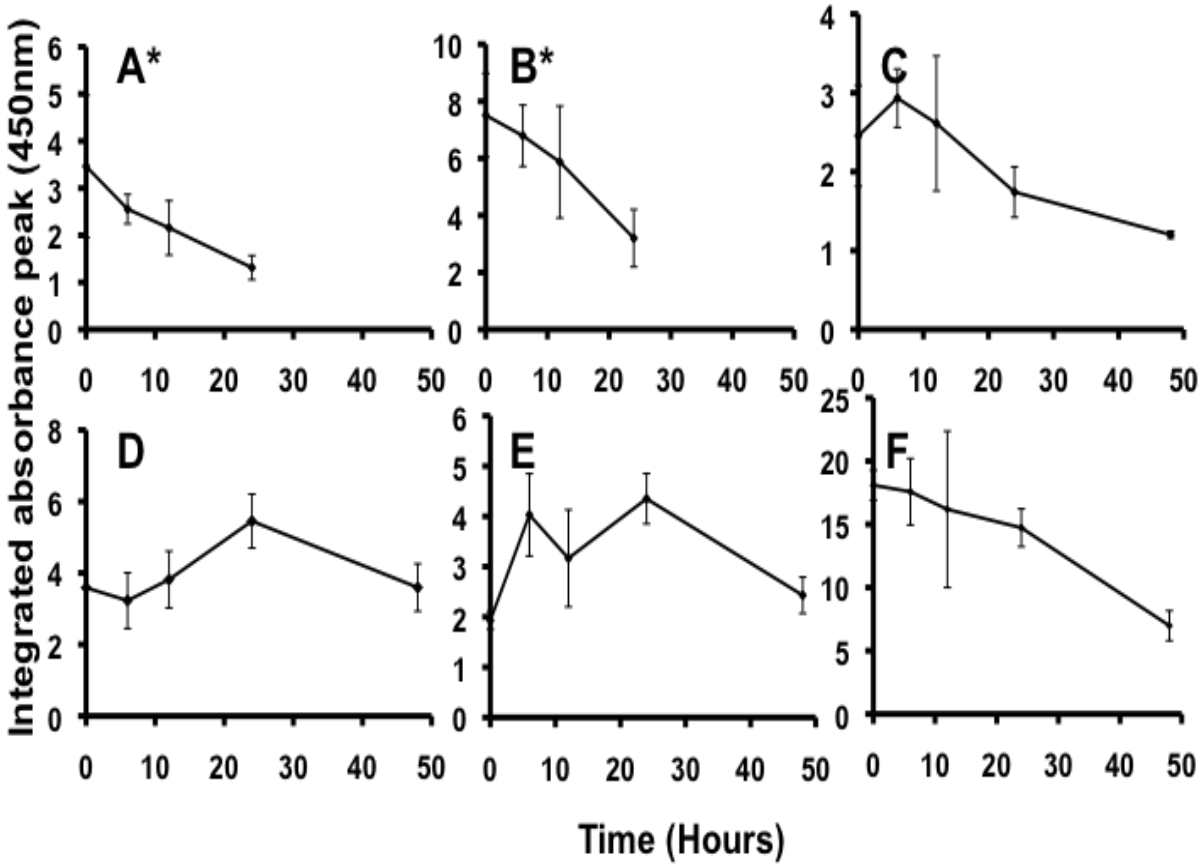

Figure 2.5. Carotenoid levels. Carotenoid levels at successive times following N deprivation determined by extraction, HPLC separation and measurement of absorbance at 450nm compared to authentic standards. A) Violaxanthin, B) Neoxanthin, C) Loroxanthin, D) β-carotene, E) Zeaxanthin, F) Lutein. * Indicates that the pigment was not detected at 48 hrs. Error bars indicate standard error, N=3.

Thylakoid lipid levels and composition

Over the course of N deprivation, we observed a decrease in the levels of thylakoid membranes lipids. This includes the glycolipids monogalactosyldiacylglycerol (MGDG), digalactosyldiacylglycerol (DGDG), and the anionic lipids sulfoquinovosyldiacylglycerol (SQGD), and phosphatidylglycerol (PG) (Benning 2010, Shimojima, et al. 2010). There was a sharp decrease in their levels in the first six hrs and then a more gradual decrease until 24 hrs (Figure 2.6). Proportions of polar (PG, SQGD) and nonpolar (MGDG, DGDG) thylakoid lipid levels did not change, which suggests that the thylakoid membrane composition and charge density are maintained. Thylakoid structure was examined by electron microscopy during the first 48 hrs of N deprivation (Fig. 2.7), revealing that the chloroplast decreases in size, consistent with the decreases observed in plastid membrane lipid levels. Thylakoid stack structure appears normal until at least 72 hrs, which contrasts with the deterioration of cytosolic structure and suggests that photosynthetic capacity is maintained.

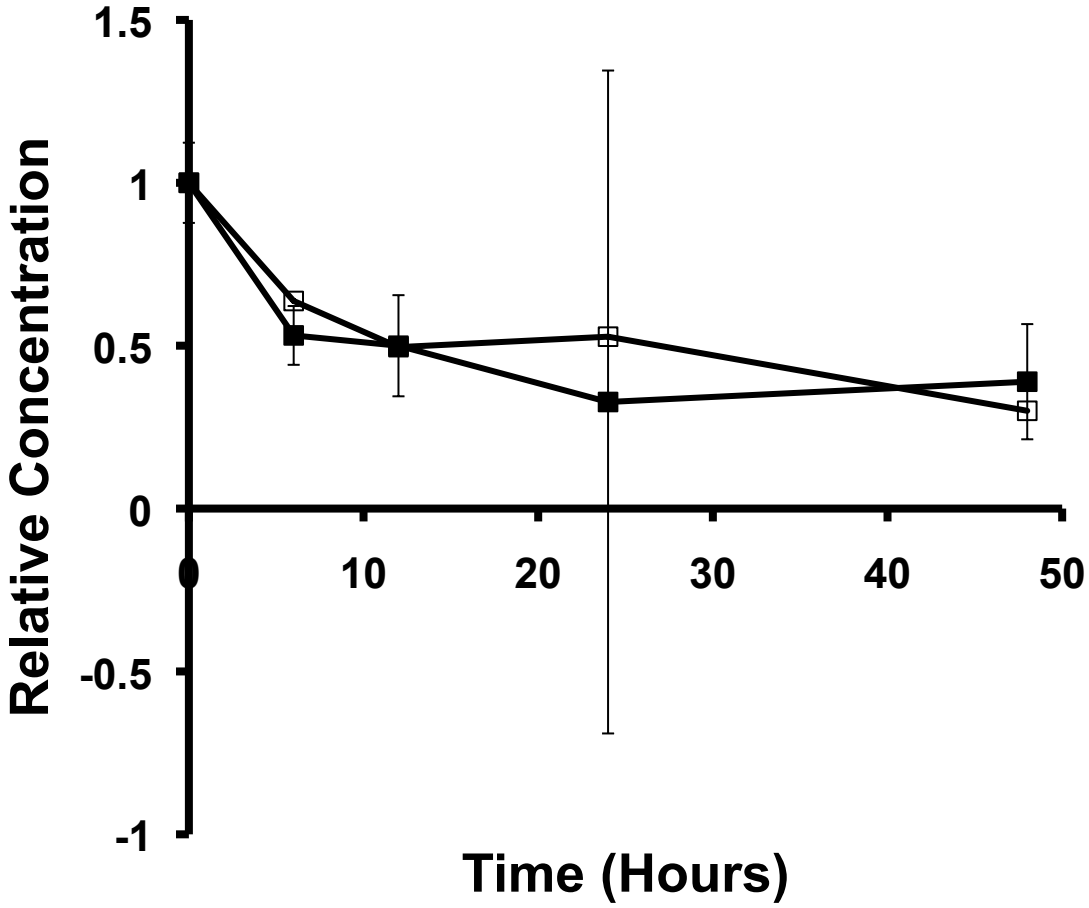

Figure 2.6. Relative changes in thylakoid lipid levels. Thylakoid Galactolipids (MGDG, DGDG) and Anionic Lipids (SQDG, PG) were quantified by high mass resolution mass spectrometry as described in the accompanying paper. Values represent the sum of ion counts for individual members of each lipid class relative to internal standards and then normalized to the values at time 0 hrs (N replete). Filled symbols represent the galactolipids, unfilled ones represent the anionic lipids. Error bars indicate standard deviation, N=3.

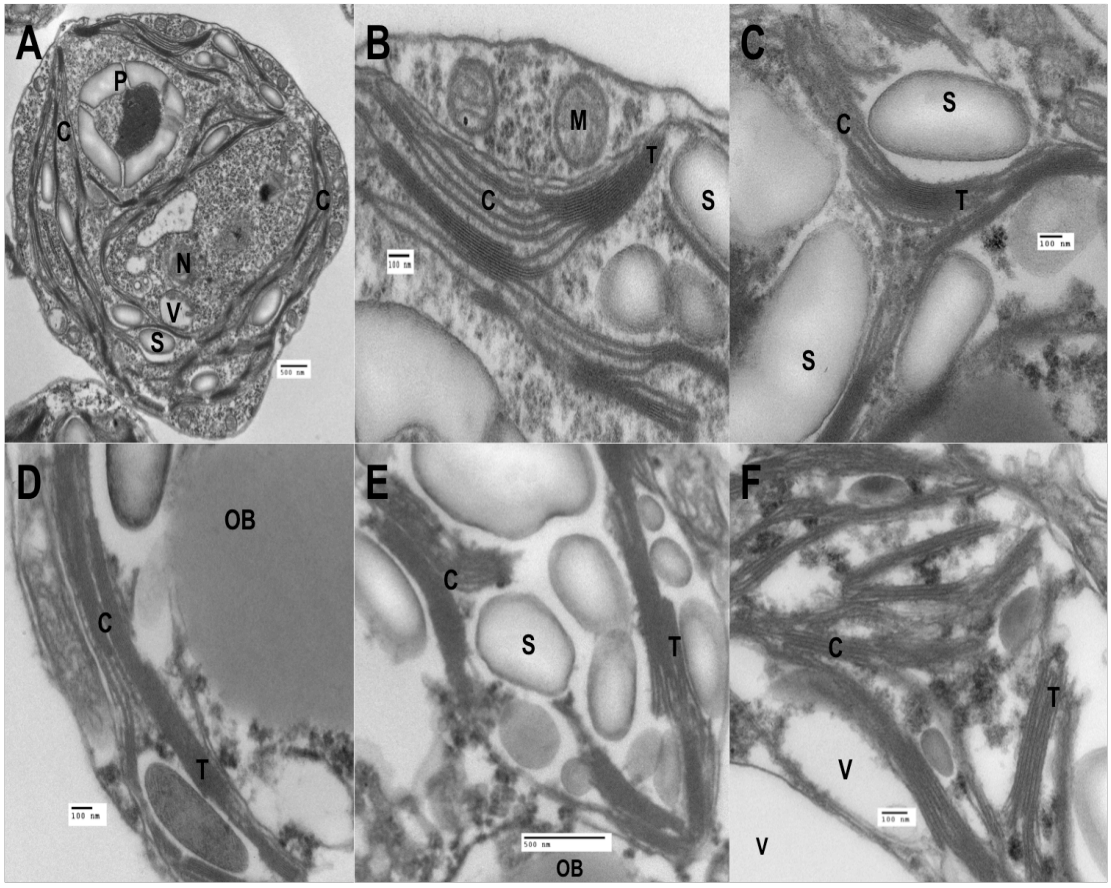

Figure 2.7. Chloroplast Imaging with electron microscopy. Images from left to right: (A) N replete cell, (B) N replete chloroplast, (C) 6 hr N- chloroplast, (D) 12 hr N- chloroplast, (E) 24 hr N- chloroplast, (F) 48 hr N- chloroplast. Bars indicate 100nm except in panels A and E where they indicate 500nm. **C**) Chloroplast; **M**) Mitochondria; **N**) Nucleus; **OB**) Oil Bodies; **P**) Pyrenoid; **S**) Starch; **T**) Thylakoids; **V)** Vacuole.

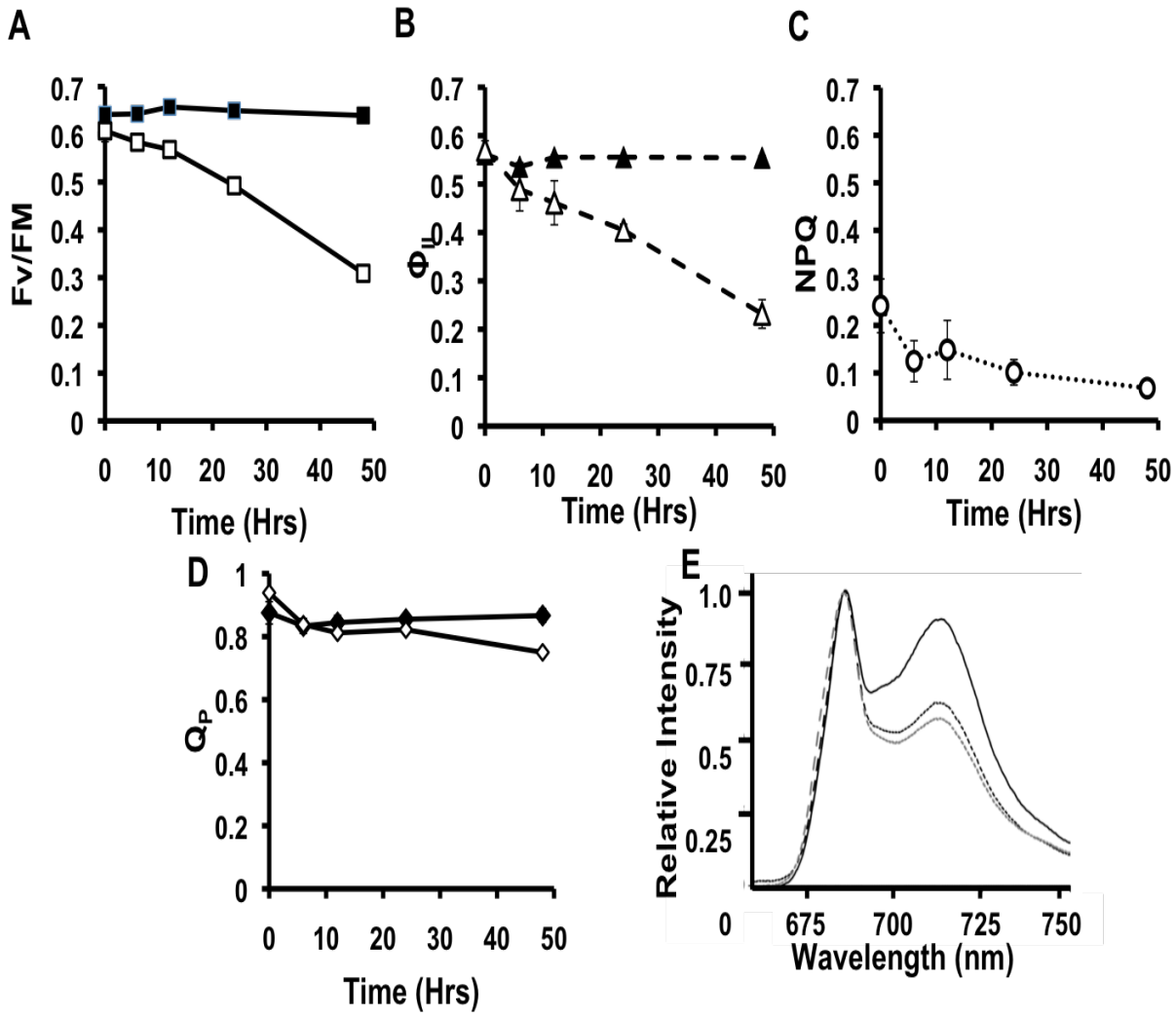

Figure 2.8. Photosynthetic fluorescence functional measurements. (A) Fv/Fm, (B) Φ_{II}, (C) NPQ, (D) qP, and (E) 77K fluorescence. Contribution to efficiency decreases were measured through Chl fluorescence experiments over 48 hr of N deprivation using PAM fluorimetry. For A, B, C, & D: solid shapes indicate N plus while empty shapes indicate N minus. (E) 77K fluorescence spectra during N deprivation. Control (solid black line), 6 hr N- (black hashed line), and 24 hr N- (gray hashed line) are shown. PSI associated fluorescence (maximum at 715nm) decreased markedly from 95% to 65% (±1%) of the fluorescence intensity at PSII (maximum at 685nm) by 6 hrs and then decreased slightly (58 ±7%) by 24 hrs. Not shown are 48 hrs and 72 hrs curves which had fluorescence signals at 715nm with 64% and 66% (±3%) of the signal at 685nm respectively. Error bars indicate standard deviation, N=3. 77K data presented as average of three measurements.

Energy capture and conversion is down regulated during N-deprivation

We used chlorophyll fluorescence spectroscopy to assess photosynthetic function during N deprivation. Over the 48-hour N deprivation time-course a slow, approximately linear, decrease in the theoretical maximum quantum efficiency of photosystem II (Fv/Fm, (Baker 2008)) occurred. After 24 hrs Fv/Fm was ~85% that of N replete values and at 48 hrs it was ~75%, similar to the levels reported by (Schmollinger, et al. 2014) and (Li, et al. 2010). The operating quantum efficiency of photosystem II photochemistry in the light (Φ_{II}) (Baker 2008, Genty *et al.* 1989) decreased continually after 6 hrs reaching close to half the initial value by 48 hrs (Fig. 2.8B). In N replete cells Φ_{II} was 15% lower than the Fv/Fm theoretical maximum while N deprived Φ_{II} was almost 55% lower. Non-photochemical quenching (NPQ) during N deprivation was also measured (Fig. 2.8C), showing that in N deprived cells, NPQ decreased from ~0.3 to ~0.07 by 48 hrs.

In PSII, the efficiency of electron transfer is partly dependent on the number of open/ oxidized quinone A (Q_A). qP and qL are two parameters used to describe the percent of open PSII reaction centers (oxidized Q_A pool) (Kramer *et al.* 2004). During N deprivation, qP fell from 0.93 to 0.82 in 6 hrs and further to 0.75 by 48 hrs indicating a decrease in the abundance of open reaction centers while in N replete control cultures its levels remained constant throughout the timecourse (Fig. 2.8D). qL is similar to qP, except that it takes in to account the lake model of shared light harvesting centers, in these experiments its values were ~1-2% lower than qP. Both qP and qL demonstrated that the Q_A pool was increasingly reduced over time (Figure 2.9)

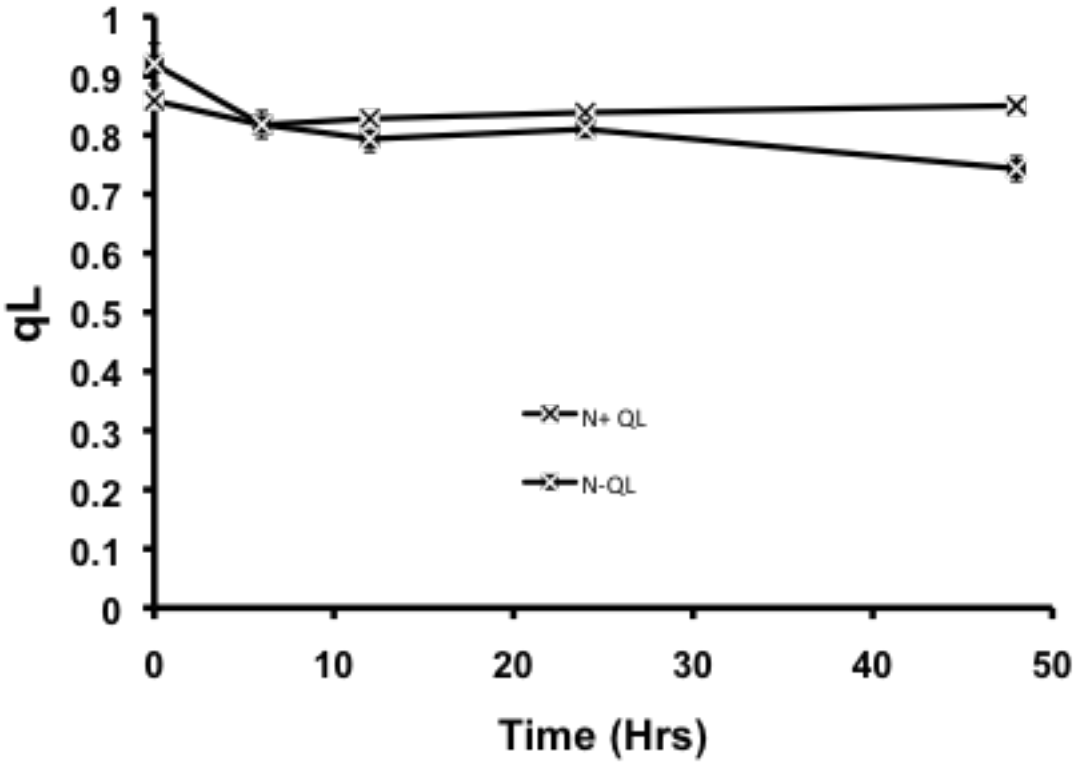

Figure 2.9. qL. Relative amount of oxidized Q_A based upon the lake model. Error bars indicates standard deviation, N=3

To probe potential changes in the allocation of light energy between photosystems, 77K fluorescence spectra, which are a measure of the amount of light harvesting complex chlorophyll associated with different photocenters, were acquired (Fig. 2.8E). A substantial fall in the fluorescence peak at 715nm relative to the PSII peak at 685nm was observed at 6h and beyond (consistent with previous reports in nitrogen limited Chlamydomonas (Plumley *et al.* 1989a)). STT7 (Class1), a protein kinase responsible for inducing state transitions and adaptation to different light conditions (Depege *et al.* 2003), increased threefold in transcript abundance within 2 hrs then returned to initial levels by 24 hrs while its protein levels decrease from 6hrs to 24 hrs.

77K spectra and protein data suggest a decreasing role for state transitions during N deprivation. Alternatively, the 77K spectra could represent rapid remodeling of antennae and photocenter arrangements.

Oxygen evolution

Photosynthetic oxygen evolution in the light and its consumption immediately upon transfer to the dark were measured over the N- time course (Fig. 2.10A). Under the growth conditions of this study (160 microEinsteins (uE m^{-2} s^{-1}), light driven gross oxygen evolution and consumption rates per cell decreased by half in the first 12 hrs with minor decreases through 48 hrs. Similar trends in oxygen exchange rates were recently reported by (Schmollinger, et al. 2014) using higher light levels for measurement than for culturing. Thus the electron flux through PSII was down regulated over the first 24 hrs after nitrogen deprivation, and this can be accounted for by the measured decreases in the efficiency of PSII and Chl levels.

Total PSI turnover rate falls during N deprivation

The absorbance changes at 705nm under PSII inhibited conditions are proportional to the oxidation/reduction of PSI (Alric 2010, Johnson *et al.* 2012). These P700 absorbance changes shown in Fig 2.10 are attributed to redox turnover at PSI due to cyclic electron flow (CEF, Fig. 2.10B). Thus CEF rates fall by ~50% over 48hrs when expressed on a per cell basis when expressed on a per Chl basis the decreases are more modest. This indicates that cellular rates of CEF fall more because of decreases in the numbers of photocenters per cell (as reflected in chl levels) than because of the turnover rates of each photocenter.

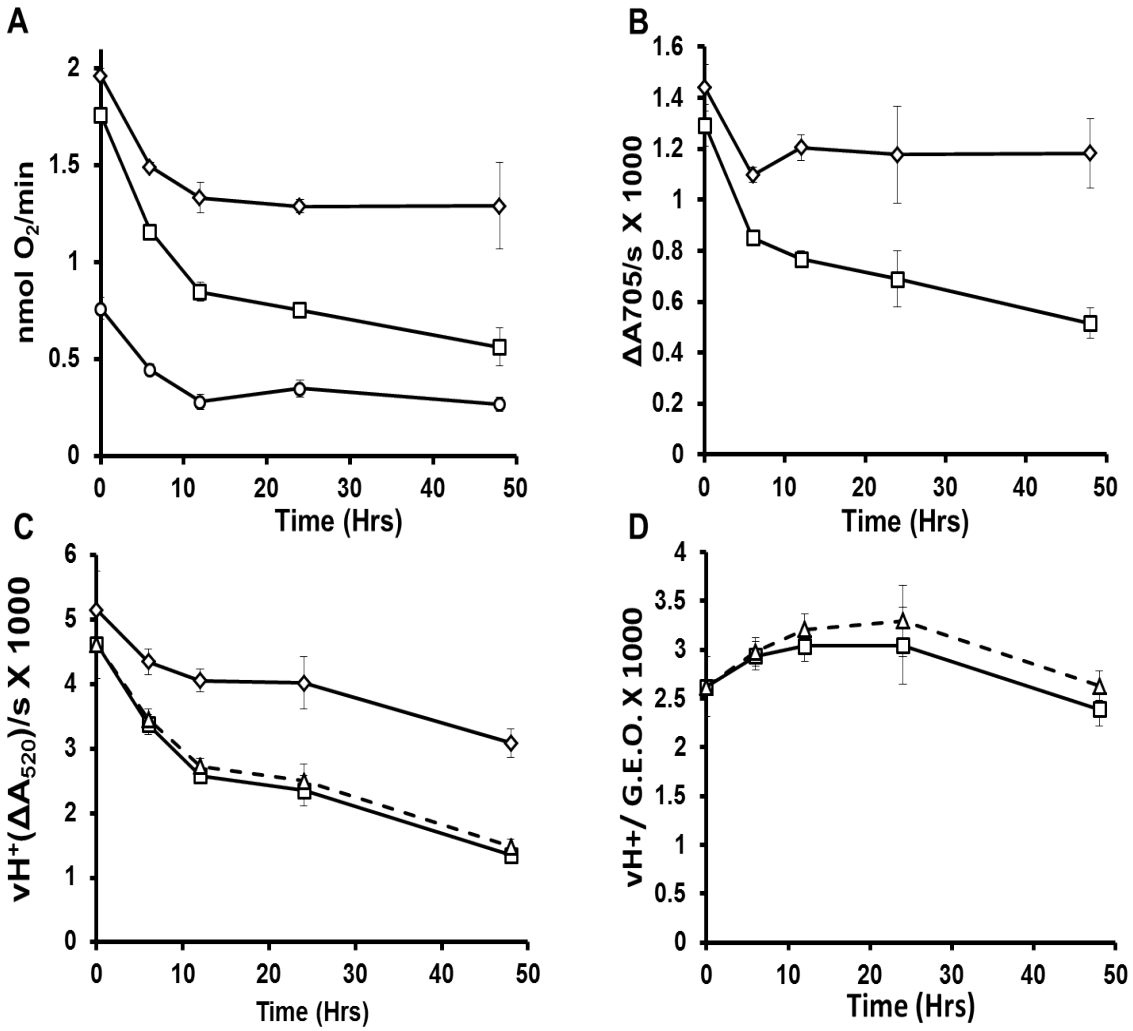

Figure 2.10. Oxygen evolution, ECS, and P700 spectroscopy. For A, B, and C, hollow squares indicate per million cells and hollow diamonds indicates per µg Chl. (A) Gross Oxygen evolution and consumption (open circle) (nmol/min), (B) P700 (ΔA_{705} /s) X 1000, (C) v_H^+ (ΔA_{520} /s) X 1000 (Hollow triangle, dashed line indicates samples normalized to PSII inhibited P700/ECS ratios), (D) v_H^+ / Gross evolved Oxygen (G.E.O.) X 1000. v_H^+/ G.E.O: hollow square, solid line, dashed line; v_H^+ / G.E.O. normalized to PSII inhibited P700/ v_H^+ ratios: hollow triangle.. Error bars indicate standard deviation, N=3

Electrochromic shift measurements to probe thylakoid proton motive force and fluxes

The electrochemical potential across thylakoid membranes was assessed using electrochromic shift (ECS) induced absorbance changes at 520nm (Avenson *et al.* 2005, Bailleul, et al. 2010, Lucker *et al.* 2013). When pigments are immobilized within an electric potential, a shift in the dipole moment can be induced and changing the spectral properties of the pigment absorbance changes during brief periods of dark are due to the dissipation of the thylakoid proton motive force (*pmf*). This is believed to occur primarily through proton translocation through the ATP synthase. The initial slope of ECS induced absorbance change during light to dark transitions give estimates of total proton efflux ($\boldsymbol{v}_{\mathbf{H}}^{+}$) during steady state photosynthesis. Figure 2.10 C shows that $\boldsymbol{v}_{\mathbf{H}}^{+}$ decreased by ~50% in the first 12hrs after N deprivation, then another 20% of by 48hrs.

The amplitude of the ECS signal is proportional to the concentration of the relevant pigments and the amplitude of the electrochemical potential. Therefore, to account for any changes in pigment concentrations on the $\boldsymbol{v}_{\mathbf{H}}^{+}$ calculation during the N deprived timecourse, we normalized the ECS signal using the P700 absorbance changes in the presence of DCMU, this was rationalized as follows. Under PSII inhibited conditions, changes in absorbance at 705nm during light to dark transitions are directly proportional to PSI turnovers under PSII inhibited conditions, and are linearly proportional to the ECS_{520} signal (Lucker, et al. 2013). We can therefore calibrate changes in the ECS signal due to pigment changes with the PSI signal. The PSII inhibited Δ705nm to Δ520nm ratio (Figure 2.11) was found to increase only approximately 10% by 48 hrs, demonstrating that pigment changes had minimal impact on measured ECS absorbance changes over the time course and allowing greater confidence in the estimates of proton flux. Normalized υH^{+} is presented in Figure 2.10C.

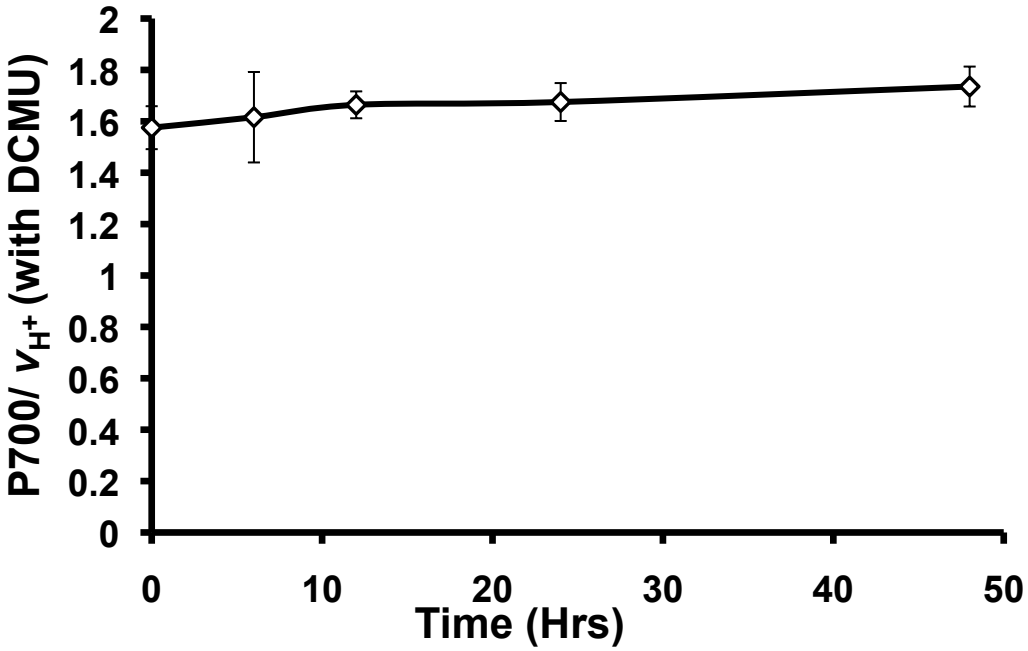

Figure 2.11 PSII inhibited P700/ υH^+ during N deprivation. Error bars indicates standard deviations, N=3

To determine the relative contributions of linear and cyclic electron flows to total photosynthetic electron, we compared v_H^+ to gross evolved oxygen rates (G.E.O) during nutrient deprivation in. Figure 2.10D shows that during N deprivation, v_H^+ / G.E.O increases ~15% by 24 hrs indicating modest increases in the contribution of CEF relative to LEF to the chloroplastic pmf. From 24 to 48 hrs, v_H^+/ G.E.O decreased to N replete levels. Calibrated v_H^+ / G.E.O shows a small increase in favor of CEF vs. LEF over the timecourse, most significant at 24 hrs.

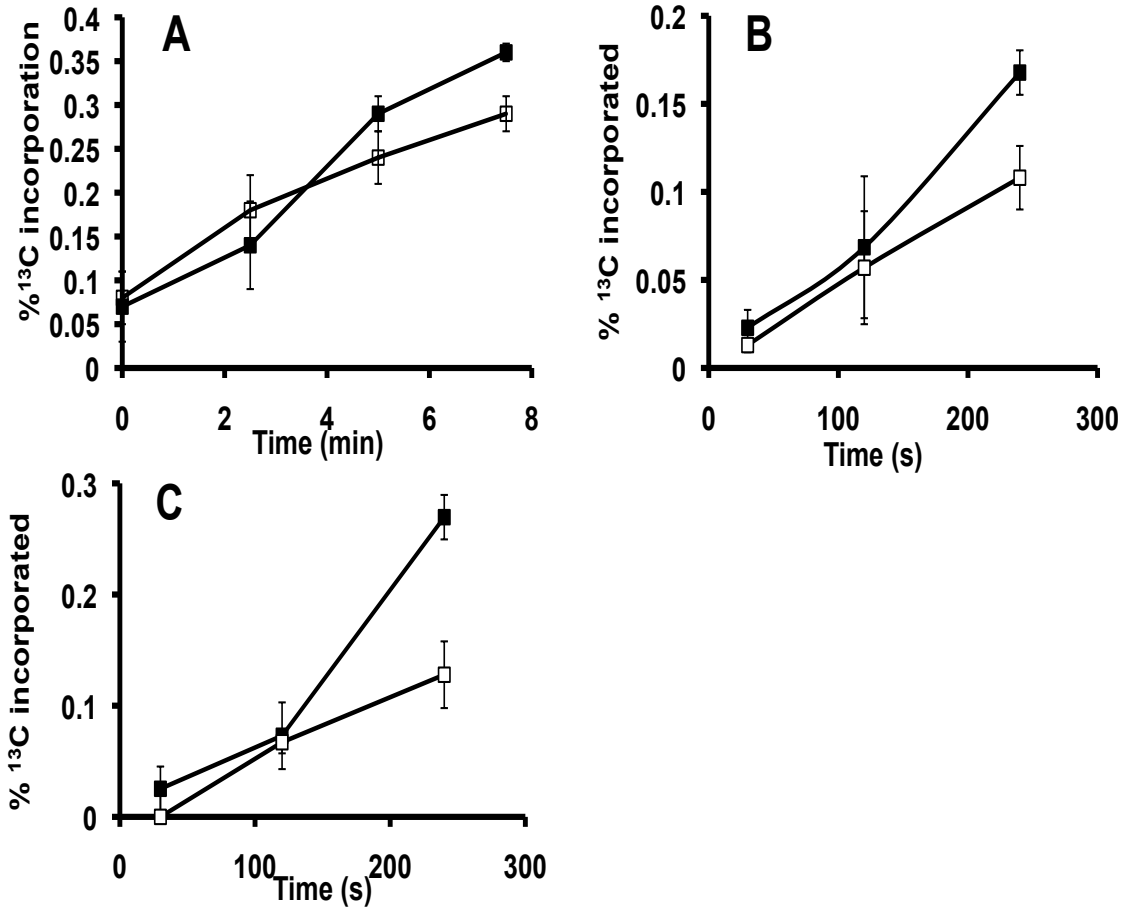

Figure 2.12. **^{13}C Incorporation.** Time course of ^{13}C incorporated into glucose-6P (A), glycine (B), and serine (C) after addition of ^{13}C bicarbonate to *Chlamydomonas* cultures in TAP medium deprived of N for 6 hr. The proportion of molecules containing ^{13}C label was determined by GC mass spectrometry after rapid quenching of cells in -70^{o}C methanol and subsequent extraction. Error bars indicate standard deviation, N=3

Photosynthetic carbon fixation

Steady state ^{13}C labeling experiments showed that under nutrient replete conditions, photosynthetic carbon fixation contributed approximately a third of carbon used for growth. To assess changes in flux from photosynthetic carbon fixation into soluble metabolite pools, cells were pulse-labeled with ^{13}C bicarbonate before or 6 hrs after N deprivation (Figure 2.12) The rate of labeling of glucose-6-phosphate and particularly of glycine and serine, was reduced by between 15 and 50% within 6 hrs of N deprivation, indicating that fluxes through the photosynthetic dark reactions of the Calvin cycle are substantially reduced before any significant changes in the relevant enzyme levels.

Starch Synthesis

In Chlamydomonas, N deprivation induces the accumulation of starch sooner and to a greater extent than TAG, (Fan, et al. 2012, Siaut, et al. 2011). Starch levels (Figure 2.13), show a linear increase starting within 6 hrs and increasing from 5μg/million cells to ~25μg/million cells by 48 hrs. Transcripts for genes related to starch synthesis (2.13A) especially soluble starch synthase I, are up regulated within 30 minutes of N deprivation while most genes related to starch degradation were down regulated early on. The levels of most of the corresponding protein closely followed changes in transcripts. Interestingly, the expression of some starch degradation genes, including many starch binding and debranching enzymes, are upregulated after 4 hrs. Such findings suggest that the starch pool may be turned over during N- which would point to starch metabolism having more than a simple storage function. Starch turnover has been demonstrated during normal growth (Klein 1987) and has been suggested to occur during N deprivation based on observations on starch breakdown mutants (Tuncay *et al.* 2013). Starch

accumulation occurs during a time when cells are downregulating photosynthesis, decreasing carbon fixation, and reducing ATP and NADPH production. While oxygen production rates before N deprivation are sufficient to sustain the initial starch accumulation rates, within ~12 hrs this is no longer the case and we therefore suggest that starch accumulation is not primarily driven by photosynthetic carbon or energy overflow under these conditions.

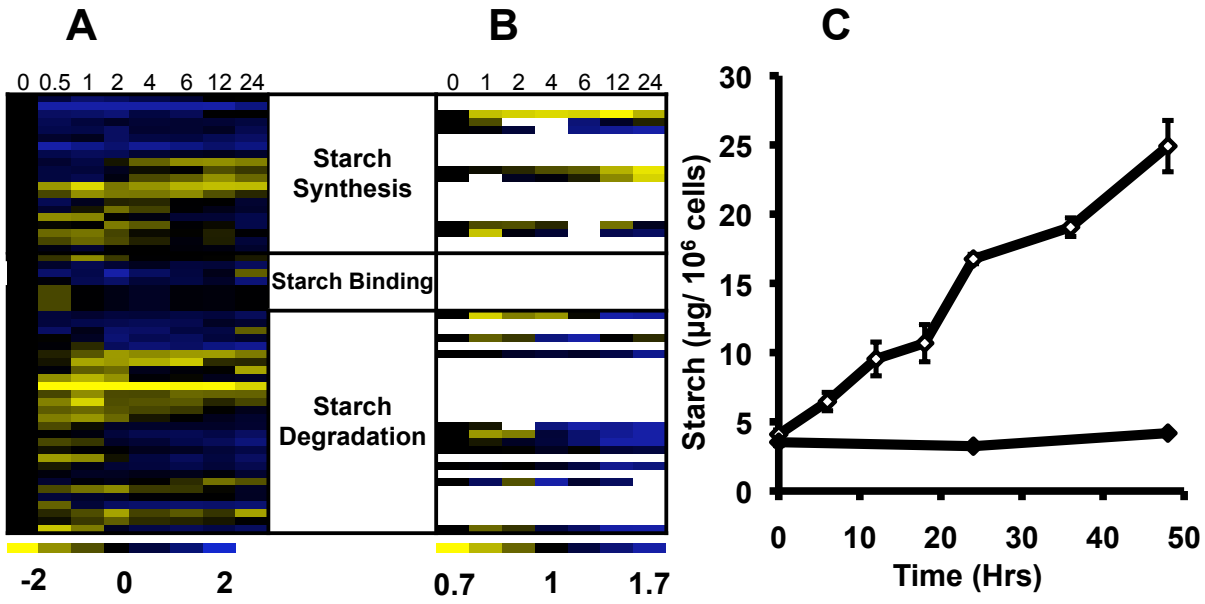

Figure 2.13. Starch Analysis. Transcript (A) and protein (B) abundance values over a 24 hrs N-time course for genes related to starch metabolism. Transcript values expressed as log fold change, and protein values expressed as ratios of value at time point to original value at time = 0 hrs; both follow the color scales denoted below their respective panels, with blue representing an increase in expression and yellow representing a decrease. Panel C shows N replete (solid diamonds) and starved (hollow diamonds) starch levels in µg per10^6 cells. Error bars indicate standard deviation, N=3.

DISCUSSION

Regulation of Photosynthetic Activity

When microalgae are deprived of nitrogen or other inorganic nutrients, growth slows, photosynthesis is down regulated, and starch and oil accumulate. Pronounced and rapid decreases in transcripts for most genes encoding the photosynthetic complexes, electron transport, light harvesting centers, photosynthetic pigments, and the Calvin-Benson cycle were observed here and in other studies (Blaby, et al. 2013, Miller, et al. 2010, Schmollinger, et al. 2014) pointing to a central role for transcriptional regulation in reducing photosynthetic rates. Protein levels for many of these genes also decreased, albeit to a substantially lesser extent and with delays generally in the 6 to 12 hr range. However, analyses of photosynthetic energy fluxes and of ^{13}C labeling rates show that regulation at the post translational level is at least as important as expression changes in the short term response to nutrient deprivation. Thus photosynthetic CO_2 fixation and chlorophyll synthesis rates are both markedly inhibited before the corresponding protein levels are significantly decreased. Likewise, the timing of changes in the photosynthetic apparatus and in electron and proton fluxes does not correlate with the expression levels of the relevant genes. For example as a whole, expression of almost all PSI genes are decreased relative to that of PSII genes, whereas CEF fluxes at PSI increase relative to LEF, which are initiated at PSII. Another significant posttranslational change is the relative partitioning of light harvesting complexes between the photosystems, which occurs within 6 hrs, before the levels of the antennae proteins have changed significantly. Post-translational regulation of photosynthesis is known to be important in a range of stress responses as well as in diurnal changes (de Vitry *et al.* 1989, Geiger *et al.* 1994, Pfalz *et al.* 2012, Turkina *et al.* 2006). Such changes include structural modifications of individual proteins and photosynthetic complexes as well as allosteric regulation of enzyme activities.

Differential Regulation of PSI and PSII

It has been reported that PSI and PSII respond quite differently during N deprivation with PSII protein and activity decreasing more than that of PSI (Berges, et al. 1996, Plumley, et al. 1989a, Wykoff, et al. 1998). Plumley et al. 1989 (in Chlamydomonas) and Berges et al 1996 (in *Thalassiosira weissflogii*, *Dunaliella tertiolecta*, and Synechococcus), concluded that "the major effects of nitrogen deprivation are in PSII" and that "there is a relatively large capacity for cyclic electron flow" under these conditions. Similarly, Wykoff et al. 1998 studying Chlamydomonas under S and P deprivation found that "electron flow was inhibited at PSII, whereas PSI activity was essentially unchanged in starved cells". By using multiple measurement methods of to assess photosynthetic fluxes we conclude that under the culture conditions used, fluxes through the two photosystems are both reduced, and that while linear electron fluxes fall more than cyclic ones in the first day of nutrient deprivation, the difference is much less dramatic than previously concluded.

At the transcript level PSII gene expression is increased within 2 hrs of N deprivation (Class1) while PSI transcript levels are fall (Class 6). This suggests that PSII protein levels should stay higher longer than PSI, however this is not the case. Second, from 77K fluorescence data we find a higher proportion of chlorophyll fluorescence associated with PSII than PSI over time, which is the reverse of findings in Nannochloropsis (Simionato, et al. 2013). In contrast, the gross oxygen evolution rate, a measure of PSII activity, decreases somewhat more than the υH^+ during the first 24 hrs, indicating a decrease in the contribution of LEF compared to CEF. From 24 to 48 hrs, there appears to be a rebalancing of photosynthetic electron fluxes with LEF increasing relative to CEF. Interestingly, the maximum quantum efficiency of PSII does not

decrease rapidly suggesting that PSII complexes remain functional and that LEF is being downregulated in another manner partly due to dilution of Chl per cell. As mentioned above, the PTOX protein abundance increases and may be involved in redirecting electrons from linear electron transport towards chlororespiration (Peltier, et al. 1991) while the increases in PGR5, PGRL1B, and NDA2 transcript and protein levels suggest increased CEF capacity (Johnson, et al. 2014). The increase over the first 24 hrs of the proportion of proton efflux apparently driven by CEF implies there is an increase in demand for photosynthetically generated ATP relative to NADPH. We postulate that such a shift reflects a decreasing demand for NADPH for de-novo biosynthesis as growth slows while ATP demands for maintenance and remodeling of the proteome remain closer to those during normal growth.

Photosynthesis is Down Regulated in a Controlled and Orderly Manner

During N deprivation, it has been suggested that photosynthesis induces significant stress via energetic overflows leading to potential oxidative damage, and driving starch and oil accumulation as energy sinks (Hu, et al. 2008, Li, et al. 2012b, Roessler 1990). Consistent with this, GPX5, a gene associated with reactive oxygen species (ROS), was upregulated. The PSBS gene, believed to be involved in NPQ (Bonente *et al.* 2008, Miller, et al. 2010), the LHCSR genes and the PSBA D1 protein are also upregulated and zeaxanthin levels doubled within 6 hrs. While Zeaxanthin accumulation and LHCSR and PSBS upregulation are typically associated with light induced stress and thylakoid acidification (Gilmore *et al.* 1993, Horton *et al.* 1994, Peers, et al. 2009), our other results provide evidence that photosynthetic fluxes are down regulated sufficiently to prevent significant stress. NPQ, which is elevated markedly under photosynthetic stress conditions such as drought or high light exposure (Muller *et al.* 2001,

Niyogi *et al.* 1997), did not increase following N deprivation. It seems likely that the moderate light levels at which Chlamydomonas is cultured, and at which NPQ was measured here are too low to induce significant stress or quenching. Also we observed little or no increase in the levels of ROS related proteins, (with the exception of modest increases in GPX5), which is consistent with a recent study in which no increases in ROS levels were detected during N deprivation in wild type Chlamydomonas (Li, et al. 2012b). Chl levels per cell decrease strongly, and this together with changes in photosynthetic light use efficiency can be estimated to reduce energy capture by approximately threefold within 24 hrs, consistent with the observation of strong reduction in the light-driven oxygen production rate. It is likely that during the first 24 hrs decreased light capture is a more important factor than changes in Calvin cycle enzyme levels or activities in the decreased carbon fixation rates. Also consistent with a picture of an orderly down regulation of photosynthesis that preserves structure and function while avoiding stress from energy overflow are the findings that Chl levels fall by dilution without the induction of degradation, and the same apparent pattern in the decreasing levels of thylakoid membranes, with their proportions and organization in the thylakoid stacks being preserved. The fact that starch and later TAG accumulation increase while photosynthetic energy capture is greatly decreased, suggests that photosynthetic energy overflow may not be the primary driver of storage compound accumulation. Thus for example, maximal starch production rates are achieved before growth rates have slowed significantly. A full energetic and carbon balance under autotrophic as well as mixotrophic conditions would be needed to quantitatively assess the contribution of photosynthesis to storage compound accumulation. As algae in nature commonly face nutrient deprivation (Grossman 2000, Grossman, et al. 2010a, Merchant *et al.* 2012a) it should perhaps

not be surprising that they are able to respond in an orderly manner, preventing substantial energetic overflows and oxidative damage.

METHODS

Culturing

Chlamydomonas reinhardtii strain cc400 cw-15 mt++ was obtained from the Chlamydomonas Research Center and grown at 23 °C in liquid Tris-Acetate-Phosphate (TAP) media (Gorman *et al.* 1965) in flasks shaken at 125 rpm under continuous illumination at 160 μmol photons m^{-2} s^{-1} and ambient CO_2 concentrations. Cell growth was determined by optical density measurements at 750 nm using a DU 800 spectrophotometer (Beckman-Coulter). Cultures were grown to cell densities of between 0.15 and 0.3 O.D. to minimize self-shading which becomes significant in denser cultures. Cells were counted using and Z series Coulter Counter cell and particle counter (Beckman-Coulter). For N deprivation, cells were centrifuged and resuspended in TAP media lacking Ammonium Chloride (nitrogen source). For labeling studies, acetate was replaced with $^{13}C_2$ acetate.

Transcriptomics

Transcript analysis was conducted as described in (Park, et al. 2014), which includes the mapping, parameters for SNP analysis, statistical data tools, and functional annotations. Briefly, cells were harvested by centrifugation at 0^oC and resuspended in RNAlater solution (Qiagen Sciences, Gaithersburg MD, USA) and stored at between -80 and -60^oC; RNA was extracted from two biological replicates for each time point using TRIzol reagent (Invitrogen, Karlsruhe, Germany) according to the manufacturer's protocol. cDNA library preparation and RNA-seq analyses were performed as previously described by He. et al. (He *et al.* 2012).

Proteomics

Cells were harvested by centrifugation and frozen in liquid N. Proteins were extracted and trypsin digested as described in (Wang *et al.* 2012). 100 µg of each digested sample was labeled using 4plex iTRAQ reagents according to the manufacturer's instructions (AB Sciex, Foster City, USA). Two 4plex iTRAQ experiments were performed for each biological replicate of the seven time-points as described in the accompanying paper. Labeled samples from each experiment with iTRAQ labels 114-117 were mixed and fractionated via SCX as in (Alvarez *et al.* 2011). Fractions from 5 to 24 min were analyzed by nano-LC-MS/MS using an LTQ-Orbitrap Velos mass spectrometer (ThermoFisher Scientific, Rockford, USA) coupled with a nanoLC Ultra (Eksigent, Dublin, USA). Mascot Distiller v2.4 was used to process data Mascot Daemon (Matrix Science, London, UK) was used to search data against the *Chlamydomonas* protein database from Phytozome 9 and the Chlamydomonas chloroplast and nuclearsome database from NCBInr (Phytozome 9, 7 Jan, 2013, 17,114 sequences, 12,173,409 residues). The false positives rate of protein identification was assessed with an automatic decoy database search and identified proteins were grouped based on 98% homology with Scaffold v3.1 (Proteome Software, Portland, USA). Full details can be found in (Park et al., 2014).

Annotation and expression analysis

Transcripts and proteins identified during sequencing were filtered for relatedness to photosynthetic function based upon annotation in Phytozome 10.1 (translated from 9.1), Kyoto Encyclopedia of Genes and Genomes (KEGG), the Chlamydomonas sourcebook (Harris E *et al.* 2008). Genes with unknown function were further checked for similarity to arabidopsis protein

and DNA sequences provided on TAIR (The Arabidopsis Information Resource), as well as papers cited in this work.

Kmeans and agglomerative hierarchical clustering for transcript expression was carried out using XLSTAT (Addinsoft) in Microsoft Excel. Kmeans clustering randomly picks a designated number of centroids randomly in the clustering space and then determines the number of members in the cluster based upon their Euclidean distance from the centroid. A new centroid is then calculated based upon the center of each of the clusters and the distance between members and the centroid is calculated again. This is repeated until a true class center is determined. The number of expression classes was chosen based upon least number of classes with least amount of within class variance generated after 500 iterations. Agglomerative hierarchical clustering was then carried out on the expression classes based upon their Euclidean distances between eachother and presented in dendogram format.

Chlorophyll Concentration

Cells were collected by centrifugation of 1 ml culture and Chl was extracted in 1 ml of 80 % acetone for 20 minutes from pelleted samples after supernatant was removed. After extraction, samples were pelleted by centrifugation and the supernatant was used for analysis. Chl was quantified spectroscopically as described in (Ritchie 2006) using a DU 800 spectrophotometer (Beckman Coulter).

Phytol Isotopic Labeling

For determination of Chl synthesis rates, ^{13}C incorporation into the phytol side chain of the Chl molecule was measured using GC-MS. Exponentially growing cells were centrifuged

and transferred to $^{13}C_2$ acetate TAP media with and without N. 2 mL of cells (~0.15 mg CDW) were harvested at various time points. Lipids were extracted with chloroform-methanol (2:1) and dried under a stream of N. The dried lipid extract was saponified using methanolic potassium hydroxide at 100 ºC for 2 h in a 2ml screw capped tube. The unsaponified components which contained the phytol chain was then extracted using hexane and dried under N. The extract was derivatized to its TMS derivative using 50 µL of N-Methyl-N-(trimethylsilyl)trifluoroacetamide with 1 % trimethylchlorosilane (Sigma Aldrich, USA) by incubating at 80 °C for 1 h. One µL of the derivative was injected into the gas chromatography-mass spectrometry (GC/MS) consisting of HP 6890 GC (Hewlett Packard, Palo Alto, CA, USA) equipped with DB-5MS column (5 % phenyl-methyl-siloxan-diphenylpolysiloxan; 30 m × 0.251 mm × 0.25 µm, Agilent, Waldbronn, Germany) and a quadrupole mass spectrometer (MS 5975, Agilent, Waldbronn, Germany). Electron ionization was carried out at 70 eV. The separation was carried out in GC (carrier gas 1.1 mL min^{-1} helium) with the following temperature program: initial column temperature of 100 ºC, increase of 20 ºC min^{-1} until 150 ºC, 4 ºC min^{-1} until 225 ºC, 30 ºC min^{-1} until 325 ºC with a final holding time of 5 min. The inlet and quadrople both had temperature set to 320 ºC and the quadrupole of 320 ºC. The ions 143, 144, 145, 146 and 147 of the mass spectra were monitored, which represent a four carbon fragment of the phytol chain. The obtained mass spectrometric data were corrected for the natural abundance of the elements to give fractional ^{13}C labeling.

Carotenoid Quantification

Folch extracts were analyzed for free carotenoid content via HPLC as described by (Rodriguez-Uribe *et al.* 2012). Extracts were diluted in $CHCl_3$:MeOH (2:1, v/v) and a 20 µL aliquot was separated on an 4.6 x 250 mm YMC carotenoid column. Carotenoid peaks were

detected by a 996 PDA detector 400-600 nm (Waters, Milford, USA), peak detection and integration was performed using the extracted 450 nm absorbance chromatogram. Peak areas were integrated for relative quantification by peak area using the Empower software (Waters, Milford, USA). Astaxanthin, loroxanthin and neoxanthin was identified by comparison of the UV absorbance spectra to their respective referenced UV spectra in the *Carotenoids:Handbook* (Britton *et al.* 2009).

Lipid analyses

Cells were centrifuged at 0^{o}C, lyophilized and total lipids were extracted from ~10 mg of dry cell mass by the method of Folch (Folch *et al.* 1957). Briefly, the lyophilized tissue was weighed into 2 mL eppendorf vials and extracted with 200 µL of $CHCl_3$:MeOH (2:1, vol/vol) shaking on a vortexer for 30 min. The sample was then centrifuged and the supernatant was collected, dried under N and stored at -20 °C until analysis. Thylakoid membrane lipids were quantified by direct infusion into an FT-ICR MS as previously described (Holguin *et al.* 2013).

Electron microscopy

During N deprivation at selected time points, 50ml cells at .2 O.D. 750nm were harvested, pelleted and resuspended in fixation solution of TAP media with + 0.5% glutaraldehyde + 10 µL H_2O_2 to 10 mL, for 1h in the dark at 4°C on a rotary plate. After fixation, cells were pelleted (3500rpm) and then resuspend 0.5 ml TAP media. Cells were packaged at MSU and sent to Cambridge for analysis. Fixed cell samples were then treated with 1% osmium ferricyanide at 25°C for 2 hrs then were rinsed in deionized water five times. Pelleted cells were then treated with 2% uranyl acetate in 0.05M maleate buffer at pH 5.5 for 2 hrs at 25°C. They

were again rinsed in dionized water and dehydrated in an ascending series of ethanol solutions from 70% to 100and then treated with 2 changes of dry acetonitrile and infiltration with Quetol epoxy resin. Sections were cut at 50 nm on a Leica Ultracut S. Samples were stained with uranyl acetate and lead citrate and viewed at 120kV in an FEI Tecnai G2. Images were captured with an AMT XR60B camera using Deben software.

Oxygen evolution and consumption

Changes in dissolved oxygen was measured with an NEOFOX analyzer FOXY-R probe with a FOXY-AF-MG coating (Ocean Optics). Probe was placed in 2 ml of culture in a capped 3ml cuvette with stir bar to keep samples mixed. Net oxygen evolution was measured for 5 minutes at 160 μmol photons m^{-2} s^{-1} and consumption was measured in the dark immediately after the light period for 1 minute. Gross oxygen evolution was calculated as net oxygen evolution minus consumption.

As cells consume acetate in the dark, they are net CO_2 producers during the period of dark adaptation, increasing the concentration of CO_2 and decreasing O_2 during this period. It was found that cells were carbon limited under our growth regime (see chapter three) and adjusting the amount of time cells spent during the dark conditions had an affect on the illuminated O_2 production. While O_2 rates reported in this study were done under as consistent conditions as possible, these values may not represent true growth O_2 production rates.

In vivo spectroscopy

All spectroscopic measurements were performed with biological triplicates at each timepoint. Light-induced absorbance and chlorophyll fluorescence yield were measured using a

kinetic spectrophotometer/fluorimeter (Hall C *et al.* 2011, Livingston *et al.* 2010, Sacksteder *et al.* 2001) modified for liquid samples by replacing the leaf holder with a temperature-controlled, stirring enabled cuvette holder (standard 1 cm pathlength). Cells were treated with a far red light LED (730nm) in otherwise darkness for 20 min to oxidize the plastoquinone pool for accurate F_0 measurements. After dark/ far red adaptation, the first saturating pulse for Chl fluorescence measurements was taken with a pulsed measuring beam (505 nm peak emission LED) filtered through a BG18 (Edmund Optics) glass filter. The sample was then illuminated with 160 μmol photons $m^{-2}s^{-1}$ of photosynthetic photon flux density (PPFD), provided by a pair of light emitting diodes (LEDs) (Luxeon III LXHL-PD09, Philips) with maximal emission at 620 nm, directed towards opposite sides of the cuvette, perpendicular to the measuring beam. Fluorescence yields from saturating pulses were measured under actinic light and averaged over 6 measurements, separated by 120 s intervals. Both absorption and fluorescence measuring pulses were 20-35 μs in duration and attenuated to produce less than 0.1% increase in chlorophyll fluorescence yield in dark-adapted samples. The first dark interval relaxation kinetics (DIRK) trace measuring the electrochromic shift kinetics (one trace per biological replicate) was measured after three minutes of actinic illumination, followed by one minute of actinic light. Actinic LEDs were calibrated using a Licor LI190 PAR quantum sensor.

The kinetics of PSI primary donor ($P700^+$) oxidation/reduction kinetics measurements were performed 5 minutes after the cells had been treated with 10 μM 3(3,4-dichlorophenyl)-1,1-dimethylurea (DCMU, Sigma Aldrich) as described in (Lucker, et al. 2013). Briefly, absorbance changes attributed to P700 redox changes were monitored using a measuring LED (peak emission: 720 nm) filtered through a 5 nm band pass filter centered at 700 nm, giving an emission peak at ~705 nm. A Schott RG695 color glass filter was used to protect the detector

from actinic light. The kinetics of $P700^+$ reduction were measured by the absorbance changes during light to dark transition after 10 seconds of actinic illumination with 160 μmol photons $m^{-2}s^{-1}$.

77K Chl fluorescence emission spectra

Cell cultures were taken directly from the incubator at the specified times and poured into a 3ml styrene cuvette in triplicates at 3μg Chl/ml. The cuvettes were immediately placed in a liquid N filled dewar, freezing the cells, and then stored at -80°C until further analysis. Immediate freezing of samples was important to prevent state transitions. For analysis, cuvettes were placed in a liquid N filled Dewar. A beam of blue excitation light from an LED (peak 440nm) was directed through an optic fiber (Murakami 1997). Fluorescence emission spectra from 187-1110nm were detected using a fiber optic spectrophotometer (USB2000+ UV-VIS, Ocean Optics, Florida, USA) (Hill *et al.* 2012). To determine relative intensity values, data from a TAP media blank was first subtracted. Samples were then normalized to the 685nm (PSII associated peak). PSI associated fluorescence was maximal at 715 nm and was used from comparison between samples.

^{13}C Bicarbonate Labeling

^{13}C bicarbonate from a stock solution was added to a final concentration of 17mM to 400 ml cultures of cells growing with or without N for 6h. Cells were harvested at 0, 1, 2.5, 5, 7, 10 and 15 minutes after the addition of label by quenching 40 ml culture aliquots with 10ml methanol at -80^{o}C. Samples were centrifuged at 0°C, the supernatant discarded and intracellular metabolites were extracted with 100% methanol then extracts were dried under a stream of N_2.

Methoxyamine-pyridine (50 µL of a 25 mg Methoxyamine-HCl/ mL solution in pyridine) was added to the dried extract and incubated for 45 min at 80 °C followed by TMS derivatization as described above for phytol analysis. One microliter of derivative was used for GC-MS. For gas chromatographic separation helium was the carrier gas at a flow rate of 1.1 mL min^{-1} with the following temperature program: initial column temperature of 100 ºC, increasing at 10 ºC min^{-1} to 325ºC with a final holding time of 5 min. The inlet and quadrupole had temperatures of 320ºC. Ions corresponding to TMS derivatives of amino acids and sugar phosphates were monitored and corrected for the natural abundance of the elements to give fractional ^{13}C labeling.

Starch Analysis

Total glucose contained in starch was measured after amyloglucosidase and amylase digestion with the Megazyme total starch anaylsis kit (Megazyme, Ireland), similar to Work et al. (Work, et al. 2010) Briefly, starch pellets remaining after 2:1 methanol:chloroform lipid extraction was autoclaved for 1 hr in 0.1 M Acetate buffer pH 4.8 then was treated with α-amylase and amyloglucosidase for 1 hour at 55ºC. Free glucose was quantitated with a colorimetric assay at 510nm as described in the Total Starch Assay kit (Megazyme, Ireland).

ACKNOWLEDGEMENTS

We thank Dr. Bruria Shachar-Hill for electron microscopy.

REFERENCES

REFERENCES

Allen, M.M. and Smith, A.J. (1969) Nitrogen chlorosis in blue-green algae. *Archiv fur Mikrobiologie*, **69**, 114-120.

Alric, J. (2010) Cyclic electron flow around photosystem I in unicellular green algae. *Photosynth Res*, **106**, 47-56.

Alvarez, S., Hicks, L.M. and Pandey, S. (2011) ABA-dependent and -independent G-protein signaling in Arabidopsis roots revealed through an iTRAQ proteomics approach. *Journal of proteome research*, **10**, 3107-3122.

Atabani, A.E., Silitonga, A.S., Badruddin, I.A., Mahlia, T.M.I., Masjuki, H.H. and Mekhilef, S. (2012) A comprehensive review on biodiesel as an alternative energy resource and its characteristics. *Renew. Sust. Energ. Rev.*, **16**, 2070-2093.

Avenson, T.J., Cruz, J.A., Kanazawa, A. and Kramer, D.M. (2005) Regulating the proton budget of higher plant photosynthesis. *Proc Natl Acad Sci U S A*, **102**, 9709-9713.

Bailleul, B., Cardol, P., Breyton, C. and Finazzi, G. (2010) Electrochromism: a useful probe to study algal photosynthesis. *Photosynth Res*, **106**, 179-189.

Baker, N.R. (2008) Chlorophyll fluorescence: a probe of photosynthesis in vivo. *Annu Rev Plant Biol*, **59**, 89-113.

Baker, N.R., Harbinson, J. and Kramer, D.M. (2007) Determining the limitations and regulation of photosynthetic energy transduction in leaves. *Plant Cell Environ*, **30**, 1107-1125.

Beardall, J., Griffiths, H. and Raven, J.A. (1982) Carbon Isotope Discrimination and the Co2 Accumulating Mechanism in Chlorella-Emersonii. *J Exp Bot*, **33**, 729-737.

Beardall, J., Roberts, S. and Millhouse, J. (1991) Effects of Nitrogen Limitation on Uptake of Inorganic Carbon and Specific Activity of Ribulose-1,5-Bisphosphate Carboxylase Oxygenase in Green Microalgae. *Can J Bot*, **69**, 1146-1150.

Benning, C. (2010) The Anionic Chloroplast Membrane Lipids: Phosphatidylglycerol and Sulfoquinovosyldiacylglycerol. In *Chloroplast: Basics and Applications* (Rebeiz, C.A., Benning, C., Bohnert, H.J., Daniell, H., Hoober, J.K., Lichtenthaler, H.K., Portis, A.R. and Tripathy, B.C. eds). Dordrecht: Springer, pp. 171-183.

Berges, J.A., Charlebois, D.O., Mauzerall, D.C. and Falkowski, P.G. (1996) Differential effects of nitrogen limitation on photosynthetic efficiency of photosystems I and II in microalgae. *Plant Physiol*, **110**, 689-696.

Blaby, I.K., Glaesener, A.G., Mettler, T., Fitz-Gibbon, S.T., Gallaher, S.D., Liu, B.S., Boyle, N.R., Kropat, J., Stitt, M., Johnson, S., Benning, C., Pellegrini, M., Casero, D. and Merchant, S.S. (2013) Systems-Level Analysis of Nitrogen Starvation-Induced Modifications of Carbon Metabolism in a Chlamydomonas reinhardtii Starchless Mutant. *The Plant cell*, **25**, 4305-4323.

Bölling, C. and Fiehn, O. (2005) Metabolite Profiling of Chlamydomonas reinhardtii under Nutrient Deprivation. *Plant Physiol*, **139**, 1995-2005.

Bonente, G., Passarini, F., Cazzaniga, S., Mancone, C., Buia, M.C., Tripodi, M., Bassi, R. and Caffarri, S. (2008) The Occurrence of the psbS Gene Product in *Chlamydomonas reinhardtii* and in Other Photosynthetic Organisms and Its Correlation with Energy Quenching. *Photochem. Photobiol.*, **84**, 1359-1370.

Boudière, L., Michaud, M., Petroutsos, D., Rébeillé, F., Falconet, D., Bastien, O., Roy, S., Finazzi, G., Rolland, N., Jouhet, J., Block, M.A. and Maréchal, E. (2013) Glycerolipids in photosynthesis: Composition, synthesis and trafficking. *Biochimica et Biophysica Acta (BBA) - Bioenergetics*.

Britton, G., Liaaen-Jensen, S. and Pfander, H. (2009) *Carotenoids Volume 5: Nutrition and Health*: Birkhäuser Basel.

Cardol, P., Bailleul, B., Rappaport, F., Derelle, E., Beal, D., Breyton, C., Bailey, S., Wollman, F.A., Grossman, A., Moreau, H. and Finazzi, G. (2008) An original adaptation of photosynthesis in the marine green alga Ostreococcus. *Proc Natl Acad Sci U S A*, **105**, 7881-7886.

Chisti, Y. (2007) Biodiesel from microalgae. *Biotechnology Advances*, **25**, 294-306.

Coleman, J.R., Berry, J.A., Togasaki, R.K. and Grossman, A.R. (1984) Identification of Extracellular Carbonic Anhydrase of Chlamydomonas reinhardtii. *Plant Physiol*, **76**, 472-477.

Collier, J.L. and Grossman, A.R. (1992) Chlorosis induced by nutrient deprivation in Synechococcus sp. strain PCC 7942: not all bleaching is the same. *Journal of bacteriology*, **174**, 4718-4726.

de Vitry, C., Olive, J., Drapier, D., Recouvreur, M. and Wollman, F.A. (1989) Posttranslational events leading to the assembly of photosystem II protein complex: a study using photosynthesis mutants from Chlamydomonas reinhardtii. *The Journal of cell biology*, **109**, 991-1006.

Dent, R.M., Han, M. and Niyogi, K.K. (2001) Functional genomics of plant photosynthesis in the fast lane using *Chlamydomonas reinhardtii*. *Trends in plant science*, **6**, 364-371.

Depege, N., Bellafiore, S. and Rochaix, J.D. (2003) Role of chloroplast protein kinase Stt7 in LHCII phosphorylation and state transition in *Chlamydomonas*. *Science*, **299**, 1572-1575.

Dong, H.P., Williams, E., Wang, D.Z., Xie, Z.X., Hsia, R.C., Jenck, A., Halden, R., Li, J., Chen, F. and Place, A.R. (2013) Responses of *Nannochloropsis oceanica* IMET1 to Long-Term Nitrogen Starvation and Recovery. *Plant Physiol*, **162**, 1110-1126.

Fan, J., Yan, C., Andre, C., Shanklin, J., Schwender, J. and Xu, C. (2012) Oil accumulation is controlled by carbon precursor supply for fatty acid synthesis in *Chlamydomonas reinhardtii*. *Plant & cell physiology*, **53**, 1380-1390.

Feng, X., Tang, K.H., Blankenship, R.E. and Tang, Y.J. (2010) Metabolic flux analysis of the mixotrophic metabolisms in the green sulfur bacterium Chlorobaculum tepidum. *J Biol Chem*, **285**, 39544-39550.

Fischer, B.B., Dayer, R., Schwarzenbach, Y., Lemaire, S.D., Behra, R., Liedtke, A. and Eggen, R.I. (2009) Function and regulation of the glutathione peroxidase homologous gene GPXH/GPX5 in *Chlamydomonas reinhardtii*. *Plant molecular biology*, **71**, 569-583.

Folch, J., Lees, M. and Sloane Stanley, G.H. (1957) A simple method for the isolation and purification of total lipides from animal tissues. *J Biol Chem*, **226**, 497-509.

Frentzen, M. (2004) Phosphatidylglycerol and sulfoquinovosyldiacylglycerol: anionic membrane lipids and phosphate regulation. *Curr Opin Plant Biol*, **7**, 270-276.

Geider, R.J., Macintyre, H.L., Graziano, L.M. and McKay, R.M.L. (1998) Responses of the photosynthetic apparatus of Dunaliella tertiolecta (Chlorophyceae) to nitrogen and phosphorus limitation. *European Journal of Phycology*, **33**, 315-332.

Geiger, D.R. and Servaites, J.C. (1994) DIURNAL REGULATION OF PHOTOSYNTHETIC CARBON METABOLISM IN C-3 PLANTS. *Annu Rev Plant Phys*, **45**, 235-256.

Genty, B., Briantais, J.M. and Baker, N.R. (1989) The Relationship between the Quantum Yield of Photosynthetic Electron-Transport and Quenching of Chlorophyll Fluorescence. *Biochimica et biophysica acta*, **990**, 87-92.

Gilmore, A.M. and Yamamoto, H.Y. (1993) Linear models relating xanthophylls and lumen acidity to non-photochemical fluorescence quenching. Evidence that antheraxanthin explains zeaxanthin-independent quenching. *Photosynth Res*, **35**, 67-78.

Goodenough, U., Blaby, I., Casero, D., Gallaher, S.D., Goodson, C., Johnson, S., Lee, J.H., Merchant, S.S., Pellegrini, M., Roth, R., Rusch, J., Singh, M., Umen, J.G., Weiss, T.L. and Wulan, T. (2014) The path to triacylglyceride obesity in the sta6 strain of Chlamydomonas reinhardtii. *Eukaryot Cell*, **13**, 591-613.

Gorman, D.S. and Levine, R.P. (1965) CYTOCHROME F AND PLASTOCYANIN - THEIR SEQUENCE IN PHOTOSYNTHETIC ELECTRON TRANSPORT CHAIN OF *CHLAMYDOMONAS REINHARDTII*. *P Natl Acad Sci USA*, **54**, 1665-&.

Granum, E., Kirkvold, S. and Myklestad, S.M. (2002) Cellular and extracellular production of carbohydrates and amino acids by the marine diatom Skeletonema costatum: diel variations and effects of N depletion. *Mar Ecol Prog Ser*, **242**, 83-94.

Grossman, A. (2000) Acclimation of *Chlamydomonas reinhardtii* to its nutrient environment. *Protist*, **151**, 201-224.

Grossman, A.R., Gonzalez-Ballester, D., Shibagaki, N., Pootakham, W., Moseley, J. and Pootakham, W. (2010) *Responses to Macronutrient Deprivation*.

Hall C, Cruz J, Wood M, Zegara R, De Mars D, Carpenter J, Kanazawa A and D, K. (2011) Photosynthesis: research for food, fuel and future-15th international conference on photosynthesis. *Zhejiang University Press, Bejing*, 184-188.

Harris E, Stern D and Witman G (2008) *Chlamydomonas Sourcebook (Second Edition)* 2nd edn.: Elsevier

He, R.F., Kim, M.J., Nelson, W., Balbuena, T.S., Kim, R., Kramer, R., Crow, J.A., May, G.D., Thelen, J.J., Soderlund, C.A. and Gang, D.R. (2012) Next-Generation Sequencing-Based Transcriptomic and Proteomic Analysis of the Common Reed, Phragmites Australis (Poaceae), Reveals Genes Involved in Invasiveness and Rhizome Specificity. *Am J Bot*, **99**, 232-247.

Hertle, A.P., Blunder, T., Wunder, T., Pesaresi, P., Pribil, M., Armbruster, U. and Leister, D. (2013) PGRL1 is the elusive ferredoxin-plastoquinone reductase in photosynthetic cyclic electron flow. *Molecular cell*, **49**, 511-523.

Hill, R., Larkum, A.W.D., Prasil, O., Kramer, D.M., Szabo, M., Kumar, V. and Ralph, P.J. (2012) Light-induced dissociation of antenna complexes in the symbionts of scleractinian corals correlates with sensitivity to coral bleaching. *Coral Reefs*, **31**, 963-975.

Holguin, F.O. and Schaub, T. (2013) Characterization of microalgal lipid feedstock by direct-infusion FT-ICR mass spectrometry. *Algal Research*, **2**, 43-50.

Horton, P., Ruban, A.V. and Walters, R.G. (1994) Regulation of Light Harvesting in Green Plants (Indication by Nonphotochemical Quenching of Chlorophyll Fluorescence). *Plant Physiol*, **106**, 415-420.

Houille-Vernes, L., Rappaport, F., Wollman, F.A., Alric, J. and Johnson, X. (2011) Plastid terminal oxidase 2 (PTOX2) is the major oxidase involved in chlororespiration in Chlamydomonas. *Proc Natl Acad Sci U S A*, **108**, 20820-20825.

Hu, Q., Sommerfeld, M., Jarvis, E., Ghirardi, M., Posewitz, M., Seibert, M. and Darzins, A. (2008) Microalgal triacylglycerols as feedstocks for biofuel production: perspectives and advances. *Plant J*, **54**, 621-639.

Iwai, M., Takahashi, Y. and Minagawa, J. (2008) Molecular remodeling of photosystem II during state transitions in *Chlamydomonas reinhardtii*. *The Plant cell*, **20**, 2177-2189.

Jahns, P. and Holzwarth, A.R. (2012) The role of the xanthophyll cycle and of lutein in photoprotection of photosystem II. *Biochimica et biophysica acta*, **1817**, 182-193.

Jamers, A., Blust, R. and De Coen, W. (2009) Omics in algae: paving the way for a systems biological understanding of algal stress phenomena? *Aquat Toxicol*, **92**, 114-121.

Jans, F., Mignolet, E., Houyoux, P.A., Cardol, P., Ghysels, B., Cuine, S., Cournac, L., Peltier, G., Remacle, C. and Franck, F. (2008) A type II NAD(P)H dehydrogenase mediates light-independent plastoquinone reduction in the chloroplast of Chlamydomonas. *Proc Natl Acad Sci U S A*, **105**, 20546-20551.

Jarvis, P., Dormann, P., Peto, C.A., Lutes, J., Benning, C. and Chory, J. (2000) Galactolipid deficiency and abnormal chloroplast development in the Arabidopsis MGD synthase 1 mutant. *Proc Natl Acad Sci U S A*, **97**, 8175-8179.

Johnson, X. and Alric, J. (2012) Interaction between starch breakdown, acetate assimilation, and photosynthetic cyclic electron flow in Chlamydomonas reinhardtii. *J Biol Chem*, **287**, 26445-26452.

Johnson, X. and Alric, J. (2013) Central Carbon Metabolism and Electron Transport in Chlamydomonas reinhardtii: Metabolic Constraints for Carbon Partitioning between Oil and Starch. *Eukaryotic Cell*, **12**, 776-793.

Johnson, X., Steinbeck, J., Dent, R.M., Takahashi, H., Richaud, P., Ozawa, S., Houille-Vernes, L., Petroutsos, D., Rappaport, F., Grossman, A.R., Niyogi, K.K., Hippler, M. and Alric, J. (2014) Proton gradient regulation 5-mediated cyclic electron flow under ATP- or redox-limited conditions: a study of DeltaATpase pgr5 and DeltarbcL pgr5 mutants in the green alga Chlamydomonas reinhardtii. *Plant Physiol*, **165**, 438-452.

Jones, M.R. (2007) Lipids in photosynthetic reaction centres: Structural roles and functional holes. *Prog. Lipid Res.*, **46**, 56-87.

Klein, U. (1987) Intracellular Carbon Partitioning in Chlamydomonas reinhardtii. *Plant Physiol*, **85**, 892-897.

Kramer, D.M., Johnson, G., Kiirats, O. and Edwards, G.E. (2004) New fluorescence parameters for the determination of q(a) redox state and excitation energy fluxes. *Photosynth Res*, **79**, 209-218.

Lee, D.Y., Park, J.-J., Barupal, D.K. and Fiehn, O. (2012) System Response of Metabolic Networks in *Chlamydomonas reinhardtii* to Total Available Ammonium. *Molecular & Cellular Proteomics*, **11**, 973-988.

Leng, J., Sakurai, I., Wada, H. and Shen, J.R. (2008) Effects of phospholipase and lipase treatments on photosystem II core dimer from a thermophilic cyanobacterium. *Photosynth. Res.*, **98**, 469-478.

Li, X., Moellering, E.R., Liu, B., Johnny, C., Fedewa, M., Sears, B.B., Kuo, M.H. and Benning, C. (2012) A galactoglycerolipid lipase is required for triacylglycerol accumulation and survival following nitrogen deprivation in Chlamydomonas reinhardtii. *The Plant cell*, **24**, 4670-4686.

Li, Y., Han, D., Hu, G., Sommerfeld, M. and Hu, Q. (2010) Inhibition of starch synthesis results in overproduction of lipids in Chlamydomonas reinhardtii. *Biotechnology and bioengineering*, **107**, 258-268.

Liu, B.S. and Benning, C. (2013) Lipid metabolism in microalgae distinguishes itself. *Current Opinion in Biotechnology*, **24**, 300-309.

Livingston, A.K., Cruz, J.A., Kohzuma, K., Dhingra, A. and Kramer, D.M. (2010) An Arabidopsis mutant with high cyclic electron flow around photosystem I (hcef) involving the NADPH dehydrogenase complex. *The Plant cell*, **22**, 221-233.

Lohr, M. (2009) Chapter 21 - Carotenoids. In *The Chlamydomonas Sourcebook (Second Edition)* (Elizabeth, H.H., Ph.D, David, B.S., Ph.D and George B. Witman, P.D. eds). London: Academic Press, pp. 799-817.

Longworth, J., Noirel, J., Pandhal, J., Wright, P.C. and Vaidyanathan, S. (2012) HILIC- and SCX-based quantitative proteomics of Chlamydomonas reinhardtii during nitrogen starvation induced lipid and carbohydrate accumulation. *Journal of proteome research*, **11**, 5959-5971.

Lucker, B. and Kramer, D.M. (2013) Regulation of cyclic electron flow in Chlamydomonas reinhardtii under fluctuating carbon availability. *Photosynth Res*, **117**, 449-459.

Martin, N.C. and Goodenough, U.W. (1975) Gametic differentiation in Chlamydomonas reinhardtii. I. Production of gametes and their fine structure. *The Journal of cell biology*, **67**, 587-605.

Maruyama, S., Tokutsu, R. and Minagawa, J. (2014) Transcriptional regulation of the stress-responsive light harvesting complex genes in Chlamydomonas reinhardtii. *Plant & cell physiology*, **55**, 1304-1310.

Merchant, S.S. and Helmann, J.D. (2012a) Elemental economy: microbial strategies for optimizing growth in the face of nutrient limitation. *Advances in microbial physiology*, **60**, 91-210.

Merchant, S.S., Kropat, J., Liu, B., Shaw, J. and Warakanont, J. (2012b) TAG, You're it! *Chlamydomonas* as a reference organism for understanding algal triacylglycerol accumulation. *Current Opinion in Biotechnology*, **23**, 352-363.

Merchant, S.S., Prochnik, S.E., Vallon, O., Harris, E.H., Karpowicz, S.J., Witman, G.B., Terry, A., Salamov, A., Fritz-Laylin, L.K., Marechal-Drouard, L., Marshall, W.F., Qu, L.H., Nelson, D.R., Sanderfoot, A.A., Spalding, M.H., Kapitonov, V.V., Ren, Q., Ferris, P., Lindquist, E., Shapiro, H., Lucas, S.M., Grimwood, J., Schmutz, J., Cardol, P., Cerutti, H., Chanfreau, G., Chen, C.L., Cognat, V., Croft, M.T., Dent, R., Dutcher, S., Fernandez, E., Fukuzawa, H., Gonzalez-Ballester, D., Gonzalez-Halphen, D., Hallmann, A., Hanikenne, M., Hippler, M., Inwood, W., Jabbari, K., Kalanon, M., Kuras, R., Lefebvre, P.A., Lemaire, S.D., Lobanov, A.V., Lohr, M., Manuell, A., Meier, I., Mets, L., Mittag, M., Mittelmeier, T., Moroney, J.V., Moseley, J., Napoli, C., Nedelcu, A.M., Niyogi, K., Novoselov, S.V., Paulsen, I.T., Pazour, G., Purton, S., Ral, J.P., Riano-Pachon, D.M., Riekhof, W., Rymarquis, L., Schroda, M., Stern, D., Umen, J., Willows, R., Wilson, N., Zimmer, S.L., Allmer, J., Balk, J., Bisova, K., Chen, C.J., Elias, M., Gendler, K., Hauser, C., Lamb, M.R., Ledford, H., Long, J.C., Minagawa, J., Page, M.D., Pan, J., Pootakham, W., Roje, S., Rose, A., Stahlberg, E., Terauchi, A.M., Yang, P., Ball, S., Bowler, C., Dieckmann, C.L., Gladyshev, V.N., Green, P., Jorgensen, R., Mayfield, S., Mueller-Roeber, B., Rajamani, S., Sayre, R.T., Brokstein, P., Dubchak, I., Goodstein, D., Hornick, L., Huang, Y.W., Jhaveri, J., Luo, Y., Martinez, D., Ngau, W.C., Otillar, B., Poliakov, A., Porter, A., Szajkowski, L., Werner, G., Zhou, K., Grigoriev, I.V., Rokhsar, D.S. and Grossman, A.R. (2007) The *Chlamydomonas* genome reveals the evolution of key animal and plant functions. *Science*, **318**, 245-250.

Miller, R., Wu, G., Deshpande, R.R., Vieler, A., Gartner, K., Li, X., Moellering, E.R., Zauner, S., Cornish, A.J., Liu, B., Bullard, B., Sears, B.B., Kuo, M.H., Hegg, E.L., Shachar-Hill, Y., Shiu, S.H. and Benning, C. (2010) Changes in transcript abundance in *Chlamydomonas reinhardtii* following nitrogen deprivation predict diversion of metabolism. *Plant Physiol*, **154**, 1737-1752.

Mizusawa, N. and Wada, H. (2012) The role of lipids in photosystem II. *Biochim. Biophys. Acta-Bioenerg.*, **1817**, 194-208.

Moseley, J.L., Allinger, T., Herzog, S., Hoerth, P., Wehinger, E., Merchant, S. and Hippler, M. (2002) Adaptation to Fe-deficiency requires remodeling of the photosynthetic apparatus. *Embo J*, **21**, 6709-6720.

Msanne, J., Xu, D., Konda, A.R., Casas-Mollano, J.A., Awada, T., Cahoon, E.B. and Cerutti, H. (2012) Metabolic and gene expression changes triggered by nitrogen deprivation

in the photoautotrophically grown microalgae Chlamydornonas reinhardtii and Coccomyxa sp C-169. *Phytochemistry*, **75**, 50-59.

Muller, P., Li, X.P. and Niyogi, K.K. (2001) Non-photochemical quenching. A response to excess light energy. *Plant Physiol*, **125**, 1558-1566.

Munekage, Y., Hojo, M., Meurer, J., Endo, T., Tasaka, M. and Shikanai, T. (2002) PGR5 is involved in cyclic electron flow around photosystem I and is essential for photoprotection in Arabidopsis. *Cell*, **110**, 361-371.

Murakami, A. (1997) Quantitative analysis of 77K fluorescence emission spectra in Synechocystis sp. PCC 6714 and Chlamydomonas reinhardtii with variable PS I/PS II stoichiometries. *Photosynth. Res.*, **53**, 141-148.

Myouga, F., Hosoda, C., Umezawa, T., Iizumi, H., Kuromori, T., Motohashi, R., Shono, Y., Nagata, N., Ikeuchi, M. and Shinozaki, K. (2008) A Heterocomplex of Iron Superoxide Dismutases Defends Chloroplast Nucleoids against Oxidative Stress and Is Essential for Chloroplast Development in Arabidopsis. *The Plant cell*, **20**, 3148-3162.

Nguyen, H.M., Baudet, M., Cuine, S., Adriano, J.M., Barthe, D., Billon, E., Bruley, C., Beisson, F., Peltier, G., Ferro, M. and Li-Beisson, Y. (2011) Proteomic profiling of oil bodies isolated from the unicellular green microalga *Chlamydomonas reinhardtii*: With focus on proteins involved in lipid metabolism. *Proteomics*, **11**, 4266-4273.

Niyogi, K.K., Bjorkman, O. and Grossman, A.R. (1997) Chlamydomonas xanthophyll cycle mutants identified by video imaging of chlorophyll fluorescence quenching. *The Plant cell*, **9**, 1369-1380.

Ohlrogge, J., Allen, D., Berguson, B., DellaPenna, D., Shachar-Hill, Y. and Stymne, S. (2009) Driving on Biomass. *Science*, **324**, 1019-1020.

Park, J., Wang, H., Gargouri, M., Deshpande, R., Skepper, J., Holguin, F.O., Juergens, M., Shachar-Hill, Y., Hicks, L. and Gang, D.R. (2014) The response of Chlamydomonas reinhardtii to nitrogen deprivation: A systems biology analysis. *Submitted*.

Peers, G., Truong, T.B., Ostendorf, E., Busch, A., Elrad, D., Grossman, A.R., Hippler, M. and Niyogi, K.K. (2009) An ancient light-harvesting protein is critical for the regulation of algal photosynthesis. *Nature*, **462**, 518-U215.

Peltier, G. and Schmidt, G.W. (1991) Chlororespiration: an adaptation to nitrogen deficiency in Chlamydomonas reinhardtii. *Proc Natl Acad Sci U S A*, **88**, 4791-4795.

Petroutsos, D., Terauchi, A.M., Busch, A., Hirschmann, I., Merchant, S.S., Finazzi, G. and Hippler, M. (2009) PGRL1 participates in iron-induced remodeling of the photosynthetic apparatus and in energy metabolism in Chlamydomonas reinhardtii. *J Biol Chem*, **284**, 32770-32781.

Pfalz, J., Liebers, M., Hirth, M., Grubler, B., Holtzegel, U., Schroter, Y., Dietzel, L. and Pfannschmidt, T. (2012) Environmental control of plant nuclear gene expression by chloroplast redox signals. *Frontiers in plant science*, **3**, 257.

Philipps, G., Happe, T. and Hemschemeier, A. (2012) Nitrogen deprivation results in photosynthetic hydrogen production in *Chlamydomonas reinhardtii*. *Planta*, **235**, 729-745.

Plumley, F.G., Douglas, S.E., Switzer, A.B. and Schmidt, G.W. (1989a) Nitrogen-dependent biogenesis of chlorophyll-protein complexes. *Plant Biology (New York)*, **8**, 311-329.

Plumley, F.G. and Schmidt, G.W. (1989b) NITROGEN-DEPENDENT REGULATION OF PHOTOSYNTHETIC GENE-EXPRESSION. *P Natl Acad Sci USA*, **86**, 2678-2682.

Ritchie, R.J. (2006) Consistent sets of spectrophotometric chlorophyll equations for acetone, methanol and ethanol solvents. *Photosynth Res*, **89**, 27-41.

Rochaix, J.D. (2002) Chlamydomonas, a model system for studying the assembly and dynamics of photosynthetic complexes. *FEBS Lett*, **529**, 34-38.

Rodriguez-Uribe, L., Guzman, I., Rajapakse, W., Richins, R.D. and O'Connell, M.A. (2012) Carotenoid accumulation in orange-pigmented Capsicum annuum fruit, regulated at multiple levels. *J Exp Bot*, **63**, 517-526.

Roessler, P.G. (1990) Environmental-Control of Glycerolipid Metabolism in Microalgae - Commercial Implications and Future-Research Directions. *Journal of Phycology*, **26**, 393-399.

Rumeau, D., Peltier, G. and Cournac, L. (2007) Chlororespiration and cyclic electron flow around PSI during photosynthesis and plant stress response. *Plant Cell Environ*, **30**, 1041-1051.

Sacksteder, C.A., Jacoby, M.E. and Kramer, D.M. (2001) A portable, non-focusing optics spectrophotometer (NoFOSpec) for measurements of steady-state absorbance changes in intact plants. *Photosynth Res*, **70**, 231-240.

Schmollinger, S., Muhlhaus, T., Boyle, N.R., Blaby, I.K., Casero, D., Mettler, T., Moseley, J.L., Kropat, J., Sommer, F., Strenkert, D., Hemme, D., Pellegrini, M., Grossman, A.R., Stitt, M., Schroda, M. and Merchant, S.S. (2014) Nitrogen-Sparing Mechanisms in Chlamydomonas Affect the Transcriptome, the Proteome, and Photosynthetic Metabolism. *The Plant cell*.

Shastri, A.A. and Morgan, J.A. (2007) A transient isotopic labeling methodology for 13C metabolic flux analysis of photoautotrophic microorganisms. *Phytochemistry*, **68**, 2302-2312.

Shifrin, N.S. and Chisholm, S.W. (1981) Phytoplankton Lipids - Interspecific Differences and Effects of Nitrate, Silicate and Light-Dark Cycles. *Journal of Phycology*, **17**, 374-384.

Shimojima, M., Ohta, H. and Nakamura, Y. (2010) Biosynthesis and Function of Chloroplast Lipids. In *Lipids in Photosynthesis* (Wada, H. and Murata, N. eds): Springer Netherlands, pp. 35-55.

Siaut, M., Cuine, S., Cagnon, C., Fessler, B., Nguyen, M., Carrier, P., Beyly, A., Beisson, F., Triantaphylides, C., Li-Beisson, Y.H. and Peltier, G. (2011) Oil accumulation in the model green alga *Chlamydomonas reinhardtii*: characterization, variability between common laboratory strains and relationship with starch reserves. *Bmc Biotechnol*, **11**.

Simionato, D., Block, M.A., La Rocca, N., Jouhet, J., Marechal, E., Finazzi, G. and Morosinotto, T. (2013) Response of *Nannochloropsis Gaditana* to Nitrogen Starvation Includes a De Novo Biosynthesis of Triacylglycerols, a Decrease of Chloroplast Galactolipids and a Reorganization of the Photosynthetic Apparatus. *Eukaryot Cell*.

Takaichi, S. (2011) Carotenoids in Algae: Distributions, Biosyntheses and Functions. *Mar. Drugs*, **9**, 1101-1118.

Tokutsu, R. and Minagawa, J. (2013) Energy-dissipative supercomplex of photosystem II associated with LHCSR3 in *Chlamydomonas reinhardtii*. *Proc Natl Acad Sci U S A*, **110**, 10016-10021.

Tuncay, H., Findinier, J., Duchene, T., Cogez, V., Cousin, C., Peltier, G., Ball, S.G. and Dauvillee, D. (2013) A forward genetic approach in Chlamydomonas reinhardtii as a strategy for exploring starch catabolism. *PloS one*, **8**, e74763.

Turkina, M.V., Kargul, J., Blanco-Rivero, A., Villarejo, A., Barber, J. and Vener, A.V. (2006) Environmentally modulated phosphoproteome of photosynthetic membranes in the green alga Chlamydomonas reinhardtii. *Molecular & cellular proteomics : MCP*, **5**, 1412-1425.

Urzica, E.I., Vieler, A., Hong-Hermesdorf, A., Page, M.D., Casero, D., Gallaher, S.D., Kropat, J., Pellegrini, M., Benning, C. and Merchant, S.S. (2013) Remodeling of Membrane Lipids in Iron Starved Chlamydomonas. *J Biol Chem*.

Van, K. and Spalding, M.H. (1999) Periplasmic carbonic anhydrase structural gene (Cah1) mutant in chlamydomonas reinhardtii. *Plant Physiol*, **120**, 757-764.

Wang, H., Alvarez, S. and Hicks, L.M. (2012) Comprehensive comparison of iTRAQ and label-free LC-based quantitative proteomics approaches using two Chlamydomonas reinhardtii strains of interest for biofuels engineering. *Journal of proteome research*, **11**, 487-501.

Wang, Y.J., Duanmu, D.Q. and Spalding, M.H. (2011) Carbon dioxide concentrating mechanism in *Chlamydomonas reinhardtii*: inorganic carbon transport and CO2 recapture. *Photosynth. Res.*, **109**, 115-122.

Wang, Z.T., Ullrich, N., Joo, S., Waffenschmidt, S. and Goodenough, U. (2009) Algal lipid bodies: stress induction, purification, and biochemical characterization in wild-type and starchless *Chlamydomonas reinhardtii*. *Eukaryot Cell*, **8**, 1856-1868.

Wijffels, R.H. and Barbosa, M.J. (2010) An Outlook on Microalgal Biofuels. *Science*, **329**, 796-799.

Williams, P.J.L. and Laurens, L.M.L. (2010) Microalgae as biodiesel & biomass feedstocks: Review & analysis of the biochemistry, energetics & economics. *Energ Environ Sci*, **3**, 554-590.

Work, V.H., Radakovits, R., Jinkerson, R.E., Meuser, J.E., Elliott, L.G., Vinyard, D.J., Laurens, L.M., Dismukes, G.C. and Posewitz, M.C. (2010) Increased lipid accumulation in the Chlamydomonas reinhardtii sta7-10 starchless isoamylase mutant and increased carbohydrate synthesis in complemented strains. *Eukaryot Cell*, **9**, 1251-1261.

Wykoff, D.D., Davies, J.P., Melis, A. and Grossman, A.R. (1998) The regulation of photosynthetic electron transport during nutrient deprivation in Chlamydomonas reinhardtii. *Plant Physiol*, **117**, 129-139.

Yang, Z.-K., Ma, Y.-H., Zheng, J.-W., Yang, W.-D., Liu, J.-S. and Li, H.-Y. (2013a) Proteomics to reveal metabolic network shifts towards lipid accumulation following nitrogen deprivation in the diatom *Phaeodactylum tricornutum*. *J. Appl. Phycol.*

Yang, Z.K., Niu, Y.F., Ma, Y.H., Xue, J., Zhang, M.H., Yang, W.D., Liu, J.S., Lu, S.H., Guan, Y. and Li, H.Y. (2013b) Molecular and cellular mechanisms of neutral lipid accumulation in diatom following nitrogen deprivation. *Biotechnology for biofuels*, **6**, 67.

Yoshida, K., Igarashi, E., Mukai, M., Hirata, K. and Miyamoto, K. (2003) Induction of tolerance to oxidative stress in the green alga, Chlamydomonas reinhardtii, by abscisic acid. *Plant Cell Environ*, **26**, 451-457.

Young, E.B. and Beardall, J. (2005) Modulation of photosynthesis and inorganic carbon acquisition in a marine microalga by nitrogen, iron, and light availability. *Can J Bot*, **83**, 917-928.

Young, J.D., Shastri, A.A., Stephanopoulos, G. and Morgan, J.A. (2011) Mapping photoautotrophic metabolism with isotopically nonstationary C-13 flux analysis. *Metab Eng*, **13**, 656-665.

CHAPTER-3

The Relationship of Triacylglycerol and Starch Accumulation to Carbon and Energy Flows During Nutrient Deprivation in Chlamydomonas.[1]

[1]This Manuscript has been submitted for Publication to Plant Physiology under the same title. Authors: Matthew T. Juergens, Bradley Disbrow, and Yair Shachar-Hill. I generated and analyzed all data presented in this chapter as well as wrote this chapter. Bradley Disbrow assisted in sample processing and Yair Shachar-Hill assisted with writing and data interpretation.

ABSTRACT

Because of the potential importance of algae for green biotechnology, considerable effort has been invested in understanding their responses to nitrogen deprivation. The most frequently invoked reasons proposed for the accumulation of high cellular levels of triacylglycerol (TAG) and starch are variants of what may be termed the Overflow Hypothesis. According to this, growth inhibition results in the rate of photosynthetic energy and/or carbon input exceeding cellular needs; the excess input is directed into the accumulation of TAG and/or starch to prevent damage. The present study was aimed at providing a quantitative dataset and analysis of the main energy and carbon flows before and during nitrogen deprivation in a model system to assess alternative explanations. Cellular growth, biomass, starch and lipid levels as well as several measures of photosynthetic function were recorded for cells of *Chlamydomonas reinhardtii* cultured under 9 different autotrophic, mixotrophic and heterotrophic conditions during nutrient-replete growth and for the first four days of nitrogen deprivation. The results of a 13C labeling time course indicated that in mixotrophic culture, starch is predominantly made from CO_2 and fatty acid synthesis is largely supplied by exogenous acetate, with considerable turnover of membrane lipids, so that total lipid rather than TAG is the appropriate measure of product accumulation. Heterotrophic cultures accumulated TAG and starch during N-deprivation, showing that these are not dependent on photosynthesis. We conclude that the overflow hypothesis is insufficient and suggest that storage may be a more universally important reason for carbon compound accumulation during nutrient deprivation.

INTRODUCTION

The current rate of utilization of fossil fuel products for energy and the chemical industry is unsustainable. Among the alternative renewable replacements, microalgal oil and biomass production have shown considerable promise (Atabani, et al. 2012, Chisti 2007, Ohlrogge, et al. 2009, Williams, et al. 2010) because many algae are capable of rapid photoautotrophic growth to high cell densities and can accumulate high dry weight percentages of triacylglycerol (TAG) (Hu, et al. 2008, Jones, et al. 2012, Wijffels, et al. 2010). TAG accumulation is induced in many microalgal taxa by a number of stresses including salt and nutrient deprivation (Murphy 2001). Beginning over 100 years ago (Beijerinck 1904) many researchers have reported that nitrogen (N) deprivation induces high levels of accumulation of TAG and starch in a range of microalgal species at the expense of decreased cell growth and slower metabolism (Granum, et al. 2002, Hu, et al. 2008, Liu, et al. 2013, Martin, et al. 1975a, Shifrin, et al. 1981, Spoehr, et al. 1949). This has led to interest in understanding the underlying physiological and adaptive functions of algal TAG production during N deprivation to help guide engineering of higher oil yields.

In recent years, studies of the effects of nutrient deprivation have revealed many changes in the structure and function of networks across metabolism and other cellular functions, (Blaby, et al. 2013, Goodenough, et al. 2014, Juergens, et al. 2015, Miller, et al. 2010, Schmollinger, et al. 2014). Such studies and mutant screens have led to the identification of enzymes involved in TAG synthesis (Li, et al. 2012b, Merchant, et al. 2012b) and pointed to putative regulatory networks (Gargouri *et al.* 2015). However the interpretation of system-wide molecular changes and the choice of which among them to target for further investigation and practical purposes is

uncertain and is strongly influenced by the prevailing views of the function of TAG accumulation.

Several explanations have been proposed for the induction of TAG accumulation in algae under stress, ranging from storing reduced carbon as an energy source for survival and/or future recovery, to lipid reorganization during photosynthetic down-regulation and/or subsequent up-regulation, to photo-protection (Akita, et al. 2015, Grossman, et al. 2010a, Khozin-Goldberg, et al. 2005, Klok, et al. 2014, Kohlwein 2010, Murphy 2001). Roessler (Roessler 1990) appears to have been the first to postulate that algae accumulate TAG as a sink for excess photosynthetic energy and reductant to prevent photochemical damage. In this explanation, photosynthetic carbon and energy assimilation that can no longer be directed to growth when population increase is inhibited by nutrient deficiency or other stresses results in overflow products, particularly TAG. The concept of overflow metabolism has traditionally been associated with the export of metabolites by heterotrophic microbes (Neijssel, et al. 1975) and has more recently also been applied to photosynthetic metabolism in cyanobacteria (Courchesne, et al. 2009, Grundel, et al. 2012, Hays, et al. 2015) and higher plants (Weise, et al. 2011). In microalgal work, the idea of photosynthetic overflow (excess photosynthetic energy and carbon) as the driver of oil accumulation has become a widely accepted explanation (see for example (Hu, et al. 2008, Klok, et al. 2014, Li, et al. 2012b, Li, et al. 2013, Solovchenko 2012). This Overflow Hypothesis (OH) strongly influences research efforts and the interpretation of results in biological and engineering studies of microalgal metabolism and TAG accumulation and also has important implications for the ecophysiology of photosynthetic microbes. While frequently invoked in interpreting the results of nutrient deprivation studies, the OH has not been systematically assessed.

Such systematic assessments should include a quantitative analysis of the major carbon and energy flows during stress-induced oil accumulation, and should be carried out over a range of eco-physiologically and practically meaningful conditions in relevant model organisms (Smith *et al.* 2010). Despite a burgeoning literature on microalgal TAG accumulation under N deprivation, such studies are lacking. The green alga *Chlamydomonas reinhardtii* is the most widely studied species in research on microalgal oil production. Although it produces less TAG than some species and has a low tolerance of extreme conditions, its robust growth, ease of culture, ability to grow heterotrophically and the wealth of existing data and available genetic tools (including mutant collections, transformation tools, and a well annotated genome sequence), make it attractive for biofuel research (Merchant, et al. 2012b, Merchant, et al. 2007, Rochaix 2002).

Carbon (C) and Energy (E) balances are established tools in ecology and metabolic engineering and are employed to assess growth and yields during commercial applications. Widely used for monitoring and improving bacterial and yeast fermentation processes, measuring cellular C and E influxes and outflows has also been used in several cyanobacterial and algal studies (Chapman, et al. 2015, Slade *et al.* 2013, Wagner *et al.* 2006, Watanabe *et al.* 1995). Figure 1 shows the C and E entering a Chlamydomonas cell (photosynthesis and/or acetate uptake) as well as the major C and E outputs (growth, maintenance, dissipation, and TAG and Starch production. Figure 1 also illustrates the overflow hypothesis, in which nutrient deprivation causes a redirection of output fluxes from reproduction to TAG and starch synthesis. Quantifying the relationships between C and E fluxes before and during stress conditions can point to processes such as dissipative metabolic or photochemical processes and can be used to

make quantitative tests of predictions implied by the OH and alternative explanations for TAG accumulation.

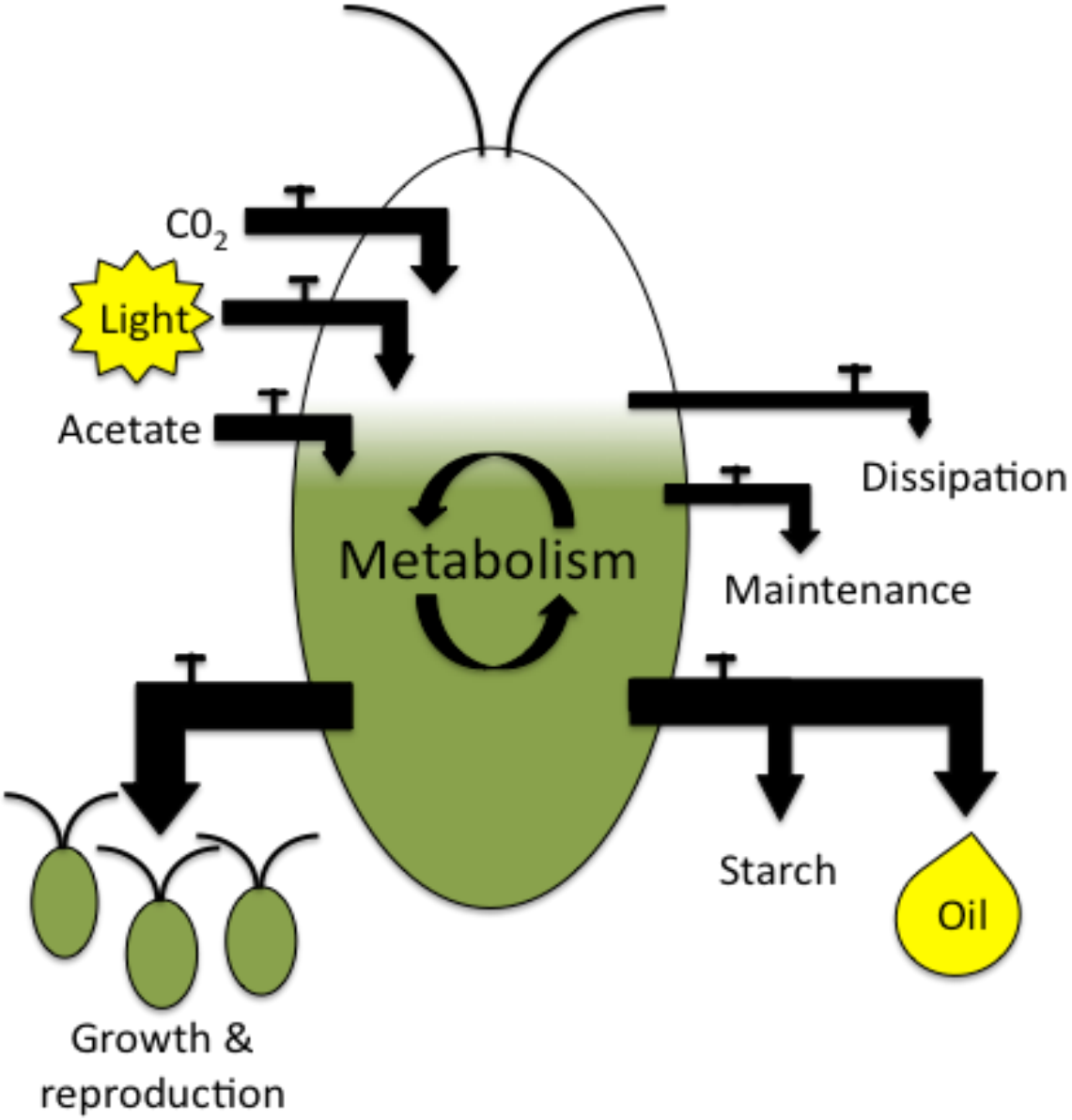

Figure 3.1. The main Carbon and Energy inputs and outputs of Chlamydomonas cells. CO_2 provides C input, light provides energy input and acetate provides both. Incoming energy can be dissipated as heat, consumed for maintenance, or used in cell growth or biosynthesis of storage compounds (starch and oil). Incoming carbon is used in growth, stored in starch or oil, or respired as CO_2.

Here we present measurements of cellular growth, biomass, starch, TAG, and total fatty acid accumulation, changes in photosynthetic fluxes and acetate uptake rates across 5 light levels and 2 media compositions before and during the course of 96 h of N deprivation. Results from a ^{13}C labeling time course experiment highlight the involvement of multiple lipid pools during N deprivation, so that (a) total lipid rather than TAG alone is the appropriate pool for C & E balances; and (b) lipid is preferentially formed from exogenous fixed carbon (when available) rather than from photosynthate, the latter contributing more to starch production. TAG and starch accumulated to significant levels in the dark after N depletion, demonstrating that TAG accumulation is not dependent upon photosynthetic activity. Using the photosynthetic, biomass and uptake rates, C and E influxes and outflows are reported and compared to predictions deduced from the overflow hypothesis. Several aspects of the findings do not support the OH in its straightforward form. We conclude that the overflow hypothesis is insufficient to explain carbon accumulation during nutrient deprivation and suggest that storage of biosynthetic precursors and/or chemical energy as adaptive survival traits may be more universal reasons.

RESULTS

Growth rates in N-replete conditions

To characterize the effect of light and trophic conditions on *Chlamydomonas reinhardtii* growth rates, cells were grown in defined media either with acetate as a fixed carbon source (Tris Acetate Phosphate, TAP media) or without acetate (High Salt, HS media) at light levels of 0, 5, 15, 40, and 160 μmol photons m^{-2} s^{-1}. Cell growth measured during exponential (steady state) growth is presented as specific growth rate in Figure 3.2. This range of light intensity spans heterotrophic growth in the dark in TAP media, light-limited autotrophic and mixotrophic conditions and saturating light levels. Illumination was kept below levels (at or above 200 μmol photons m^{-2} s^{-1}) where cells showed chlorosis and reduced growth rates indicative of light stress and/or photo-inhibition (Bonente *et al.* 2012, Juergens, et al. 2015, Peers, et al. 2009). Increasing illumination from 40 to 160 μmol photons m^{-2} s^{-1} did not increase growth rate, suggesting that these cells are carbon limited (Ref on C limitation in Algae) (Goldman *et al.* 1974, Spalding 1989). This suggestion was supported by the observation that growth rates increased approximately twofold when humidified ambient air was circulated through the culture flasks to increase CO_2 availability.

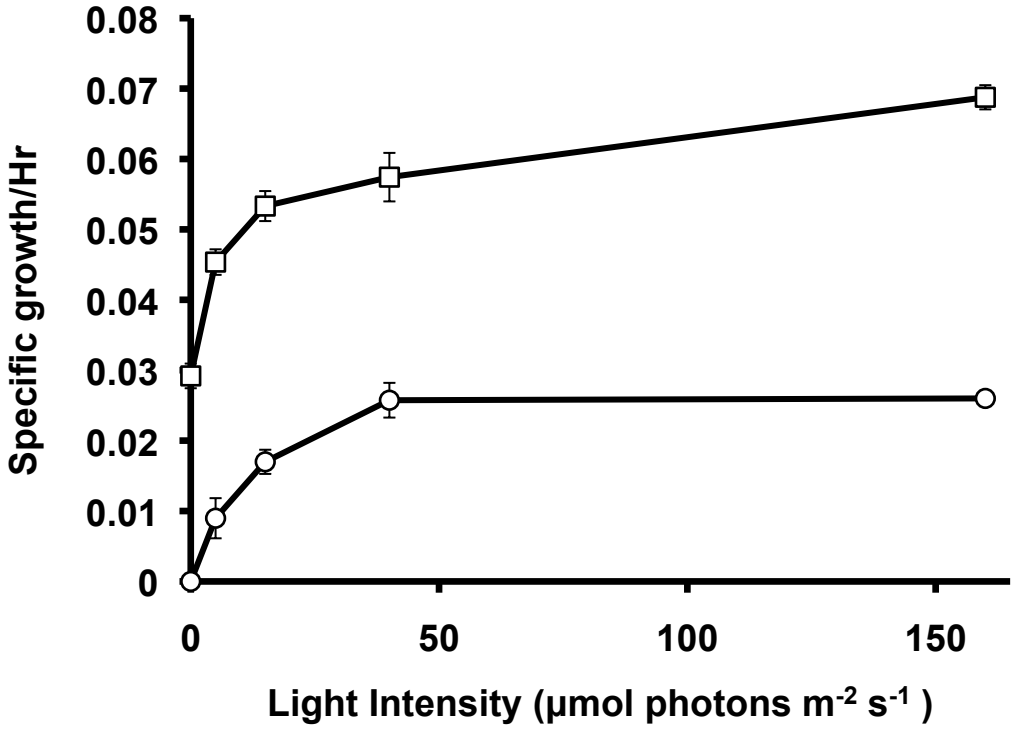

Figure 3.2. Specific growth rates during exponential growth in nitrogen replete media. Growth with acetate (TAP media, squares) and or without (HS media, circles) under continuous illumination at light levels from 0 to 160 µ mol photons m^{-2} s^{-1}. Specific growth rate (SG) is the rate constant for log growth and is inversely related to doubling time as SG = Ln (2)/ (doubling time). Error bars indicate +/- SD (n=3 biological replicates).

Biomass

Biomass measured as ash free dry weight (AFDW) is shown in Figure 3.3A and Figure 3.3B. Cellular biomass in N replete cells is very similar across light levels, with mixotrophic and heterotrophic cultures (TAP medium) having approximately 25% more AFDW than autotrophic cultures. Cells cultured in TAP medium increased ~2 fold in cell biomass over 96 hrs whereas HS cells increased less in biomass, especially in the first 48h of deprivation.

Biomass and C and N contents of cells were measured to quantify net carbon accumulation rates and cellular nitrogen contents as a proxy for nitrogenous biomass (protein plus nucleic acids). Cellular C and N contents measured by elemental analysis are shown in Figure 3.3C to Figure 3.3F and C:N ratio is shown in Figure 3.4. Carbon accounts for ~40-47% of cell dry weight during growth in N replete media (Figure 3.3C and Figure 3.3D), levels which changed little during N deprivation in TAP media - whereas C levels decreased in cells deprived of N in HS media. Nitrogen levels as a percentage of dry weight were higher in nitrogen replete cells growing autotrophically than in TAP media and fell significantly during N deprivation (except for heterotrophic cultures). The falling cellular %N during deprivation is due to the accumulation of biomass components lacking N, so that total N contents per cell were little changed.

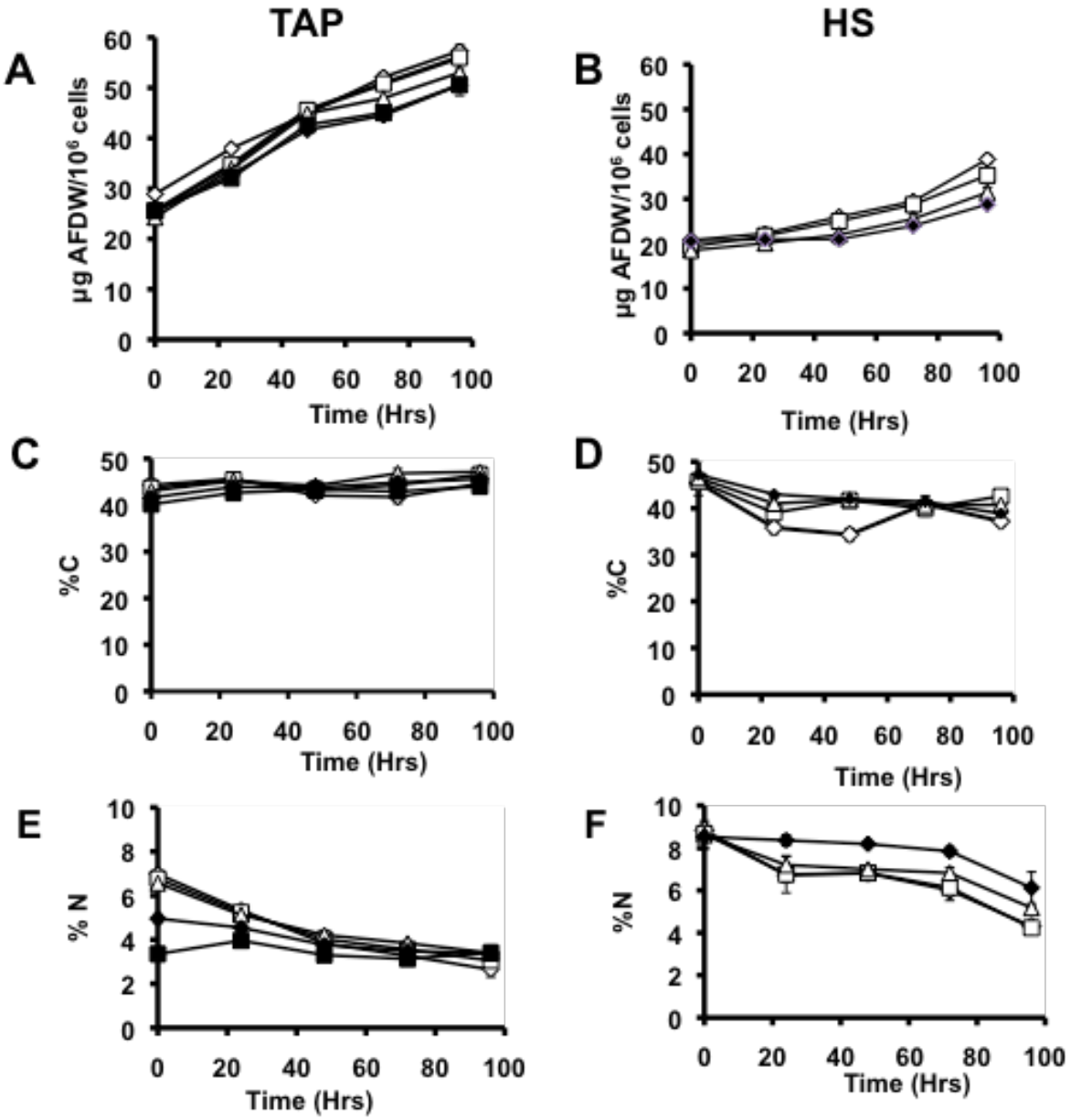

Figure 3.3. Cellular Biomass and % Carbon and Nitrogen before and during nitrogen deprivation. Biomass is given as Ash Free Dry Weight (AFDW) per million cells (**A** and **B**), %C (**C** and **D**), and %N (**E** and **F**) is reported for cultures grown in TAP (**A C,** and **E**) and HS (**B, D** and **F**) media and deprived of N at time 0. Empty diamonds, cells cultured at 160 µmol photons m^{-2} $s^{-}1$ (µE); empty squares, 40 µE; empty triangles, 15 µE; filled diamonds, 5 µE; filled squares, 0 µE. Error bars indicate +/- SD (n=3).

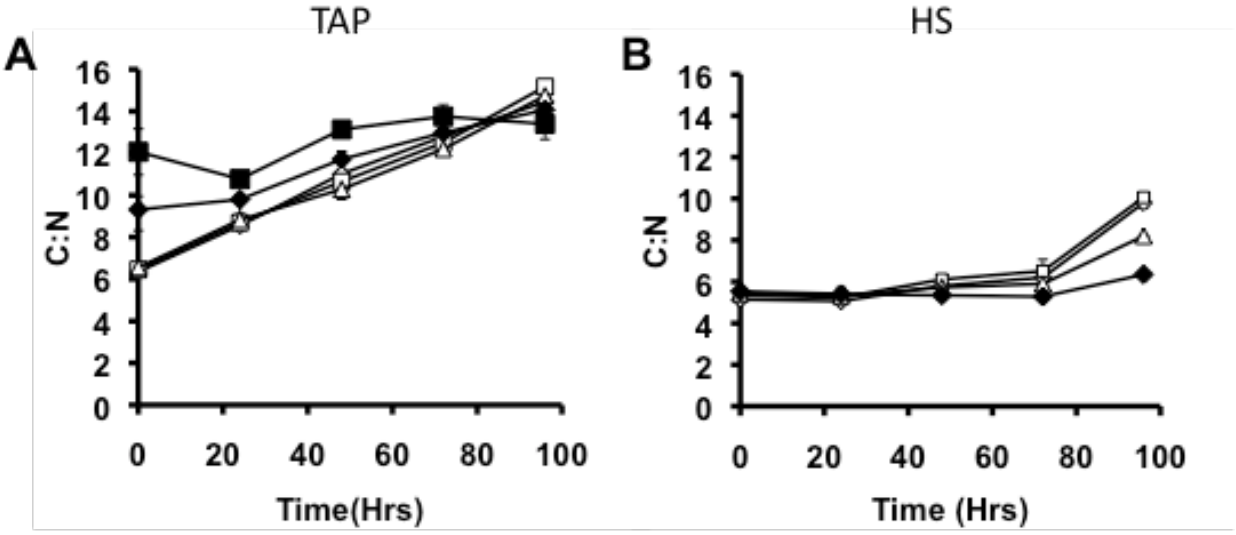

Figure 3.4. Carbon to Nitrogen (C:N) ratios during N deprivation. Data for TAP(A) and HS(B) cultures were taken before and during N deprivation. In all cases, 160 μmol m^{-1} s^{-1} is indicated by hollow diamonds, 40 μmol m^{-1} s^{-1} by hollowed squares, 15 μmol m^{-1} s^{-1} indicated by hollowed triangles , 5 μmol m^{-1} s^{-1} by solid diamonds, and 0 μmol m^{-1} s^{-1} by solid squares. Error bars indicate SD (n=3).

The Accumulation of TAG and Starch

The first compound known to accumulate to high levels during N deprivation is starch (Klein 1987) and the upregulation of starch synthesis gene expression has been reported during N deprivation (Ball, et al. 1990, Juergens, et al. 2015, Miller, et al. 2010). Increases in starch levels during N deprivation are shown in Figure 3.5; they account for the majority of the increases in cellular dry weight. Starch levels rose linearly for 48 hrs after N deprivation in both TAP and HS media, with higher rates at higher light levels and in TAP compared to HS media. After 48 hrs starch accumulation rates decreased, with cessation of starch accumulation by 96 hrs for all but the cells cultures at the highest light level in TAP media and those at the lowest light levels in HS media.

During nitrogen-replete growth cultures contained close to 5µg of total fatty acid per million cells (Figure 3.5B and Figure 3.5C) and no TAG was detected (Figure 3.5E and 3.5F). During N deprivation in mixotrophic cultures, TAG levels were detected at 24 hours while little or no TAG was detected in HS cultures until 48h. Levels of starch and TAG were previously reported by Fan et al. (Fan, et al. 2012) and by Siaut *et al*. (Siaut, et al. 2011) for several *C. reinhardtii* strains cultured at 50 and 150 µmol photons m^{-2} s^{-1} respectively, after 2 or 3 days of N deprivation. Our results for these time points in cells supplied with 40 and 160 µmol photons m^{-2} s^{-1} are similar to those previously reported (except for mutant strains lacking starch). The observation that TAG accumulates during nitrogen deprivation in Chlamydomonas cells cultured heterotrophically in the dark separates the induction of TAG accumulation from photosynthesis. High levels of TAG accumulation have been reported in heterotrophically grown Chlorella species (Liu *et al.* 2011, Miao *et al.* 2004) and TAG accumulation was also observed in heterotrophically cultured Chlamydomonas after carbon starvation (Singh *et al.* 2014) and during N deprivation in the presence of high levels (60mM) of acetate (Fan, et al. 2012).

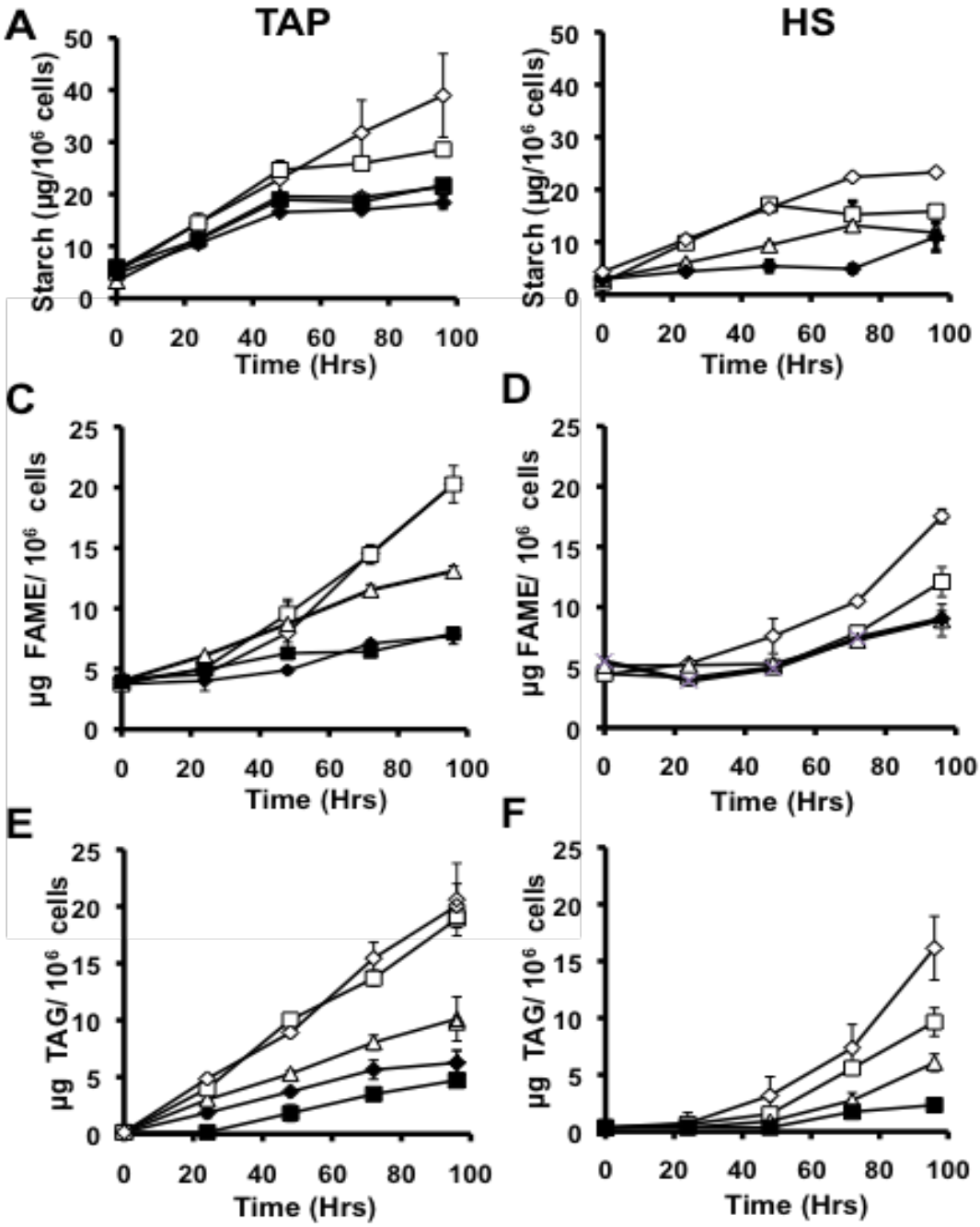

Figure 3.5. **Starch, FAME and TAG levels before and during nitrogen deprivation**. Starch (**A,B**), FAME (**C,D**), and TAG (**E,F**) levels are reported in ug per million cells for cultures in TAP (**A, C, E**) and HS (**B, D, F**) media. Empty diamonds, cells cultured at 160 µmol photons m^{-2} $s^{-}1$ (µE); empty squares, 40 µE; empty triangles, 15 µE; filled diamonds, 5 µE; filled squares, 0 µE. Error bars indicate +/- SD (n=3).

The increases in total cellular FAME levels we observed were lower and slower to start than increases in TAG. This is consistent with previous reports that membrane lipid levels fall during N deprivation and that some fatty acids used in TAG synthesis come from membrane lipids (Juergens, et al. 2015, Moellering *et al.* 2011, Yoon *et al.* 2012). However the extent to which fatty acids newly synthesized during N deprivation enter bulk membrane lipid pools is not known. The source(s) of carbon entering TAG and the fate of carbon assimilated during nutrient deprivation are relevant to the consideration of cellular metabolic input and output fluxes during TAG synthesis and were therefore probed in a labeling experiment.

^{13}C labeling Results

Chlamydomonas cells growing in nitrogen-replete TAP media were transferred to TAP media without N and containing ^{13}C labeled acetate (100% $^{13}C_{1,2}$). After 40 h cells were transferred to TAP media containing unlabeled acetate and lacking N for the remainder of the 96 h deprivation period. Cells cultured mixotrophically at 160 μmol photons m^{-2} s^{-1} were used as these conditions are similar to those used in many prior studies and showed the highest sustained starch and lipid accumulation rates. After 40 h of N deprivation in the presence of ^{13}C-acetate, the proportion of starch-derived ions detected that were labeled with ^{13}C was found to be low, with over 65% of the ions containing no ^{13}C label (Figure 3.6A) and over 80% of the total carbon being ^{12}C. Label levels increased modestly during the initial washout period between 40 and 72 h (~28% of starch carbon at 72 h originated from the ^{13}C acetate taken up between 0 and 40 h). Label levels in starch did not significantly change between 72 and 96 h. Thus photosynthetic CO_2 fixation and/or cellular biomass components made before deprivation is the dominant source of carbon for net starch synthesis during N deprivation under mixotrophic conditions. In

such cultures the total starch levels per cell doubled between 40 and 96 h (Figure 3.5A), during which time no ^{13}C label was present in the medium, so we had expected a dilution of the ^{13}C label in starch. The lack of a decrease in fractional labeling level between 40 and 96 h shows that ^{13}C assimilated during nitrogen deprivation (0-40 h) contributed significantly to starch synthesis later.

Labeling in fatty acids from the experiment described above is also shown in Figure 3.6. Figure 3.6B shows the distribution of mass isomers from a representative mass spectrum of palmitate (C16:0, as the methyl ester) from cells collected at 40 h. Labeling results for C16:0 from TAG and two membrane lipid fractions (galactolipids, which are major components of chloroplast membranes, and a polar lipid fraction containing lipids from both chloroplast and extra-plastidic membranes) are shown in Figure 3.6 C to Figure 3.6E. Analogous data for other abundant fatty acids are given in the Figures 3.7 and 3.8. After 40 h of labeling and nitrogen deprivation, approximately 70% of the fatty acid molecules from TAG and membrane lipids contained one or more ^{13}C labeled carbons. In the majority of fatty acid molecules over half the carbon atoms were ^{13}C and the most abundant labeled mass isomer was the fully labeled one (^{13}C in all positions) and approximately half the total carbon in cellular fatty acids was ^{13}C. The preponderance of fatty acid molecules in all pools were either unlabeled or highly labeled, and since the total fatty acid content of the cultures approximately doubled during the 40 h labeling period we infer that 75% or more of the carbon used to synthesize fatty acids during N deprivation is derived from acetate taken up during deprivation.

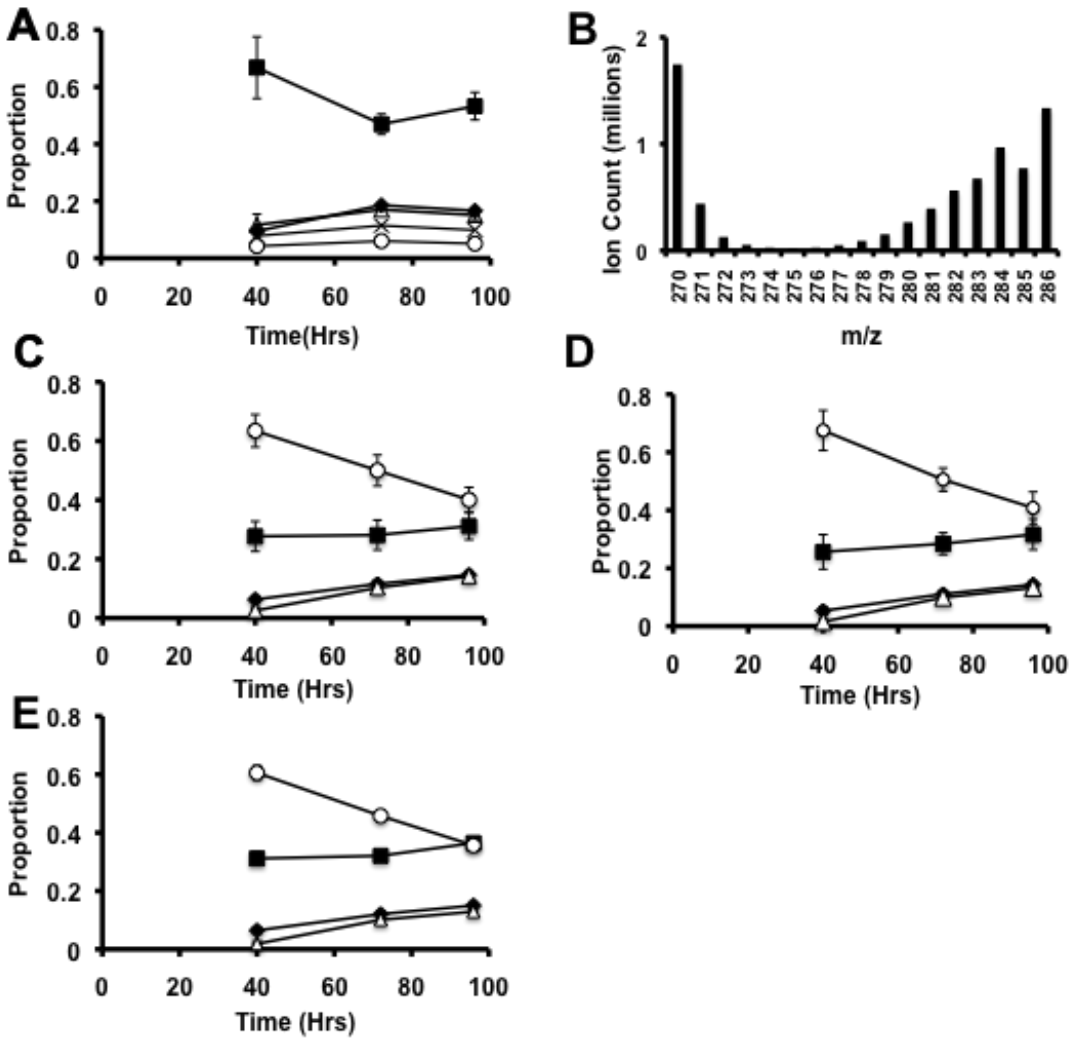

Figure 3.6. ^{13}C labeling of fatty acids and starch during N deprivation in cells cultured in TAP media at 160 µmol photons m^{-2} s^{-1}. Cells grown to log phase in N replete media were moved at time 0 to TAP media lacking N with 100% uniformly labelled ^{13}C acetate. After 40hrs the media was replaced with TAP media lacking N and containing unlabeled acetate for the remainder of the time course. The proportions of different mass isomers are plotted as a function of time. Panel **A** shows mass isomers of the m/z = **319** fragment ion containing carbons **2-6** of the glucose monomers of starch. Filled squares represent M+0, filled diamonds M+1, empty triangles m+2, **X**'s M+3, and empty circles M+4. Panel **B** is a histogram of the mass isomer distributions for a representative 16:0 FAME mass spectrum showing the abundance of highly labeled molecules together with unlabeled molecules (M+0 and naturally-occurring M+1 masses). Panel **C**, **D**, and **E** represent mass isomer distributions for ions of intact C16:0 FAME molecules from TAG, MGDG, and Polar Lipid fractions respectively. Filled squares represent unlabeled molecules (M+0); filled diamonds, M+1 (one ^{13}C atom); empty triangles, M+2; empty circles, the sum of M+3 through M+16 (fully labeled), Error bars indicate range (n=2).

High fractional labeling in galactolipids and polar lipids (Figure 5C and Figure 5D) after 40 h of N deprivation shows that membrane lipids are synthesized at a significant rate during nitrogen deprivation. Since the cellular levels of membrane lipids fall by more than 50% during this time (Juergens, et al. 2015), it is clear that substantial rates of simultaneous synthesis and breakdown of membrane lipids are occurring, suggesting acyl chain trafficking through these lipid classes. Therefore we consider that total cellular lipid rather than TAG is the appropriate pool to be measured when evaluating net carbon and energy fluxes into accumulated intracellular compounds during nitrogen deprivation.

After replacement of labeled with unlabeled acetate the proportion of fatty acid molecules that were highly 13C-labeled fell while the proportion of unlabeled molecules rose; this is consistent with dilution of highly labeled with newly synthesized unlabeled fatty acids. The similarity in C16:0 labeling patterns in different lipid pools is consistent with the continued flux of newly synthesized fatty acids into membrane lipids as well as TAG between 40 and 9 6h. In addition, during this "chase" period there is an increase in the proportion of fatty acid molecules with low levels of labeling (M+1 and M+2) which we attribute to flow of C from non-lipid compounds synthesized during the initial stages of N deprivation into lipid synthesis at later stages.

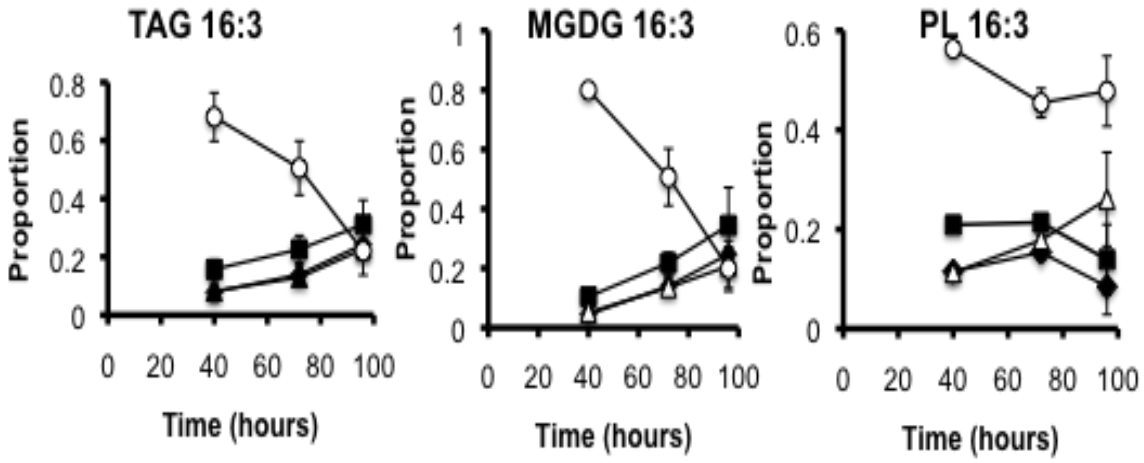

Figure 3.7. ^{13}C labeling of C16:3 fatty acids during N deprivation in cells cultured in TAP media at 160 µmol m^{-1} s^{-1} . Cells grown to log phase in N replete media were moved at time 0 to TAP media lacking N with 100% uniformly labelled ^{13}C acetate. After 40hrs the media was replaced with TAP media lacking N and containing unlabeled acetate for the remainder of the time course. The proportions of different mass isomers are plotted as a function of time. Panel A, B, and C represent mass isomer distributions for ions of intact C16:3 FAME molecules from TAG, MGDG, and Polar Lipid fractions respectively. Filled squares represent unlabeled molecules (M+0); filled diamonds, M+1 (one ^{13}C atom); empty triangles, M+2; empty circles, the sum of M+3 through M+16 (fully labelled), Error bars indicate range (n=2).

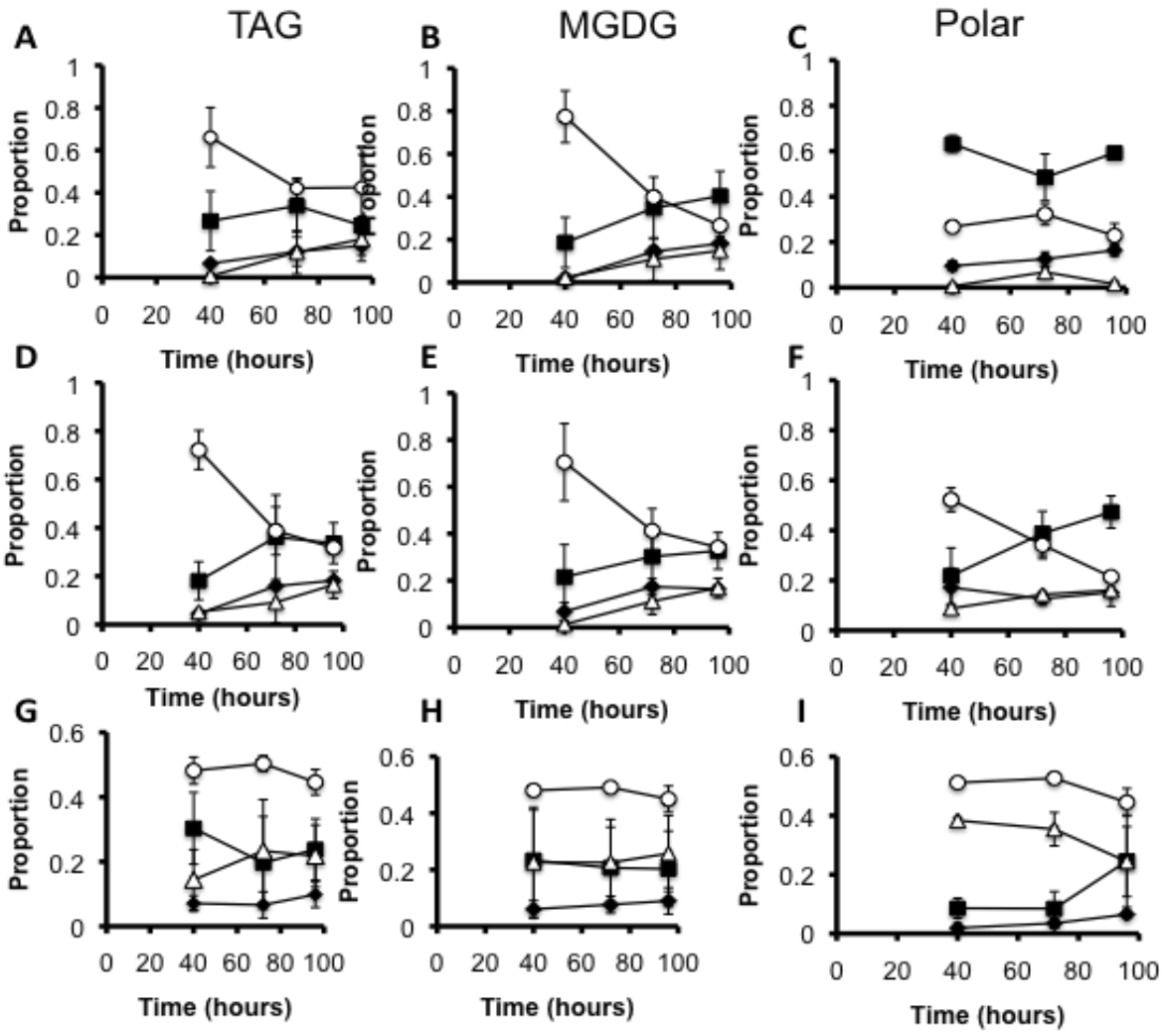

Figure 3.8. ^{13}C labeling of C18 fatty acids during N deprivation in cells cultured in TAP media at 160 µmol m^{-1} s^{-1} . Cells grown to log phase in N replete media were moved at time 0 to TAP media lacking N with 100% uniformly labeled ^{13}C acetate. After 40hrs the media was replaced with TAP media lacking N and containing unlabeled acetate for the remainder of the time course. The proportions of different mass isomers are plotted as a function of time. Panel A, B, and C represent mass isomer distributions for ions of intact C18:1 FAME molecules from TAG, MGDG, and Polar Lipid fractions respectively. Panel D, E, and F represent mass isomer distributions for ions of intact C18:2 FAME molecules from TAG, MGDG, and Polar Lipid fractions respectively. Panel G, H, and I represent mass isomer distributions for ions of intact C18:3 FAME molecules from TAG, MGDG, and Polar Lipid fractions respectively. Filled squares represent unlabeled molecules (M+0); filled diamonds, M+1 (one ^{13}C atom); empty triangles, M+2; empty circles, the sum of M+3 through M+16 (fully labeled), Error bars indicate range (n=2).

Light Absorption, Utilization Efficiency and Dissipation

To gauge photosynthetic light capture rates, levels of chlorophyll (chl) and the efficiency of photosystem II were measured. Chl levels are shown in Figure 3.9A and Figure 3.9B for cells cultured in TAP and HS medium respectively. Nitrogen-replete cells growing under mixotrophic conditions contained more Chl than autotrophically growing cells, with the exception of mixotrophic cells at the lowest light levels. During nitrogen deprivation chl levels fell continuously in mixotrophically cultured cells, whereas under autotrophic conditions chl levels fell during the first two days and did not change significantly thereafter.

Both theoretical quantum yield at photosystem II (F_V/F_M) and light driven yields (Φ_{II}) were measured by fluorescence spectroscopy as measures of the efficiency with which absorbed light drives linear electron flow. In TAP media F_V/F_M and Φ_{II} (Figure 3.9C and Figure 3.9E respectively) declined through the nitrogen deprivation period, with the exception of cells under 5 μmol photons m^{-2} s^{-1}. In autotrophic cells F_V/F_M and Φ_{II} (Figure 3.9D and Figure 3.9F) did not significantly change during nitrogen deprivation.

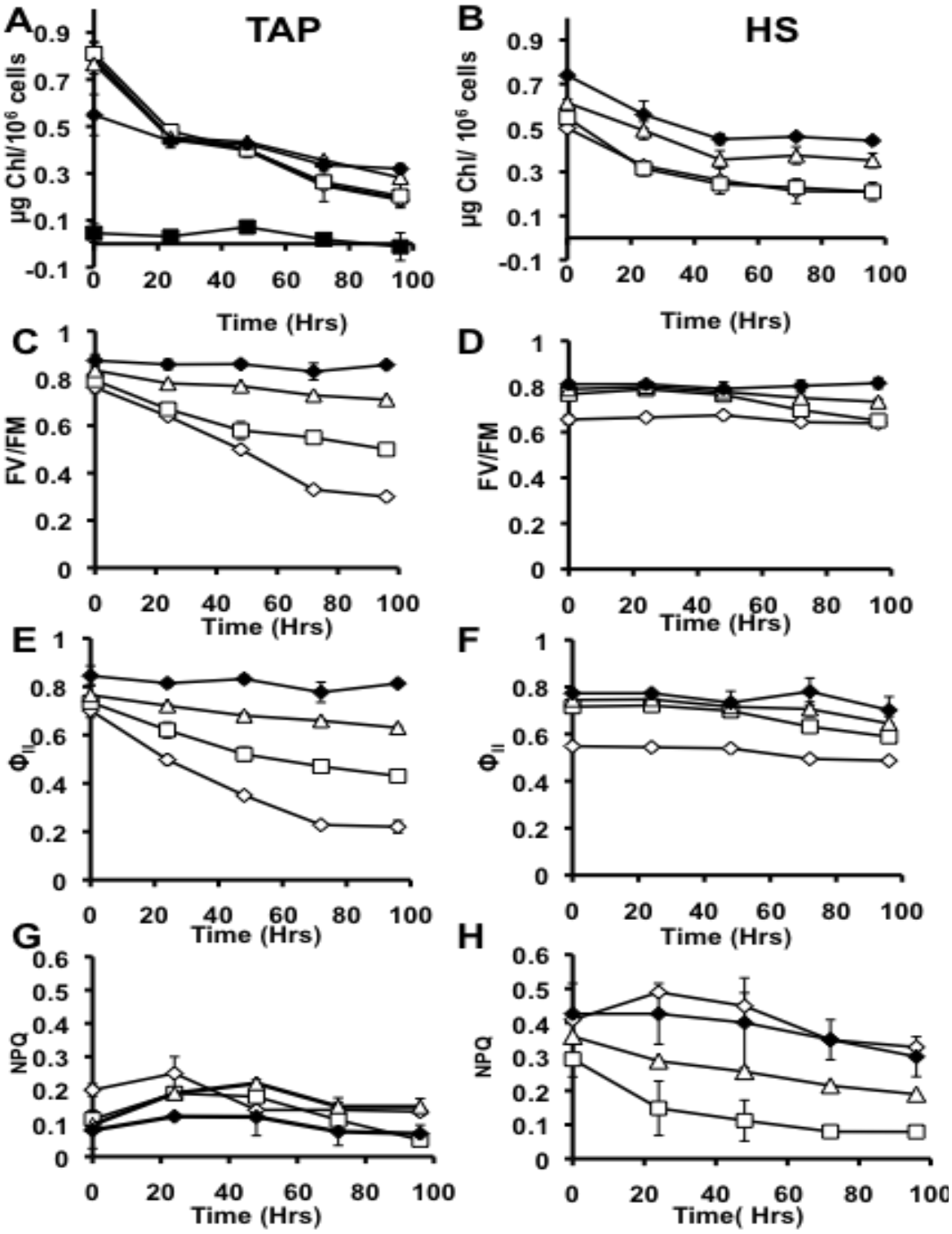

Figure 3.9. Chlorophyll, Photosynthetic efficiency and Non Photochemical Quenching.

Figure 3.9 (cont'd). Panel **A** and **B** represent Chlorophyll levels in Tap and HS conditions respectively. Panels **C** and **D** represent Maximum photosynthetic efficiency from dark adapted cells for TAP and HS conditions respectively. Panels **E** and **F** represent photosynthetic efficiency in the light for TAP and HS conditions respectively. Panels **G** and **H** represent photosynthetic efficiency in TAP and HS conditions respectively. In all cases, 160 μmol m^{-1} s^{-1} is indicated by hollow diamonds, 40 μmol m^{-1} s^{-1} by hollowed squares, 15 μmol m^{-1} s^{-1} indicated by hollowed triangles , 5 μmol m^{-1} s^{-1} by solid diamonds, and 0 μmol m^{-1} s^{-1} by solid squares. Error bars indicate SD (n=3).

During photosynthetic stress conditions and at high light levels, cells dissipate excess absorbed light energy, by non- photochemical quenching (NPQ) (Muller, et al. 2001). We measured NPQ before and during N deprivation under mixotrophic (Figure 3.9G) and autotrophic (Figure 3.9H) conditions using the same light level for NPQ measurement as the level under which the cells had been cultured. NPQ levels recorded before and throughout nitrogen deprivation for all cultures were lower than values reported in previous studies in which much higher light levels were used for measurement than for growth (Niyogi, et al. 1997, Peers, et al. 2009, Terauchi *et al.* 2010). The absence of significant increases in NPQ after N-deprivation suggests that there is little or no light stress due to excess energy intake under these conditions.

Photosynthetic Fluxes

Photosynthetic fluxes were assessed by measuring oxygen evolution and electrochromic shift (ECS) absorbance spectroscopy as indicators of linear and cyclic electron flow respectively (Figure 3.10). Oxygen evolution rates at 160 μmol photons m^{-2} s^{-1} for both autotrophic and heterotrophic cultures decreased markedly during N deprivation (Figure 3.10A and Figure 3.10b). At 40 μmol photons m^{-2} s^{-1} and below, net oxygen fluxes were much less during nitrogen replete growth but remained largely unchanged during deprivation. Mixtrophically

cultured cells at lower light levels and autotrophic cells were net oxygen consumers. ECS decay rates, which reflect the proton fluxes across thylakoid membranes that drive photosynthetic ATP synthesis, decreased several fold during nitrogen deprivation for cells under the highest light level for both mixotrophic and autotrophic cells (Figure 3.10C and Figure 3.10D). At lower light levels ECS values for N replete cells were significantly less than at 160 μmol photons m^{-2} s^{-1} and decreased moderately or were not significantly changed during nitrogen deprivation.

Figure 3.10. Oxygen evolution and electrochromic shift measurements. Net oxygen evolution (**A** and **B**) and electrochromic shift decay rates (indicating proton fluxes across the

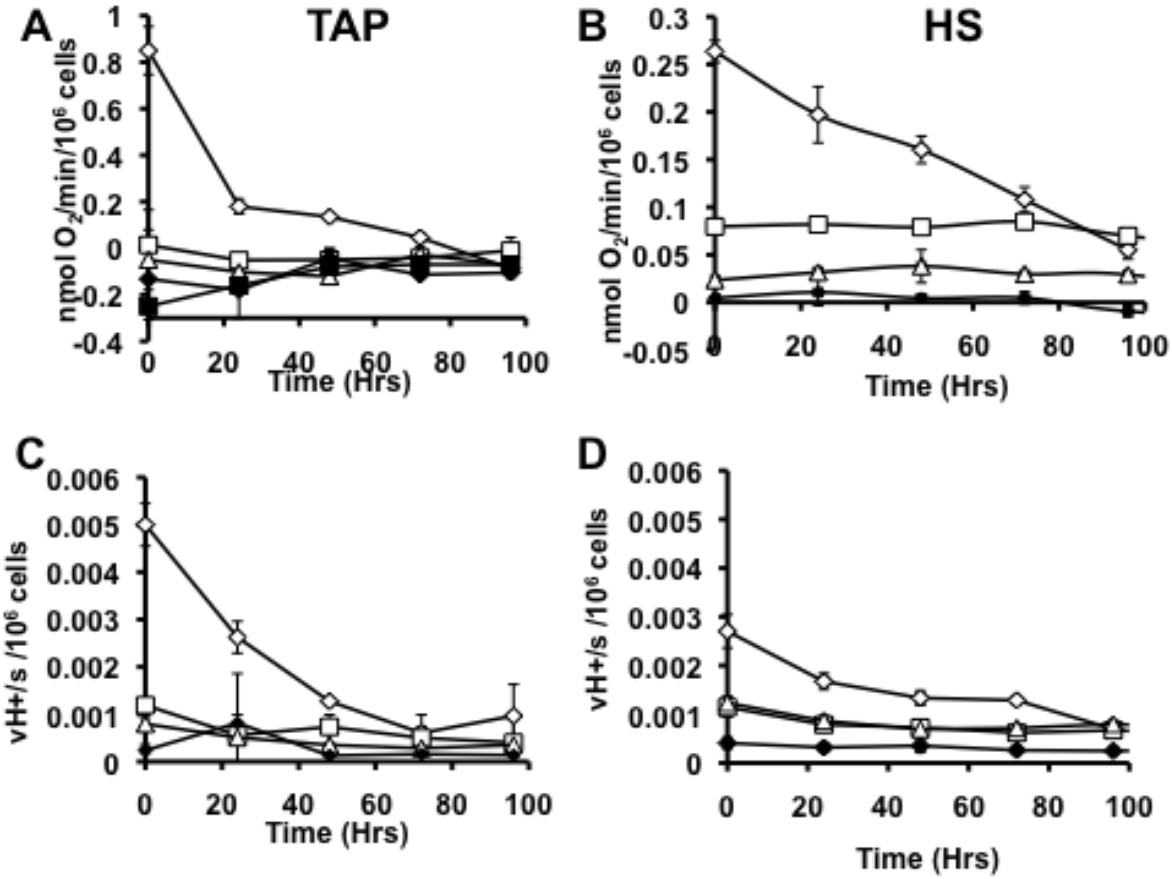

thylakoid membrane, **C** and **D**) for cells grown in TAP (**A** and **C**) and HS (**B** and **D**) media. Results for cells cultured at 160 μmol m^{-2} s^{-1} are indicated by empty diamonds, 40 μmol m^{-2} s^{-1} empty squares, 15 μmol m^{-2} s^{-1} empty triangles, 5 μmol m^{-2} s^{-1} filled diamonds, and 0 μmol m^{-2} s^{-1} filled squares. Error bars indicate SD (n=3).

Carbon Assimilation and Release

Net CO_2 uptake and efflux rates were measured before and during N deprivation (Figure 3.11A and Figure 3.11B). In TAP media, cultures under 160 and 40 μmol photons m^{-2} s^{-1} of illumination and in HS media at all light levels showed net CO_2 assimilation when provided with nitrogen while cultures exposed to lower light levels or in the dark in TAP media were net CO_2 producers. During nitrogen deprivation, net CO_2 uptake and output rates decreased, with TAP-grown cells at 40 μmol photons m^{-2} s^{-1} becoming net CO_2 producers after 2d of deprivation. Acetate uptake rates for mixotrophic and heterotrophic cultures (Figure 3.11C) were higher for cells at lower light intensities and in the dark and decreased during nitrogen deprivation. Thus both photosynthetic CO_2 assimilation and consumption of external fixed carbon decreased strongly during N deprivation, with decreases being more marked at higher light levels.

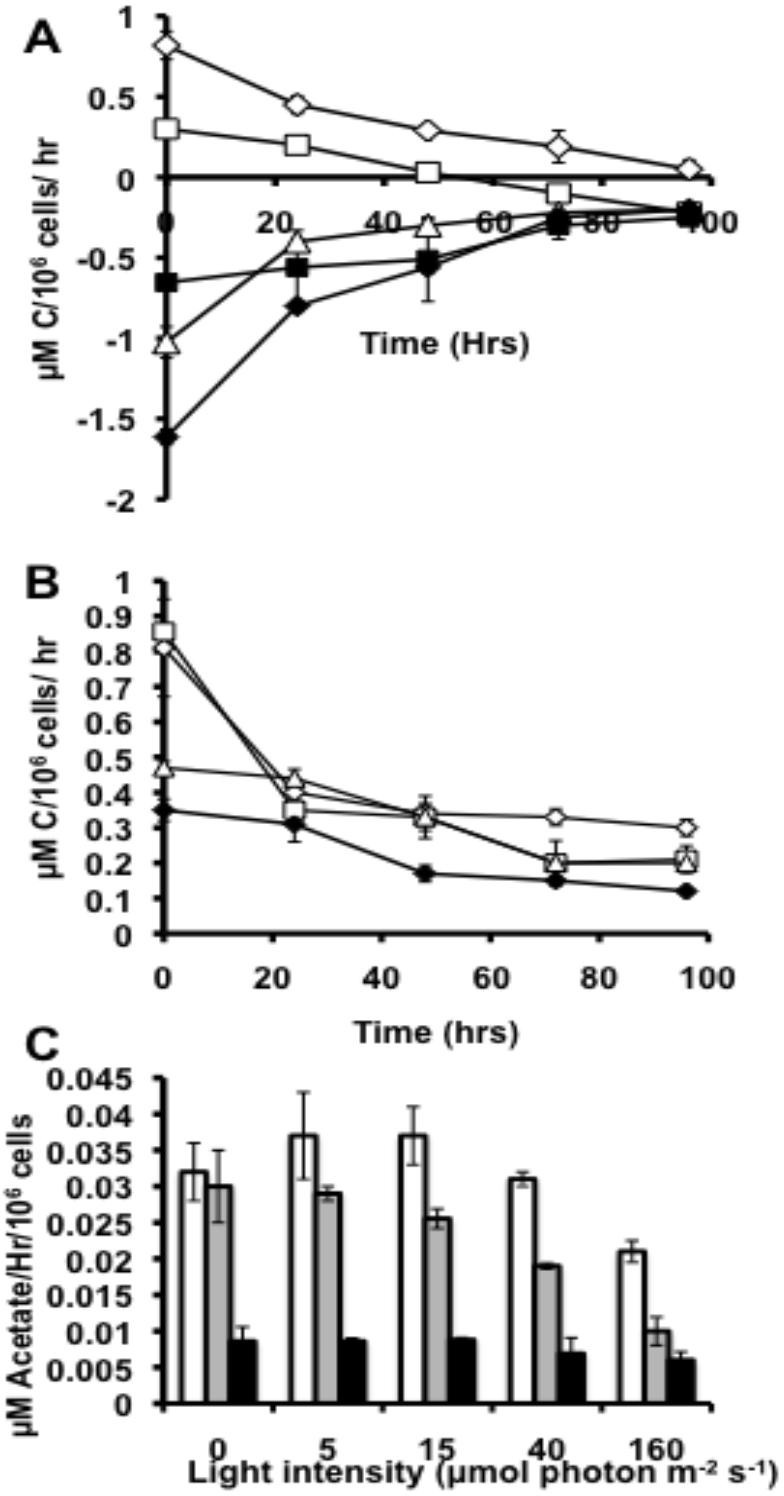

Figure 3.11. **Carbon assimilation rates.**

Figure 3.11. **(cont'd).** Net CO_2 uptake in TAP (**A**) and HS (**B**) media. Measurements of cells cultured 160 μmol m^{-2} s^{-1} are indicated by empty diamonds, 40μmol m^{-2} s^{-1} by empty squares, 15μmol m^{-2} indicated by empty triangles , 5μmol m^{-2} s^{-1} by filled diamonds, and 0 μmol m^{-1} s^{-1} by filled squar Acetate uptake in TAP cultures are in panel **C** for Nitrogen replete cells (White), 0-24hrs of deprivation (grey), and 24-96hrs of deprivation (black). Error bars indicate SD (n=3).

ANALYSIS AND DISCUSSION

The first observation of microalgal TAG accumulation under nitrogen deprivation was made over a century ago (Beijerinck 1904) and the potential to utilize this phenomenon for biofuels has been recognized for over 70 years (Harder *et al.* 1942a, Harder *et al.* 1942b). Among several explanations offered, the overflow hypothesis (OH), now at least 25 years old (Roessler 1990), currently holds sway over much of the interpretation of algal TAG accumulation data. The OH explains the synthesis of TAG and/or starch by algae during nutrient deprivation as a response to excess photosynthetic energy and/or carbon assimilation. The results of this study allow an assessment to be made of the OH in its straightforward form by making a series of inferences from it about the relationships between photosynthetic carbon and energy uptake rates and the rates of accumulation of TAG and starch and comparing these expectations to the data(Table 3.1). First, if accumulation is driven by surplus energy or carbon from photosynthesis, no accumulation is expected to occur in the dark. Starch accumulation rates in the dark were equal to or greater than rates for autotrophic cultures at all light levels and were exceeded only by mixotrophic cultures at the higher two light levels. We conclude either that starch accumulation during nitrogen deprivation is primarily driven by factors unrelated to photosynthetic overflow or that there is a separate additional explanation for its accumulation under heterotrophic conditions. TAG accumulation in the dark was also significant, although net

fatty acid accumulation was modest compared to cultures in the light. Indeed heterotrophic cells from taxa as diverse as fungi bacteria and mammals have been shown to accumulate TAG under nutrient deprivation (Alvarez *et al.* 2002, Frenk *et al.* 1958, Morin *et al.* 2011, Murphy 2001, Packter *et al.* 1995).

	Predictions	Supported?
1	Tag accumulates when PS fluxes are still high	No
2	Increasing light gives proportionate increase in oil	No
3	Tag accumulation is dependent upon photosynthesis	No
4	All the carbon in TAG will come from photosynthesis	No
5	N dep would induce reduction in photosynthesis	Yes
6	N dep induces significant NPQ	No
7	The rate of photosynthetic carbon assimilation rather than total carbon uptake drives TAG accumulation	No

Table 3.1. Overflow Hypothesis predictions and verification. This table summarizes the predictions associated with the Overflow Hypothesis of TAG accumulation and whether they were supported or not by this study.

Second, the OH links growth before nutrient deprivation to TAG production afterwards; initially we examine carbon balances. Figure 3.12 shows a comparison of carbon accumulation rates before and during the first 24 h after N deprivation. The first 24 h after deprivation were selected for comparison with N-replete growth since at this time photosynthetic function is most similar to pre-deprivation rates. In this work, as elsewhere (Fan, et al. 2012, Siaut, et al. 2011) starch was found to be the dominant carbon sink, with total FAME accounting for less than 15% of net carbon accumulation during the first 24 h. Total FAME accumulation rates only match and begin to exceed those for starch after 48 h, by which time photosynthetic fluxes are substantially lower. For autotrophic cells across all light levels the total carbon accumulation rates after deprivation are close to 90% of those during N replete growth, which is consistent with the OH as applied to total C. For cells cultured under mixotrophic or heterotrophic conditions, total carbon accumulation rates after deprivation are not well explained by the rates during N replete growth. Although there is a trend with increasing light levels in TAP media towards greater total C accumulation rates before and after deprivation, the slope corresponds to only 11% and the trend does not extrapolate meaningfully to low light and lower growth rates. Concerning the origins of carbon from which TAG and starch are synthesized, ^{13}C acetate labeled both these pools in mixotrophic cultures that were grown at the highest light level to maximize photosynthetic inputs. Photosynthesis is therefore not the dominant metabolic source of acetyl-CoA used in TAG synthesis in mixotrophy. Fan et al. (Fan, et al. 2012) have suggested that TAG accumulation is dependent upon total carbon precursor availability rather than only CO_2 from photosynthesis.

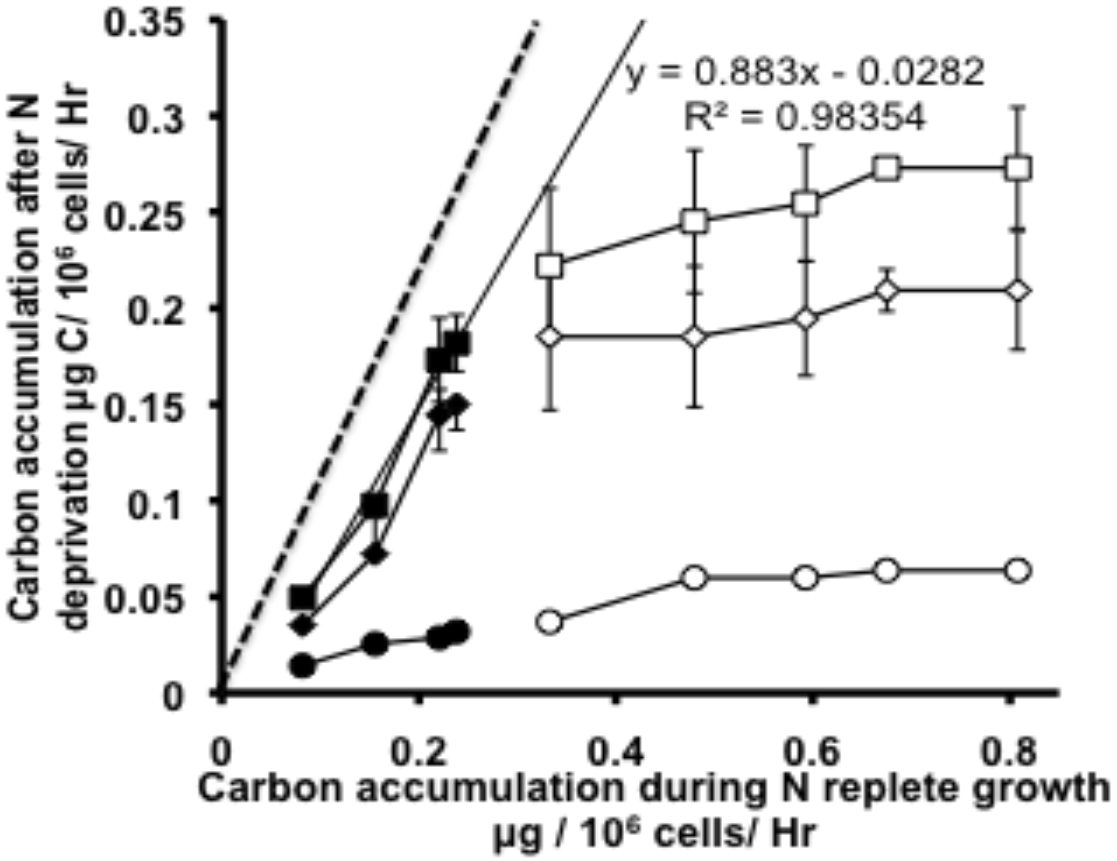

Figure 3.12. Cellular carbon accumulation rates before and during the first 24hrs after nitrogen deprivation. Accumulation during nitrogen replete growth was derived from growth rates and total cellular carbon contents; carbon accumulation after deprivation is due to starch and lipid production. Filled symbols represent autotrophic conditions (HS media), while empty ones represent mixotrophic and heterotrophic conditions (TAP media). Squares indicate values for total Carbon accumulation (starch plus total FAME) while diamonds and circles represent starch and total FAME respectively. Within each series, increasing light levels correspond to symbols from left to right Error bars depict +/- SD (n=3). The dashed line corresponds to a slope of 1 and the solid line is the least-squares best fit to the autotrophic total carbon accumulation results.

Third, regarding redox energy balance the OH posits that the function of TAG synthesis during nutrient deprivation is to consume excess photosynthetically produced reductant and thereby prevent photodamage due to over reduction of electron transport chain components. We would expect from this that cellular fatty acid levels should rise most rapidly when net oxygen production is highest (early on in nutrient deprivation), which is not the case (compare Figure 4C and 4D with Figure 7A and 7B). Since cells at the highest light level were CO_2 limited during N-replete growth, these might be expected to show either high rates of NPQ or elevated fatty acid accumulation rates compared to starch early during deprivation, neither of which was observed.

Related to the potential role of TAG synthesis in mitigating over reduction in the electron transport chain is a fourth prediction, one that has received apparent support from past studies. In this version of the OH, following N deprivation cells experience stress from excess light energy uptake leading to the activation of energy dissipative mechanisms such as non-photochemical quenching and/or the Mehler reaction in addition to TAG synthesis. Increases in NPQ under nutrient deprivation have been previously observed, reaching levels that account for a substantial proportion of light energy reaching the photosystems (Allen *et al.* 2008, Antal *et al.* 2006, White *et al.* 2011, Wilson *et al.* 2007). However, those measurements of NPQ were made under much higher light levels than those under which cultures were maintained. Measurements of NPQ under light levels under which cells had been cultured (Figure 3.9) show stable or decreasing NPQ in TAP media while in HS media cells exhibit decreasing NPQ following N deprivation. Slow decreases in photosynthetic efficiency, Chl levels and gas exchange rates in parallel with low and decreasing levels of NPQ indicate that a coordinated downregulation of photosynthetic structure and function that is used to match energy supply and demand under a wide range of

energy input rates, making the idea of overflow from a mismatch of supply and demand less appealing.

An alternative perspective on energy balances is to assess the relationship between photosynthetic energy input and the accumulation of TAG and starch. Figure 3.13A and Figure 3.13B show the values of an estimate of the rates of cellular light energy intake: the product of illumination level, chlorophyll content and Φ_{II}. This parameter accounts for light absorbed and the quantum efficiency with which light drives photosynthetic electron flow (Genty, et al. 1989). While only part of the energy capture estimated by this parameter becomes available to cellular functions in the form of ATP and NADPH, the dominant losses involved, such as that associated with light of wavelength < 680nm and the stoichiometries and/or irreversibilities of electron transport and H+/ATP'ase fluxes are such that the proportion lost is likely to be similar across the conditions used here. The photosynthetic energy capture rates span a range of approximately 50 fold under nitrogen-replete conditions, a range which narrows during N deprivation since the capture rates fall more strongly in cells cultured with lower light levels. The extent to which light capture rate is reflected in lipid, starch and total C accumulation rate is shown in Figure 3.13C to Figure 3.13H as the ratio of carbon accumulated to the light capture parameter. This ratio varies widely among culture conditions at any given time, with cells exposed to higher light levels accumulating less starch or FAME as a proportion of apparent light energy captured. The OH would lead one to expect higher rather than lower proportions of light energy to be used for carbon accumulation at higher light levels. Alternatively or additionally a threshold of light capture rates might be expected to be needed to result in photosynthetic energy overflow that triggers C accumulation; a comparison of Figures 3.13A and 3.13B with Figure 3.5 shows that no such threshold is evident. Starch and TAG rates vs. acetate is presented in Figure 3.14.

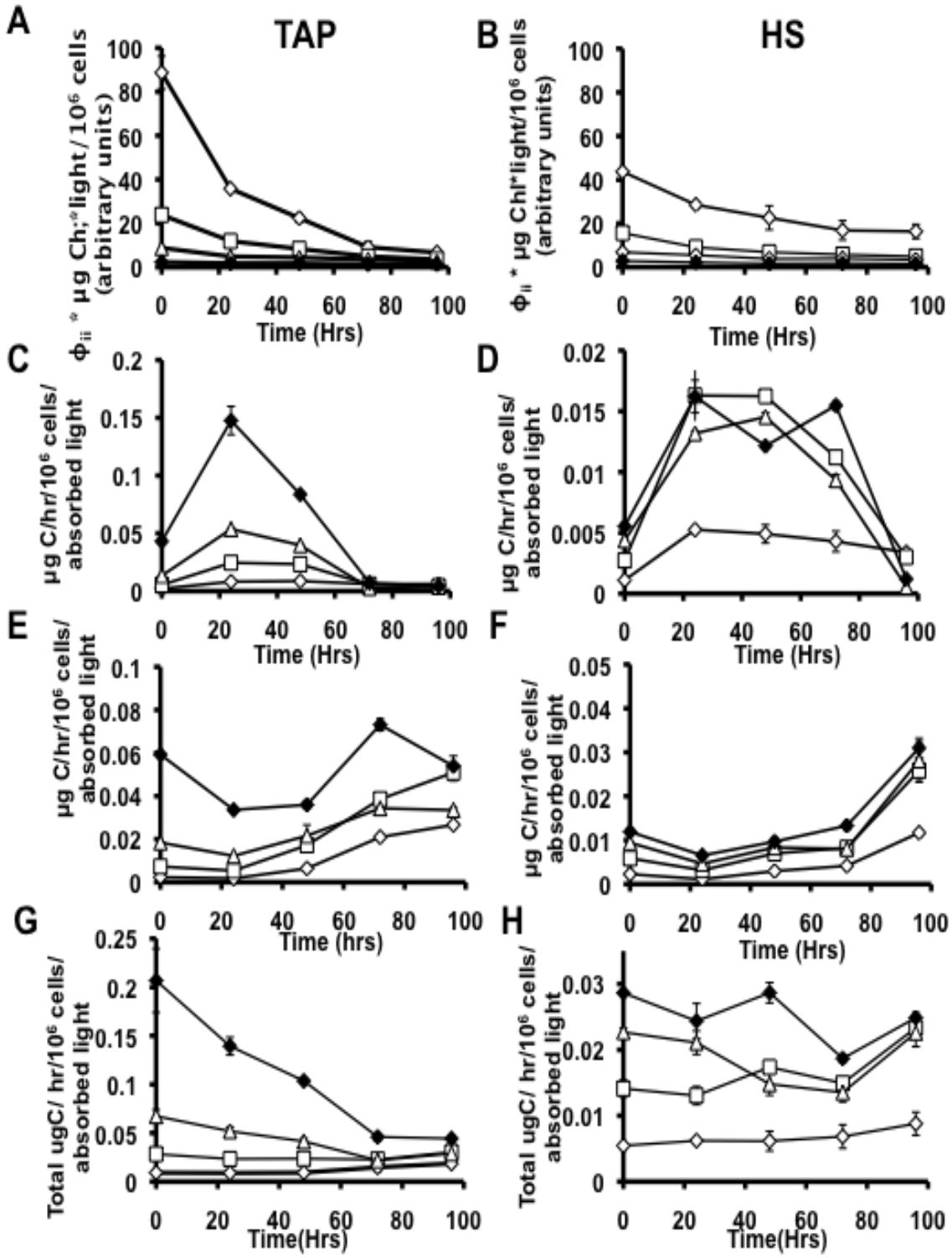

Figure 3.13. Accumulated Carbon V.S Potential absorbed light

Figure 3.13 (Cont'd). A metric of potential usable light by photosystem II was calculated from Φ_{II} times Chl levels* light intensity per million cells. TAP cultures are in panel A and HS culture data is in panel B. Panel C and D show the rate of starch accumulation vs. absorbed light for TAP and HS respectively. Panel E and F show rates of FAME accumulation vs. absorbed light for TAP and HS respectively. G and H display rates of total carbon accumulation vs. absorbed light. For TAP and HS repectively In all cases, 160 μmol photons m^{-2} s^{-1} (μE) is indicated by hollow diamonds, 40 μE by hollowed squares, 15 μE indicated by hollowed triangles , 5 μE by solid diamonds. Error bars indicate SD (n=3).

The OH can also be considered in terms of the relationship between captured light energy and the energy deposited in accumulated compounds; for the latter we used heats of combustion for starch and glycerolipid (and for nitrogen replete growth also of protein/nucleic acids). This comparison is made in Figure 3.15A and Figure 3.15B for mixotrophic and autotrophic cultures respectively. For autotrophic cells at lower light levels and during N deprivation but not before, there is a correlation between photosynthetic energy input (X axis of figure 3.15B) and the accumulation of chemical potential energy in starch plus TAG (Y axis). For N replete, mixotrophic cultures and higher light levels, this correlation is not evident. The ratio of light energy input to chemical energy accumulated is shown as a function of deprivation time in Figure 3.15C and 3.15D. This ratio ranges by 20 fold across light levels with cells having higher light input rates accumulating less of it in starch and TAG, which is not expected if C compound accumulation is a large contributor to coping with light energy input.

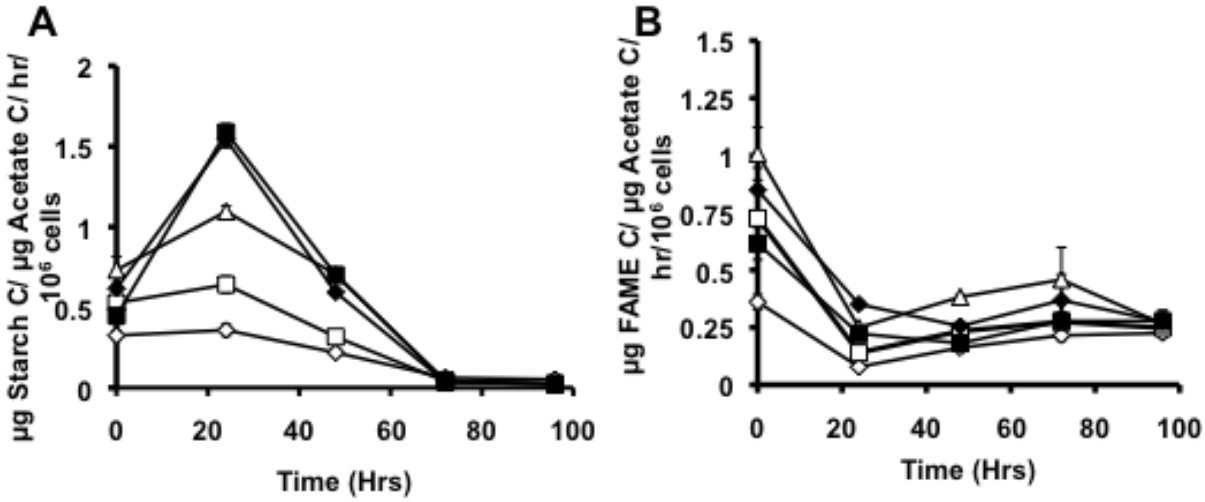

Figure 3.14. µg Starch and FAME per uptaken acetate. Panels A and B represent Starch and FAME accumulation rates respectively for TAP conditions. In all cases, 160 µmol m^{-1} s^{-1} is indicated by hollow diamonds, 40 µmol m^{-1} s^{-1} by hollowed squares, 15 µmol m^{-1} s^{-1} indicated by hollowed triangles , 5 µmol m^{-1} s^{-1} by solid diamonds, and 0 µmol m^{-1} s^{-1} by solid squares. Error bars indicate SD (n=3).

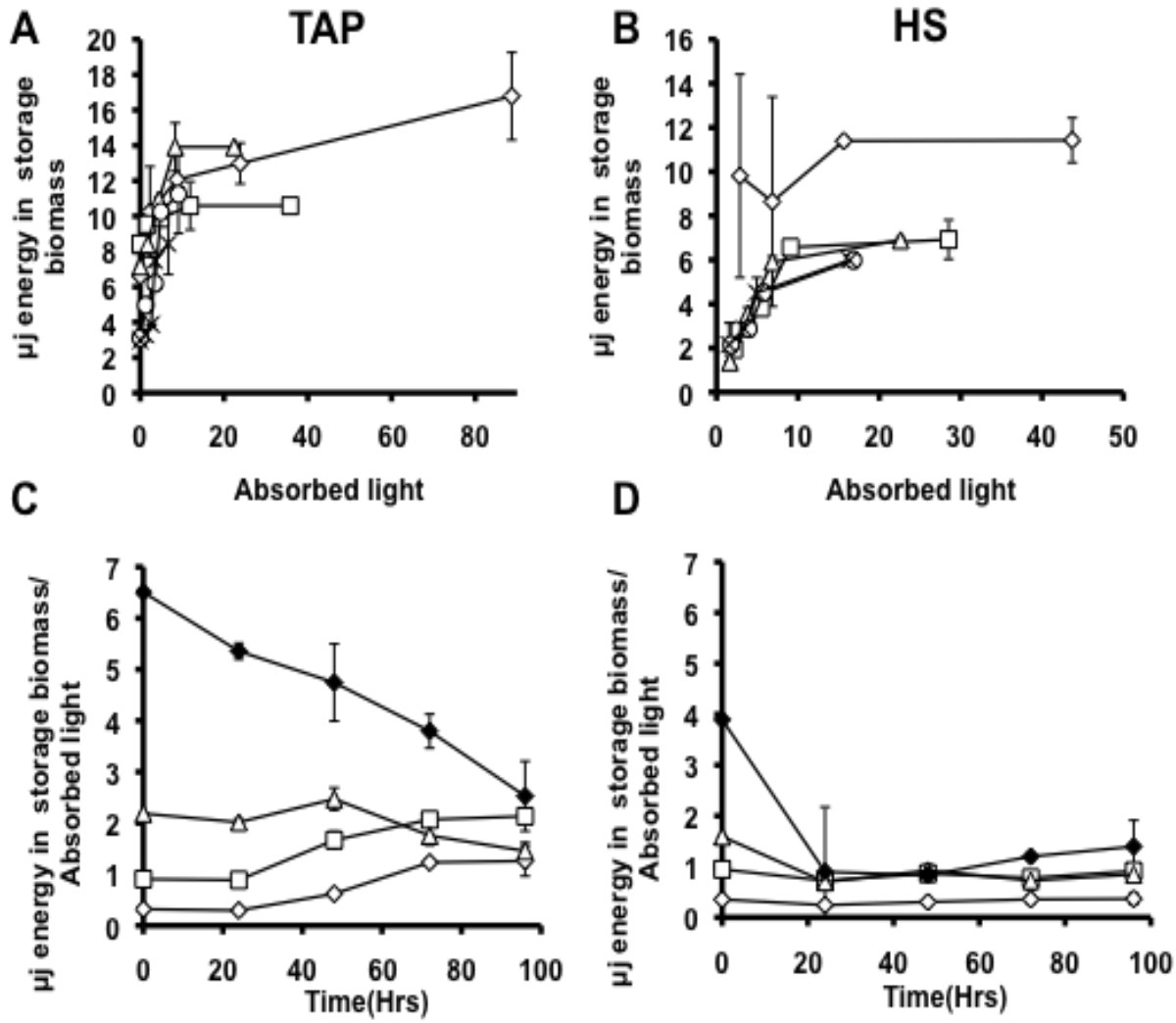

Figure 3.15 Light energy intake and energy stored in accumulated biomass (as heat of combustion) in TAP (panels A and C) and HS (panels B and D). The relationship between this energy output into biomolecules and the energy input from photosynthetic light capture is shown in panels **A** and **B**. The ratio of chemical potential energy accumulated in each 24 h period to the light energy intake rate is shown in panels **C** and **D**. For A and B, Time 0 hrs is indicated by empty diamonds, 24hrs N- is indicated by empty squares, 48 hrs N- is indicated by empty triangles, 72hrs N- is indicated by empty circles, and 96hrs is indicated by X's. For **C** and **D**, 160 µmol photons $m^{-2}s^{-1}$ (µE) is indicated by empty diamonds, 40 µE by empty squares, 15 µE indicated by empty triangles, 5 µE by filled diamonds. Error bars indicate +/- SD (n=3).

CONCLUSION

This study was aimed at obtaining sufficient data to assess of the OH. Some of the results, such as the trend towards higher rates of TAG accumulation at higher light levels, and the correlation between total net carbon assimilation before and after nutrient deprivation in autotrophic cells are consistent with the OH, although that they are also compatible with alternative, storage based explanations. Other observations, including starch and TAG accumulation in heterotrophic cultures, the timing of TAG accumulation relative to maximal photosynthetic rates, and the apparent absence of correlation between light stress or excess reductant and TAG or starch accumulation show that the OH is insufficient as an explanation for the C accumulating response of algae during nutrient deprivation.

The results of a number of studies have been interpreted in terms of the OH hypothesis. One such study concerns the Chlamydomonas PGD1 galactolipase mutant. This mutant accumulates half as much TAG as wild type cells and is found to undergo severe chlorosis and cell death during N deprivation unless it is given DCMU (an inhibitor of PSII electron transfer). If excess photosynthetic energy is normally used for fatty acid synthesis when growth is halted by nutrient deprivation, reduction of TAG synthesis in this mutant could cause cell damage due to energy overflow. In light of the fact that most carbon and energy during N deprivation enter starch rather than TAG it would be important to measure starch levels to determine C and E balances. Also the OH explanation for the PDG1 phenotype assumes that the mutation has no significant effect on the chloroplast membrane and thus the environmnent around the photocenters, which may induce stress on the organism during N deprivation that would be alleviated by inhibiting PSII. It would also be of interest to measure such dissipative mechanisms as NPQ and the Mehler reactions in the PDG1 mutant under N deprived culture conditions, to

verify whether there is evidence for increased light stress. Finally, while PGD1 cells accumulate ROS, this was only found to accumulate 7 days after N deprivation - well past the point where photosynthetic fluxes are substantial. This suggests (as the authors note) that ROS is more likely linked to autophagy than to energy overflow.

We suggest that alternative explanations for starch and TAG accumulation by microalgae under nutrient deprivation should also be assessed experimentally. A plausible alternative role for TAG accumulation during N is that TAG serves as a storage site for, and a subsequent source of, acyl chains to aid in membrane degradation and resynthesis. One study following 14C labeled arachidonic acid found that this fatty acid was mobilized from TAG to chloroplast membrane during recovery {Khozin-Goldberg, 2005 #921}. The correlation between nutrient deprivation and the accumulation of TAG in photosynthetic algae has been known for over a century, its significance for green biotechnology development as well as for the ecophysiology of nutrient cycles makes understanding the adaptive causal links involved important and should be subjected to further experimental assessment. Future experiments should include 14C labeling during N deprivation and following the label during N recovery in total biomass, starch, TAG, amino acids and membrane lipids.

METHODS

Culturing

Chlamydomonas reinhardtii strain cc400 cw-15 mt++ was obtained from the Chlamydomonas Research Center and grown at 23 °C in liquid Tris-Acetate-Phosphate (TAP) media (Gorman, et al. 1965) and Sueoka High Salt (HS) media (Sueoka 1960) in 1L flasks shaken at 125 rpm under continuous illumination at 160, 40, 15, 5 and 0 μmol photons m^{-2} s^{-1} and ambient CO_2 concentrations. Cell growth was determined by optical density measurements at 750 nm using a DU 800 spectrophotometer (Beckman-Coulter). Cultures were grown to cell densities of between 0.15 and 0.3 O.D. to minimize self-shading which becomes significant in denser cultures. Cells were counted using a Z series Coulter Counter cell and particle counter (Beckman-Coulter). For N deprivation, cells were centrifuged and resuspended in TAP media lacking ammonium chloride (nitrogen source).

Chlorophyll Concentration

Cells were collected by centrifugation of 1 ml culture and Chl was extracted in 1 ml of 80 % acetone for 20 minutes from pelleted samples after the supernatant culture medium was removed. After extraction, samples were pelleted by centrifugation and the supernatant was used for analysis. Chl was quantified spectroscopically as described in (Ritchie 2006) using a DU 800 spectrophotometer (Beckman Coulter).

Ash Free dry weight

50 ml culture volume was harvested at each time point and cells were filtered onto Millipore Glass Fibre Prefilters (Millipore) under reduced pressure. Filtered cells were dried in an oven at 100°C for 4 h and weighed on a Sartorius CP225D analytical balance. Weighed samples were then heated 540°C to incinerate the cell biomass and the filters were reweighed (Zhu *et al.* 1997). Ash free dry weight (AFDW) was taken as the difference between sample weights before and after incineration.

Carbon and Nitrogen Contents

Aliquots of 50 ml of culture were harvested by centrifugation at each time point. Cells were then pelleted by centrifugation and frozen at -78°C then lyophilized for 12h. Dried samples were weighed on a Sartorius CP225D analytical balance in tin capsules, which were then submitted to Duke Environmental Stable Isotope Laboratory (Duke University) for elemental analysis.

Lipid analyses

Cells harvested by centrifugation at 0^{o}C and total lipids were extracted from samples containing the equivalent of ~10 mg of dry cell mass by the method of Folch (Folch, et al. 1957). Briefly, cells were extracted with 1ml of $CHCl_3$:MeOH (1:2, vol/vol), vortexing samples for 2 min. The sample was then centrifuged and the supernatant was collected; the extraction was repeated two more times and the supernatant extracts were pooled. Extracts were dried under flowing N_2 gas at room temperature and stored at -20 °C until analysis.

Total TAG was quantified using Thin Layer Chromatography (TLC) separation and densitometry. Briefly total lipid extracts were loaded onto Analtech *uniplate* silica gel HL plates

(Analtech) and separated with hexane: diethyl ether: acetic acid (70:30:1 vol/vol). After iodine staining, samples were scanned with a Cannon image class mf4690 scanner. ImageJ software (National Institute of Health) was used to quantitate TAG levels from the images. Conversion of integrated density into weight of TAG was performed by comparison with a biological standard sample (96hN-deprived Chlamydomonas TAG extract quantified by Gas Chromatography Flame Ionization Detection (GCFID) of its Fatty Acid Methyl Esters (FAMEs).

FAMEs were quantified by GCFID after derivatization of lipid samples. C15 TAG in toluene was first added to total cell lipid extracts as internal standard. Total lipid extracts were treated with 150ul 2M methanolic KOH in 1ml hexane and vortexed for 5 min at room temperature completion. 6N HCl was added to neutralize the pH, samples were vortexed for 1 min and the hexane phase was transferred to another glass tube and dried under flowing N_2 gas at room temperature and stored at -20°C. Remaining free fatty acids were derivatized with silylation agent N-tert-butyldimethylsilyl- N-methyltrifluoroacetamide (MTBSTFA) (Sigma, Saint Louis, MO) in pyridine. Samples were dried, resuspended in 1 ml hexane, and quantified using an Agilent GCFID with a DB-23 column (Agilent) as previously described(Pollard *et al.* 2015).

Oxygen Production and Consumption Rates

Changes in dissolved oxygen in cell suspensions were measured with a NEOFOX analyzer FOXY-R probe with a FOXY-AF-MG coating (Ocean Optics) as previously described (Juergens, et al. 2015).The O_2 sensor was immersed in 2 ml of culture in a capped 3ml cuvette with stirring. Net oxygen evolution was measured for 5 minutes at the same illumination level as

the culture had been grown in and O_2 consumption was measured for 1 minute in the dark immediately after the light period.

In vivo fluorescence spectroscopy

All spectroscopic measurements were performed with biological triplicates at each time point as previously described (Juergens, et al. 2015). Light-induced absorbance and chlorophyll fluorescence yield were measured using a kinetic spectrophotometer/fluorometer (Hall C, et al. 2011, Livingston, et al. 2010, Sacksteder, et al. 2001) modified for liquid samples by replacing the leaf holder with a temperature-controlled, stirring enabled cuvette holder (standard 1 cm pathlength). Cells were maintained under far red light LED (730nm) 20 min to oxidize the plastoquinone pool for accurate F_0 measurements. After dark/ far red adaptation, the first saturating pulse for Chl fluorescence measurements was applied with a pulsed measuring beam (505 nm peak emission LED) filtered through a BG18 (Edmund Optics) glass filter. The sample was then illuminated with the its respective photosynthetic photon flux density (PPFD) using a pair of light emitting diodes (LEDs) (Luxeon III LXHL-PD09, Philips) with maximal emission at 620 nm, directed towards opposite sides of the cuvette, perpendicular to the measuring beam. Fluorescence yields from saturating pulses were measured under actinic light and averaged over 6 measurements, separated by 120s intervals. Both absorption and fluorescence measuring pulses were 20-35 μs in duration and attenuated to produce less than 0.1% increase in chlorophyll fluorescence yield in dark-adapted samples. The first dark interval relaxation kinetics trace measuring the electrochromic shift (ECS) kinetics (one trace per biological replicate) was recorded after three minutes of actinic illumination, followed by one

minute of dark. Actinic LEDs were calibrated using a Licor LI190 PAR quantum sensor.

CO_2 Production and Consumption Rates

CO_2 exchange measurements were carried out with a LICOR XT 6400 (LICOR) infrared gas analyzer. Air was continuously circulated through 250ml flasks flask containing 50ml cultures, which were maintained under culture incubation conditions, and CO_2 levels were recorded for the air entering and leaving the flask. Input CO_2 levels were adjusted so that returning air contained 400 ppm.

Starch Analysis

Total glucose contained in starch was measured after amyloglucosidase and amylase digestion with the Megazyme total starch analysis kit (Megazyme, Ireland), similar to Work et al. (Work, et al. 2010). Briefly, pellets remaining after extraction of lipids from cells with 2:1 methanol:chloroform were autoclaved for 1 hour in 0.1 M Acetate buffer pH 4.8 then treated with α-amylase and amyloglucosidase for 1 hour at 55^{o}C. Free glucose was quantitated with a colorimetric assay at 510nm using a starch assay kit (Megazyme, Ireland) according to the manufacturer's instructions.

Acetate Analysis

Total acetate in culture media was measured with an acetate analysis Kit (K-ACETRM, Megazyme, Ireland). TAP media samples were diluted fivefold to be within the linear response range and 1.5 ml sub-samples were used for NADH consumption measurement by absorbance changes at 340nm. Briefly, acetic acid and ATP are converted to acetyl phosphate and ADP by

acetate kinase. The forward reaction is maintained by phosphotransacetlyase reaction of acetyl phosphate and coenzyme A to form acetyl-CoA and inorganic phosphate. Added phosphoenolpyruvate and ADP are converted to pyruvate and ATP by pyruvate kinase to maintain ATP levels and to produce pyruvate in proportion to the original levels of acetate. D-lactate dehydrogenase then converts the pyruvate and NADH into D-lactic acid and NAD^+.

Calculation of Carbon and Energy Balances

Acetate and oxygen uptake rates were converted into μg C/ 10^6 cells/ hr. Net oxygen fluxes were assumed to represent net CO_2 fluxes at a 1:1 ratio with 12g C/mol O_2. Acetate consumption was multiplied by 2 moles C/mole acetate. Carbon accumulation rates in biomass were obtained from the percent carbon of the biomass and the biomass accumulated. FAME and Starch mass accumulation rates were converted to μg C/ 10^6 cells/ h by multiplying the by the mass fraction of carbon for those molecules (72 g C per 162g polymerized starch and 204gC /267g FAME).

^{13}C labeling

Algal cells were fed 100% uniformly 13C labeled Acetate in TAP media without N for the first 40h after N deprivation. Cells were then centrifuged and resuspended in unlabeled TAP media without N for a further 56 h (96 h of deprivation total). Samples were collected at 40, 72, and 96 h following N deprivation. Starch and Lipids were extracted and treated as above, glucose from starch samples was derivatized with methoxyamine and TMS as described in (Roessner *et al.* 2001). Labeling in FAME samples was analyzed by GC-MS as described previously (Allen *et al.* 2007) while glucose labeling was analyzed on GC-MS using the same chromatography and MS parameters previously used for amino acids by (Chen *et al.* 2011b).

ACKNOWLEDGEMENTS

We thank Dr.'s David Kramer and Thomas Sharkey for generously making available to us equipment for making photosynthesis-related measurements and Dr. Sean Weise for advice on CO_2 gas exchange measurements.

REFERENCES

REFERENCES

Akita, T. and Kamo, M. (2015) Theoretical lessons for increasing algal biofuel: Evolution of oil accumulation to avert carbon starvation in microalgae. *Journal of theoretical biology*, **380**, 183-191.

Allen, A.E., Laroche, J., Maheswari, U., Lommer, M., Schauer, N., Lopez, P.J., Finazzi, G., Fernie, A.R. and Bowler, C. (2008) Whole-cell response of the pennate diatom Phaeodactylum tricornutum to iron starvation. *Proc Natl Acad Sci U S A*, **105**, 10438-10443.

Allen, D.K., Shachar-Hill, Y. and Ohlrogge, J.B. (2007) Compartment-specific labeling information in 13C metabolic flux analysis of plants. *Phytochemistry*, **68**, 2197-2210.

Alvarez, H.M. and Steinbuchel, A. (2002) Triacylglycerols in prokaryotic microorganisms. *Appl. Microbiol. Biotechnol.*, **60**, 367-376.

Antal, T.K., Volgusheva, A.A., Kukarskikh, G.P., Krendeleva, T.E., Tusov, V.B. and Rubin, A.B. (2006) [Examination of chlorophyll fluorescence in sulfur-deprived cells of Chlamydomonas reinhardtii]. *Biofizika*, **51**, 292-298.

Atabani, A.E., Silitonga, A.S., Badruddin, I.A., Mahlia, T.M.I., Masjuki, H.H. and Mekhilef, S. (2012) A comprehensive review on biodiesel as an alternative energy resource and its characteristics. *Renew. Sust. Energ. Rev.*, **16**, 2070-2093.

Ball, S.G., Dirick, L., Decq, A., Martiat, J.C. and Matagne, R.F. (1990) Physiology of Starch Storage in the Monocellular Alga Chlamydomonas-Reinhardtii. *Plant Sci*, **66**, 1-9.

Beijerinck, M. (1904) Das Assimilationsprodukt der Kohlensäure in den Chromatophoren der Diatomeen. *Recueil Travaux Botaniques Néerlandais*, **1**, 28-32.

Blaby, I.K., Glaesener, A.G., Mettler, T., Fitz-Gibbon, S.T., Gallaher, S.D., Liu, B.S., Boyle, N.R., Kropat, J., Stitt, M., Johnson, S., Benning, C., Pellegrini, M., Casero, D. and Merchant, S.S. (2013) Systems-Level Analysis of Nitrogen Starvation-Induced Modifications of Carbon Metabolism in a Chlamydomonas reinhardtii Starchless Mutant. *The Plant cell*, **25**, 4305-4323.

Bonente, G., Pippa, S., Castellano, S., Bassi, R. and Ballottari, M. (2012) Acclimation of Chlamydomonas reinhardtii to different growth irradiances. *J Biol Chem*, **287**, 5833-5847.

Chapman, S.P., Paget, C.M., Johnson, G.N. and Schwartz, J.M. (2015) Flux balance analysis reveals acetate metabolism modulates cyclic electron flow and alternative glycolytic pathways in Chlamydomonas reinhardtii. *Frontiers in plant science*, **6**, 474.

Chen, X.W., Alonso, A.P., Allen, D.K., Reed, J.L. and Shachar-Hill, Y. (2011) Synergy between C-13-metabolic flux analysis and flux balance analysis for understanding metabolic adaption to anaerobiosis in *E. coli*. *Metab Eng*, **13**, 38-48.

Chisti, Y. (2007) Biodiesel from microalgae. *Biotechnology Advances*, **25**, 294-306.

Courchesne, N.M., Parisien, A., Wang, B. and Lan, C.Q. (2009) Enhancement of lipid production using biochemical, genetic and transcription factor engineering approaches. *Journal of biotechnology*, **141**, 31-41.

Fan, J., Yan, C., Andre, C., Shanklin, J., Schwender, J. and Xu, C. (2012) Oil accumulation is controlled by carbon precursor supply for fatty acid synthesis in *Chlamydomonas reinhardtii*. *Plant & cell physiology*, **53**, 1380-1390.

Folch, J., Lees, M. and Sloane Stanley, G.H. (1957) A simple method for the isolation and purification of total lipides from animal tissues. *J Biol Chem*, **226**, 497-509.

Frenk, S., Gomez, F., Ramos-Galvan, R. and Cravioto, J. (1958) Fatty liver in children; kwashiorkor. *The American journal of clinical nutrition*, **6**, 298-309.

Gargouri, M., Park, J.J., Holguin, F.O., Kim, M.J., Wang, H., Deshpande, R.R., Shachar-Hill, Y., Hicks, L.M. and Gang, D.R. (2015) Identification of regulatory network hubs that control lipid metabolism in Chlamydomonas reinhardtii. *J Exp Bot*, **66**, 4551-4566.

Genty, B., Briantais, J.M. and Baker, N.R. (1989) The Relationship between the Quantum Yield of Photosynthetic Electron-Transport and Quenching of Chlorophyll Fluorescence. *Biochimica et biophysica acta*, **990**, 87-92.

Goldman, J.C., Oswald, W.J. and Jenkins, D. (1974) Kinetics of Inorganic Carbon Limited Algal Growth. *J Water Pollut Con F*, **46**, 554-574.

Goodenough, U., Blaby, I., Casero, D., Gallaher, S.D., Goodson, C., Johnson, S., Lee, J.H., Merchant, S.S., Pellegrini, M., Roth, R., Rusch, J., Singh, M., Umen, J.G., Weiss, T.L. and Wulan, T. (2014) The path to triacylglyceride obesity in the sta6 strain of Chlamydomonas reinhardtii. *Eukaryot Cell*, **13**, 591-613.

Gorman, D.S. and Levine, R.P. (1965) CYTOCHROME F AND PLASTOCYANIN - THEIR SEQUENCE IN PHOTOSYNTHETIC ELECTRON TRANSPORT CHAIN OF *CHLAMYDOMONAS REINHARDTII*. *P Natl Acad Sci USA*, **54**, 1665-&.

Granum, E., Kirkvold, S. and Myklestad, S.M. (2002) Cellular and extracellular production of carbohydrates and amino acids by the marine diatom Skeletonema costatum: diel variations and effects of N depletion. *Mar Ecol Prog Ser*, **242**, 83-94.

Grossman, A.R., Gonzalez-Ballester, D., Shibagaki, N., Pootakham, W., Moseley, J. and Pootakham, W. (2010) *Responses to Macronutrient Deprivation*.

Grundel, M., Scheunemann, R., Lockau, W. and Zilliges, Y. (2012) Impaired glycogen synthesis causes metabolic overflow reactions and affects stress responses in the cyanobacterium Synechocystis sp. PCC 6803. *Microbiology*, **158**, 3032-3043.

Hall C, Cruz J, Wood M, Zegara R, De Mars D, Carpenter J, Kanazawa A and D, K. (2011) Photosynthesis: research for food, fuel and future-15th international conference on photosynthesis. *Zhejiang University Press, Bejing*, 184-188.

Harder, R. and Witsch, H.v. (1942a) Bericht über Versuche zur Fettsynthese mittels autotropher Microorganismen. . *Forschungsdienst Sonderheft*, 270-275.

Harder, R. and Witsch, H.v. (1942b) Die Massenkultur von Diatomeen. *Ber Deutsch Bot Ges*, 146-152.

Hays, S.G. and Ducat, D.C. (2015) Engineering cyanobacteria as photosynthetic feedstock factories. *Photosynth. Res.*, **123**, 285-295.

Hu, Q., Sommerfeld, M., Jarvis, E., Ghirardi, M., Posewitz, M., Seibert, M. and Darzins, A. (2008) Microalgal triacylglycerols as feedstocks for biofuel production: perspectives and advances. *Plant J*, **54**, 621-639.

Jones, C.S. and Mayfield, S.P. (2012) Algae biofuels: versatility for the future of bioenergy. *Curr Opin Biotechnol*, **23**, 346-351.

Juergens, M.T., Deshpande, R.R., Lucker, B.F., Park, J.J., Wang, H., Gargouri, M., Holguin, F.O., Disbrow, B., Schaub, T., Skepper, J.N., Kramer, D.M., Gang, D.R., Hicks, L.M. and Shachar-Hill, Y. (2015) The Regulation of Photosynthetic Structure and Function during Nitrogen Deprivation in Chlamydomonas reinhardtii. *Plant Physiol*, **167**, 558-573.

Khozin-Goldberg, I., Shrestha, P. and Cohen, Z. (2005) Mobilization of arachidonyl moieties from triacylglycerols into chloroplastic lipids following recovery from nitrogen starvation of the microalga Parietochloris incisa. *Bba-Mol Cell Biol L*, **1738**, 63-71.

Klein, U. (1987) Intracellular Carbon Partitioning in Chlamydomonas reinhardtii. *Plant Physiol*, **85**, 892-897.

Klok, A.J., Lamers, P.P., Martens, D.E., Draaisma, R.B. and Wijffels, R.H. (2014) Edible oils from microalgae: insights in TAG accumulation. *Trends in biotechnology*, **32**, 521-528.

Kohlwein, S.D. (2010) Triacylglycerol homeostasis: insights from yeast. *J Biol Chem*, **285**, 15663-15667.

Li, X., Moellering, E.R., Liu, B., Johnny, C., Fedewa, M., Sears, B.B., Kuo, M.H. and Benning, C. (2012) A galactoglycerolipid lipase is required for triacylglycerol accumulation and survival following nitrogen deprivation in Chlamydomonas reinhardtii. *The Plant cell*, **24**, 4670-4686.

Li, Y., Han, D., Yoon, K., Zhu, S., Sommerfeld, M. and Hu, Q. (2013) Molecular and Cellular Mechanisms for Lipid Synthesis and Accumulation in Microalgae: Biotechnological Implications. In *Handbook of Microalgal Culture*.

Liu, B.S. and Benning, C. (2013) Lipid metabolism in microalgae distinguishes itself. *Current Opinion in Biotechnology*, **24**, 300-309.

Liu, J., Huang, J., Sun, Z., Zhong, Y., Jiang, Y. and Chen, F. (2011) Differential lipid and fatty acid profiles of photoautotrophic and heterotrophic Chlorella zofingiensis: assessment of algal oils for biodiesel production. *Bioresour Technol*, **102**, 106-110.

Livingston, A.K., Cruz, J.A., Kohzuma, K., Dhingra, A. and Kramer, D.M. (2010) An Arabidopsis mutant with high cyclic electron flow around photosystem I (hcef) involving the NADPH dehydrogenase complex. *The Plant cell*, **22**, 221-233.

Martin, N.C. and Goodenough, U.W. (1975) Gametic differentiation in Chlamydomonas reinhardtii. I. Production of gametes and their fine structure. *The Journal of cell biology*, **67**, 587-605.

Merchant, S.S., Kropat, J., Liu, B., Shaw, J. and Warakanont, J. (2012) TAG, You're it! *Chlamydomonas* as a reference organism for understanding algal triacylglycerol accumulation. *Current Opinion in Biotechnology*, **23**, 352-363.

Merchant, S.S., Prochnik, S.E., Vallon, O., Harris, E.H., Karpowicz, S.J., Witman, G.B., Terry, A., Salamov, A., Fritz-Laylin, L.K., Marechal-Drouard, L., Marshall, W.F., Qu, L.H., Nelson, D.R., Sanderfoot, A.A., Spalding, M.H., Kapitonov, V.V., Ren, Q., Ferris, P., Lindquist, E., Shapiro, H., Lucas, S.M., Grimwood, J., Schmutz, J., Cardol, P., Cerutti, H., Chanfreau, G., Chen, C.L., Cognat, V., Croft, M.T., Dent, R., Dutcher, S., Fernandez, E., Fukuzawa, H., Gonzalez-Ballester, D., Gonzalez-Halphen, D., Hallmann, A., Hanikenne, M., Hippler, M., Inwood, W., Jabbari, K., Kalanon, M., Kuras, R., Lefebvre, P.A., Lemaire, S.D., Lobanov, A.V., Lohr, M., Manuell, A., Meier, I., Mets, L., Mittag, M., Mittelmeier, T., Moroney, J.V., Moseley, J., Napoli, C., Nedelcu, A.M., Niyogi, K., Novoselov, S.V., Paulsen, I.T., Pazour, G., Purton, S., Ral, J.P., Riano-Pachon, D.M., Riekhof, W., Rymarquis, L., Schroda, M., Stern, D., Umen, J., Willows, R., Wilson, N., Zimmer, S.L., Allmer, J., Balk, J., Bisova, K., Chen, C.J., Elias, M., Gendler, K., Hauser, C., Lamb, M.R., Ledford, H., Long, J.C., Minagawa, J., Page, M.D., Pan, J., Pootakham, W., Roje, S., Rose, A., Stahlberg, E., Terauchi, A.M., Yang, P., Ball, S., Bowler, C., Dieckmann, C.L., Gladyshev, V.N., Green, P., Jorgensen, R., Mayfield, S., Mueller-Roeber, B., Rajamani, S., Sayre, R.T., Brokstein, P., Dubchak, I., Goodstein, D., Hornick, L., Huang, Y.W., Jhaveri, J., Luo, Y., Martinez, D., Ngau, W.C., Otillar, B., Poliakov, A., Porter, A., Szajkowski, L., Werner, G., Zhou, K., Grigoriev, I.V., Rokhsar, D.S. and Grossman, A.R. (2007) The *Chlamydomonas* genome reveals the evolution of key animal and plant functions. *Science*, **318**, 245-250.

Miao, X.L. and Wu, Q.Y. (2004) High yield bio-oil production from fast pyrolysis by metabolic controlling of Chlorella protothecoides. *Journal of biotechnology*, **110**, 85-93.

Miller, R., Wu, G., Deshpande, R.R., Vieler, A., Gartner, K., Li, X., Moellering, E.R., Zauner, S., Cornish, A.J., Liu, B., Bullard, B., Sears, B.B., Kuo, M.H., Hegg, E.L., Shachar-Hill, Y., Shiu, S.H. and Benning, C. (2010) Changes in transcript abundance in *Chlamydomonas reinhardtii* following nitrogen deprivation predict diversion of metabolism. *Plant Physiol*, **154**, 1737-1752.

Moellering, E.R. and Banning, C. (2011) Galactoglycerolipid metabolism under stress: a time for remodeling. *Trends in plant science*, **16**, 98-107.

Morin, N., Cescut, J., Beopoulos, A., Lelandais, G., Le Berre, V., Uribelarrea, J.L., Molina-Jouve, C. and Nicaud, J.M. (2011) Transcriptomic Analyses during the Transition from Biomass Production to Lipid Accumulation in the Oleaginous Yeast Yarrowia lipolytica. *PloS one*, **6**.

Muller, P., Li, X.P. and Niyogi, K.K. (2001) Non-photochemical quenching. A response to excess light energy. *Plant Physiol*, **125**, 1558-1566.

Murphy, D.J. (2001) The biogenesis and functions of lipid bodies in animals, plants and microorganisms. *Prog Lipid Res*, **40**, 325-438.

Neijssel, O.M. and Tempest, D.W. (1975) The regulation of carbohydrate metabolism in Klebsiella aerogenes NCTC 418 organisms, growing in chemostat culture. *Archives of microbiology*, **106**, 251-258.

Niyogi, K.K., Bjorkman, O. and Grossman, A.R. (1997) Chlamydomonas xanthophyll cycle mutants identified by video imaging of chlorophyll fluorescence quenching. *The Plant cell*, **9**, 1369-1380.

Ohlrogge, J., Allen, D., Berguson, B., DellaPenna, D., Shachar-Hill, Y. and Stymne, S. (2009) Driving on Biomass. *Science*, **324**, 1019-1020.

Packter, N.M. and Olukoshi, E.R. (1995) Ultrastructural studies of neutral lipid localisation in Streptomyces. *Archives of microbiology*, **164**, 420-427.

Peers, G., Truong, T.B., Ostendorf, E., Busch, A., Elrad, D., Grossman, A.R., Hippler, M. and Niyogi, K.K. (2009) An ancient light-harvesting protein is critical for the regulation of algal photosynthesis. *Nature*, **462**, 518-U215.

Pollard, M., Martin, T.M. and Shachar-Hill, Y. (2015) Lipid analysis of developing Camelina sativa seeds and cultured embryos. *Phytochemistry*, **118**, 23-32.

Ritchie, R.J. (2006) Consistent sets of spectrophotometric chlorophyll equations for acetone, methanol and ethanol solvents. *Photosynth Res*, **89**, 27-41.

Rochaix, J.D. (2002) Chlamydomonas, a model system for studying the assembly and dynamics of photosynthetic complexes. *FEBS Lett*, **529**, 34-38.

Roessler, P.G. (1990) Environmental-Control of Glycerolipid Metabolism in Microalgae - Commercial Implications and Future-Research Directions. *Journal of Phycology*, **26**, 393-399.

Roessner, U., Luedemann, A., Brust, D., Fiehn, O., Linke, T., Willmitzer, L. and Fernie, A. (2001) Metabolic profiling allows comprehensive phenotyping of genetically or environmentally modified plant systems. *The Plant cell*, **13**, 11-29.

Sacksteder, C.A., Jacoby, M.E. and Kramer, D.M. (2001) A portable, non-focusing optics spectrophotometer (NoFOSpec) for measurements of steady-state absorbance changes in intact plants. *Photosynth Res*, **70**, 231-240.

Schmollinger, S., Muhlhaus, T., Boyle, N.R., Blaby, I.K., Casero, D., Mettler, T., Moseley, J.L., Kropat, J., Sommer, F., Strenkert, D., Hemme, D., Pellegrini, M., Grossman, A.R., Stitt, M., Schroda, M. and Merchant, S.S. (2014) Nitrogen-Sparing Mechanisms in Chlamydomonas Affect the Transcriptome, the Proteome, and Photosynthetic Metabolism. *The Plant cell*.

Shifrin, N.S. and Chisholm, S.W. (1981) Phytoplankton Lipids - Interspecific Differences and Effects of Nitrate, Silicate and Light-Dark Cycles. *Journal of Phycology*, **17**, 374-384.

Siaut, M., Cuine, S., Cagnon, C., Fessler, B., Nguyen, M., Carrier, P., Beyly, A., Beisson, F., Triantaphylides, C., Li-Beisson, Y.H. and Peltier, G. (2011) Oil accumulation in the model green alga *Chlamydomonas reinhardtii*: characterization, variability between common laboratory strains and relationship with starch reserves. *Bmc Biotechnol*, **11**.

Singh, H., Shukla, M.R., Chary, K.V. and Rao, B.J. (2014) Acetate and bicarbonate assimilation and metabolite formation in Chlamydomonas reinhardtii: a 13C-NMR study. *PloS one*, **9**, e106457.

Slade, R. and Bauen, A. (2013) Micro-algae cultivation for biofuels: Cost, energy balance, environmental impacts and future prospects. *Biomass Bioenerg*, **53**, 29-38.

Smith, V.H., Sturm, B.S., Denoyelles, F.J. and Billings, S.A. (2010) The ecology of algal biodiesel production. *Trends Ecol Evol*, **25**, 301-309.

Solovchenko, A.E. (2012) Physiological Role of Neutral Lipid Accumulation in Eukaryotic Microalgae under Stresses. *Russ. J. Plant Physiol.*, **59**, 167-176.

Spalding, M.H. (1989) Photosynthesis and Photorespiration in Fresh-Water Green-Algae. *Aquat Bot*, **34**, 181-209.

Spoehr, H.A. and Milner, H.W. (1949) The Chemical Composition of Chlorella - Effect of Environmental Conditions. *Plant Physiol*, **24**, 120-149.

Sueoka, N. (1960) Mitotic Replication of Deoxyribonucleic Acid in Chlamydomonas Reinhardi. *Proc Natl Acad Sci U S A*, **46**, 83-91.

Terauchi, A.M., Peers, G., Kobayashi, M.C., Niyogi, K.K. and Merchant, S.S. (2010) Trophic status of Chlamydomonas reinhardtii influences the impact of iron deficiency on photosynthesis. *Photosynth Res*, **105**, 39-49.

Wagner, H., Jakob, T. and Wilhelm, C. (2006) Balancing the energy flow from captured light to biomass under fluctuating light conditions. *New Phytol*, **169**, 95-108.

Watanabe, Y., Delanoue, J. and Hall, D.O. (1995) Photosynthetic Performance of a Helical Tubular Photobioreactor Incorporating the Cyanobacterium Spirulina-Platensis. *Biotechnology and bioengineering*, **47**, 261-269.

Weise, S.E., van Wijk, K.J. and Sharkey, T.D. (2011) The role of transitory starch in C(3), CAM, and C(4) metabolism and opportunities for engineering leaf starch accumulation. *J Exp Bot*, **62**, 3109-3118.

White, S., Anandraj, A. and Bux, F. (2011) PAM fluorometry as a tool to assess microalgal nutrient stress and monitor cellular neutral lipids. *Bioresour Technol*, **102**, 1675-1682.

Wijffels, R.H. and Barbosa, M.J. (2010) An Outlook on Microalgal Biofuels. *Science*, **329**, 796-799.

Williams, P.J.L. and Laurens, L.M.L. (2010) Microalgae as biodiesel & biomass feedstocks: Review & analysis of the biochemistry, energetics & economics. *Energ Environ Sci*, **3**, 554-590.

Wilson, A., Boulay, C., Wilde, A., Kerfeld, C.A. and Kirilovsky, D. (2007) Light-induced energy dissipation in iron-starved cyanobacteria: roles of OCP and IsiA proteins. *The Plant cell*, **19**, 656-672.

Work, V.H., Radakovits, R., Jinkerson, R.E., Meuser, J.E., Elliott, L.G., Vinyard, D.J., Laurens, L.M., Dismukes, G.C. and Posewitz, M.C. (2010) Increased lipid accumulation in the Chlamydomonas reinhardtii sta7-10 starchless isoamylase mutant and increased carbohydrate synthesis in complemented strains. *Eukaryot Cell*, **9**, 1251-1261.

Yoon, K., Han, D., Li, Y., Sommerfeld, M. and Hu, Q. (2012) Phospholipid:Diacylglycerol Acyltransferase Is a Multifunctional Enzyme Involved in Membrane Lipid Turnover and Degradation While Synthesizing Triacylglycerol in the Unicellular Green Microalga *Chlamydomonas reinhardtii*. *The Plant cell*, **24**, 3708-3724.

Zhu, C.J. and Lee, Y.K. (1997) Determination of biomass dry weight of marine microalgae. *J. Appl. Phycol.*, **9**, 189-194.

CHAPTER-4

Flux Balance Analysis of Chlamydomonas during Nitrogen Deprivation

ABSTRACT

Algae have been suggested as sources for biofuel production due to their ability to grow quickly and accumulate carbon in the form of starch and triacylglycerols. Despite much research on these accumulations, there is little consensus on the best approaches to increase production as well as the reasons behind the accumulations. In Chapter 3 we measured various carbon accumulations, photosynthetic properties, acetate uptake, and gas exchange rates during nitrogen deprivation in Chlamydomonas across 5 light levels and two media conditions. In this chapter we use that data as constraints for flux balance analysis using a genome scale model of Chlamydomonas, iCre1355. Flux results demonstrate that the model is robust across multiple growth conditions and representative of current knowledge about metabolism under each condition. Nitrogen deprivation experiments show a single pathway for starch accumulation across all light and media conditions but different metabolic routes for TAG accumulation depending upon the growth condition used. We additionally correct the iCre1355 model to have proper photosynthetic reaction stoichiometry as well as add several reactions left out in the original model. This work provides a foundation for a deeper metabolic understanding of carbon accumulation during nutrient deprivation.

INTRODUCTION

The current utilization of petroleum resources as fuel and chemical substrate is unsustainable (Solomon 2010). Further, variable fluctuations in the prices of these foreign derived commodities has dramatic effects on our economy (Brown *et al.* 2013). Additional costs of petroleum usage are found in deleterious effects on our environment, global warming, and public health. Developing dependable, clean, and sustainable renewable carbon and energy sources to replace petroleum is at the forefront of current bioenergy research. Renewable resources being developed rely on wind, solar, and the burning of photosynthetically derived biomass for energy. Biomass sources can be burned directly for electricity or processed through natural or artificial means to produce liquid and gas fuels as well as syngas and target molecules for the chemical industry. Crop plants such as maize and sugar cane were initially studied as feedstocks for biofuel (bioethanol); however, the focus has significantly shifted to developing fuels from single celled photosynthetic microalgae (Chisti 2007, Martin 2010, Ohlrogge, et al. 2009, Solomon 2010).

Many algae have been studied for their capacity as industrial biofuel strains including Nannochloropsis (Radakovits, et al. 2012), Chlorella (Liu, et al. 2011), and Galdiaria (Selvaratnam, et al. 2014). Much of the research on biofuel production in microalgae however has been done on the model green alga *Chlamydomonas reinhardtii* (Fan, et al. 2012, Liu, et al. 2013, Siaut, et al. 2011). This alga has been studied extensively over the last fifty years (Goodenough 2015, Harris 2009b, Merchant, et al. 2012b) and has a plentiful list of resources such as a fully sequenced genome (Blaby, et al. 2014, Merchant, et al. 2007), multiple transcriptomic and proteomic analyses (Wang, et al. 2014), as well as various metabolic libraries (Bolling, et al. 2005, Lee do, et al. 2008, May, et al. 2008). Further, an extensive library of

characterized mutants have been generated for Chlamydomonas enabling more rapid and extensive studies on gene-phenotype relationships (Li, et al. 2016). In recent years, several large scale studies have been done on Chlamydomonas during biofuel accumulation conditions, especially various nutrient deprivation regimes. These studies provide guidance for rational engineering and strain development for biofuel and engineering purposes.

Aside from describing the mechanisms behind a given phenotype, one of the ultimate goals of systems biology is to be able to accurately direct genetic engineering efforts through predictive modeling. Omics data can be used to determine the set of enzymes, metabolic reactions and metabolites present in an organism and allow the formation of a metabolic model (Borodina *et al.* 2005). Metabolic reactions are then described in the form of linear reaction stoichiometries, accounting for all energy, reductant, carbon, and other components necessary for biology. Measured physiological data such as biomass, metabolite uptake rates, and known reaction rates can be used as constraints for Flux Balance Analysis (FBA), a systems biology techniqueused to study the generated metabolic model (Baroukh *et al.* 2015, Shachar-Hill 2013). FBA uses linear computational programming to balance all of the reaction stoichiometries in the model based upon the given constraints, with flux values for each reaction as output. Generated fluxes are used to describe the flow of carbon/ metabolites/ energy in an organism and, through perturbation, aid in the predictions of hypothesis driven genetic engineering efforts. FBA has been used in the prediction of several successful engineering efforts, including those in *Corynebacterium glutamicum* (Vallino *et al.* 1993), *Sacchromyces cerevisiae* (Famili *et al.* 2003), and *Staphylococcus aureus* (Heinemann *et al.* 2005).

Despite the importance of understanding the relationship between phenotypes and metabolic flux, FBA has only recently been applied to photosynthetic organisms. Early phototrophic

metabolic models of cyanobacteria Synechocystis and Spirulina were simplistic in nature, modeling only central metabolism and simplistic photosynthetic expressions (Cogne *et al.* 2003, Yang *et al.* 2000). Shastri and Morgan generated another model of Synechocystis, this time taking into consideration the reactions validated by the sequenced genome (Shastri *et al.* 2005). At the same time, efforts to characterize higher plant metabolism involved single network C13 metabolic flux analysis, a steady state analysis requiring expensive C^{13} label and intensive analytical chemistry analysis (Allen *et al.* 2009, Kruger *et al.* 2009, Libourel *et al.* 2008). This process only allowed for the description of a network, unable to predict the effects of gene knockouts or other genetic engineering perturbations. Boyle and Morgan built upon the Synechocystis model, generating one to describe the eukaryotic, green alga *Chlamydomonas reinhardtii* and metabolic compartmentation (Boyle, et al. 2009). This provided groundwork for the production of larger scale models in algae and higher plants. FBA genome scale models have thus been generated for *Arabidopsis thaliana* (de Oliveira Dal'Molin *et al.* 2010, Poolman *et al.* 2009) and *Zea maize* (Saha *et al.* 2011) with smaller, literature based models generated for barley (Grafahrend-Belau *et al.* 2009) and *Brassica napus* seeds (Hay *et al.* 2011, Pilalis *et al.* 2011). These models have helped determined where gaps are in our genome annotations, what reactions are in the same network, as well as described some interactions between metabolites in different compartments such as the cytosol, plastid, and mitochondria.

Due to the vast amount of omic data generated and genome sequencing (Merchant, et al. 2007) in recent years, FBA has been applied to the green alga Chlamydomonas. Morgan and Boyle generated the first metabolic reconstruction of central metabolism in *Chlamydomonas reinhardtii*. This model included three compartments (plastid, cytosol, and mitochondria), 484 metabolic reactions, and led to enzyme annotation (Boyle, et al. 2009). This model was then

followed by a transcript verified model (Manichaikul *et al.* 2009). Significant improvements were made in three larger, genome scale models (GEMs), AlgaGEM (derived from an Arabidopsis model (Dal'Molin, et al. 2011), iRC1080 (generated from a bottom up approach) (Chang *et al.* 2011b), and iCre1355 (a recently updated iRC1080) (Imam, et al. 2015). These models have been used to study the effect of CO_2 and acetate upon photosynthesis (Chapman, et al. 2015, Melo *et al.* 2014), transcript regulation of nitrogen deprivation (Imam, et al. 2015, Lopez Garcia de Lomana, et al. 2015), and network reduction (Rugen *et al.* 2012). While these models are highly informed from genome, transcript, and protein systems analysies, they lack rigorous constraints based upon functional physiological measurements.

In this work we used flux balance analysis to study the metabolic carbon and energy fluxes during normal growth and nutrient deprivation in Chlamydomonas. The iCre1355 metabolic model was modified to correct photosynthetic reaction stoichiometries and physiological measurements taken in chapter 3 were used to constrain the feasible flux space solutions. Carbon flux solutions generated gave results in congruence with current dogma on heterotrophic, autotrophic, and mixotrophic growth demonstrating the robustness of the model across several conditions. Photosynthetic fluxes and cellular photon demand results also provided support to conclusions of chapter 3. Nutrient deprivation experiments demonstrated a single source for starch synthesis in the plastid across all conditions while triacylglycerol carbon can be derived from several metabolic pathways depending upon the growth conditions of the cell. This work provides a foundation to explore ways to increase biofuel production in algae as well as study how metabolism responds to different growth environments.

METHODS

Model Curation

In the work we chose to use the genome scale model iCre1355 updated by Imam et al. (Imam, et al. 2015) from the iCR1080 model by Chang (Chang, et al. 2011b). This model includes updated gene annotation and gene protein relations as well as deletions of unsupported gene reactions. Further, while other models for Chlamydomonas such as AlgaGem were generated from other organisms including Arabidopsis (Dal'Molin, et al. 2011, de Oliveira Dal'Molin, et al. 2010), iCre1355/ iCR1080 were built from the ground up and separate network reactions such as photosynthesis were separated into multiple equations instead of single stoichiometries. One example of this is linear electron flow where in AlgaGEM there is a single reaction while in iCre1355/iCR1080 there are separate reactions for PSII, b_6f complex, PSI, ferredoxin NADPH reductase, and so on, allowing the model to more realistically demonstrate biology.

Pathway	Reaction ID	Name	Equation- iCre1355	Changes- iCre1357_Juergens
Photosynthesis	Pcount	photon counter	NA	count[e] <=> count[u]
	CBFC	cytochrome b6/f complex	(2) h[h] + (2) pccu2p[u] + pqh2[u] --> (4) h[u] + (2) pccu1p[u] + pq[u]	1 pccu2p[u] + pqh2[u] => 2 h[u] + 1 pccu1p[u] + 1eq
	Qcyc	Q cycle	NA	2 eq[u] +pq[u] +2h[h] => pqh2[u]
	CEF	Cyclic Electron Flow	fdxrd[u] + (2) h[h] + (2) pccu2p[u] --> fdxox[u] + (4) h[u] + (2) pccu1p[u]	2 fdxrd[u] + 2 h[h] + pq[u] => 2 fdxox[u] + pqh2[u]
	FNORh	ferredoxin---NADP+ reductase	fdxrd[u] + nadp[h] --> fdxox[u] + nadph[h] + h[h]	2 fdxrd[u] + h[h] + nadp[h] => 2 fdxox[u] + nadph[h]
	PSIblue	photosystem I (blue light-activated)	[u] : fdxox + (2) pccu1p + (2) photon437 + (2) h --> fdxrd + (2) pccu2p	count[u] + fdxox[u] + pccu1p[u] + photon437[u] => count[e] + fdxrd[u] + pccu2p[u]
	PSIIblue	photosystem II (blue light-activated)	[u] : (2) h2o + (4) photon438 + (2) pq --> o2D + (2) pqh2	4 count[u] + 4 h[h] + 2 h2o[u] + 4 photon438[u] + 2 pq[u] => 4 count[e] + 4 h[u] + o2[u] + 2 pqh2[u]
	PSIred	photosystem I (red light-activated)	[u] : fdxox + (2) pccu1p + (2) photon680 + (2) h --> fdxrd + (2) pccu2p	count[u] + fdxox[u] + pccu1p[u] + photon680[u] => count[e] + fdxrd[u] + pccu2p[u]
	PSIIred	photosystem II (red light-activated)	[u] : (2) h2o + (4) photon673 + (2) pq --> o2D + (2) pqh2	4 count[u] + 4 h[h] + 2 h2o[u] + 4 photon673[u] + 2 pq[u] => 4 count[e] + 4 h[u] + o2[u] + 2 pqh2[u]
	NDHq	NADPH dehydrogenase quinone	NA	h[h] + nadph[h] + pq[u] => nadp[h] + pqh2[u]
	PTOX	Plastid Terminal Oxidase	NA	o2[h] + 2 pqh2[u] => 2 h2o[h] + 2 pq[u]
	Mehler	Mehler	NA	fdxrd[u] + o2[u] => fdxox[u] + o2R[u]
Ascorbate	ASCBOR	L-ascorbate:oxygen oxidoreductase	2 ascb_L[u] + o2[u] => 2 dhdascb[u] + 2 h2o[u]	2 ascb_L[u] + o2R[u] => 2 dhdascb[u] + 2 h2o[u]
Demand	DM_na1_c	sodium demand	na1[c] =>	deleted
	DM_na1_h	sodium demand	na1[h] =>	deleted
	DM_na1_m	sodium demand	na1[m] =>	deleted
	DM_na1_x	sodium demand	na1[x] =>	deleted
	DM_o2D_u	demand removing dummy o2 from system	o2D[u] =>	deleted
	NADPH burn	Burns NADPH in plastid	NA	NADPH[h] => NADP[h] +h[h]

Table 4.1. **Changes made to model related to photosynthesis.** Reactions were corrected to match current stoichiometric understandings as well as remove free energy generation from sodium fluxes.

Despite other works having used iCR1080 and iCre1355 and "updated" them, we found several cases of incorrect photosynthetic stoichiometries and free energy generation through sodium transport reactions (Chapman, et al. 2015, Cogne *et al.* 2011, Gomez *et al.* 2016, Lopez Garcia de Lomana, et al. 2015, Rugen, et al. 2012). Presented in Table 4.1, we show corrections in the stoichiometries of photosystem I and II, cyclic electron flow (CEF), and Ferredoxin NADPH reductase, and b6f complex. Chapman et al. 2015 claimed to correct CEF stoichiometries and send flux through plastoquinone instead of plastocyanin pools; however, these are not found in their published model. Additionally, four reactions were added for photosynthesis; the Mehler reaction which generates oxygen radicals at PSI(Mehler 1951a, Mehler 1951b, Mehler *et al.* 1952), the Plastid Terminal Oxidase (PTOX2, Cre03.g172500) which dissipates excess photosynthetic electrons by dumping them onto water (Houille-Vernes, et al. 2011), the second CEF pathway through NADPH dehydrogenase (NDH), using NADPH to reduce the quinone pool (Peng *et al.* 2009, Saroussi *et al.* 2016), and finally the Q cycle used by the b_6f complex. The radical oxygen generated from the Mehler reaction "o2R" is now reduced to water through the ascorbate peroxidase pathway, whereas previously this pathway was non-functional. Additional photosynthetic changes included removing the "dummy O_2" demand function and adding a useful photon count reaction to aid photon constraints. PSII generated oxygen now enters the thylakoid O_2 pool instead of simply dissipating away. Finally the Q cycle is split into two reactions, the first takes one electron from plastoquinol and sends it to the plastocyanin while the second reaction takes the second electron and uses it to reduce another plastoquinone. Figure 4.1 shows the current photosynthetic pathways and areas of possible perturbation in the model.

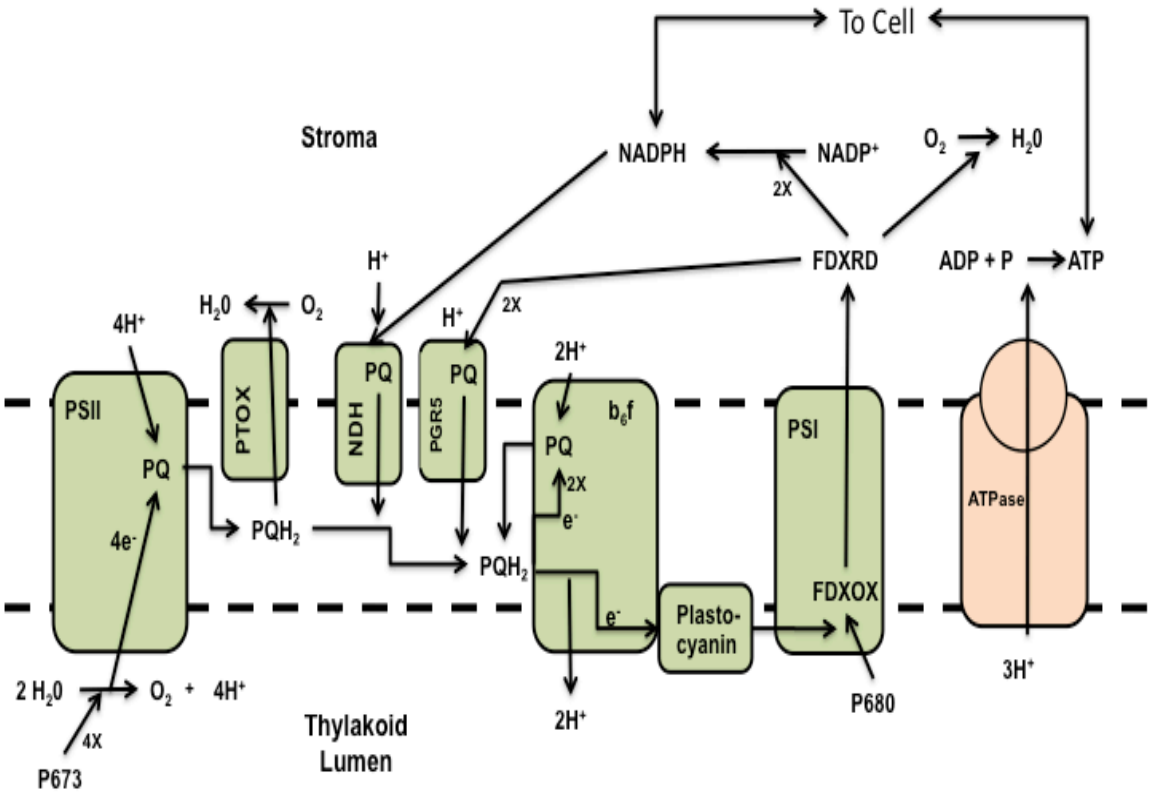

Figure 4.1 Photosynthetic fluxes allowed in model. Fluxes at each of these sites can be constrained or knocked out depending on the needs of the modeler. **ATPase**: ATP synthase; **B_6F**: B_6F complex with quinone cycle; **P680**: 680nm photons; **P673**: 673nm photons; **PQ**: Plastoquinone; **PGH2**: Plastoquinol; **PSI**: Photosystem I; **PSII**: Photosystem II; **FDXOX**: oxidized ferrodoxin; **FDXRD**; reduced ferrodoxin; **PTOX**: Plastid Terminal Oxidase; **NDH**: NADPH hydrogenase; **PGR5**: Proton Gradient Regulation 5

Other general changes include the deletion of sodium demand functions from organelles which generated free energy for the cell through sodium flows. The model was additionally altered to remove constraints on oxygen evolution, RuBisCO activity, CO_2 and other components not strictly controlled in the media. Next, from our experiments, the ATP maintenance costs used in Imam et al. were too high (model was infeasible with our constraints) so we used the lower ATP value in Chang et al. Further, the ATP maintenance cost flux was moved from the cytosol

to the plastid to remove a H_2O_2 and proton gradient generating reaction that helped moved ATP from the plastid to the cytosol. The biomass equations presented in the model were adjusted placing half of the ATP demand in the cytosol and half in the plastid. Finally, a NADPH burning reaction was added to the plastid as a feature to allow the study of the effects of increased reductant upon the system.

Flux Balance Analysis

FBA was performed using a curated form of the pre-existing model of *C. reinhardtii* metabolism, iCre1355, as mentioned above. Measured CO_2, biomass, TAG, starch, and acetate uptake rates were constrained in the models. Minimizing light use for autotrophic and CO_2 emission for mixo- and heterotrophic cultures was used as an objective function. Flux predictions were generated for the various light and nutrient environments measured in Chapter 3. These constraints included growth rates, acetate uptake, light intensity, Ash free dry weights, carbon uptake, starch and TAG accumulation rates, and photosynthetic efficiencies. The Growth LED designed by Chang et al. (year) was chosen as the light source for the model to simplify the photon fluxes to either PSI or PSII.

Flux Balance simulations were carried out using the COBRA Toolbox in the MATLAB programming environment (MathWorks, Inc. http://www.mathworks.com/ products/matlab). Gurobi Optimizer was used as the linear solver (www.Gurobi.com). Flux variability analysis was used to determine the max and min flux for each of the reactions during N+ and N- conditions (Mahadevan *et al.* 2003).

Cell Cultivation, growth, and constraint measurements

See Chapter 3 for growth and uptake measurement details. These include measurements of biomass % carbon, starch and TAG levels, as well as acetate, O_2, and CO_2 fluxes at 0, 5, 15, 40, and 160 μmol photons/m^2/s light intensities in Tris-acetate- phosphate (mixotrophic) and high salt (autotrophic) conditions.

RESULTS

Measurements of biomass composition, oxygen evolution, carbon dioxide fluxes, and acetate uptake from chapter 3 were used as constraints for flux balance analysis in *Chlamydomonas reinhardtii*. Conditions tested included autotrophic, mixotrophic, and heterotrophic growth regimes during N replete growth, and 24 and 96 hrs after nitrogen depletion. N-depleted samples were constrained additionally with measured starch and triacylglycerol (TAG) accumulations with their respective demand functions. For cultures grown in the light (mixotrophic and autotrophic), the objective function was the minimization of light use (Pcount flux) as otherwise the model could use as much light as possible and lead to wasteful energy usage. Heterotrophic cultures objective function was set to minimize CO_2 emissions, forcing a conservative use of carbon. Flux data generated from the balance analysis is presented in figure 4.2, simplified to primary carbon metabolism. Numbers presented indicate mmol Carbon/ gDW/Hr.

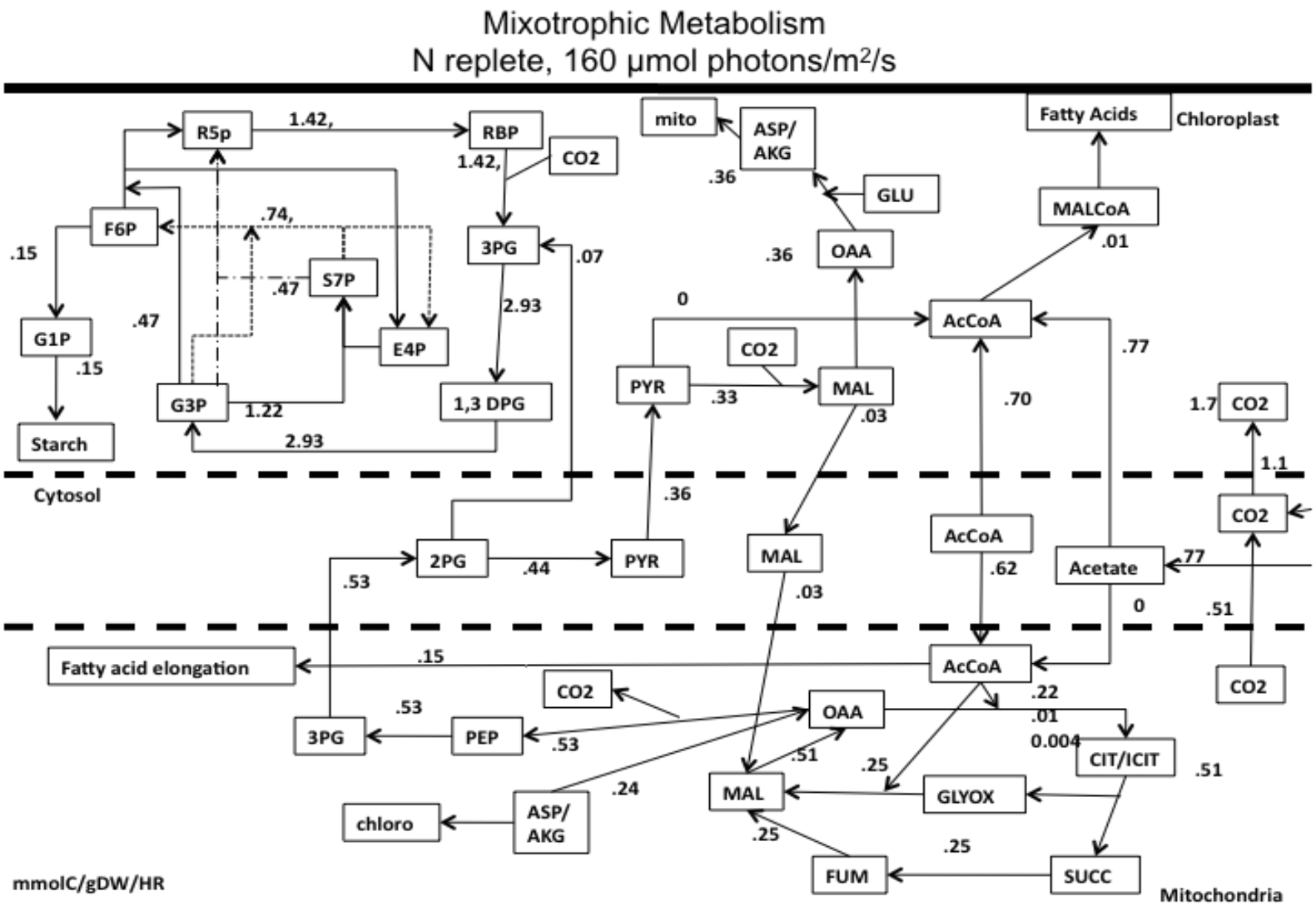

Figure 4.2 A. Nitrogen Replete Mixotrophic Growth

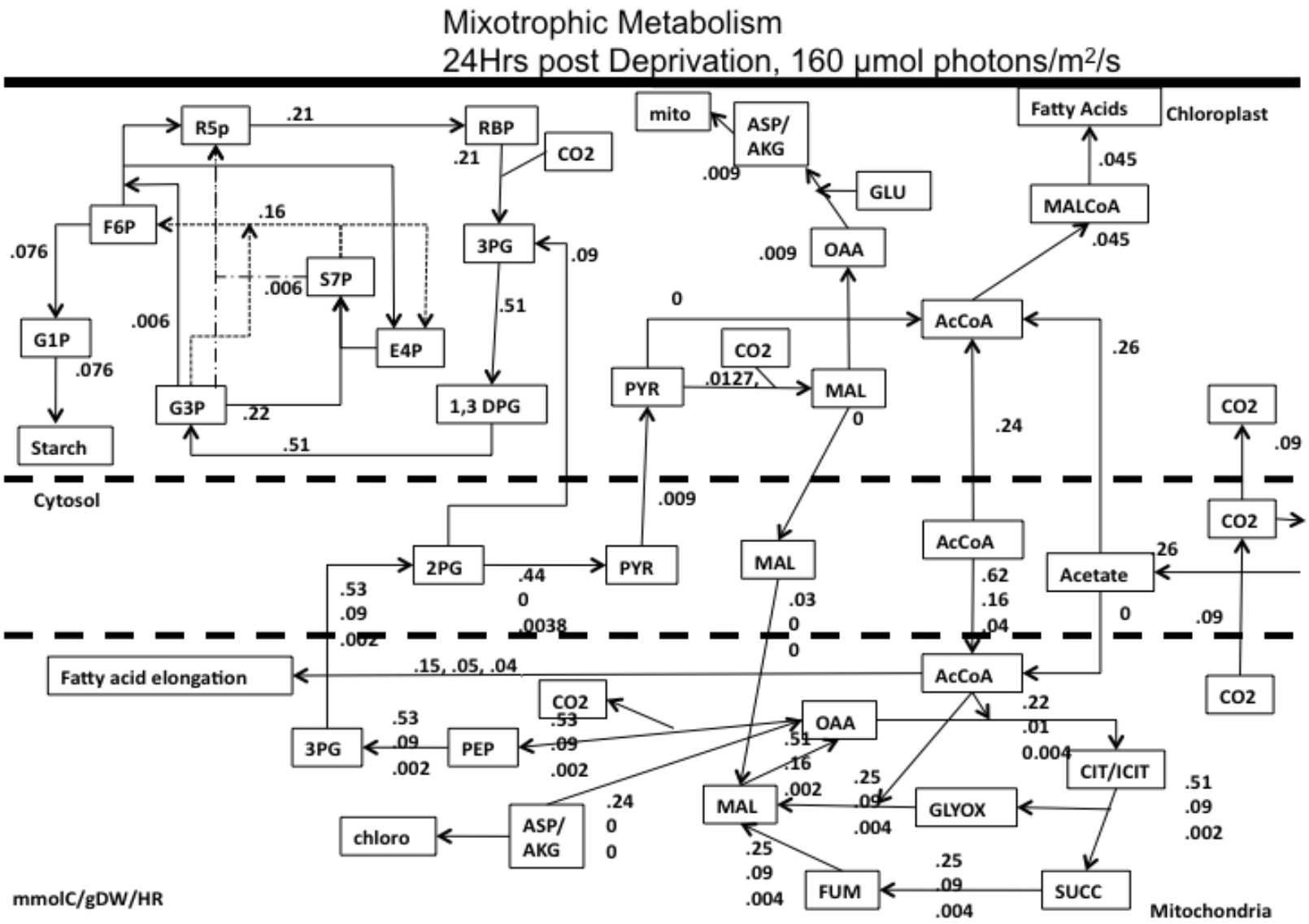

Figure 4.2 B. Nitrogen Deplete Mixotrophic Growth. 24 hrs post N deprivation

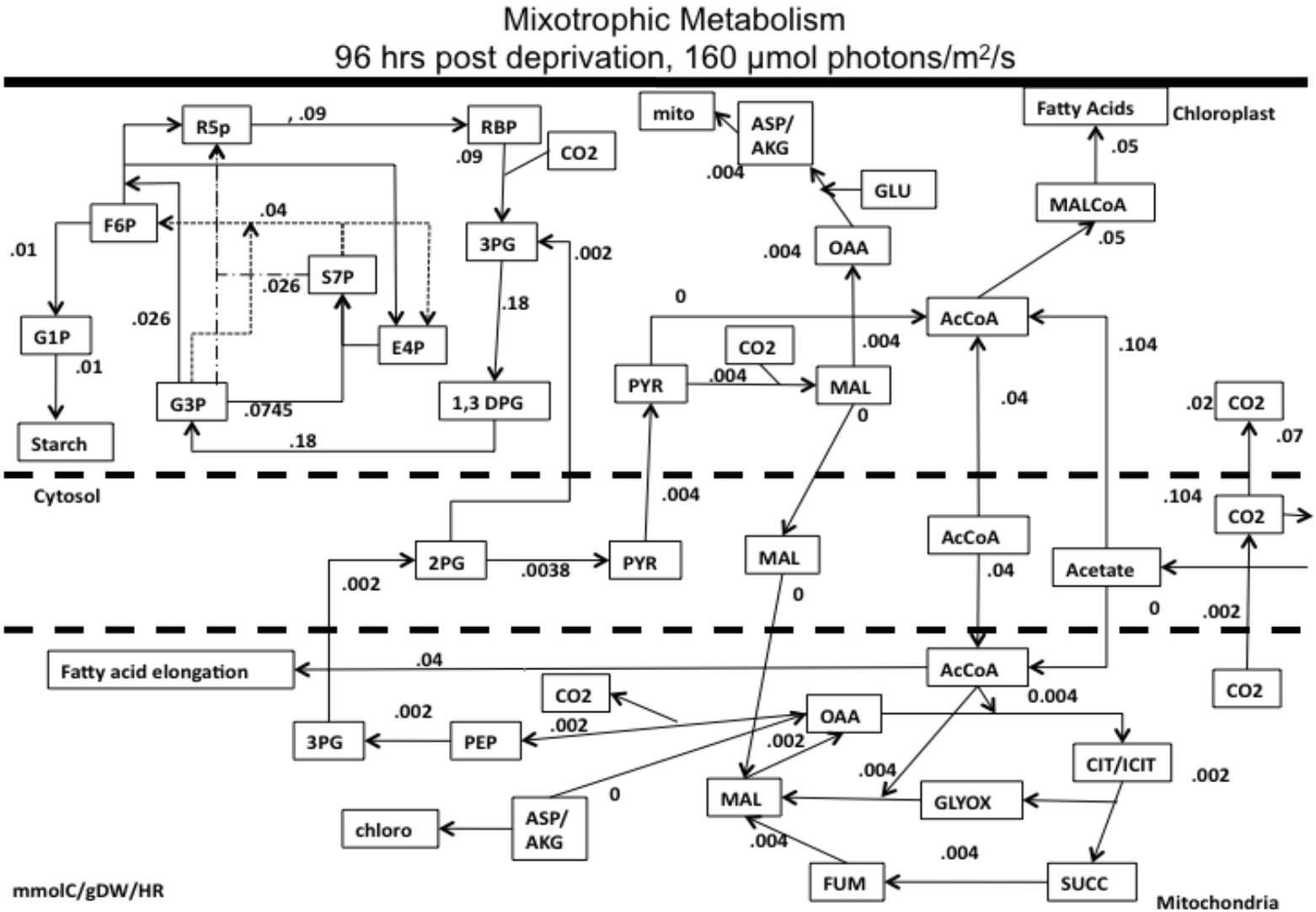

Figure 4.2 C. Nitrogen Deplete Mixotrophic Growth. 96 hrs post N deprivation

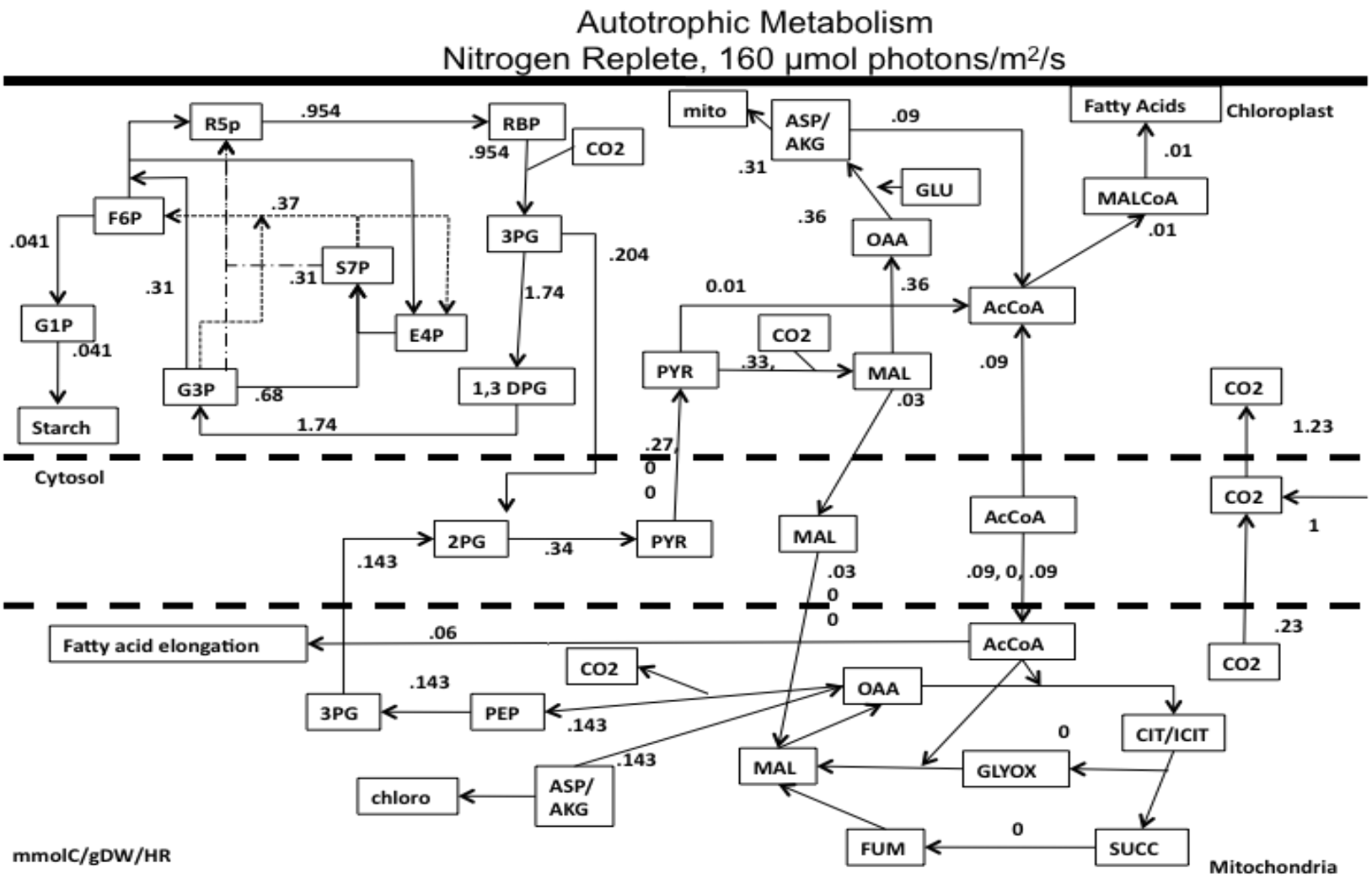

Figure 4.2 D. Nitrogen Replete Autotrophic Growth.

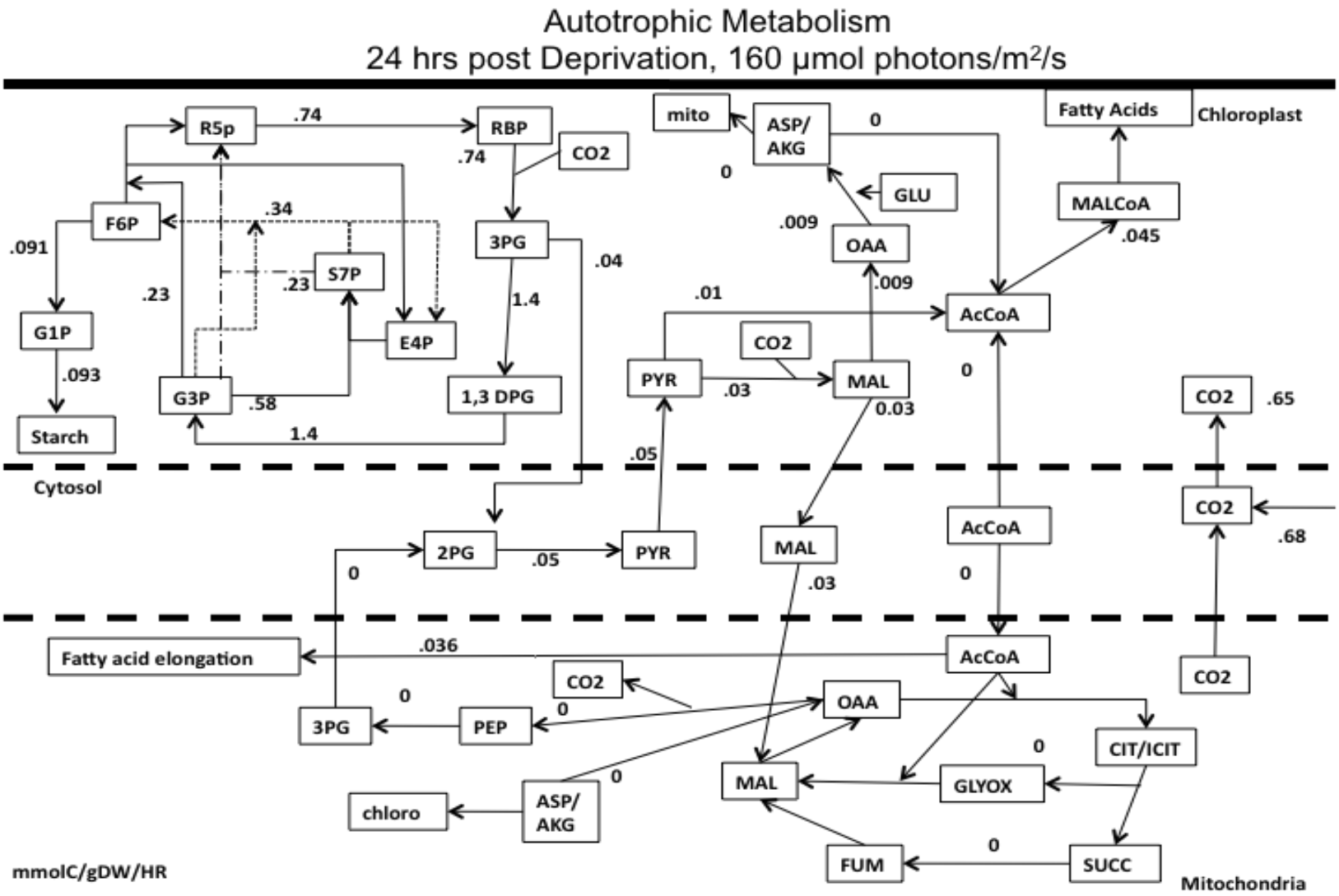

Figure 4.2 E. Nitrogen Deplete Autotrophic Growth. 24 hrs post N deprivation

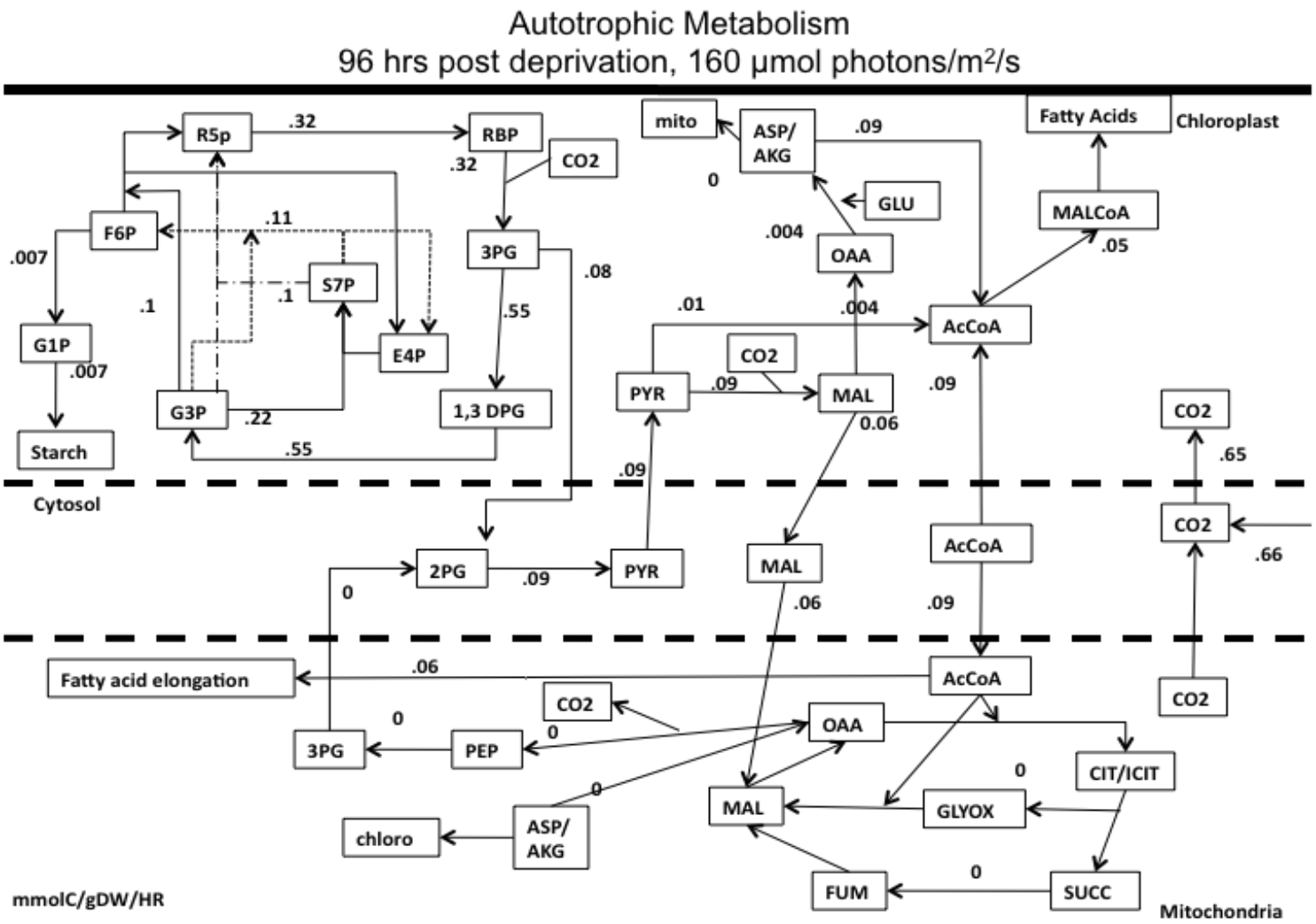

Figure 4.2 F. Nitrogen Deplete Autotrophic Growth. 96 hrs post N deprivation.

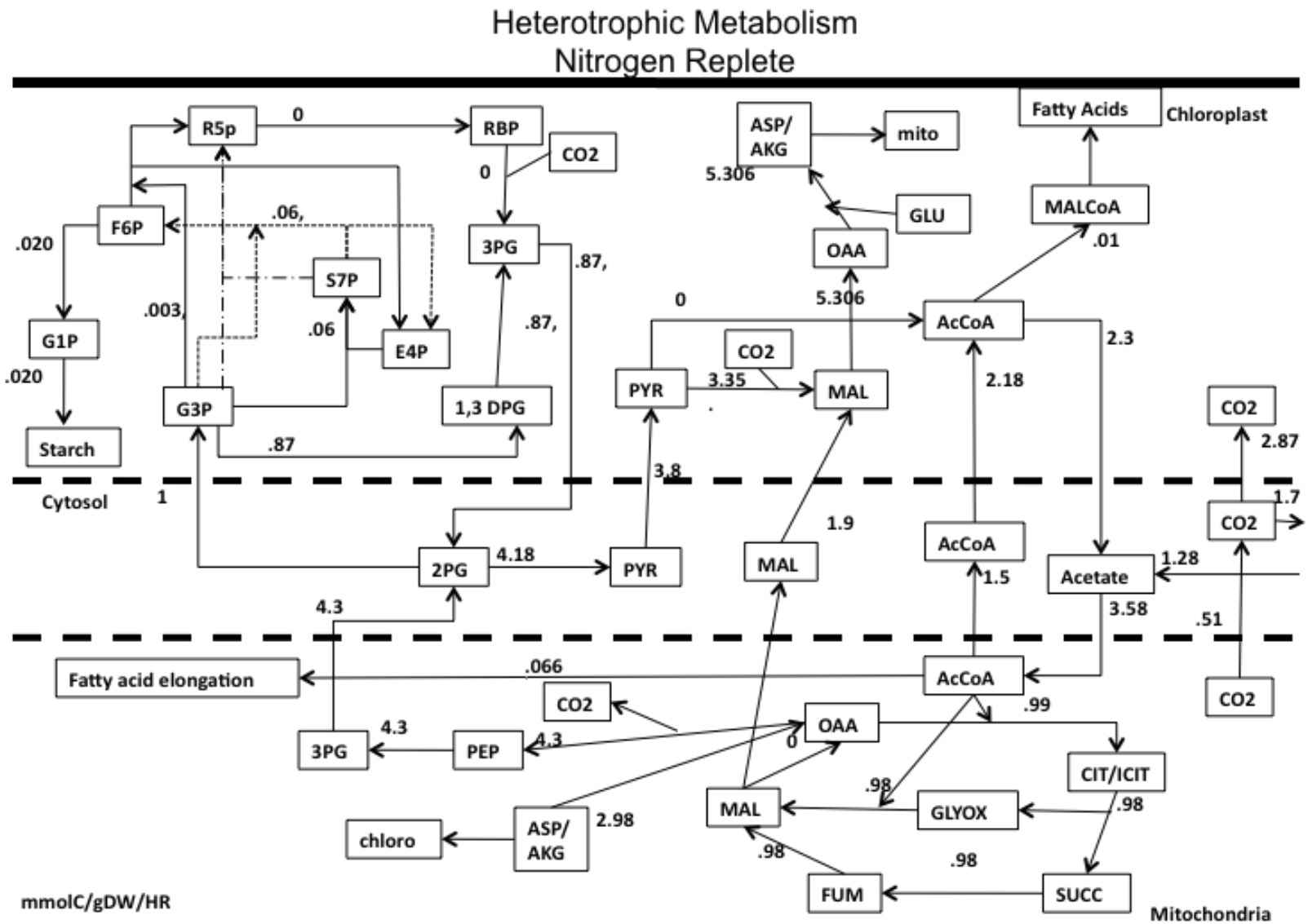

Figure 4.2 G. Nitrogen Replete Heterotrophic Growth.

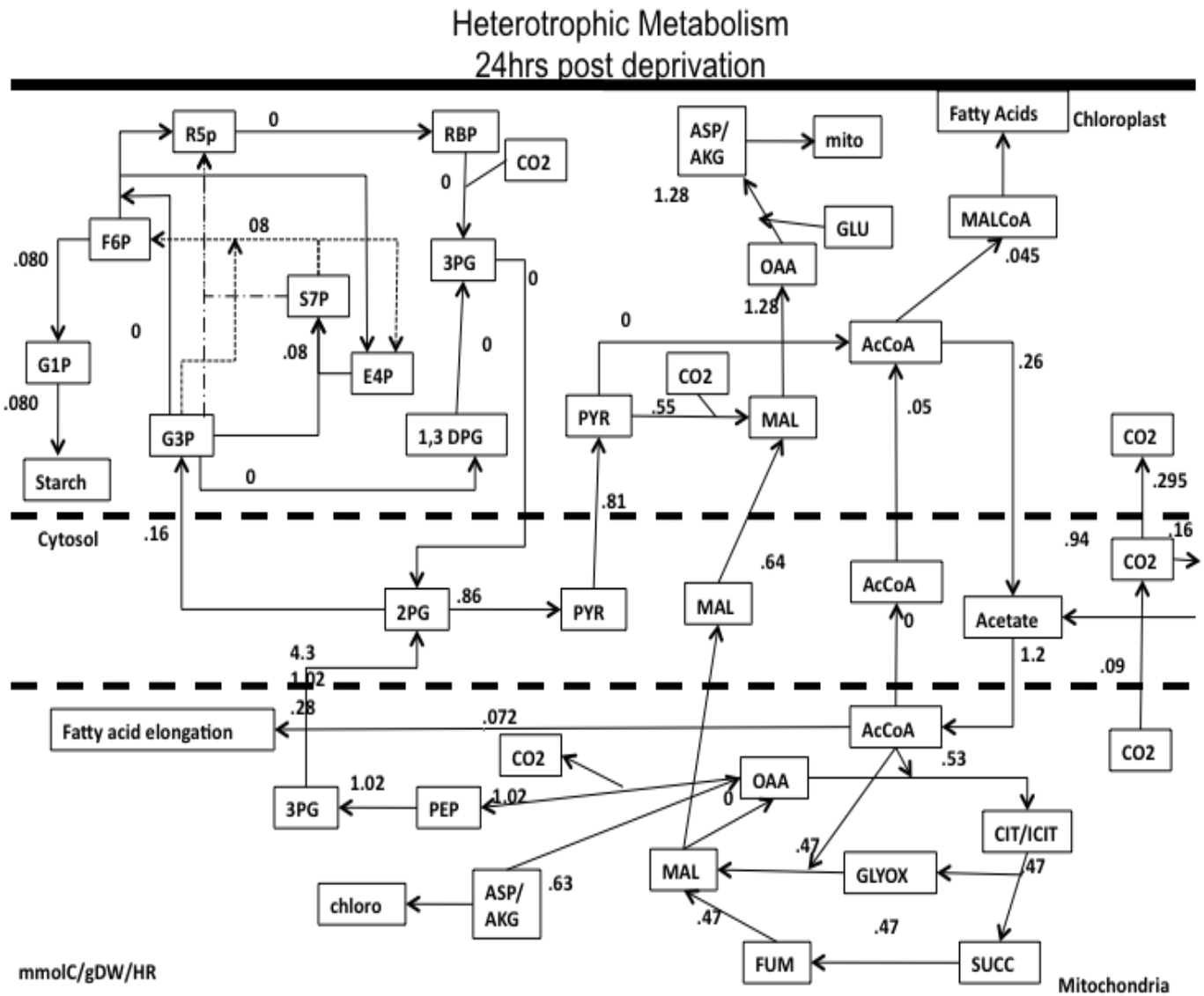

Figure 4.2 H. Nitrogen Deplete Heterotrophic Growth. 24 hrs post N deprivation

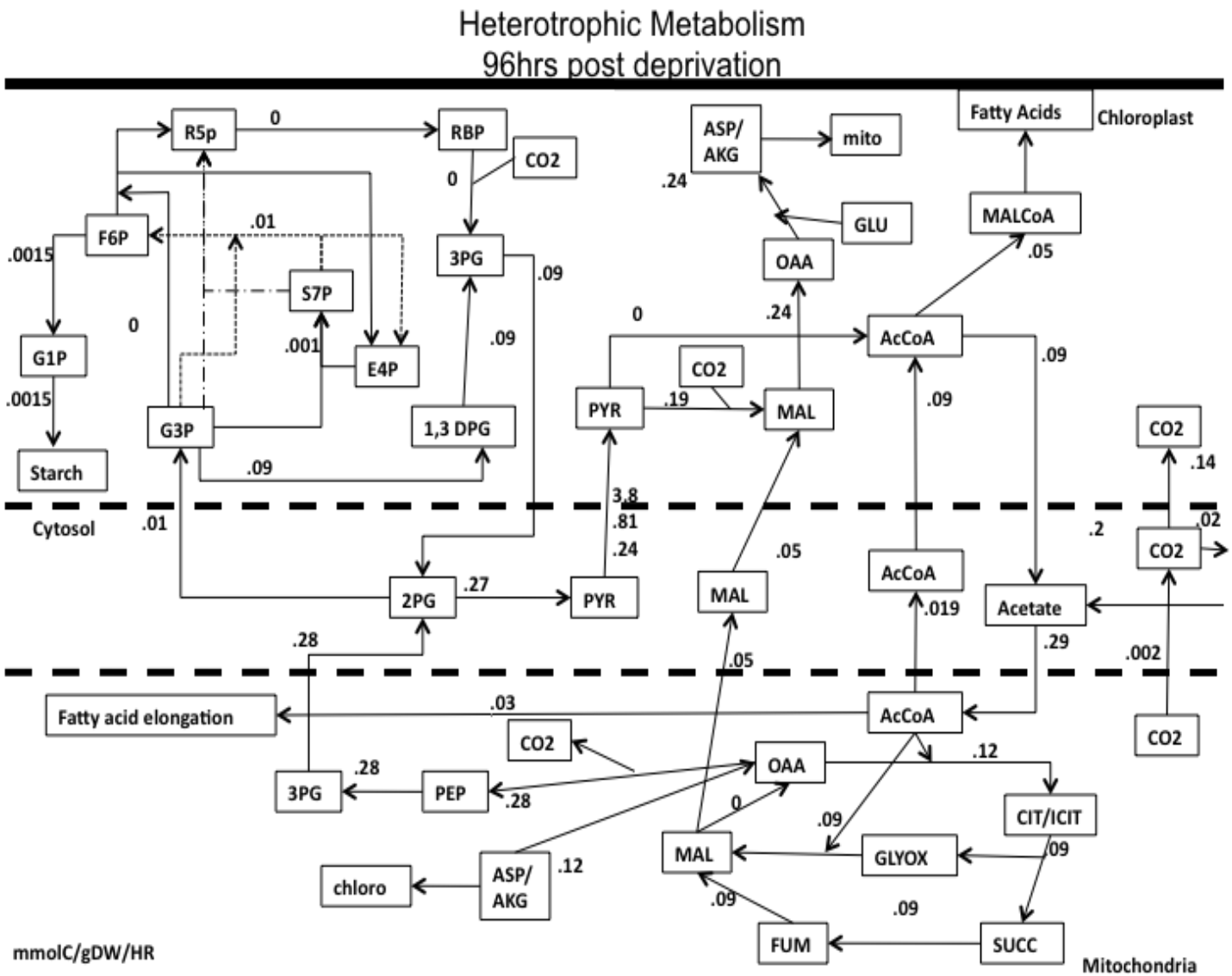

Figure 4.2 I. Nitrogen Deplete Heterotrophic Growth. 96 hrs post N deprivation

Nitrogen Replete Conditions

The flux maps presented under each of the three conditions demonstrates the robustness of the model to study various media conditions. Known metabolic activities of cells under each condition are supported - i.e., autotrophic growth has dominant fluxes through the Calvin cycle, mixotrophic uses both acetate and Calvin Benson cycle for carbon and energy, and the heterotrophic condition uses acetate and has an inactive Calvin Benson cycle. Both light using autotrophic and mixotrophic conditions also show a linear relationship between light consumed and growth rates demonstrating the models ability to represent different light conditions (Figure 4.3). Also, mixotrophic conditions receive more biomass per photon as acetate is present to aid biosynthesis and growth.

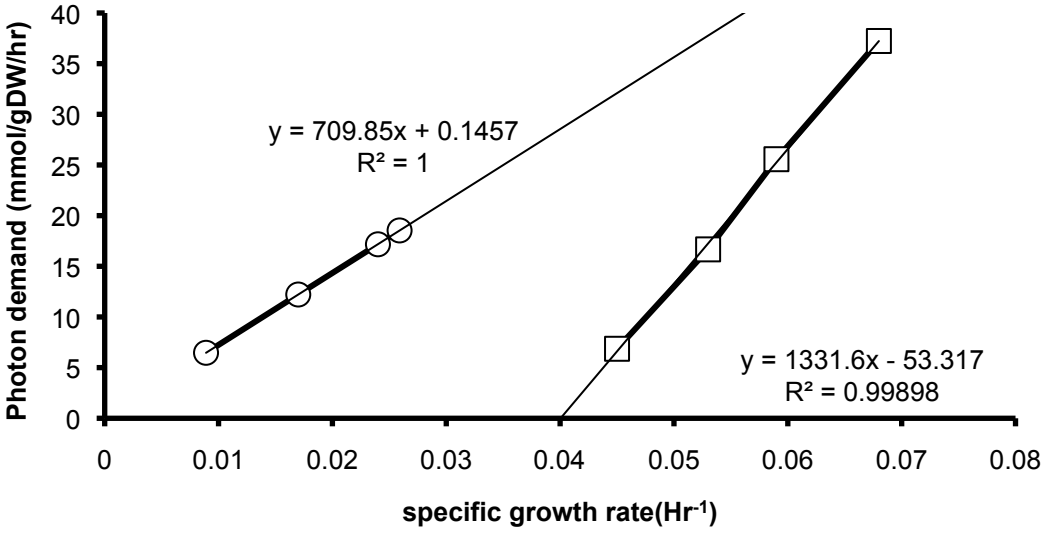

Figure 4.3. Photon demand vs. growth rate at 5, 40, 15, and 160 µmol photon/m^2/s. Hollow circle represent autotrophic conditions and hollow squares represent mixotrophic conditions.

These models additionally support the idea that cells at even moderate light intensities are exposed to more light than than needed. Figure 4.4 shows the calculated photon demands at 5, 40, 15, and 160 μmol photon/m^2/s. vs. the relative light absorbed by the cell that was calculated in chapter 3. Here we find that although cells have the capacity to absorb significant amounts of light with increasing light intensity, only a small amount is actually needed. From chapter 3 we also found that our cells are carbon limited which will account for decreased photon demands. Autotrophic data shows this the most with almost no increase in light demand from 40 to 160 μmol photon/m^2/s even though the potential absorbed light increases 3 fold.

Aside from interesting photosynthetic outputs, these flux balances present insight into general metabolism. First, none of the maps showed flux through plastidic fructose bisphospate aldolase, instead using oxidative pentose phosphate pathway (OPP) reactions to generate fructose bisphosphate for starch production. This is interesting as this is normally a major gluconeogenic pathway. Second, we find 3-phosphoglycerate to be the dominant triose phosphate exported from the plastid from photosynthesis while glyceraldehyde-3-phosphate is generally depicted of as the main trios exported. Next, the maps generally depict little to no flux through traditional citric acid cycle, opting for flux through the glyoxolate cycle in the mitochondria(activity naturally found in the peroxisome). Finally, for all the maps there is a general flux from the plastid to the mitochondria in the form of aspartate and alpha ketoglutarate to oxaloacetate, moving ammonia and carbon.

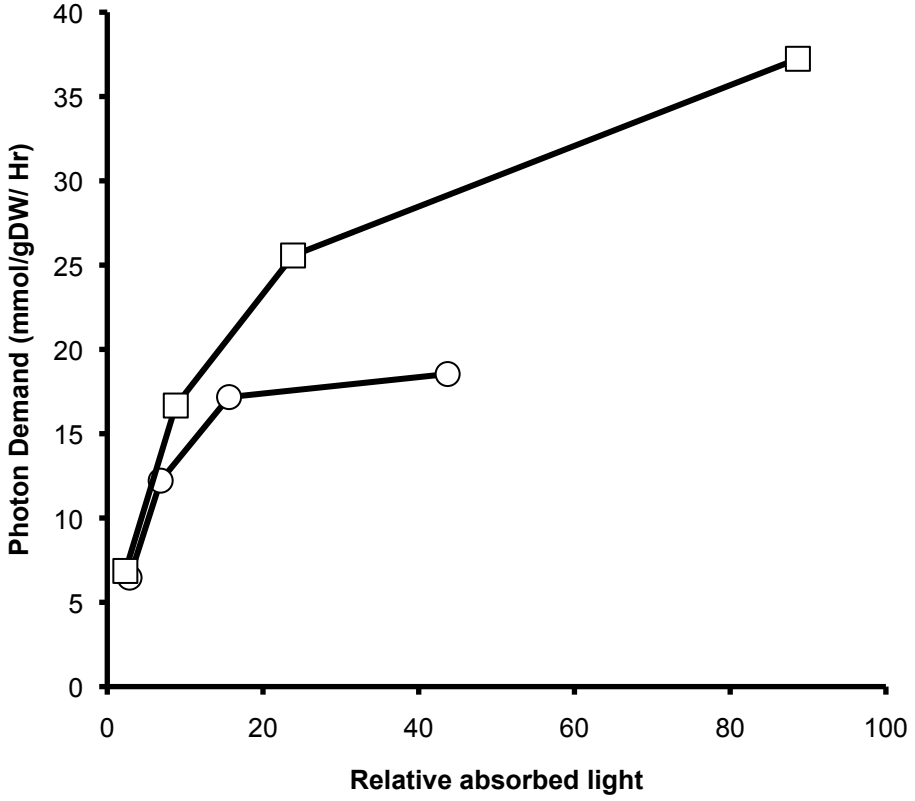

Figure 4.4. Photon demand vs. relative absorbed light at 5, 40, 15, and 160 µmol photon/m^2/s. Hollow circle represent autotrophic conditions and hollow squares represent mixotrophic conditions. Relative absorbed light calculated from φii * µg Chlorophyll/million cells* light intensity from data in chapter 3 for each light intensity.

Photosynthesis During N Deprivation

In chapter three, I measured decreases in photosynthesis during nitrogen deprivation in both mixorophic and autotrophic conditions. Here it was found that mixotrophic cultures had higher photosynthetic activities during nitrogen replete conditions than autotrophic conditions and fell to values significantly lower than autotrophic during later timepoints of N deprivation. We linked this to mixotrophic cells being able to rely on fed acetate while autotrophic cells were reliant upon photosynthesis for energy and carbon even under N deprivation. We find the same trends in each growth condition with the flux modeling, presented in Figure 4.5.

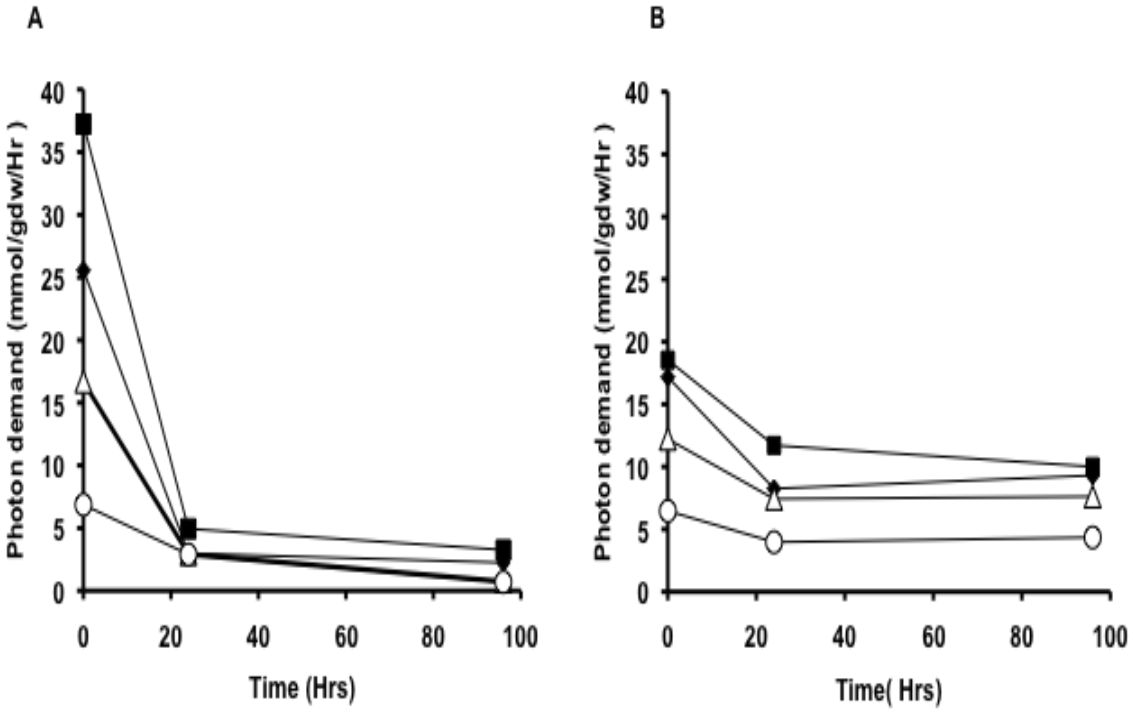

Figure 4.5. Light Demand predictions during N deprivation. A represents mixotrophic cultures while B represents autotrophic cultures. Black squares are 160, black diamonds are 40, hollow triangles are 15, and hollow circles are 5 μmol photons/ m^2/s light intensities. Mixotrophic cells demonstrate a higher flux during N replete conditions and a lower photosynthetic flux during nutrient depletion.

To assess how efficient cells are using light at different light intensities, we compared flux balance predictions to measured maximum available photons. Predicted photon demands were converted from mmol photon/gdw/hr to μmol photon/million cells/hr. Total available photons were calculated from measured light intensity, chlorophyll(capacity to abosorb light) and Φ_{II}(efficiency of light use around PSII), making the assumption that light was hitting both photosynthetic complexes equally and that each complex uses light with the same efficiency. Absorbed light was calculated using the extinction coefficient of chlorophyll, chlorophyll abundance, and Beer's law, Absorbance = ε(extinction coefficienct)*chlorophyll concentration*L (path length of light). FBA predicted photon use divided by the calculated maximum available light to the cell is presented in Figure 4.6. There are a number of conclusions one can derive from this figure. First, as light intensity increases, there is a decreasing efficiency of use from 80% at low light intensities down to 13% for higher light intensities. Second, both autotrophic and mixotrophic have similar light use efficiencies at higher light intensities but less so at low light intensities. Finally, it shows light constraints are relieved with increasing light intensity. The decreases in photosynthesis found under mixotrophic conditions extends beyond just photon demand. Table 4.2 shows how each photosynthetic flux changes during N deprivation.

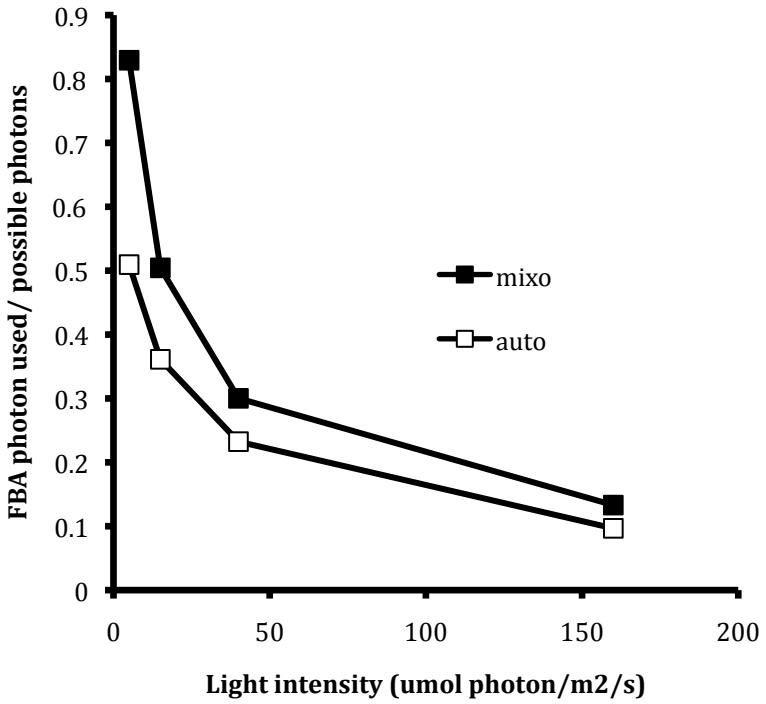

Figure 4.6. FBA predicted light use vs. calculated light available for photosynthesis. Predicted photons from FBA were divided by the calculated photons available to photosynthesis under nutrient replete conditions across multiple light intensities. Filled squares indicate mixotrophic conditions(TAP media) while hollow squares indicate autotrophic conditions(HS media).

Autotrophic	N+				24 hrs post deprivation				96 hrs Post Deprivation			
	160	40	15	5	160	40	15	5	160	40	15	5
ATP synthase	7.213	6.686	4.769	2.533	4.391	3.093	2.786	1.488	3.752	3.488	2.854	1.629
Photosystem II	2.056	1.900	1.339	0.699	1.464	1.031	0.929	0.496	1.251	1.163	0.951	0.543
Photosystem I	10.314	9.572	6.861	3.668	5.855	4.125	3.714	1.985	5.002	4.650	3.806	2.172
Cytochrome b6/f complex	10.314	9.572	6.861	3.668	5.855	4.125	3.714	1.985	5.002	4.650	3.806	2.172
Qcycle	5.157	4.786	3.431	1.834	2.927	2.062	1.857	0.992	2.501	2.325	1.903	1.086
Ferredoxin-NADP+ reductase	4.111	3.798	2.675	1.396	2.927	2.062	1.857	0.992	2.501	2.325	1.903	1.086
Cyclic Electron Flow	1.046	0.988	0.755	0.439	0	0	0	0	0	0	0	0
Plastid Terminal Oxidase	0.001	0.001	0.001	0.001	0	0	0	0	0	0	0	0
Mehler	2.48E-05	2.30E-05	1.63E-05	8.53E-06	0	0	0	0	0	0	0	0

Mixotrophic	N+				24 hrs Post Deprivation				96 hrs Post Deprivation			
	160	40	15	5	160	40	15	5	160	40	15	5
ATP synthase	14.931	10.557	6.919	2.632	1.852	1.116	1.092	1.085	1.219	0.839	0.304	0.289
Photosystem II	3.688	2.229	1.417	0.798	0.617	0.373	0.364	0.362	0.406	0.280	0.060	0.055
Photosystem I	22.486	16.655	11.004	3.668	2.469	1.487	1.457	1.447	1.626	1.118	0.488	0.470
Cytochrome b6/f complex	22.486	16.655	11.004	3.668	2.469	1.487	1.457	1.447	1.626	1.118	0.488	0.470
Qcycle	11.243	8.328	5.502	1.834	1.235	0.743	0.728	0.723	0.813	0.559	0.244	0.235
Ferredoxin-NADP+ reductase	7.374	4.456	2.831	1.594	1.235	0.743	0.728	0.723	0.813	0.559	0.119	0.107
Cyclic Electron Flow	3.870	3.872	2.671	0.240	0	0	0	0	0	0	0.125	0.128
Plastid Terminal Oxidase	0.001	0.001	0.001	0.001	0	0.001	0	0	0	0	0.001	0.001
Mehler	5.109E-07	4.433E-07	3.982E-07	3.381E-07	0	0	0	0	0	0	0	0

Table 4.2 Photosynthetic Fluxes. Flux values generated through flux balance analysis at each light intensity and media condition at N+, 24 hrs after N- and 96 hrs after N-. All values are in units of mmol C/gDW/Hr.

Nitrogen Deprivation Metabolism

Chlamydomonas was studied using Flux balance analysis at 24 and 96 hrs after deprivation. Under these conditions, nitrate and ammonium sources were constrained to zero, eliminating all biomass production. During these conditions the only drivers of synthesis are that of starch and TAG, removing all metabolism related to normal biomass production. During the first 24 hrs, we measured some cell growth as reported in chapter 3 but were unable to factor that in for this experiment. Under all growth conditions, starch precursors are produced from the fructose bisphosphate to glucose 1 phosphate and so on using the OPP pathway reactions. TAG carbon is derived from multiple sources depending upon the growth condition with primary chains coming from the plastid and elongation reactions derived from the mitochondria AcCoA pools. Mixotrophic TAG is derived predominantly from acetate (in congruence with chapter 3 conclusions) while autotrophic TAG is derived from plastidic pyruvate to amino acid to AcCoa metabolism. Meanwhile heterotrophic TAG is predicted to come from the mitochondrial AcCoA derived from acetate and transported to the plastid for fatty acid synthesis. With much interest in biofuel production this data suggests that the route to increased biofuel production depends upon the growth conditions one uses.

DISCUSSION

Here, the stoichiometric model *i*Cre1355 was used to explore Chlamydomonas metabolism during both nitrogen replete and deplete conditions and found to produce accurate representations of known metabolism under three different growth conditions. Further, imposing measured constraints such as biomass and substrate uptakes upon the system gave photosynthetic results similar to those suggested in chapter three. In congruence with that data, actual light needed for starch and TAG biosynthesis is many times lower than that available to the cell. This is in congruence with evidence against the overflow hypothesis provided in chapter three. Finally this work showed that while nitrogen deprivation starch production comes from the plastid through fructose bisphosphate, TAG accumulations can come from various sources and pathways dependent upon growth conditions.

The *i*Cre1355 model (Imam, et al. 2015, Lopez Garcia de Lomana, et al. 2015), although newly updated with current gene lists, has been found to be missing correct reaction stoichiometries and known gene reactions for photosynthesis. This model did present itself as functioning and somewhat predictive but requires more intensive biochemistry annotation. Updates that I have added to the model allow for a number of activities. First, photosynthetic reactions have been corrected allowing for more realistic modeling results. Second, a counter of photons as well as an NADPH burning reaction have been added to control photon usage and system reduction respectively. Finally,

The next step is to push the model to its limits, determining how much starch and TAG the system can make with current and potential carbon and energy inputs and how those more active metabolisms work and move carbon and energy. Metabolic pathways

with heightened fluxes may give rise to insight for engineering efforts. Additionally, the actual movement of fatty acids through membranes can be more fully characterized to give insight into lipid trafficking pathways and possible metabolic reasons for using one or another for TAG filling during nutrient deprivation. One way to do this might include adding an endoplasmic reticulum compartment and link the plastid lipids to it instead of the mitochondria as in this model.

MODEL CHALLENGES

Before the model demonstrated fluxes representing known activities, several problems had to become overcome. Initial modeling efforts in both autotrophic and mixotrophic conditions demonstrated large fluxes through small molecule, radical oxygen, and fermentative pathways. Small molecule (carbon monoxide and nitrous oxide), and hydrogen peroxide production pathways were constrained (set to .001 mmol C/gDW/Hr), forcing flux through the fermentative pathways to produce ethanol, acetate, formate, and lactate. Attempts to constrain (limit) these pathways led to protons being dumped from NADPH onto O_2, forming water though the added photosynthetic PTOX reaction. Limiting PTOX caused PSII fluxes to remain unchanged. We believed that PSII activity was too high in relation to the needs of the cell, causing an overly reduced environment. Attempts to minimize PSII gave the same flux as before suggesting PSII or downstream NADPH production and dissipation was necessary for the modeling environment. Interestingly, if we constrained PSII to a low value while keeping minimization of light use as an objective function, cycle electron flow activity increased.

There are a number of transporters requiring a proton motive force to move molecules across membranes including those for ATP. Moving the ATP maintenance cost from the cytosol to the plastid reduced the small molecule/ peroxide/ fermentative fluxes several fold demonstrating protons requirements in transport were partly responsible for the NADPH consumption. Attempts to further pin point the exact cause of the NADPH consumption and the hidden roles of proton generation in the model led to several dead ends and infeasible models. To address the problem, we installed a NADPH consumption reaction in the plastid that simply dissipates NADPH into NADP+ and H+.

Solving the model with this flux removed most reactions that appeared to be wastefully burning NADPH or producing excessive amounts of small molecules. All flux maps presented in this work were carried out with the NADPH burning reaction active. Intensive probing and revaluation of reaction stoichiometries of the system will be required to determine the true cause of the NADPH burn requirement.

As mentioned before, another challenge laid in making sure the photosynthetic stoichiometries were correct. iCre1355 and its predecessor iCre1080 both demonstrated incorrect photosynthetic proton transport, incomplete cyclic electron flow reactions, and lack of Q cycle, Mehler reaction, PTOX, or NADPH Plastoquinone reductase. Previous studies demonstrated no flux through cyclic electron flow during autotrophic conditions however after correcting the reactions and constraining the system, we find significant flux though this reaction under nitrogen repletion. Additionally, the original model allowed for free energy generation through free sodium transport. Sodium was generated outside the cell and destroyed inside the cell generating a free flow of sodium that allowed free transmembrane transport of various metabolites. Further, the original model used a "dummy O_2" reaction that removed PSII generated oxygen instead of it entering the thylakoid lumen oxygen pool.

FUTURE DIRECTIONS

The work presented in this chapter is ongoing. While the fluxes calculated through our modeling efforts are representative of actual trends measured in the lab, they may not be completely true in respect to the actual metabolism active in the organism. The genome scale model used in this study is extensive and has been generated from all gene reactions currently supported by transcript and proteomic analysis or required for basic metabolism activity however only roughly half of the Chlamydomonas genome has been functionally annotated at this time (Blaby, et al. 2014, Grossman *et al.* 2010b). This leaves large room for improvement to the total reactome (summation of all reactions) of the model, which may drastically alter the final fluxes. Further, the model used is static, stoichiometric one meaning without extensive user given constraints, it does not have the ability to reflect changes in substrate concentrations, negative or positive feedback regulation, changes in proton and other gradients, or other dynamic situations. Additionally, without extensive constraints on metabolisms known to be nonfunctional under tested conditions, they may be active. In our case we saw extensive nitric oxide, carbon monoxide, fermentation, and reactive oxygen species generation under normal N+ growth conditions before constraining to low fluxes. Groups such as Imam et al. (Imam, et al. 2015) used transcript data during N deprivation to constrain their flux space but again only half of the known genes have been annotated and may leave much room for improvement upon further annotation.

Similarly, we chose light or CO_2 use as the objective functions in this study however this may not be the actual. During normal growth it is not known what the primary objective function of an algae is and simply saying it is to grow as much as

possible or use as little light as possible may be very misleading. Further, using these constraints during nutrient deprivation may be equally far off the actual function of the cell. Cells are already flush with more light than they need under these conditions, what is stopping them from using as much light as they want wastefully, would it not provide an advantage in nature to absorb as much light as possible and prevent competitors from growing? Using different objective functions can give wildly different results and should be explored in future studies.

To more properly constrain flux maps in the future and have a more accurate representation of the metabolism in Chlamydomonas, ^{13}C metabolic flux analysis should be used(Allen, et al. 2009, Chen, et al. 2011b, Kim *et al.* 2008, Libourel, et al. 2008, O'Grady *et al.* 2012, Shachar-Hill 2013, Young, et al. 2011, Zamboni *et al.* 2009). This methodology uses ^{13}C labeled substrate such as acetate or bicarbonate to monitor metabolism. Chlamydomonas grown in labeled substrate containing media will reach steady state incorporation and percent ^{13}C labeling and patterning which can be analyzed through analytical methods such as mass spectrometry or nuclear magnetic resonance. Only a certain range of possible flux solutions exist to give rise to the labeling pattern seen in the organism and that can be calculated computationally. As this is a measure of actual metabolism in the organism, it can be used to check the validity of and guide constraints in flux balance analysis. Nitrogen deprivation is a continuously changing condition and will require more intensive dynamic labeling experiments instead of the steady state ones used for nitrogen replete conditions. Models can be further validated by using ^{13}C substrates labeled at different positions as different carbons on a molecule may be directed to different metabolic end points.

In conclusion, while the model used in this study may be extensive it is by no means complete and further, more intensive work needs to be done to constrain the models so they are more representative of current metabolism. Once validated, the flux balance modeling technique can be used to predict the outcomes of gene knockouts, over expressions, and other genetic engineering efforts.

ACKNOWLEDGEMENTS

We would like the thank Saheed Imam, Stephen Chapman, and Jean-Marc Schwartz for their help in understanding their models and flux balance assistance.

REFERENCES

REFERENCES

Allen, D.K., Libourel, I.G.L. and Shachar-Hill, Y. (2009) Metabolic flux analysis in plants: coping with complexity. *Plant Cell Environ*, **32**, 1241-1257.

Baroukh, C., Munoz-Tamayo, R., Steyer, J.P. and Bernard, O. (2015) A state of the art of metabolic networks of unicellular microalgae and cyanobacteria for biofuel production. *Metab Eng*, **30**, 49-60.

Blaby, I.K., Blaby-Haas, C.E., Tourasse, N., Hom, E.F., Lopez, D., Aksoy, M., Grossman, A., Umen, J., Dutcher, S., Porter, M., King, S., Witman, G.B., Stanke, M., Harris, E.H., Goodstein, D., Grimwood, J., Schmutz, J., Vallon, O., Merchant, S.S. and Prochnik, S. (2014) The Chlamydomonas genome project: a decade on. *Trends in plant science*, **19**, 672-680.

Bolling, C. and Fiehn, O. (2005) Metabolite profiling of *Chlamydomonas reinhardtii* under nutrient deprivation. *Plant Physiol*, **139**, 1995-2005.

Borodina, I. and Nielsen, J. (2005) From genomes to in silico cells via metabolic networks. *Curr Opin Biotechnol*, **16**, 350-355.

Boyle, N.R. and Morgan, J.A. (2009) Flux balance analysis of primary metabolism in *Chlamydomonas reinhardtii*. *BMC systems biology*, **3**, 4.

Brown, S.P.A. and Kennelly, R. (2013) Consequences of U.S. Dependence on Foreign Oil. University of Nevada, Las Vegas: National Energy Policy Institute.

Chang, R.L., Ghamsari, L., Manichaikul, A., Hom, E.F.Y., Balaji, S., Fu, W., Shen, Y., Hao, T., Palsson, B.Ø., Salehi-Ashtiani, K. and Papin, J.A. (2011) Metabolic network reconstruction of Chlamydomonas offers insight into light-driven algal metabolism. *Molecular systems biology*, **7**, 518-518.

Chapman, S.P., Paget, C.M., Johnson, G.N. and Schwartz, J.M. (2015) Flux balance analysis reveals acetate metabolism modulates cyclic electron flow and alternative glycolytic pathways in Chlamydomonas reinhardtii. *Frontiers in plant science*, **6**, 474.

Chen, X.W., Alonso, A.P., Allen, D.K., Reed, J.L. and Shachar-Hill, Y. (2011) Synergy between C-13-metabolic flux analysis and flux balance analysis for understanding metabolic adaption to anaerobiosis in *E. coli*. *Metab Eng*, **13**, 38-48.

Chisti, Y. (2007) Biodiesel from microalgae. *Biotechnology Advances*, **25**, 294-306.

Cogne, G., Gros, J.B. and Dussap, C.G. (2003) Identification of a metabolic network structure representative of Arthrospira (spirulina) platensis metabolism. *Biotechnology and bioengineering*, **84**, 667-676.

Cogne, G., Rügen, M., Bockmayr, A., Titica, M., Dussap, C.-G., Cornet, J.-F. and Legrand, J. (2011) A model-based method for investigating bioenergetic processes in autotrophically growing eukaryotic microalgae: Application to the green algae Chlamydomonas reinhardtii. *Biotechnology progress*, **27**, 631-640.

Dal'Molin, C.G., Quek, L.E., Palfreyman, R.W. and Nielsen, L.K. (2011) AlgaGEM--a genome-scale metabolic reconstruction of algae based on the *Chlamydomonas reinhardtii* genome. *Bmc Genomics*, **12 Suppl 4**, S5.

de Oliveira Dal'Molin, C.G., Quek, L.E., Palfreyman, R.W., Brumbley, S.M. and Nielsen, L.K. (2010) AraGEM, a genome-scale reconstruction of the primary metabolic network in Arabidopsis. *Plant Physiol*, **152**, 579-589.

Famili, I., Förster, J., Nielsen, J. and Palsson, B.O. (2003) Saccharomyces cerevisiae phenotypes can be predicted by using constraint-based analysis of a genome-scale reconstructed metabolic network. *P Natl Acad Sci USA*, **100**, 13134-13139.

Fan, J., Yan, C., Andre, C., Shanklin, J., Schwender, J. and Xu, C. (2012) Oil accumulation is controlled by carbon precursor supply for fatty acid synthesis in *Chlamydomonas reinhardtii*. *Plant & cell physiology*, **53**, 1380-1390.

Gomez, J.A., Hoffner, K. and Barton, P.I. (2016) From sugars to biodiesel using microalgae and yeast. *Green Chemistry*, **18**, 461-475.

Goodenough, U. (2015) Historical perspective on Chlamydomonas as a model for basic research: 1950–1970. *The Plant Journal*, **82**, 365-369.

Grafahrend-Belau, E., Schreiber, F., Koschutzki, D. and Junker, B.H. (2009) Flux Balance Analysis of Barley Seeds: A Computational Approach to Study Systemic Properties of Central Metabolism. *Plant Physiol*, **149**, 585-598.

Grossman, A.R., Karpowicz, S.J., Heinnickel, M., Dewez, D., Hamel, B., Dent, R., Niyogi, K.K., Johnson, X., Alric, J., Wollman, F.A., Li, H. and Merchant, S.S. (2010) Phylogenomic analysis of the Chlamydomonas genome unmasks proteins potentially involved in photosynthetic function and regulation. *Photosynth Res*, **106**, 3-17.

Harris, E.H. (2009) Preface to Volume 1. In *The Chlamydomonas Sourcebook (Second Edition)* (Harris, E.H., Stern, D.B. and Witman, G.B. eds). London: Academic Press, pp. ix.

Hay, J. and Schwender, J. (2011) Metabolic network reconstruction and flux variability analysis of storage synthesis in developing oilseed rape (Brassica napus L.) embryos. *Plant J*, **67**, 526-541.

Heinemann, M., Kummel, A., Ruinatscha, R. and Panke, S. (2005) In silico genome-scale reconstruction and validation of the Staphylococcus aureus metabolic network. *Biotechnology and bioengineering*, **92**, 850-864.

Houille-Vernes, L., Rappaport, F., Wollman, F.A., Alric, J. and Johnson, X. (2011) Plastid terminal oxidase 2 (PTOX2) is the major oxidase involved in chlororespiration in Chlamydomonas. *Proc Natl Acad Sci U S A*, **108**, 20820-20825.

Imam, S., Schauble, S., Valenzuela, J., Lopez Garcia de Lomana, A., Carter, W., Price, N.D. and Baliga, N.S. (2015) A refined genome-scale reconstruction of Chlamydomonas metabolism provides a platform for systems-level analyses. *Plant J*, **84**, 1239-1256.

Kim, H.U., Kim, T.Y. and Lee, S.Y. (2008) Metabolic flux analysis and metabolic engineering of microorganisms. *Mol. Biosyst.*, **4**, 113-120.

Kruger, N.J. and Ratcliffe, R.G. (2009) Insights into plant metabolic networks from steady-state metabolic flux analysis. *Biochimie*, **91**, 697-702.

Lee do, Y. and Fiehn, O. (2008) High quality metabolomic data for *Chlamydomonas reinhardtii*. *Plant methods*, **4**, 7.

Li, X., Zhang, R., Patena, W., Gang, S.S., Blum, S.R., Ivanova, N., Yue, R., Robertson, J.M., Lefebvre, P., Fitz-Gibbon, S.T., Grossman, A.R. and Jonikas, M.C. (2016) An indexed, mapped mutant library enables reverse genetics studies of biological processes in Chlamydomonas reinhardtii. *The Plant cell*.

Libourel, I.G.L. and Shachar-Hill, Y. (2008) Metabolic flux analysis in plants: From intelligent design to rational engineering. *Annu Rev Plant Biol*, **59**, 625-650.

Liu, B.S. and Benning, C. (2013) Lipid metabolism in microalgae distinguishes itself. *Current Opinion in Biotechnology*, **24**, 300-309.

Liu, J., Huang, J., Sun, Z., Zhong, Y., Jiang, Y. and Chen, F. (2011) Differential lipid and fatty acid profiles of photoautotrophic and heterotrophic Chlorella zofingiensis: assessment of algal oils for biodiesel production. *Bioresour Technol*, **102**, 106-110.

Lopez Garcia de Lomana, A., Schauble, S., Valenzuela, J., Imam, S., Carter, W., Bilgin, D.D., Yohn, C.B., Turkarslan, S., Reiss, D.J., Orellana, M.V., Price, N.D. and Baliga, N.S. (2015) Transcriptional program for nitrogen starvation-induced lipid accumulation in Chlamydomonas reinhardtii. *Biotechnology for biofuels*, **8**, 207.

Mahadevan, R. and Schilling, C.H. (2003) The effects of alternate optimal solutions in constraint-based genome-scale metabolic models. *Metab Eng*, **5**, 264-276.

Manichaikul, A., Ghamsari, L., Hom, E.F., Lin, C., Murray, R.R., Chang, R.L., Balaji, S., Hao, T., Shen, Y., Chavali, A.K., Thiele, I., Yang, X., Fan, C., Mello, E., Hill, D.E., Vidal, M., Salehi-Ashtiani, K. and Papin, J.A. (2009) Metabolic network analysis integrated with transcript verification for sequenced genomes. *Nature methods*, **6**, 589-592.

Martin, M.A. (2010) First generation biofuels compete. *New biotechnology*, **27**, 596-608.

May, P., Wienkoop, S., Kempa, S., Usadel, B., Christian, N., Rupprecht, J., Weiss, J., Recuenco-Munoz, L., Ebenhoh, O., Weckwerth, W. and Walther, D. (2008) Metabolomics- and proteomics-assisted genome annotation and analysis of the draft metabolic network of Chlamydomonas reinhardtii. *Genetics*, **179**, 157-166.

Mehler, A.H. (1951a) Studies on reactions of illuminated chloroplasts. I. Mechanism of the reduction of oxygen and other Hill reagents. *Archives of biochemistry and biophysics*, **33**, 65-77.

Mehler, A.H. (1951b) Studies on reactions of illuminated chloroplasts. II. Stimulation and inhibition of the reaction with molecular oxygen. *Archives of biochemistry and biophysics*, **34**, 339-351.

Mehler, A.H. and Brown, A.H. (1952) Studies on reactions of illuminated chloroplasts. III. Simultaneous photoproduction and consumption of oxygen studied with oxygen isotopes. *Archives of biochemistry and biophysics*, **38**, 365-370.

Melo, D.O.P., Moncada, R.J.-P., Winck, F.V. and Barrios, A.F.G. (2014) In Silico Analysis for Biomass Synthesis under Different CO2 Levels for Chlamydomonas reinhardtii Utilizing a Flux Balance Analysis Approach. In *Advances in Computational Biology: Proceedings of the 2nd Colombian Congress on Computational Biology and Bioinformatics (CCBCOL)* (Castillo, F.L., Cristancho, M., Isaza, G., Pinzón, A. and Rodríguez, C.J.M. eds). Cham: Springer International Publishing, pp. 279-285.

Merchant, S.S., Kropat, J., Liu, B., Shaw, J. and Warakanont, J. (2012) TAG, You're it! *Chlamydomonas* as a reference organism for understanding algal triacylglycerol accumulation. *Current Opinion in Biotechnology*, **23**, 352-363.

Merchant, S.S., Prochnik, S.E., Vallon, O., Harris, E.H., Karpowicz, S.J., Witman, G.B., Terry, A., Salamov, A., Fritz-Laylin, L.K., Marechal-Drouard, L., Marshall, W.F., Qu, L.H., Nelson, D.R., Sanderfoot, A.A., Spalding, M.H., Kapitonov, V.V., Ren, Q., Ferris, P., Lindquist, E., Shapiro, H., Lucas, S.M., Grimwood, J., Schmutz, J., Cardol, P., Cerutti, H., Chanfreau, G., Chen, C.L., Cognat, V., Croft, M.T., Dent, R., Dutcher, S., Fernandez, E., Fukuzawa, H., Gonzalez-Ballester, D., Gonzalez-Halphen, D., Hallmann, A., Hanikenne, M., Hippler, M., Inwood, W., Jabbari, K., Kalanon, M., Kuras, R., Lefebvre, P.A., Lemaire, S.D., Lobanov, A.V., Lohr, M., Manuell, A.,

Meier, I., Mets, L., Mittag, M., Mittelmeier, T., Moroney, J.V., Moseley, J., Napoli, C., Nedelcu, A.M., Niyogi, K., Novoselov, S.V., Paulsen, I.T., Pazour, G., Purton, S., Ral, J.P., Riano-Pachon, D.M., Riekhof, W., Rymarquis, L., Schroda, M., Stern, D., Umen, J., Willows, R., Wilson, N., Zimmer, S.L., Allmer, J., Balk, J., Bisova, K., Chen, C.J., Elias, M., Gendler, K., Hauser, C., Lamb, M.R., Ledford, H., Long, J.C., Minagawa, J., Page, M.D., Pan, J., Pootakham, W., Roje, S., Rose, A., Stahlberg, E., Terauchi, A.M., Yang, P., Ball, S., Bowler, C., Dieckmann, C.L., Gladyshev, V.N., Green, P., Jorgensen, R., Mayfield, S., Mueller-Roeber, B., Rajamani, S., Sayre, R.T., Brokstein, P., Dubchak, I., Goodstein, D., Hornick, L., Huang, Y.W., Jhaveri, J., Luo, Y., Martinez, D., Ngau, W.C., Otillar, B., Poliakov, A., Porter, A., Szajkowski, L., Werner, G., Zhou, K., Grigoriev, I.V., Rokhsar, D.S. and Grossman, A.R. (2007) The *Chlamydomonas* genome reveals the evolution of key animal and plant functions. *Science*, **318**, 245-250.

O'Grady, J., Schwender, J., Shachar-Hill, Y. and Morgan, J.A. (2012) Metabolic cartography: experimental quantification of metabolic fluxes from isotopic labelling studies. *J Exp Bot*, **63**, 2293-2308.

Ohlrogge, J., Allen, D., Berguson, B., DellaPenna, D., Shachar-Hill, Y. and Stymne, S. (2009) Driving on Biomass. *Science*, **324**, 1019-1020.

Peng, L., Fukao, Y., Fujiwara, M., Takami, T. and Shikanai, T. (2009) Efficient operation of NAD(P)H dehydrogenase requires supercomplex formation with photosystem I via minor LHCI in Arabidopsis. *The Plant cell*, **21**, 3623-3640.

Pilalis, E., Chatziioannou, A., Thomasset, B. and Kolisis, F. (2011) An In Silico Compartmentalized Metabolic Model of Brassica Napus Enables the Systemic Study of Regulatory Aspects of Plant Central Metabolism. *Biotechnology and bioengineering*, **108**, 1673-1682.

Poolman, M.G., Miguet, L., Sweetlove, L.J. and Fell, D.A. (2009) A Genome-Scale Metabolic Model of Arabidopsis and Some of Its Properties. *Plant Physiol*, **151**, 1570-1581.

Radakovits, R., Jinkerson, R.E., Fuerstenberg, S.I., Tae, H., Settlage, R.E., Boore, J.L. and Posewitz, M.C. (2012) Draft genome sequence and genetic transformation of the oleaginous alga *Nannochloropsis gaditana*. *Nature Communications*, **3**.

Rugen, M., Bockmayr, A., Legrand, J. and Cogne, G. (2012) Network reduction in metabolic pathway analysis: elucidation of the key pathways involved in the photoautotrophic growth of the green alga Chlamydomonas reinhardtii. *Metab Eng*, **14**, 458-467.

Saha, R., Suthers, P.F. and Maranas, C.D. (2011) Zea mays iRS1563: A Comprehensive Genome-Scale Metabolic Reconstruction of Maize Metabolism. *PloS one*, **6**.

Saroussi, S.I., Wittkopp, T.M. and Grossman, A.R. (2016) The type II NADPH dehydrogenase facilitates cyclic electron flow, energy dependent quenching and chlororespiratory metabolism during acclimation of Chlamydomonas reinhardtii to nitrogen deprivation. *Plant Physiol*.

Selvaratnam, T., Pegallapati, A.K., Montelya, F., Rodriguez, G., Nirmalakhandan, N., Van Voorhies, W. and Lammers, P.J. (2014) Evaluation of a thermo-tolerant acidophilic alga, Galdieria sulphuraria, for nutrient removal from urban wastewaters. *Bioresour Technol*, **156**, 395-399.

Shachar-Hill, Y. (2013) Metabolic network flux analysis for engineering plant systems. *Current Opinion in Biotechnology*, **24**, 247-255.

Shastri, A.A. and Morgan, J.A. (2005) Flux balance analysis of photoautotrophic metabolism. *Biotechnology progress*, **21**, 1617-1626.

Siaut, M., Cuine, S., Cagnon, C., Fessler, B., Nguyen, M., Carrier, P., Beyly, A., Beisson, F., Triantaphylides, C., Li-Beisson, Y.H. and Peltier, G. (2011) Oil accumulation in the model green alga *Chlamydomonas reinhardtii*: characterization, variability between common laboratory strains and relationship with starch reserves. *Bmc Biotechnol*, **11**.

Solomon, B.D. (2010) Biofuels and sustainability. *Annals of the New York Academy of Sciences*, **1185**, 119-134.

Vallino, J.J. and Stephanopoulos, G. (1993) Metabolic flux distributions in Corynebacterium glutamicum during growth and lysine overproduction. *Biotechnology and bioengineering*, **41**, 633-646.

Wang, H., Gau, B., Slade, W.O., Juergens, M., Li, P. and Hicks, L.M. (2014) The global phosphoproteome of Chlamydomonas reinhardtii reveals complex organellar phosphorylation in the flagella and thylakoid membrane. *Molecular & cellular proteomics : MCP*, **13**, 2337-2353.

Yang, C., Hua, Q. and Shimizu, K. (2000) Energetics and carbon metabolism during growth of microalgal cells under photoautotrophic, mixotrophic and cyclic light-autotrophic/dark-heterotrophic conditions. *Biochemical Engineering Journal*, **6**, 87-102.

Young, J.D., Shastri, A.A., Stephanopoulos, G. and Morgan, J.A. (2011) Mapping photoautotrophic metabolism with isotopically nonstationary C-13 flux analysis. *Metab Eng*, **13**, 656-665.

Zamboni, N., Fendt, S.M., Ruhl, M. and Sauer, U. (2009) (13)C-based metabolic flux analysis. *Nature protocols*, **4**, 878-892.

CHAPTER-5

Conclusions and Future Directions

CARBON ACCUMULATIONS DURING NUTRIENT LIMITATIONS

In nature, one of the most common problems life faces is nutrient limitation, especially that of nitrogen. Across biology, organisms respond with slowing metabolisms and accumulations of carbon, be it glycogen (Hasunuma *et al.* 2013), starch (Ball, et al. 1990), triacylglycerols (TAGs) (Merchant, et al. 2012b, Siaut, et al. 2011), or other energy dense molecules. In the field of biofuel technology, researchers seek to use these accumulated molecules as sources of energy as fuels or for carbon substrate for the chemical industry. Algae are photosynthetic organisms that can accumulate these compounds under nutrient stress and have been the target of extensive research over the last several decades, especially for the production of TAG. Despite this work, the reasons cells accumulate one carbon compound or another as well as the role these stored carbon compounds play in the nutrient deplete/ replete life cycle of organisms remain undefined.

Several explanations have been proposed for the induction of TAG accumulation in algae under stress, ranging from storing reduced carbon as an energy source for survival and/or future recovery, to lipid reorganization during photosynthetic down-regulation and/or subsequent up-regulation, to photo-protection from excess photosynthetic energy and carbon (Akita, et al. 2015, Grossman, et al. 2010a, Hu, et al. 2008, Khozin-Goldberg, et al. 2005, Klok, et al. 2014, Kohlwein 2010, Murphy 2001, Roessler 1990). These roles can be divided into four classifications: (i) sink for excess fixed carbon, (ii) sink for excess photosynthetic energy, (iii) carbon storage to aid nutrient recovery, and (iv) energy storage to aid nutrient recovery. The work in this thesis has sought to deepen the understanding of the relationship between photosynthesis and

TAG accumulation in microalgae and either support or counter the above motivations through the analysis of carbon and energy fluxes.

PHOTOSYNTHESIS AND NUTRIENT DEPRIVATION

In Chapter 2, I present the effects of nitrogen deprivation on photosynthesis in *Chlamydomonas reinhardtii*. This work demonstrates drastic decreases in the photosynthetic capacity and efficiency during the first 48 hrs of N deprivation. Using transcript and protein profiles along with functional photosynthetic measurements we came to the conclusion that cells decrease photosynthesis in a controlled and coordinated manner. Further when non-photochemical quenching (a measure of photosynthetic stress) was calculated from chlorophyll fluorescence measurements, it was found that this parameter decreased overtime suggesting the cells were not under photosynthetic stress and were able to dissipate any "excess" energy. Evidence for posttranslational control of photosynthetic activity demonstrates cells are able to decrease photosynthetic parameters well before there are changes in protein abundances. Another manuscript from the same study found transcript and protein increases for genes related to nitrogen assimilation demonstrating that the cells focus on priming themselves for the return of nitrogen (Park, et al. 2014). This suggests algae have evolved an encoded systemic response to nutrient deprivation that provides them some advantage to survive the stress.

OVERFLOW HYPOTHESIS CONCLUSIONS

Several works have suggested the motivation for starch and TAG accumulation during nutrient deprivation is related to photosynthetic carbon or energy overflow(Hu, et al. 2008, Li, et al. 2012b, Roessler 1990). The most prominent study in support of the overflow hypothesis involves analyses of the Chlamydomonas PGD1 mutant which accumulates only half as much TAG as its parent line. My arguments against the mutants support of the overflow hypothesis are given in chapter three in more detail.

My work in chapter 2 did not support this hypothesis. To expand upon this and determine if there was evidence for these overflows I studied the relationship between photosynthesis and accumulated starch and TAG molecules during nutrient deprivation across 2 media conditions and 5 light intensities (presented in chapter 3). I chose to work at light intensities representative of normal physiological growth where the organism would not be expected to experience photosynthetic stress, allowing N deprivation to be the sole inducer if any existed. Further using both autotrophic and mixotrophic conditions would allow me to see the affects increased total carbon available on the system would be. If photosynthetic overflows are the main drivers of carbon accumulation I would expect a number of things: (i) No carbon would accumulate in the dark during N deprivation, (ii) there would be no carbon accumulation at low light intensities where light would be expected to be growth limiting, (iii) All carbon accumulations would come from photosynthetic ally fixed carbon, even under mixotrophic conditions, (iv) Cells would demonstrate significant photosynthetic stress in the form of NPQ, (v) there would be a proportionate increase in carbon accumulation per

increases in light intensity, and finally (vi) carbon accumulations would be highest when photosynthetic rates were highest, decreasing over time.

In this work I found the contrary to these points. Algae were able to accumulate significant amounts of starch and TAG at low light intensities and in the dark demonstrating carbon accumulations do not depend upon photosynthetically fixed carbon or energy. Second, under our conditions, algae demonstrated a decrease in total NPQ over the timecourse suggesting they are able to safely control their energy intake and are not under significant photosynthetic stress. Third, there was not a proportionate increase in starch or TAG accumulations with increasing light intensity for both mixotrophic and autotrophic conditions pointing to other regulatory mechanisms controlling the accumulations. Under mixotrophic conditions, through ^{13}C acetate labeling during n deprivation, we found almost all TAG carbon coming from acetate with a minority of it supporting starch accumulations suggesting TAG and starch accumulations are under separate regulatory and carbon networks. Additionally, if there indeed is a photosynthetic overflow sink, it would be starch due to accumulation of photosynthetic carbon and it being the first pool to accumulate. Finally, I found TAG accumulation rates to be at their highest during the later phases of nutrient deprivation, well after photosynthetic capacity and efficiency have decreased excessively, a result counter-intuitive to the overflow hypothesis.

While this work has not described what the fundamental motivations of algal oil accumulation are, this contributes a strong step forward in saying what are not the drivers. My data strongly suggests TAG accumulations are not induced by photosynthetic stresses. This points to a regulated storage role for these molecules that

aids recovery from nutrient deprivation through either/ both carbon and energy stores(iii and iv above). Further, chapter 3 data points to a relationship between initial N+ growth rates and carbon accumulation rates with faster growing cells consuming and utilizing environmental N at a faster rate than slower growing cells, causing them to enter the N deprived carbon accumulating stage faster. Future research efforts should then be driven to look at the regulatory network, especially that around growth, for hints on controls of carbon accumulation.

MODELING OF NUTRIENT DEPRIVED METABOLISM

In chapter 4, I used a stoichiometric model of Chlamydomonas to study N+ and N- carbon metabolism to determine the most important metabolisms for growth, starch, and TAG accumulations. Here, physiological measurements from chapter 3 were used as constraints for Flux Balance Analysis to probe the genome scale metabolic model. Nitrogen deprivation experiments showed that across all light and media conditions, starch was being produced from pentose phosphate pathway fructose generation while TAG carbon came from multiple different locations depending upon the media source and light condition. Reduced carbon such as acetate is demonstrated as a preferred substrate for oil accumulation over photosynthetically derived carbon. Further corrections made to the photosynthetic reaction stoichiometries allows for more realistic flux studies on photosynthesis and its interaction with metabolism.

FUTURE EXPERIMENTS AND DIRECTION

The preliminary data presented in Appendix 1 demonstrates interesting relationships between starch and TAG breakdown and cell growth during recovery from nutrient deprivation. First, it is demonstrated that starch degradation precedes TAG degradation suggesting unique roles for each storage pool. Second, photosynthesis was found to increase in efficiency and capacity during the first 24 hrs of N recovery suggesting starch and TAG degradation may help in the recovery process.

This data leaves many questions remaining. First, what are the individual roles of starch and TAG in nutrient recovery? Does starch carbon aid nitrogen fixation or is it burned for energy? Does TAG provide acyl chains for membrane synthesis, especially in the thylakoid where large amounts of membrane are required for photosynthesis? Finally how does the photosynthetic environment change over the course of nutrient recovery and how does that change with or without acetate?

To approach the roles of starch and TAG during nutrient recovery, I propose a ^{14}C labeling experiment where cells are labeled with ^{14}C bicarbonate during nitrogen deprivation and monitored during recovery with no label. Total counts of ^{14}C in biomass per culture volume during nutrient recovery would show whether a significant amount of labeled carbon is retained during recovery or removed. If ^{14}C is retained in total biomass, it would demonstrate that starch and TAG play carbon storage roles, providing carbon for new biomass, and if there is a small amount retained it would suggest these compounds play energy storage roles as they would simply be burned after N recovery. Next counting the change in ^{14}C label in TAG and other glycerolipid pools after TLC separation might show flows of ^{14}C label from one pool to another. I believe that there will be a significant amount of label going from TAG to MGDG

and DGDG pools as TAG would help restore photosynthetic membranes. Expanding upon this, if cells were labeled with ^{14}C during 12-40 hrs(starch labeling) and from 40 to 96 hrs (TAG labeling) (See Chapter 3) during N deprivation, one could get label dominantly into either starch or TAG pools and be able to follow specific labeling from each stored compound. Counting 14C in other biomass such as protein pools may point to the starch and TAG utility for the assimilation of nitrogen. With this data trends, one may be able to tease out of starch, TAG, or both pools are in line with photosynthetic measurement increases, contributing to its recovery. One earlier study used labeled arachidionic acid to suggest TAG is used to help MGDG production during nutrient flow however this was in a different alga strain and only one Fatty acid species (Khozin-Goldberg, et al. 2005). Understanding the roles of starch and TAG during nutrient recovery may shed light on ways to increase their production during nutrient deprivation for bioenergy purposes.

FINAL

Determining the final destination of starch and TAG carbon helps determine reasons for the accumulation of these compounds. Further, systems approaches identifying gene/ proteins responsible for storage compound degradation may provide direction for engineering efforts to have algae that accumulate large amounts of carbon during normal growth. Although an inverse relationship between cell growth and carbon storage has been continually demonstrated there may still be a way to unhinge these relations. This may lie in deregulating photosynthetic controls decreasing potential carbon and energy fixation, or in regulation controlling N+ TAG and starch pool sizes.

In this dissertation I have shown TAG accumulations are not caused by photosynthetic stress/ overflow during nutrient deprivation under mixotrophy at normal physiological conditions. Additionally, I have shown that starch increases before TAG during deprivation and is used before TAG during nutrient recovery(see Appendix). This points to a regulatory control switch between starch and TAG synthesis suggesting one look at the regulatory environment of the cell when it switches from starch to TAG synthesis. Tuning those signals may allow for increased TAG and decreased starch synthesis. Next as autotrophic cells do not decrease their photosynthetic components as much as mixotrophic cells during N dep, it may be possible to compare the two conditions and pull out what regulatory controls are at play to help engineer an organism that has heightened energy and carbon capture during N- to aid carbon accumulation.

In homage to all the general biology courses I have ever taken:

--THE MITOCHONDRIA IS THE POWERHOUSE OF THE CELL--

APPENDIX

To address the functional roles of starch and TAG accumulations, these compounds need to be studied during nutrient recovery. Very little literature exists on nutrient recovery in algae, especially on carbon metabolism and the ultimate destination of the starch and TAG carbon and energy. Here, I have gathered preliminary data on the cell physiology, photosynthetic parameters, and kinetics of nutrient recovery to aid future research endeavors in this area.

After 96 hrs of N deprivation in TAP media, nitrogen is added back to the media and the Chlamydomonas cells were followed. Figure 5.1 (Panel A) shows cells do not begin to divide until after 24 hrs. During this 24 hr lag period, cells synthesized new chlorophyll to reach near N+ level (Panel B). Further, cells decreased their Ash Free Dry Weights (AFDW) suggesting starch and TAG and being degraded within this period.

Total FAMES were also found to decrease in parallel. Both TAG and starch levels were back to N+ amounts by 36 hrs (Figure 5.2). This data demonstrates starch mobilization hrs before TAG suggesting starch is a first energy or carbon source for the cell which would enable the rapid uptake of nitrogen into amino acids. As TAG levels fall before total FAME, this demonstrates fatty acid distributions in the cell is changing and may represent movement of TAG fatty acids into membrane lipids.

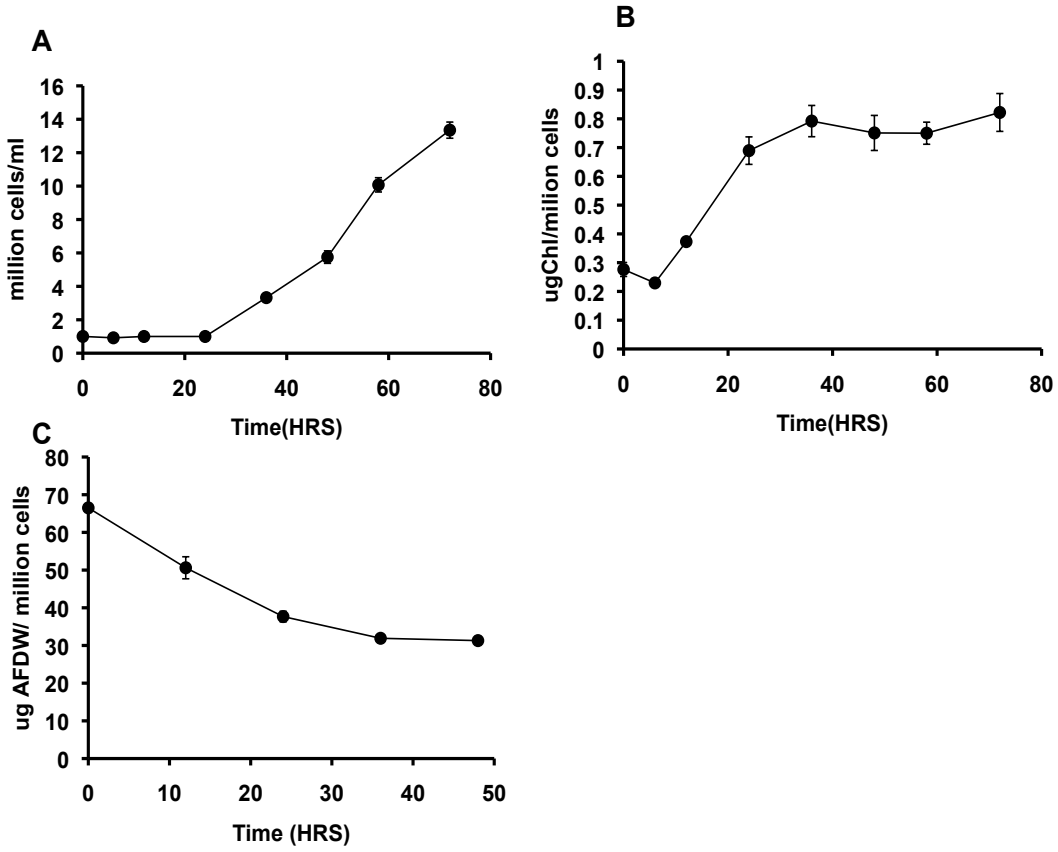

Figure 5.1. Changes in cell counts, biomass and Chl after nitrogen readdition. (A) Cell counts, (B) Chlorophyll abundance, and (C) Ash Free Dry Weights(AFDW) were measured at each timepoint after N readdition. Error bars indicate standard deviation, N=3.

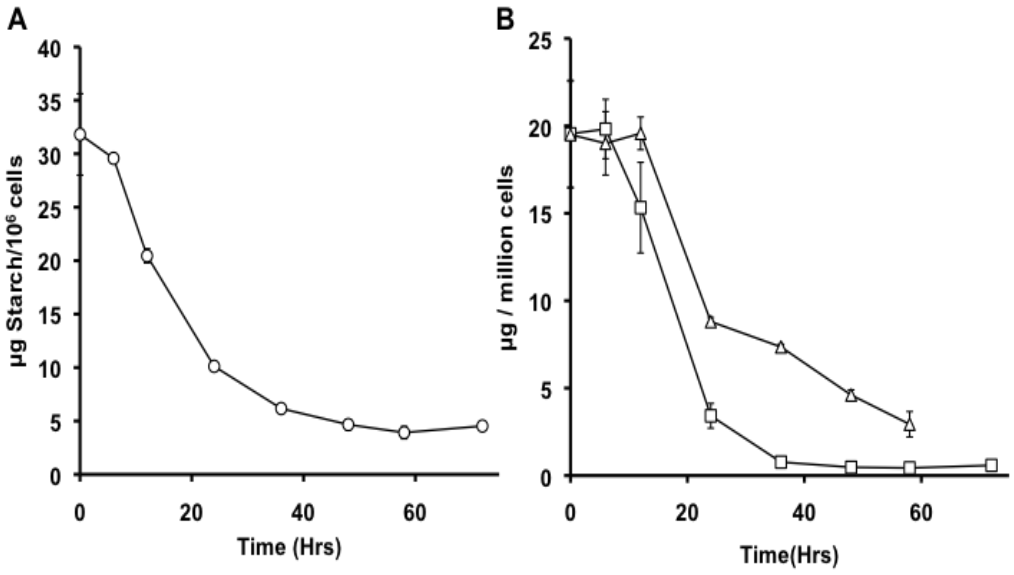

Figure 5.2. **TAG and Starch Degradation during N recovery**. Starch levels (A) begin to fall before TAG (hollow square) and FAME (hollow triangle) Levels (B) during N recovery. Error bars indicate standard deviation, N=3.

To learn about the relationship between starch and TAG and cell recovery, we measured the disappearance of these molecules (Figure 5.2). In Panel A of 5.2, starch rates were found to decrease almost immediately after the return of nitrogen. TAG levels were found to decrease starting after 6 hrs of recovery and

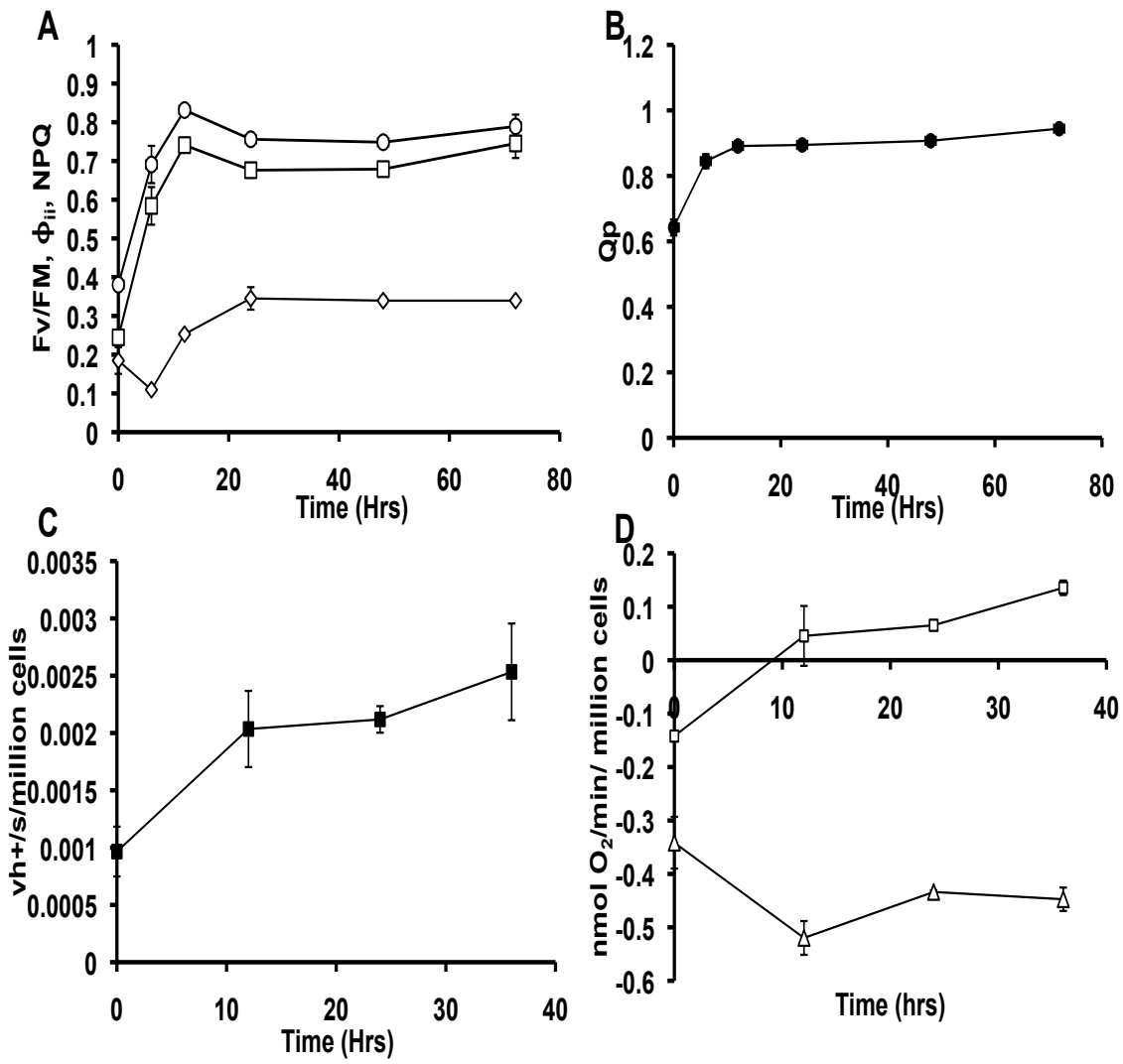

Figure 5.3. Photosynthetic measures during N recovery. Chlorophyll fluorescence measurements (A) show FV/FM(hollow square), ϕii (hollow square), and NPQ (hollow diamond) values reach N replete levels within 24 Hrs. Qp(B) measures demonstrate PSII quinone pools are open to N+ levels within 12 hrs of recovery. Thylakoid proton efflux rates (C) increase to N+ levels between 24- 36hrs. Net oxygen evolution(D) (hollow squares) and consumption (hollow triangles) reach N+ levels by 36 hours. Error bars indicate standard deviations, N=3.

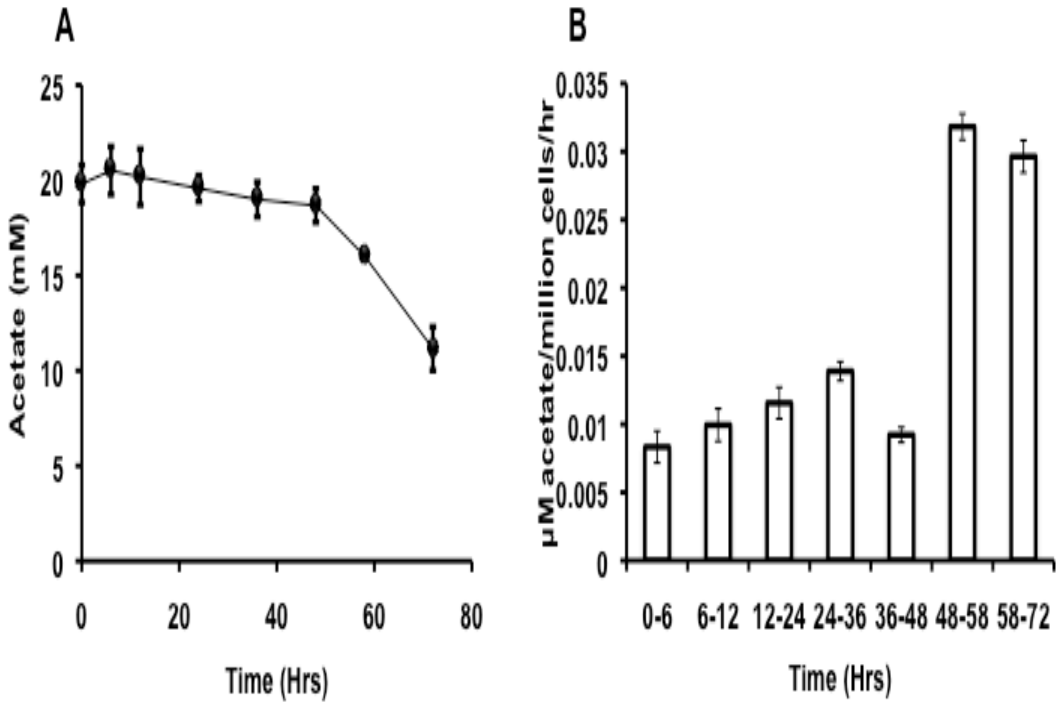

Figure 5.4. Acetate uptake during nutrient recovery. Acetate levels do not appear to decrease rapidly until after 48hrs(A). Acetate uptake levels do no increase until after 48 hrs of N recovery(B). Error bars equal ranges of measurements, N=2.

The Recovery of Photosynthesis was studied through chlorophyll fluorescence, absorbance spectroscopy, and gas measurements (Figure 5.3). PSII photosynthetic efficiency was found to return to N+ levels in the first 24 hrs of recovery and photosynthetic stress (NPQ) was found to return within the same period. The PSII quinone pool returned to N+ levels within the first 12 hrs demonstrating quick repair of PSII components. Proton efflux rates, a measure of ATP synthase, showed continued increase in rates through 36hrs suggesting cells continue to restore photosynthetic components through this time point. Oxygen evolution values show a similar trend as the total proton efflux supporting continued restoration. These collective data suggest

cells rapidly restore the intrinsic efficiency of their photosynthetic components but continue to increase their capacity for photosynthesis even after 36 hrs of recovery. It is important to note that starch and TAG decrease when photosynthetic capacity is most rapidly restored suggesting these molecules play a part in the restoration.

As a measure of metabolic demand during recovery, media acetate levels were measured. Starting off slow, acetate began to be uptake at a faster rate from 12 to 48 hs with dramatic increases in uptake from 48 to 72 hrs. Acetate uptake per cell values are presented in panel B of figure 5.4. This suggests that cells start with a slowed metabolism during n deprivation which increases to N+ levels by 48 hrs. This coincides with increases in photosynthetic activity and cell growth.

REFERENCES

REFERENCES

Akita, T. and Kamo, M. (2015) Theoretical lessons for increasing algal biofuel: Evolution of oil accumulation to avert carbon starvation in microalgae. *Journal of theoretical biology*, **380**, 183-191.

Ball, S.G., Dirick, L., Decq, A., Martiat, J.C. and Matagne, R.F. (1990) Physiology of Starch Storage in the Monocellular Alga Chlamydomonas-Reinhardtii. *Plant Sci*, **66**, 1-9.

Grossman, A.R., Gonzalez-Ballester, D., Shibagaki, N., Pootakham, W., Moseley, J. and Pootakham, W. (2010) *Responses to Macronutrient Deprivation*.

Hasunuma, T., Kikuyama, F., Matsuda, M., Aikawa, S., Izumi, Y. and Kondo, A. (2013) Dynamic metabolic profiling of cyanobacterial glycogen biosynthesis under conditions of nitrate depletion. *J Exp Bot*, **64**, 2943-2954.

Hu, Q., Sommerfeld, M., Jarvis, E., Ghirardi, M., Posewitz, M., Seibert, M. and Darzins, A. (2008) Microalgal triacylglycerols as feedstocks for biofuel production: perspectives and advances. *Plant J*, **54**, 621-639.

Khozin-Goldberg, I., Shrestha, P. and Cohen, Z. (2005) Mobilization of arachidonyl moieties from triacylglycerols into chloroplastic lipids following recovery from nitrogen starvation of the microalga Parietochloris incisa. *Bba-Mol Cell Biol L*, **1738**, 63-71.

Klok, A.J., Lamers, P.P., Martens, D.E., Draaisma, R.B. and Wijffels, R.H. (2014) Edible oils from microalgae: insights in TAG accumulation. *Trends in biotechnology*, **32**, 521-528.

Kohlwein, S.D. (2010) Triacylglycerol homeostasis: insights from yeast. *J Biol Chem*, **285**, 15663-15667.

Li, X., Moellering, E.R., Liu, B., Johnny, C., Fedewa, M., Sears, B.B., Kuo, M.H. and Benning, C. (2012) A galactoglycerolipid lipase is required for triacylglycerol accumulation and survival following nitrogen deprivation in Chlamydomonas reinhardtii. *The Plant cell*, **24**, 4670-4686.

Merchant, S.S., Kropat, J., Liu, B., Shaw, J. and Warakanont, J. (2012) TAG, You're it! *Chlamydomonas* as a reference organism for understanding algal triacylglycerol accumulation. *Current Opinion in Biotechnology*, **23**, 352-363.

Murphy, D.J. (2001) The biogenesis and functions of lipid bodies in animals, plants and microorganisms. *Prog Lipid Res*, **40**, 325-438.

Park, J., Wang, H., Gargouri, M., Deshpande, R., Skepper, J., Holguin, F.O., Juergens, M., Shachar-Hill, Y., Hicks, L. and Gang, D.R. (2014) The response of Chlamydomonas reinhardtii to nitrogen deprivation: A systems biology analysis. *Submitted*.

Roessler, P.G. (1990) Environmental-Control of Glycerolipid Metabolism in Microalgae - Commercial Implications and Future-Research Directions. *Journal of Phycology*, **26**, 393-399.

Siaut, M., Cuine, S., Cagnon, C., Fessler, B., Nguyen, M., Carrier, P., Beyly, A., Beisson, F., Triantaphylides, C., Li-Beisson, Y.H. and Peltier, G. (2011) Oil accumulation in the model green alga *Chlamydomonas reinhardtii*: characterization, variability between common laboratory strains and relationship with starch reserves. *Bmc Biotechnol*, **11**.